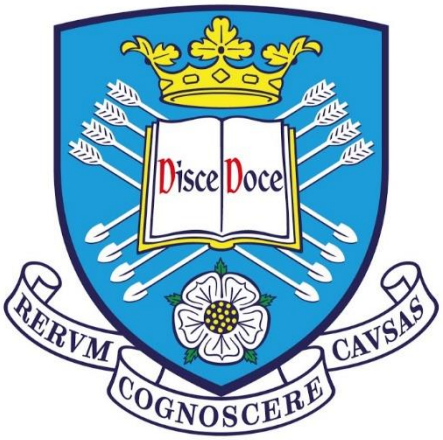

The University of Sheffield - School of Architecture

Development of a window system with optimised ventilation and noise-reduction performance: an approach using metamaterials.

A thesis submitted to the University of Sheffield for the degree of Doctor of Philosophy in the faculty of Architecture
by

GIOIA FUSARO

Supervisors:

Dr. Wen-Shao Chang

Dr. Fangsen Cui

Dr. Xiang Yu

Prof. Jian Kang

Submitted August 2021

Abstract

Noise transmission is a key factor regarding indoor comfort and energy-smart Architecture and Engineering. In most cases, occupants of the building must choose between a naturally ventilated indoor environment or a quiet one. On the other hand, the acoustic metamaterials (AMMs) allow more customisable physical properties according to their spatial configurations, proving significant merits over traditional architecture and engineering materials. This PhD study will investigate AMMs techniques to develop a window system that can control the incoming noise while allowing natural ventilation. This is a crucial point for AMMs research. So far, even if many solutions have been developed to pursue this objective, they still lack ergonomics and human perception analysis. Through a multi-disciplinary methodology, the author first a) highlighted which are the ergonomic principles that add value to the window system from the users perspective, then b) investigated a series of suitable AMMs techniques to be applied for noise reduction and natural ventilation, c) developed a specific AMM design suitable to follow those ergonomic principles previously highlighted and assessed it through human perception, and finally d) optimised a full-scale prototype for a broad acoustic range and customisable ergonomic application. Social science, ergonomic, numerical, analytical and experimental studies were used throughout the PhD project to draw a full-scale window prototype using AMMs to allow natural ventilation independently from the outdoor noise situation. The so-called acoustic metawindow (AMW) allows Transmission Loss (TL) of 10-80dB on a significant frequency range for human hearing (50-5000Hz) in an open configuration while allowing sufficient natural ventilation. In addition, the AMW is proved to positively impact the indoor environment from both physical and human perception points of view thanks to its ergonomic nature. This project will open a new AMMs field of investigation that is not limited to noise reduction but also includes outdoor stimuli optimisation towards a more comprehensive indoor comfort.

Acknowledgements

First of all, I would like to thank my supervisors, Dr Wen-Shao Chang, Professor Jian Kang, Dr Fangsen Cui, for their excellent advice, encouragement, and support throughout my PhD experience in-between The University of Sheffield and A*STAR Institute in Singapore. A special thanks go to Dr Xiang Yu from IHPC (A*STAR), who has always been a reference figure for my PhD path and has become ever since a good friend of mine. I am grateful for all the patience and expertise they all put into this project and the chance to improve my research understanding and myself. I want to thank the colleagues from the former University of Sheffield lab and the IHPC lab for their guidance, suggestions, and, most importantly, friendships. I also want to thank Professor Zhenbo Lu for his guidance and support in the experimental tests at the National University of Singapore (NUS).

I want to thank all of my friends and family. Especially my parents, for loving and supporting me in every moment of my life and throughout this PhD journey. I could not ask for better parents, and I would not be who I am today without you both. I want to thank my auntie, Elena. She is a second mother and a reference as an independent woman who inspires my life. I want to thank all the friends I have met along this journey and who stuck with me in the good and bad moments. I have met so many people that supported me throughout the PhD, and I am very grateful to all of them. However, a special thanks go to Francesco, Claudia, Tingting, Chunyang, Yussur, Gianmarco, Marion and Gioia (the first and only other Gioia), whom I met in Sheffield, and Daniela, Gianluca, Adrian, and Stefano, whom I met in Singapore. They have always been true friends and became ever since my family beyond the sea. I want to thank Katie, my marvel of a housemate, for bringing me joy, happiness and companionship during our first and most difficult pandemic lockdown. I want to thank Martina and Giada, who have been my pillars despite the distance and time difference, always showing me the best part of myself. Finally, a special thanks go to Marco, who makes me every day a better woman. Throughout this experience, we grew up together.

I have always been an enthusiastic person. I have never been able to decide between a more rationally scientific or more creative part of myself. I have always been looking for a way to fit in the number of fields I have worked on. At the end of this PhD, I have understood that I should accept myself as I am and that all the areas of research I am passionate about (and where now I have developed various yet possibly limited knowledge) are not an issue but an enrichment. I hope that the results of this project and the experience I am sharing will be useful and supportive towards the future generations of students, researchers, women.

Table of Contents

Figures and Tables

Chapter 1

Chapter 2

Chapter 3

Chapter 4

Chapter 5

Chapter 6

Chapter 7

Symbols

A	-	Cross-sectional area
c	-	Speed of sound
dB	-	Decibel
Δp	-	Pressure drop
ϵ	-	Dielectric constant
E	-	Young's modulus
F	-	Force
FS	-	Fluctuation Strength
Hz		Hertz
k	-	Bulk modulus
μ	-	Magnetic permeability
m	-	Magnification
m_{eff}	-	Effective mass
ν	-	Poisson's ratio
N	-	Loudness
P	-	Pressure
Pa	-	Pascal

q	-	Ventilation rate
ρ	-	Density
$\bar{\rho}$	-	Dynamic mass density
R	-	Roughness, or reflection coefficient
S	-	Sharpness
T		Temperature
t	-	Time
v	-	Velocity
V	-	Volume
Z	-	Impedance

Abbreviations

ACPH	-	Air Change Per Hour
ACR	-	Air Change Rate
AMM	-	Acoustic metamaterials
AMS	-	Acoustic metasurface
AMW	-	Acoustic metawindow
BSUs	-	Basic Structural Units
BEM	-	Boundary Element Method
CAD	-	Computer-Aided Design
CFD	-	Computational Fluid Dynamics
CV	-	Coefficient of variation
DMR	-	Decorated Membrane Resonator
DEs	-	Dielectric Elastomers
DNS	-	Direct Numerical Simulation
n-DOF	-	Number of Degrees Of Freedom
FDM	-	Finite-Difference Method
FEA	-	Finite Element Analysis
FEM	-	Finite Element Method
GT	-	Grounded Theory
HIE	-	Helmholtz integral equation
HR	-	Helmholtz Resonator
ICC	-	Intra-class Correlation Coefficient
IL	-	Insertion Loss
LES	-	Large Eddy Simulations
LHM	-	Left-handed Material=NIM
MEMS	-	Micro-Electro-Mechanical-System
MV	-	Mechanical Ventilation
NIM	-	Negative Index Material=LHM
NFR	-	Non Functional Requirements
ODE	-	Ordinary Differential Equation
OR	-	Opening Ratio
PC	-	Printed Circuit
PCB	-	Printed Circuit Board
PDE	-	Partial Differential Equation
PML	-	Perfectly Matched Layer

PLA	-	Polylactic Acid
RANS	-	Reynolds-Averaged Navier-Stokes
RSM	-	Reynolds Stress Model
RMS	-	Root Mean Square
RW	-	Weighted sound reduction index
SA	-	Spalart Allmaras
SPL	-	Sound Pressure Level
SRI	-	Sound Reduction Index
STC	-	Sound Transmission Class
TL	-	Transmission Loss
ZIM	-	Zero Index Material

Equations

$$v_{sound} = \sqrt{\frac{K}{\rho}} \quad \rightarrow \quad v_{light} = \sqrt{\frac{1}{\mu \cdot \epsilon}} \tag{1.1}$$

$$\nabla^2 P - \frac{\rho}{k}\frac{\delta^2 P}{\delta t^2} = 0 \tag{1.2}$$

$$f_0 = \left(\frac{c}{2\pi}\right)\sqrt{\frac{S}{V(l + 2\Delta l)}} \tag{1.3}$$

$$f_0 = \left(\frac{100R}{\sqrt{V(l + 1.6R)}}\right) \tag{1.4}$$

$$f_0 = 200\sqrt{\frac{p}{(d)(t)}} \tag{1.5}$$

$$f_0 = 216\sqrt{\frac{p}{(d)(D)}} \tag{1.6}$$

$$\bar{\rho} = -\frac{1}{\omega^2 \underline{d}}\frac{\langle P \rangle}{\langle W \rangle} \tag{1.7}$$

$$\alpha = \frac{4x_s}{(1+x_s)^2 + (y_s)^2} \quad 1.8$$

$$(\sin\theta_t - \sin\theta_i)k_0 = \xi + nG \quad 1.9$$

$$\sin\theta_i = \sin\theta_t + 2(1+n) \quad 1.10$$

$$q = AC_d\sqrt{\frac{\Delta T\, g\, h}{(T_I+273)}} \quad (m^3/s) \quad 1.11$$

$$\mathrm{IL_{AMW}} = \mathrm{SPL_{woAMW}} - \mathrm{SPL_{wAMW}} \quad (dB) \quad 1.12$$

$$\mathrm{CV} = \frac{\mathrm{RMS_1}}{\mathrm{RMS_2}} \times 100 \quad (\%) \quad 1.13$$

$$\mathrm{RMS_1} = \sqrt{\frac{\sum_{i=1}^{N}\left(\mathrm{IL_{Num,i}} - \mathrm{IL_{Exp,i}}\right)^2}{N}} \quad 1.14$$

$$\mathrm{RMS_2} = \sqrt{\frac{\sum_{i=1}^{N}\mathrm{IL_{Exp,i}}^2}{N}} \quad 1.15$$

$$Eff(N) = \frac{\Delta N}{\Delta MIN} \quad 1.16$$

$$Eff(N) = \frac{\Delta N}{\Delta MIN} \quad 1.17$$

$$Total\ ponderated\ vote = \sum X_0 \cdot 0 + X_1 \cdot 1 + X_2 \cdot 2 + X_3 \cdot 3 + X_4 \cdot 4 \quad 1.18$$

$$(\sin\theta_t - \sin\theta_i)k_0 = \xi + nG \quad 1.19$$

$$\sin\theta_i = \sin\theta_t + 2(1+n) \quad 1.20$$

$$q = AC_d\sqrt{\frac{\Delta T\ g\ h}{(T_I+273)}} \quad (m^3/s) \tag{1.21}$$

$$\mathrm{IL_{AMW}} = \mathrm{SPL_{woAMW}} - \mathrm{SPL_{wAMW}} \quad (dB) \tag{1.22}$$

$$\mathrm{CV} = \frac{\mathrm{RMS_1}}{\mathrm{RMS_2}} \times 100 \quad (\%) \tag{1.23}$$

$$\mathrm{RMS_1} = \sqrt{\frac{\sum_{i=1}^{N}\left(\mathrm{IL_{Num,i}} - \mathrm{IL_{Exp,i}}\right)^2}{N}} \tag{1.24}$$

$$\mathrm{RMS_2} = \sqrt{\frac{\sum_{i=1}^{N}\mathrm{IL_{Exp,i}}^2}{N}} \tag{1.25}$$

$$Eff(N) = \frac{\Delta N}{\Delta MIN} \tag{1.26}$$

$$Total\ ponderated\ vote = \sum X_0 \cdot 0 + X_1 \cdot 1 + X_2 \cdot 2 + X_3 \cdot 3 + X_4 \cdot 4 \tag{1.27}$$

$$SS\% = \frac{(SS_{votes} \cdot 100)}{TOT_{SS}} \tag{1.28}$$

$$AMW\ unit\ Amplitude\ Filter = \frac{SPL\ (with\ AMW\ unit)}{SPL\ (without\ AMW\ unit)} \tag{1.29}$$

$$\text{extra attenuation} = \Delta\mathrm{TL} = \mathrm{TL_{AMW}} - \mathrm{TL_{SW}} \quad (\mathrm{dB}) \tag{1.30}$$

$$\mathrm{ACPH} = \frac{\mathrm{Q}}{\mathrm{V}} \ (\mathrm{h^{-1}}) \tag{1.31}$$

$$\mathrm{ACRM} = \frac{1}{\mathrm{ACPM}} \quad (\mathrm{min}) \tag{1.32}$$

$$extra\ time = \Delta ACRM = ACRM_{AMW} - ACRM_{SW} \quad (min) \tag{1.33}$$

1. Introduction

1.1 Background

Outdoor noise façade insulation, provisions for ventilation, and overheating mitigation have been commonly considered disconnected in building design developments. Strategies to control these different systems have been developed with entirely separated approaches involving building features [2]. Conventional windows, for example, allow visual connection with the outdoors, natural ventilation, and the partial acoustics isolation when closed; however, the way these mechanisms work, forces the users to choose one function and to exclude the other and, of course, neither choice is conducive to indoor comfort [3–5]. So far, researchers have used several methodologies to overcome both problems by using, for example, mechanical ventilation [6], active or passive noise control systems [7–15]. These last ones consume less energy and can be built through several features within the window, such as perforated or microperforated (MPP) panels [8,16–18], porous materials [19–22], or acoustic metamaterials (AMMs) [23–28].

AMMs, in particular, are artificially engineered composite structures with unique acoustic properties derived from the use of modern engineering and physics, which are unlikely to be found in natural materials. Their range of applications includes sound absorption [26], noise attenuation [29], acoustic wave manipulation [30], as well as asymmetric acoustic wave propagation[31], acoustic energy harvesting [32], acoustic holography [33] and topological acoustics [34]. Among these, applications to combine noise control with air transmission have received considerable attention from acousticians. Recently methods such as resonant based acoustic meta-absorbers have been developed [16,35], evolving into subwavelength coiled channels metamaterials [36,37] and a combination of labyrinthine AMMs with porous materials such as foam and cotton[25]. However, due to their bulky and visually invasive geometrical nature, complex geometries, or relatively narrow bandwidth, they sometimes limit architectural choices, such that the design of thin and visually pleasant metastructures embedded in window systems remains a challenge. Moreover, as a product destined to be used by common people in their everyday lives, AMMs-based ventilation systems should also be evaluated from an ergonomic and human perception point of view.

1.2 Motivations

External inputs, indoor comfort needs, and ergonomics have become a fundamental part of the design innovation process [38–42]; however, published works on the built environment and its features are still limited [43]. Only a few of these studies have indeed considered using social sciences methods to investigate such fields [44] involving, for example, focus group methods. Although many methods have been developed to test the physical or psychophysical effectiveness of window design investigation [2,9,45–49], there is still a need to understand the interactions between people and windows better to optimise building systems performance and human well-being through architectural and engineering design.

Regarding the development of window design to improve the built environment, there are no indications derived from participatory ergonomics or the overall existent physical and psychophysical approaches. It is not clear how people relate actively and passively to windows, how they perceive them as a means of communication between outdoor and indoor environments, and how they think they could be improved to make a better indoor environment. The previously cited window's design studies aimed and contributed to creating an ergonomic working or living environment; however, they do not fully capture the social meaning that those environmental qualities have for the users. This disconnection has led to a window design that does not consider how people possibly relate different window shapes or materials with indoor and outdoor environment function and with the degree of privacy. So it is necessary to fill this gap to improve the manageability of this fundamental tool from users' perspective by including more in Ergonomics Social Sciences based methods, especially using participatory techniques such as Focus Group.

Finally, in order to allow a window design that is not dependent on fixed parameters (such as specific sound-absorbent materials thickness) and can be adapted to any public and private environment according to the designer will rather than the building constraint, new material must be developed. This material must also allow natural ventilation independently from the outdoor environmental noise and must be customisable according to different building indoor functions. For this reason, AMMs should be used due to their unique, customisable acoustic performance, which can be tuned in order to satisfy noise reduction requirements while keeping the shape or thickness of the window independent from it.

1.3 Aims and Objectives

This work aims to develop a new window system for natural ventilation and incoming noise reduction through AMMs. In order to achieve this, the following objectives must be met.

Investigating which are the ergonomic characteristics that would add value to the window design

As will be demonstrated later, people relate to the window system through three specific principles, which also describe the ergonomic value of the window from the users' perspective.

Individuating the most suitable available AMMs techniques for allowing noise control and air propagation and, if necessary, developing an original prototype to be adapted to a real window design and its ergonomic characteristics

A specific AMM technique must be chosen following those characteristics highlighted in the previous objective. This technique must follow the requirements for the window's ergonomic value from the users' perspective. Moreover, a careful adaptation to a standard window design must be assessed in order not only to make the new prototype useful from the physical and ergonomic point of view but also to serve engineers and architects in their building's design.

Assessing the acoustic impact of the AMM based window through the human perception experimentally.

The use of human perception is used again to close the circle of the PhD project and verify if, from the users' perspective, the adapted AMM based window system serves the purposes from the acoustic point of view (the ventilation one is guaranteed from analytical and numerical analysis).

1.4 Methodology

The methodology used to pursue the abovementioned objectives and answer the research question is mixed and uses both methods from Social Sciences, Natural Sciences, and Industrial Prototypisation (see Figure 1.1.1). Specifically, the Participatory Ergonomic Focus Group was used in Chapter **3 Participatory approach to draw ergonomic criteria for window design**. Analytical and numerical methods were used, on the other hand, for the physical investigation, including acoustic and

ventilation research questions (see Chapter **4 AMM for natural ventilation window** and **7 Development of a full-scale**). Further Psychoacoustic and Experimental analysis methods were required afterwards in Chapter **5 AMM adaptation to real window design.** To finally understand the impact of the prototype of the final acoustic metamaterial based window (acoustic metawindow = AMW), the human perception experimental method was designed, as explained in Chapter **6 AMW unit effect on the human perception**. Details of each Method and Subject will be discussed more specifically in each of the Following Chapters.

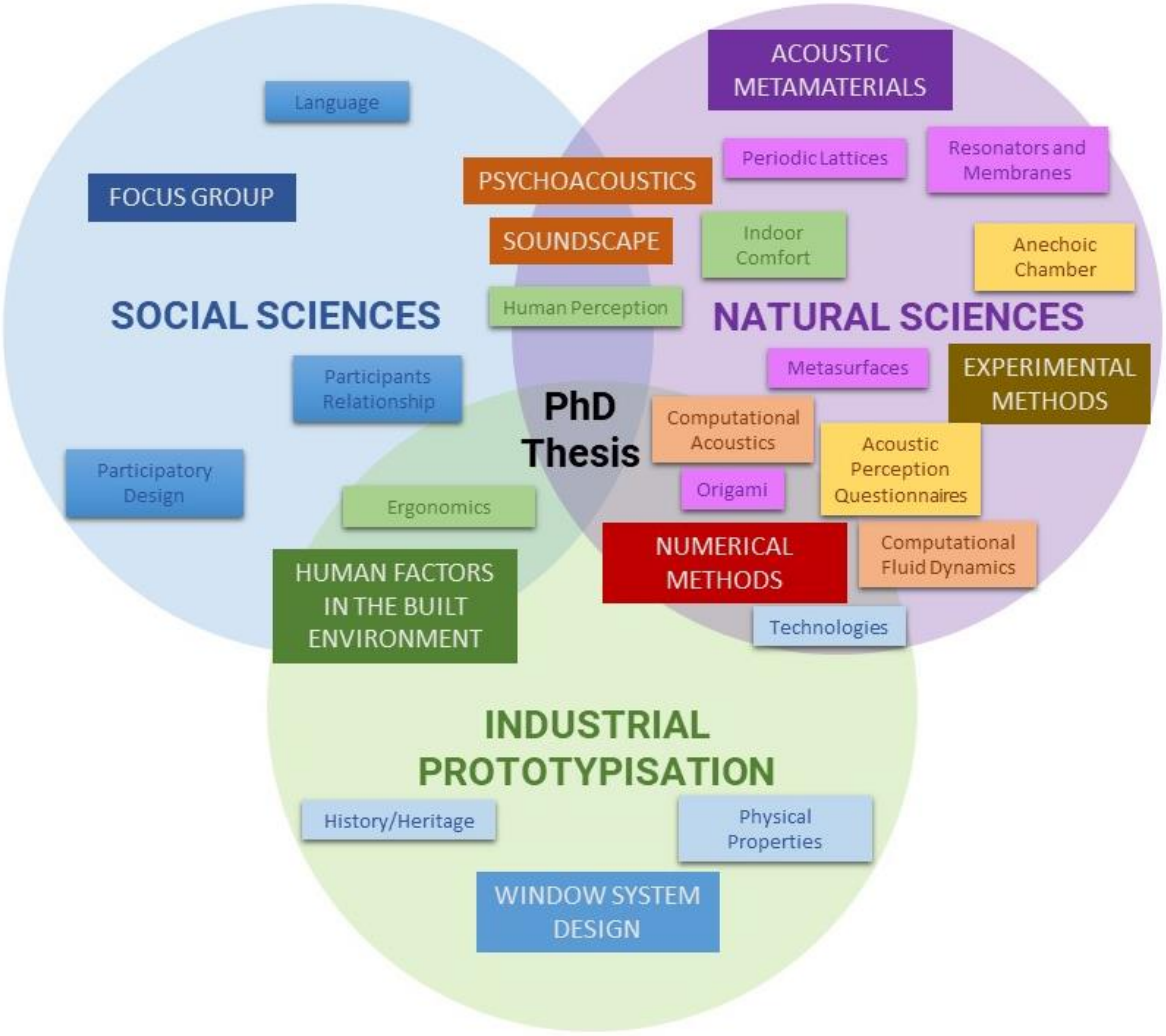

Figure 1.1.1 Schematic representing the research methods and fields involved in the presented PhD thesis.

At the end of this project, a full-scale acoustic metawindow (AMW) for broadband noise control (50 to 5000 Hz) and natural ventilation is presented, and its performances are examined numerically and supported by a previous experiment on an AMW unit following the same AMMs principle. As the complexity of designing a new window model with such characteristics is evident, methods from fields such as Natural Science, Industrial Prototypisation, and Social Science have been used (see Figure 1.1.1). By considering a window as an ergonomic feature of the building, Engineers or Architects might

think first about the technical or physical characteristics; however, it is not possible to ignore human perception and interaction meanings of such an external envelope system.

1.5 Thesis Outline

This thesis comprises eight Chapters, including this introduction, and each of them contributes to each research question (that will be described and justified in details in Section **2.7 Literature Review Highlights and Research Questions**).

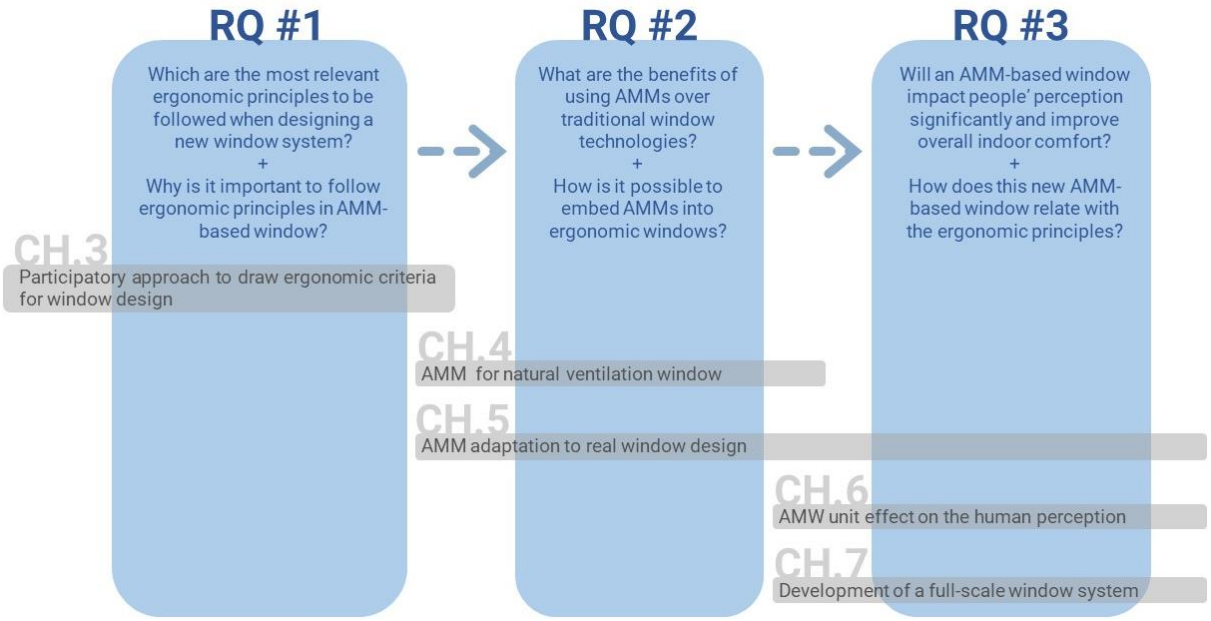

Figure 1.1.2 Diagram representing the Thesis outline with each chapter related to each research question

Chapter **2 Literature Review** introduces the theory behind the primary methodologies and subjects used in this project. An in-depth review of the previously published literature concerning the investigations carried out here shows their importance within the project and proves the relevance of the Research Question. The Literature Review includes 2.1 Windows system design, 2.2 Acoustic Metamaterials, 2.3 Numerical computational methods,
2.4 Experimental assessment methods for acoustic properties of materials, 2.5 The Human Factors in the built environment, 2.6 Focus Group - Theory.

Chapter **3 Participatory approach to draw ergonomic criteria for window design** investigates a new kind of participatory window design methodology involving social science techniques. The main aim is to understand the principles that define the value attribution of ergonomic window design from the users' perspective and draw a new methodology for window design, which considers users' preferred

aspects and combines them with specific window's technologies. Focus group technique and Grounded Theory are used.

Chapter **4 AMM for natural ventilation window** shows the numerical and analytical investigation of a variety of acoustic metamaterials (AMMs), acoustic metasurfaces (AMS), and deployability mechanism (to allow a comprehensive ventilation study too with open and closed configurations at different degrees). Section 4 includes 4.1 Acoustic Metamaterials Broad Investigation, 4.2 Origami Metacage deployability, 4.3 Development of metacage for noise control and natural ventilation in a window system.

Chapter **5 AMM adaptation to real window design** investigates for the first time the adaptability of previously effective AMMs-based systems into a metawindow unit system. The relative acoustic and ventilation performance are examined numerically and (for the acoustic part) experimentally. The numerical and experimental results show a significant *IL* within a frequency range of 300 to 5000 Hz with an effective inter-method agreement. So, the Acoustic optimisation is numerically investigated by perforating the AMM unit component and extending the resonant volume. The ventilation performance will also be assessed, proving that most of the AMW configurations are suitable for natural ventilation and that the ventilation capacity can be tuned according to different ranges by adjusting the window's ventilation opening.

Chapter **6 AMW unit effect on the human perception** investigates the effectiveness of the AMW unit through human perception based laboratory and online questionnaires. Seven environmental sounds recordings are modified through the basic model AMW unit effect. Participants evaluate both original and altered recordings (in a laboratory-based and online-based experiment), allowing the author to draw a correspondence between the impact of the AMW unit and human perception.

Chapter **7 Development of a full-scale AMW** attempts at exploring the applicability of the previously tested AMM system for noise reduction and natural ventilation in a full-scale window. A total of 120 parametric analyses are carried out to assess the effectiveness concerning two design parameters: frame's thickness and height (T and H) for both a basic AMW full-scale model and broadband optimised one. Moreover, Natural ventilation is investigated numerically for both basic and acoustically optimised models.

2. Literature Review

The research explained in this dissertation involves a series of different subjects and methodologies, which will be reviewed in this chapter. Initially, the **window development** through history and technology will be explained in detail, including the **physical properties** of window structure, such as sound or air insulation. Secondly, a series of **acoustic metamaterials** that were taken into account for the development of this overall research will be presented with the most updated literature review. Thirdly, **Numerical Analysis** methodology will be extensively explained, including different techniques (FEM, FDM, and BEM) and the theories behind them considering acoustics and fluid dynamics, followed by an **Experimental Analysis** literature review focusing on the set-up of the anechoic chamber for conducting measurements of acoustic parameters. Finally, the subject of the human perception involved in Industrial Design in terms of **Ergonomics** and the methodology that connects it with the Social Science, the **Focus Group**, are going to be reviewed to give the reader a clear context of where our study is located.

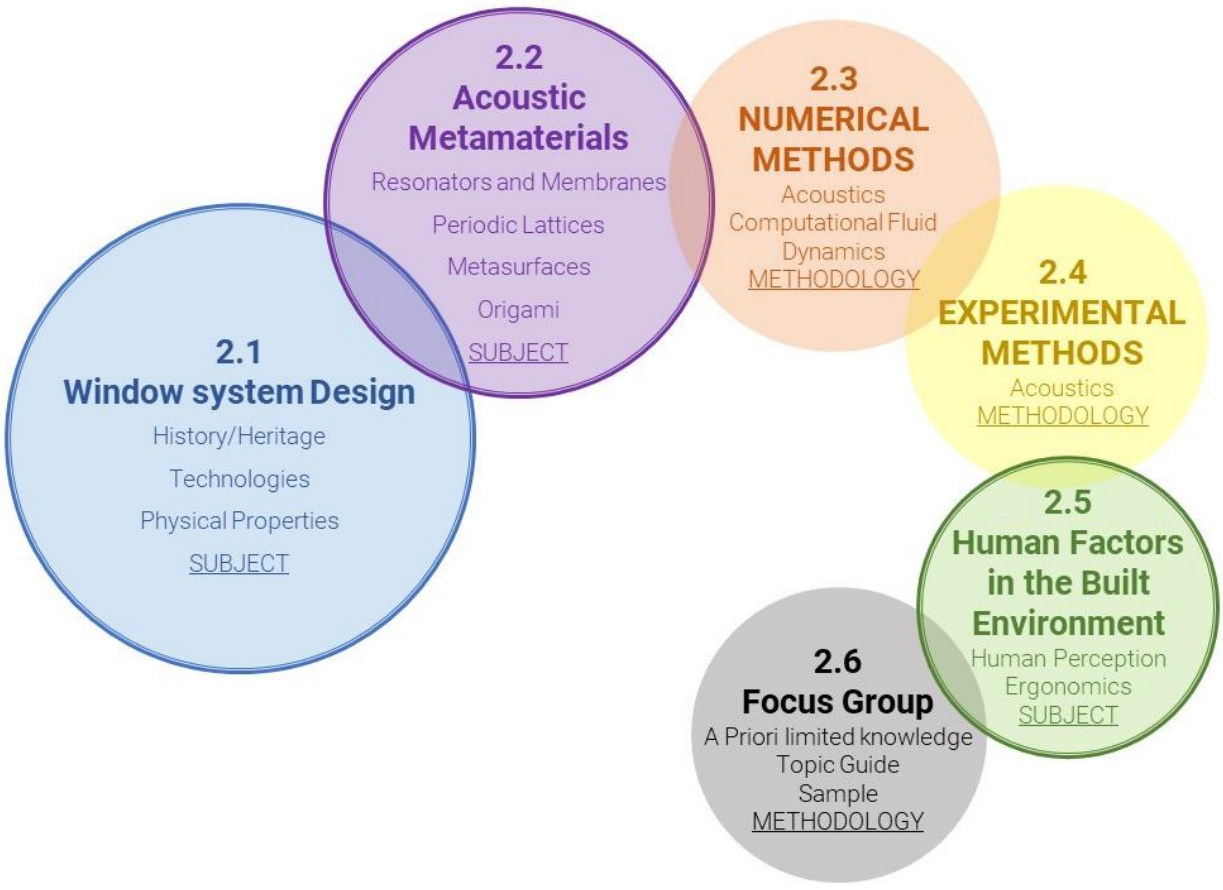

Figure 2.1 PhD project structure concept including the three subjects (window, ergonomics, and metamaterials) and the three methodologies (focus group, numerical analysis, experimental analysis).

2.1 Windows system design

2.1.1 History of windows design from Roman Empire until contemporary technology

When we think about windows, we think they have always been an undeniable part of buildings, both if they were more historical charm or modern and hi-tech. A window system tells us a lot about the building it is built on, such as its style and structure technologies, and makes us appreciate the progress accomplished by the techniques in the last centuries. Nevertheless, of course, this component has a more prehistorical origin. Let us think, for example, at the first dwellings as the caverns, where the same opening carried out the functions of door and window. Even later, the same lonely opening characterised the houses of nomads. This kind of population used to move to feed the livestock and usually used to live in tents built with tree branches and animal leather. Nevertheless, the only opening was still an important element of the first sedentary huts, made of reeds, straw and leaves.

This opening system was in use also in the first centuries of the Roman Empire. However, small sheets of coarse glass were used to close the openings with the glass industry development: they were generally not transparent and thick around one centimetre. It is possible to find evidence of this technique in the ruins of Pompeii, where the noble house of the *patricians* (the roman richest class of that age) used to have a bronze frame and inside this little and thick glass sheets. In Rome, the use of the glass became increasingly diffused, such that Cicero [50] wrote, “Tam pauper potest considerari debent Qui non habet domum operuit cum speculum laminis” which means “Really poor has to consider himself, the one who does not own a house covered by glass plates”. Once the Roman Empire ended, the glass artisans disappeared with it, and only after the 500 – 600 d.C. this type of window reappeared after discovering a new technique to produce glass. This was called flat glass, and it was produced by flowing a glass sphere and rotating it inside the hoven.

In the Mediaeval age, characterised by unrests and uncertainty, the main aim for building dwellings was defence and not comfort, so the openings did not always have glass to close them. Those in the castles' perimeter, especially, were small and had a flattened and long shape. This was used to see and check the outdoors, and, at the same time, did not allow strangers or enemies to get inside the building. More generally, in the mediaeval age, the number and the dimensions of the openings were enough to guarantee the air exchange.

In the Gothic period, a new construction method, especially related to religious buildings, allowed to concentrate the structure weights in much thinner elements than those previous: the façade was emptied and allowed wide and very high glazed openings. They were generally split into multiple

frames (*polifore*) and decorated by particulars due to the stone-cutting technique development. The massive glass walls infill the thin stone frames, so the light became an element of space definition. During this period, glass technology developed together with the lead one. The lead was used to join the glass sheets to create an airtight and statically resistant system. In civil buildings, the moving glass windows, built on non-moving steel frames, brought to a size reduction and simplification of the openings. The glass sheets were contained in lead extrusions, and wood louvres still made the shading system.

In the Renaissance, the innovation brought the dismantling of the ancient feudal structures. The windows became a crucial representative spot of the rich dwellings. More complex shapes started to be used in this historical period for the openings (for instance, the *serliana,* a triple opening window with a bigger central arch). Later, with the Mannerisms, windows systems became heavier, almost always rectangular, with protruding architrave built as a frame with decorations. Extremely common was the *aedicule* window, inspired by the Pantheon model, on which the classical architectural orders were applied. During the Baroque, the new architecture appeared more independent from the classical design schemes followed in the building production until that moment. Against the Renaissance academic criteria, based on the proportions and ancient rules, a dynamic design took a position, where each element of the building was connected to the others by the same rich decorations, spirals and other themes from the natural world. In this period, the window got together with the other elements within the façade to give the vertical rhythm (no more highlighted by the architectural orders). So the window itself was the most important element of the façade composition in the most different shapes: rectangular, squared, round or segmental arch-shaped, and tympanum shaped. The frontons were enriched through decorations, got curved and got the typical spiral shape of Baroque architecture. The articulation and the dynamism were emphasized in Rococo. The iron components were still in wrought iron, and decorations and fretworks enriched it. The first typology of wood hardware windows was with a single door, but soon also the double door and the double split in the middle door were developed.

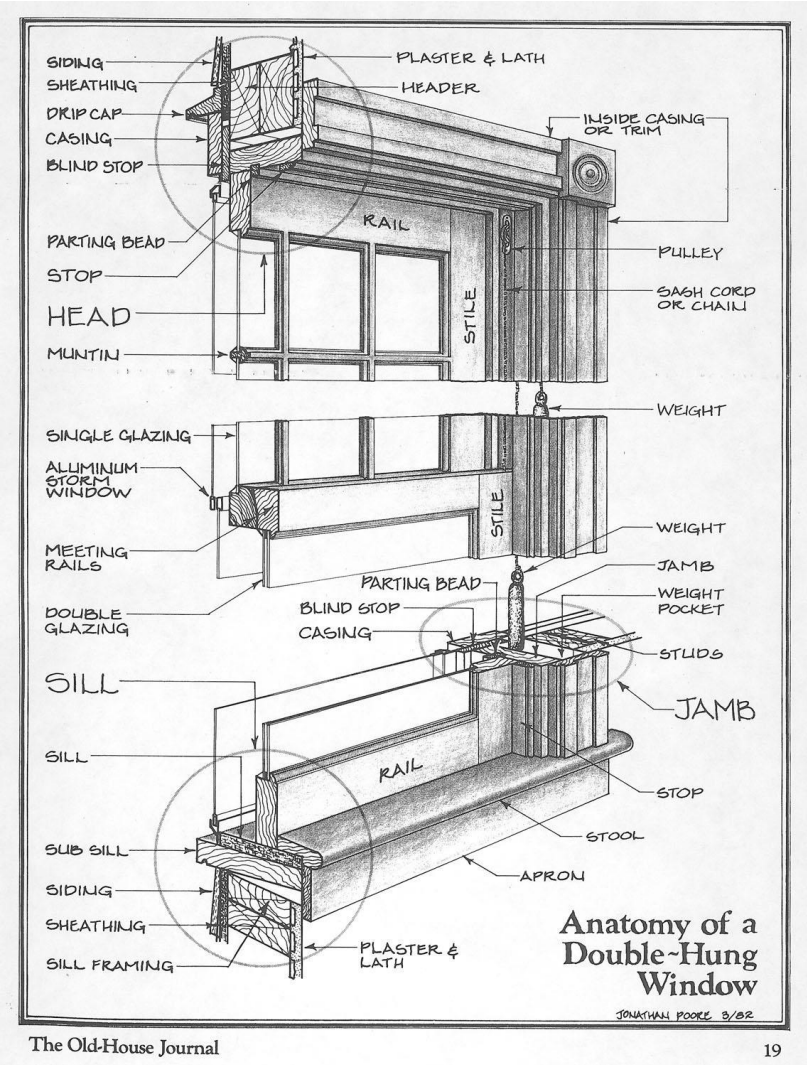

Figure 2.2 Schematic of a double-hung window which became famous as 'British window'[51].

In the 17th century in Italy, the dripstone and small intermediate frames were used to link the small glass sheets in the window panel instead of the strings of lead used previously. The frames had articulate and complex shapes with a good grip but were still limited by the water leakage and humidity resistance. One century later, the first wood windows systems started to get used even out of Italy, using wood such as durmast, teak, plane tree, and maple. In England, the double-hung window became the most common typology (Figure 2.2)[51]. This was characterised by two main parts that slid one over the other to open the window and some smaller intermediate frames for which they became famous as 'British window'. In the eighteenth century, with the Industrial Revolution, the iron in the construction industry became more popular for major engineering works such as bridges, railways, viaducts, channels, industrial buildings, ships, and major works as the constructions where to host international exhibitions. The buildings realised in iron and glass became common. The windows got significant dimensions, thanks to the thinness of the structures and the technology development, which enabled the use of glass sheets to increase dimensions, solve the problem of

intermediate frames, and amplify the design potentiality. Iron was mostly used as a construction material for the non-residential building, and the windows and doors were less important in the housing (basements or stairs), but wood was still the most used material for the residential building.

Around 1920 the façades lost all the decorations, and windows became essential. There was a general refusal of the previous century iconic architecture, and the new architects wanted to be overall technicians more than artists. They designed new typologies of windows, mostly with non-moving frames and with the only aim of lighting. Frequent were the massive *glass walls* and the so-called *ribbon windows,* which reflected the idea of more freedom in the composition, possible thanks to the advent of air conditioning systems. Thanks to modern technologies, another important innovation for the window functionality was the fixed shading system as brise soleil (literally in French sun breaker) with horizontal or vertical louvres of different materials (overall wood and concrete), an iconic element of this period architecture production. Regardless, until the advent of the new industrial technology and the new materials of the Fifties, there was no chance for the modern architects to break the classical rules for windows design, and so in a different way compared to the previous centuries. However, with the introduction of structural beams and pillars, realized through reinforced concrete, the external walls were not structural anymore, and the windows' height could be either the whole light between one pillar and the other. The industrialization of glass production and the active air conditioning allowed an open design of the transparent surfaces until the window became a wall, set to build a continuous façade. This façade system needed a frame of modular pillars and beams on which it was possible to apply transparent or opaque panels, generating a tangle that became an essential part of the façade composition. Due to air conditioning reasons, the glass technology developed an innovative system to make the external walls reflective, avoiding heat absorption. The window's main aim was not anymore the air flowing or lighting (the artificial air ventilation was preferred because it was more easily manageable). The glass was mostly requested for its versatility, its resistance to atmospheric agents, and its appearance in the architectonical composition.

In the contemporary age, buildings have windows of any possible dimension and typology. There is an extremely different idea of this element from the past, not just from the conceptual perspective but also from the architectural one. Architects and engineers have tried to improve windows systems both on the functional and appearance sides during the last decades to get better performances and get more benefits indoors. Indeed, the window has a key role in everyday life in this historical period, both inside and outside a building. A window is not anymore a mere element that divides spatially the indoor from the outdoor, but it aims to satisfy precise needs that help enhance indoor comfort. The

next section will analyse the existing window design technologies in acoustic, thermal, and ventilation comfort.

2.1.2 Windows design technologies

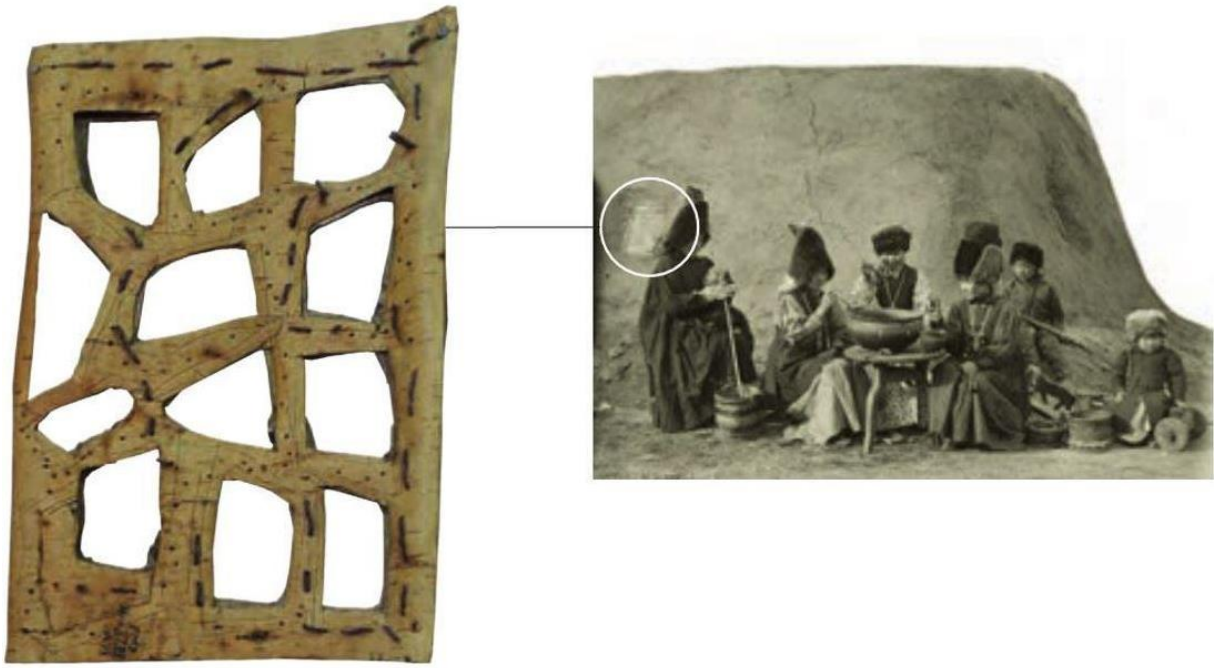

Figure 2.3 A rare Yakutian window from the Far East of Russia, made from birch bark from the Brooking National Collection (Image from Elements of R. Koolhas)[1]

Window systems have been improved much in technologies during the twentieth century. As a general knowledge, the window can be idealised as something that delimitates the space, but at the same time is space-less. Since its original use, this habitation's fundamental component allows seeing what happens outdoors while being repaired from the outdoor itself. It is useful to protect the indoor space from sensible environmental and climate changes due to multiple factors. Specifically, due to the hard climate conditions, in 1910, there was a first attempt to advance the window technology by Yakutians in Balagian dwellings (Figure 2.3) [1]. This population of North Oriental Russia used to apply on the openings of their house, a carved birch bark window.

> "The bark is softened by cooking in cow's milk, carved into shape by male members of the family, and sewn together with tendons from a horse or cow. Two windows, each of around 30cm square, are oriented to the south and one to the west." [1]

In this fragment of his work for the XIV Architectural Biennale of Venice on the fundamental architectural elements, Koolhaas brings us back to the art of adaptation of the human being expressed through windows. This first technology, affordable only by a few rich families, involved the use of oil paper, fish membranes, mica, and in rare cases, small glass shards to fill the birch bark window. However, of course, this system was suitable just in the warmer season. Due to this, the precious windows were removed from the punctured hole in the wall in the winter season to be replaced by a thick sheet of ice in a wooden frame [1]. One of the last examples of Yakutians windows is preserved in The Brooking National Collection. Thanks to Architectural museums like this one, it is possible to study many windows' variations, representing the understated evolution of this important architectural element inserted in the façade and the room through many specific components. To study a new window prototype, it is of primary importance to look at the past heritage.

In this heritage, we find that the attempts to make the window a functional element for the light and an indoor space's thermal conditions were not that many and significant until the twentieth century. Indeed, before Yakutians window, this element was seen more as part of the architectural beauty of the whole building, and due to this, the study of the design concerned more the visual details. Nevertheless, improving the building technique always brought, in every age, a new careful consideration of the window components.

A window system is generally composed of non-moving elements, which guarantee the windows' standing on the wall, and moving elements, which enable the window to open, allowing significant natural air ventilation. The non-moving part is called “frame”, and it is composed of a head, two lateral jambs, and a sill. In a double-hung window, the hardware and the interior part present a balance, connected to the moving frame through a sash, a check rail, a lower and upper rail, a lift and a sash lock. In another standard occidental window typology, the casement window, the mechanisms which allow the two different parts to move are called operator and lock handle. In the twentieth century, many of these nuanced local components have been internalized in the window’s structures by technological advances of window profiles and glass production, until becoming almost invisible. In this process, the glass took over completely until culminating in the curtain wall's invention. This is an outer covering system where outer walls are non-structural and can be substituted by lightweight materials like glass. In the next paragraphs, sound and air insulation modern and contemporary techniques will be explained.

2.1.3 Sound insulation

Acoustic insulation is fundamental in the outer building's shell. Two main methods to measure the potential sound insulation of a structure are the Sound Transmission Class (STC) [52], and the Sound Reduction Index (SRI) [53]. The first one is widely used in the US, while the second one is the reference outside the US, and basically, they only differ by the frequency range. For example, STC covers the range 125 Hz to 4000 Hz, while RW covers 100 Hz to 3150 Hz (both cover 16 one-third octave bands). Therefore, STC equals the 500 Hz band of the reference curve with 0 dB, While RW sets the 500 Hz reference value to 52 dB, equalling a standard separation between houses. However, the calculation methods show that this level does not matter. Instead, the shape of the reference curve (relative weighing) is important, which is comparable for both standards.

For example, in the field of building engineering, a well-built staggered-stud or double-stud wall might have a sound transmission class (STC) of 50 dB and provide sufficient isolation, as would a concrete-block wall. Moreover, it is important to reduce as much as possible the weak links with insufficient sound transmission loss (TL) that would seriously compromise the acoustical isolation of the wall. At the same time, we cannot exclude components as windows or doors from the building composition; otherwise, the functionality of the building itself will be null. Due to this principle, in an ideal situation where a window is placed in a wall facing an outdoor environment with loud sound levels, the sound transmission loss (TL) of the window should be equivalent to the one of the walls itself. To approach the performance described previously with a window requires very careful design and installation. According to Everest and Pohlmann, we can find a typical single pane 1/8-in (3.17 mm) glass with STC of 25 dB, prefabricated double-pane sound-insulating windows available commercially with an STC rating of 50 dB or more [52]. However, if a double-pane window is designed for thermal insulation, it may have an STC value less than a single-pane window. Most of the currently used materials for thermal insulation (such as polystyrene) are indeed closed-cell materials. Due to their physical configuration, the sound cannot penetrate them and lose energy through their vibration as it would do in an open-cell porous material. Thus, the sound propagates better, which is why thermal and soundproofing treatments are frequently in contrast.

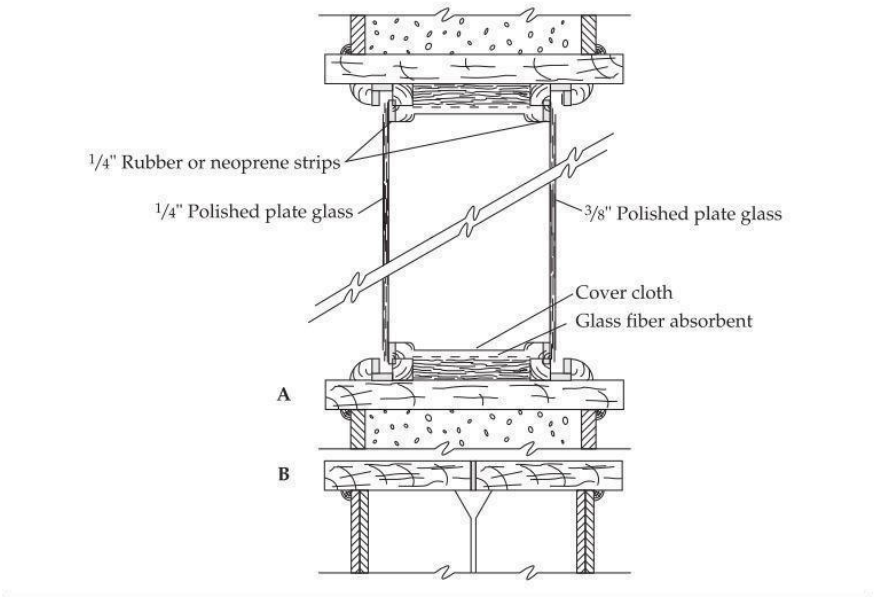

Figure 2.4 Wall construction with double-pane window from the Master Handbook of Acoustics [52]

An applied real solution of a double window on a concrete-block wall is shown in the plan of Figure 2.4A,B, indeed, shows a solution applied to a staggered-stud partition[52]ee. Generally, a sound-isolating double window is indicated in most critical applications, while to add a little to the TL, a triple window can be used instead. The mounting must minimize coupling from one wall to the other as it affects air and sound leaking.

Despite what Everest and Pohlmann assert, heavier plate glass is sometimes better used, but they will exhibit a coincidence-frequency dip nevertheless. Other systems to get a slight advantage consist of using two panes of different thicknesses or the two glass with different inclinations. This allows light or external sound reflections, but the window's TL will be affected only slightly by it. Moreover, it is important to properly design the spacing between the glass panels since even less than 3 cm con produce lower STC than a single-pane window. On the other hand, the bigger is the space, the greater is the TL; according to Everest and Pohlmann [52], there is no significant gain going beyond 10 to 20 cm. At the latter, it is common use, to isolate the glass from the frame through rubber or other elastic strips and to use an absorbent material between the pane edges around the whole periphery of the window cavity (as shown in Figure 2.2: Wall construction with double-pane window from Master Handbook of Acoustics 2) [52]. This, combined with a contained window area, discourages the airspace's resonances and makes sound insulation almost that of an STC 50 dB wall.

Apart from the noise insulation through materials mass properties, another way to control outdoor acoustic wave propagation towards indoor space is through active noise cancellation. This method consists of an electro-acoustic generation of a sound field (through a loudspeaker) for cancelling

negative existing sound fields. In these terms, the cancellation actively diminishes the unwanted noise [46]. These systems are made of a microphone to sample the disturbing acoustic wave, an electronic control system that analyses the input and generates a control signal; consequently, a loudspeaker produces the cancelling acoustic wave driven by the control signal. Finally, a second microphone, defined *error microphone,* is used to check the cancelling system's effectiveness and give additional inputs to improving it if needed, reducing as much as possible the resulting field. To the most known as a transducer, this structure is called adaptive for its dynamic nature to adapt to the variable conditions, is the most popular, and can be implemented by several microphones and loudspeakers [54]. The system becomes more accurate when increasing the number of these channels, but at the same time, the number of interactions microphones-loudspeaker grows, making the associated electronic system more complex. Overall this new technique brought an important novelty in sound field control since it offers a lower-cost solution to the problem of low-frequency noise alternatives to passive noise control [55] which, due to the long wavelength nature of such impulse, generally tends to be realised by large mufflers and massive noise control enclosures, ore visually impacting systems combined with extensive structural damping solutions. Innovative active noise cancellation solutions are currently made of multiple transducers systems applicable to building surfaces, barriers, and openings [15]. This, in turn, solves the problem of the multiple interactions complexity and enables some cases to achieve natural air ventilation with a consistent diminution of the unwanted noise. The only limitation arguable so far could be the non-optimal design configuration since a grid of transducers could negatively impact the outside's visual perception and impact the architecture of the building itself. Moreover, even though further research could achieve less visually impacting systems, the constant need for energy power would make this solution less sustainable. This is why other passive technologies need to be studied to develop a window design system that would allow the natural air to flow and stop the acoustic wave propagation simultaneously from the outside to the inside of a building.

2.1.4 Air insulation

The ventilation concept that was used to design a window in a certain building typology changed from the simple thermal study to the more complex solution to guarantee the occupants constantly have clean and fresh air without being affected by the external condition. During the last decades, the focus has been placed on the whole building’s sustainability. This has pushed the researchers to prefer natural ventilation and enhance the passive performance of a building. This could be achieved by several measures, for example, using ventilation elements with porous materials as a filter in a window

system with a typical weighted sound reduction index R_W of the whole system of about 30 dB [56]. Another one was attenuating the noise entering buildings through ventilation openings using acoustic quarter-wave resonators [57], with 6-7 dB achieved over a relatively wide frequency range. However, in all the passive control examples, the elements used for sound and ventilation management are generally made of non-transparent materials. This affects the transparent area's ratio in the window system, sometimes can generate a health hazard due to the microscopic fibres contaminating the air, and can also increase the airflow resistance in the ventilator system consuming more energy and achieve only minimum air exchange.

The above limitations motivated the new development where less invasive design techniques were developed in the following years. For example, Kang et al. studied how to integrate a micro-perforated absorber in the air space between the double glazing windows [8]. This ensures the acoustic quality and, at the same time, keeps the ventilation and daylighting efficient [8]. In addition, Huang et al. studied and tested low-frequency noise attenuation through active noise control in ventilation windows [46].

Through all their experiments, these researchers demonstrated that the acoustic and ventilation responses to the window parameters' selections were significantly sensible, so they needed more implemented predicting models. Yu et al. proposed a numerical model that allows predicting the sound attenuation performance between an inlet and an outlet acoustic domain connected by a specific bent ventilation duct [58], and they also proposed a simulation model due to predict sound insulation performance of window ventilation in buildings, estimating the SRI in the mid-to-high frequency range and providing guidelines for engineering designs [59].

Everest and Pohlmann stressed that air leaking must be prevented in a building. This idea refers to the classical concept of opening windows or fixed windows complementing an air-conditioning system. This standard idea is, in turn, reflected in the separation of acoustic and ventilation functions related to window design, forcing the users to choose one function over the other. However, during the last two decades, new technologies have been developed in the field of materials, so sound and air ventilation management could be exploited at the same time without requiring energy power. These technologies are called acoustic metamaterials.

2.2 Acoustic Metamaterials

Nowadays, the main problem regarding building materials is how to achieve efficient cooperation between material properties and structure, i.e. allowing some specific characteristics (such as thermal

and acoustic) while fitting into structure's configurations. The general approach before 1999 was to build a multi-layered material to accomplish all the acoustic and thermal tasks. This used to be an effective solution to address the physical transmission problems from the outside to the inside of a building but did not always satisfy architects in shapes and aesthetics since it generally required thick layers of materials [60]. In 1999 Pendry started the era of new composites, starting from optical lenses research, based on theory developed by Vaselago, known as negative index medium properties of particles [61]. David Smith and the company followed up by experimentally demonstrating that theory by the following year. Sir Pendry and colleagues indeed created the first metaparticles consisting of wires and split-metallic rings with a negative index of refraction and negative permittivity, and so negative permeability [62]. The first experimental demonstration of acoustic metamaterial (AMM) is attributed to Zhengyou Liu and colleagues [63]. In 2000 they found negative effective properties of a sonic crystal composed of elements with local resonance characterised by an interior space than the relevant acoustic wavelength. From this characteristic, the name of left-handed materials (LHMs) or negative-index materials (NIMs) was given to these composites. They were defined as "artificially constructed effective materials using periodic structures that are a fraction of the wavelength of the incident electromagnetic wave, resulting in effective electric and magnetic properties (permittivity and permeability) that are unavailable in natural materials." [64]. These materials were initially very attractive, especially for designing effective systems with deterministic electromagnetic properties and so for their terahertz applications. This was especially because any material at its natural state can respond well to this frequency regime (terahertz metamaterials interact at terahertz frequencies, usually defined as 0.1 to 10 THz; radiating long after the infrared band end, just after the end of the microwave band). These materials were called 'metamaterials' ten years later by Walser [65], expressing the idea of a composite which can be engineered to have properties that go beyond (from the Greek μετά) the properties that can be found in nature. Their properties do not derive only from the particles that make the material but mostly from their structure. Specific geometry, shape, size, orientation and arrangement characterises them with electromagnetic waves manipulating properties (sound waves block, absorption, enhancement, or bending). If properly customised, metamaterials can affect sound or electromagnetic waves with several advantages over standard bulk materials [66].

In Acoustics, metamaterials demonstrated to direct and manipulate sound in sonic, infrasonic or ultrasonic waves in gases, liquids and solids [67]. Acoustic and electromagnetic waves act differently in fluids: the first is longitudinal scalar waves, while the second is transverse vector waves with two polarizations. However, their wave equations can set an analogy between the two, as a map of the two constitutive parameters can be done: $\rho \rightarrow \epsilon$ and $k \rightarrow \mu^{-1}$:

$$v_{sound} = \sqrt{\frac{K}{\rho}} \quad \rightarrow \quad v_{light} = \sqrt{\frac{1}{\mu \cdot \epsilon}} \tag{2.1}$$

Where ρ and k are the constitutive parameters respectively of density and bulk modulus, and ϵ and μ are respectively dielectric constant and magnetic permeability. So, the two types of waves share most of the underlying physics, and this leads to the simultaneous development of electromagnetic/optical metamaterials and the related constituent techniques (such as negative refraction [67,68], superlens [69], and cloaking [70]) and AMMs. From Figure 2.5, it is clear that AMM can achieve an extensive range of mass density ρ and bulk modulus (stiffness) k. As explained by Habermann and Guild [71], on the upper-right quadrant (positive ρ and κ) are placed materials with conventional physical characteristics and devices made by cloaking metamaterial (e.g. ceramics, woods, metals, composites, polymers, and foams). The other quadrants and their boundaries are related only to metamaterials [26].

As Figure 2.5 shows, with the decreasing of ρ and k, we have Zero-index materials and slow-sound materials, respectively [26]. A near-zero-index metasurface (ZIM) is a medium with infinitely large phase velocity and wavelength. So, a wave in a ZIM is not affected by any phase change. Many applications such as directive emission [72], self-collimation [73], tailoring radiation phase pattern [74], and super-reflecting and cloaking [75] were possible thanks to this remarkable property. In addition, another function of ZIM is highly selective angular filtering [76] because it transmits only a wave with a near-zero incident angle (normal incidence), while it reflects all the other waves with different incidence angles. On the other side, according to Groby et al., slow sound materials are opaque mediums that exhibit enhanced transmission in narrow frequency ranges along with high dispersions that give rise to slow phase or group velocity waves whose frequency is centred on the narrow transmission band [77].

Some properties of superlenses and hyperlenses are illustrated in the lower-left quadrant of Figure 2.5, both of which defeat the diffraction limit. These lenses can bend the acoustic rays through a negative index of refraction. Consequently, the propagating waves (red arrows) and the magnification of evanescent waves (blue curve) that pass through the lenses mitigate together the effects of diffraction. This feature can be used for examples for far-field super-resolution imaging or acoustic deep-subwavelength imaging as presented in the works of Lu and Liu [78] and Zhu et al. [79]. In these two examples, super-resolution information is projected by the magnification mechanism of the hyperlenses to the far-field, while metalenses super-resolve subwavelength details and enable optical

Fourier transforms. Two basic requirements are at the base of the hyperlens realisation for far-field super-resolution imaging. First, a specific material must support wave propagation with high wave-vectors. Secondly, high wave-vector waves must be converted into one low wave-vector wave through a magnification mechanism. The main applications of such superlenses and hyperlenses are medical ultrasonography, underwater sonar and ultrasonic nondestructive evaluation. More details about superlenses and hyperlenses will be given in the further sections.

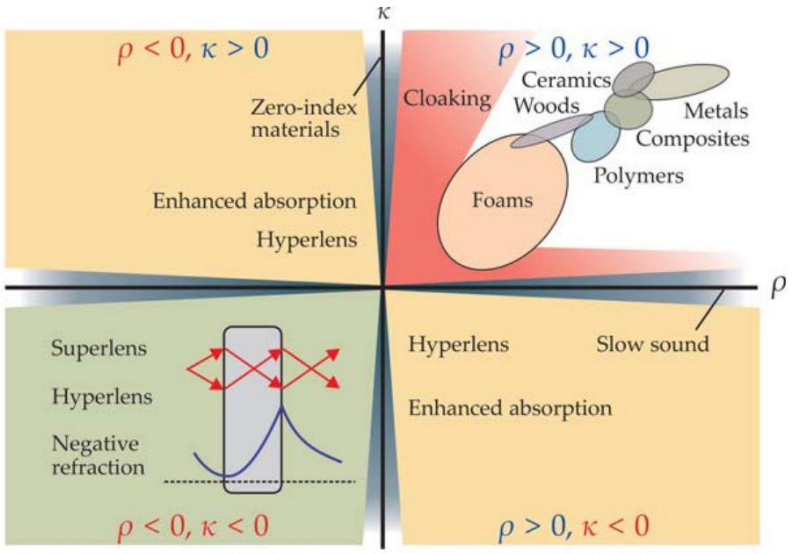

Figure 2.5 Expanded range of mass density ρ and bulk modulus (stiffness) κ [71].

So the control of sound waves is mostly accomplished through the bulk modulus k, mass density ρ, and chirality (from the Greek χειρ, which means hand, indicates that a system/molecule is distinguishable from its mirror image, so it cannot be superimposed onto it). k and ρ are the equivalents in electromagnetic metamaterials as permittivity and permeability. The relation to the mechanics of sound wave propagation in a lattice structure and strong dependence on the material's mass and intrinsic degrees of stiffness, coupled, generate a customisable resonant system.

The acoustic wave's speed manipulation is of particular interest for acoustical applications. Due to the wide range of acoustic metamaterials' effectiveness, they can generate several propagating waves (with extremely high, zero, or even negative speeds) and non propagating evanescent waves corresponding to the purely imaginary values. Negative phase speed, meaning a backwards-propagating phase front, requires both negative effective mass density and bulk modulus. A material with such properties is called double negative or left-handed, while those characterised by positive k and negative ρ or vice versa are referred to as single-negative and cannot support propagating waves. This characteristic leads to an exponential decay of acoustic waves through those materials, which have superior sound dissipation characteristics, mostly based on the coupling of local resonances.

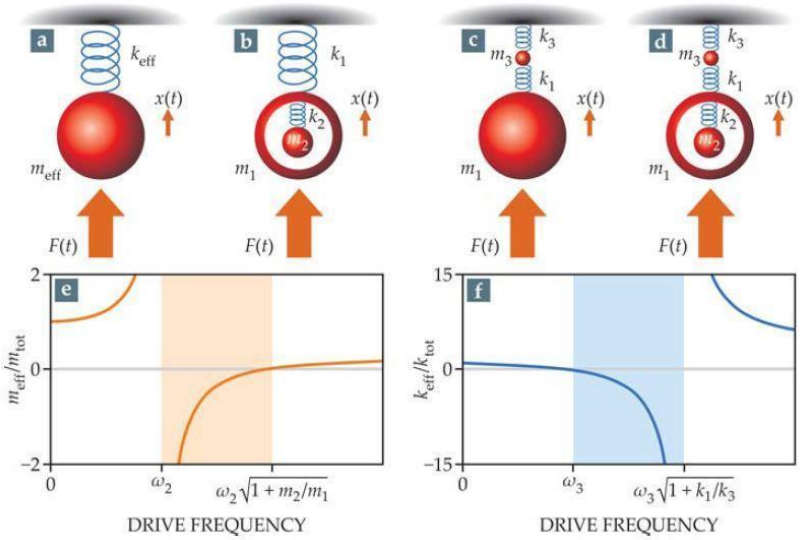

Figure 2.6 The notion of hidden degrees of freedom in AMMs with simple representative mechanical systems comprising masses and springs illustrated by Haberman and Guild [71].

It is on these local resonances (often achieved through resonant elements, that the main difference between traditional acoustic materials and metamaterials is based. When coupled, these simple systems of dynamic microstructural elements generate a large net effect even though the single element has a much smaller dimension compared to the wavelength in the background medium. In this overall view, the arrangement of those dynamic microstructural elements represents what Haberman and Guild define as degrees of freedom [71]. Through mechanical systems (masses-springs) simplification, this concept is illustrated in Figure 2.6, which highlights how they can originate the expanded material configurations. As shown in Figure 2.6a, different masses-springs arrangements result in mass displacement by a distance x(t) if a time-dependent force F(t) is applied. Haberman and Guild [71] explain that "by rearranging Newton's second law and Hooke's law, one can obtain the effective mass and spring constant of the system: $m_{eff} = F(t)/\ddot{x}$ (t) and $k_{eff} = F(t)/x(t)$, where the double dots denote the second derivative with respect to time." Hence, when the acoustic waves are governed by Newton's law of motion, fluid continuity equation, and thermodynamic equation of state (for the adiabatic process), AMMs are useful for manipulating them. The equation describing an acoustic wave in a homogeneous medium absent of a source is:

$$\nabla^2 P - \frac{\rho}{k}\frac{\delta^2 P}{\delta t^2} = 0 \qquad 2.2$$

Where *P* is the pressure and the mass density ρ and the bulk modulus k are the two constitutive parameters. The speed of sound *c* is given by $\sqrt{k/\rho}$. If considered in the effective medium sense, the

two constitutive parameters in AMMs can take unusual values (for example, negative, zero, or close to divergent) and denote acoustic wave characteristics that do not belong to ordinary composites.

According to what Haberman and Guild [71] report about the methodology to design such materials, their properties in acoustic waves can be derived by a transformation acoustics technique. First, a one-to-one map connects a target space exhibiting acoustic behaviour of interest (for example, as it could happen in a café, by redirecting acoustic waves around an enclosed object to shield it from its propagation and create a quiet area) to a physical space with conventional materials and an ordinary acoustic field. Then, the map is used to determine the target space's material properties that produce the desired effect.

A remarkable application of such materials can be found in building engineering. From the industrial revolution of the 19th Century, a new non-structural role of the building skin has been defined. Many applications are expressed through the projects of Walter Gropius, Mies van der Rohe and Le Corbusier, where new techniques, including new materials availability, led to a more energetically efficient system. More specific innovation fields, such as lighting, acoustics, and human-building interaction, have been investigated and improved in the contemporary era. Complex and adaptable architectural prototypes have been developed on a macroscale in the latest years to make the building screening system as adaptive as possible, especially in terms of motion response on external stimuli. The building's covering system is independent of the structural task allowing an innovative development of this part which respond to the external stimuli (e.g. solar radiation, heating, wind and so on) as a bioinspired function [80]. The building's screening mechanism is supposed to mimic the human body adaptation to external conditions. Further research aims to reach flexible materials [52] and a responsive skin [81] based on the free form suitability of the new Architecture and the new adaptive motion characteristics, leading to a new generation of organic and interactive buildings.

These two methods can be considered quite useful at a large scale, but can they be taken into account also for a micro-scale? The new urge to include ‘smart’ materials within the building systems must consider wide dimension systems, especially focusing on the joints of the structures. The discontinuity creates indeed a transmission (thermal and acoustic) issue to be addressed. So, dynamic systems that could change the structural configuration (for example, from a 3D spatial to one that is flat) by adapting the physical response to the external environment could advance building design technology. The acoustic metamaterials categories that will be discussed in the next sections have been set according to the realization method. Indeed, even if so far the research in the field involved new systems such as sonic crystals [63,82,83], AMM with negative reflective mass [84], and double-negative AMM [85], the way they are realised seems more relevant for this specific research. So they

are resonant systems such as 1) Helmholtz resonators and ducts or elastic membranes with attached mass (which means that when the system vibrates, it can damp some energy or change the transmission, absorption, reduction characteristics of the interbeat) or by 2) periodic lattices based on scattering and 3) metasurfaces and 4)origami metamaterials.

2.2.1 Metamaterial resonators and membranes

As explained in the introduction of Chapter **2.2 Acoustic Metamaterials**, metamaterials were applied first for optical purposes and then, for propagating waves similarities, used to design acoustic absorbers and resonators. Before metamaterials, absorbers took advantage of stiffness and multi-layered composition to efficiently absorb acoustic wave propagation. Such characteristics were inspired by the mass law, which rules the sound transmission across a solid wall or a single layer partition [52]. However, the thickness of the absorber device has always been a concerning problem when related to the architectural design or the structural issues [86], and this is why scientists have been trying to solve this problem through systems that naturally oscillate at some frequencies with greater amplitude than the normal acoustic absorbers, calling this devices resonators. The mechanical (or acoustic) oscillation produced in this system (indeed, we are not going to talk about the other resonator oscillation, the electromagnetic one) can be either used to produce sound waves of a range of specific frequencies or selectively specific frequencies from an acoustic signal. The most common examples of such systems are those used in musical instruments to produce sound waves at specific tones [87–89], or cavity resonators, in which waves are created in a hollow space inside the device [90,91]. In this kind of device, the sound is produced by the air's vibration in a cavity with one opening: they are called Helmholtz resonators.

Helmholtz resonators are the most famous devices to achieve local resonances at lower sound frequencies. At the frequency of resonance, there is a pick of maximal absorption, decreasing at nearby frequencies [52]. Thus, the resonant frequency of a Helmholtz resonator with a square opening is given by:

$$f_0 = \left(\frac{c}{2\pi}\right)\sqrt{\frac{S}{V(l+2\Delta l)}} \qquad 2.3$$

where c = speed of sound in air, 343 m/sec

S = cross-sectional area of the resonator opening, m^2

V = volume of the resonator, m^3

l = length of the resonator opening, m

$2\Delta l$ = resonator added neck length = 0.9a, where a is the edge length of the square opening

For Helmholtz resonators with circular openings, the resonant frequency is given by [52]:

$$f_0 = \left(\frac{100R}{\sqrt{V(l + 1.6R)}} \right) \quad 2.4$$

where R = radius of the circular opening, m

V = volume of the resonator, m^3

l = length of the resonator opening, m

So if we change the volume of the air cavity or the length or diameter of the neck, and the frequency of resonance changes. The width of this absorption band depends on the system friction.

The part of the sound that turns out on a Helmholtz resonator without being absorbed is reradiated. As the sound goes out from the resonator opening, it tends to be radiated in a hemisphere, meaning that the unabsorbed energy is diffused. Sound diffusion is a characteristic that in places like studios or listening rooms is very desirable.

Since very old ages, these devices were used as acoustic systems. Indeed, Helmholtz resonator's far predecessors have been found in the ancient Greek and Roman open-air theatres: large bronze jars used to absorb sound at lower frequencies, and groups of smaller jars to supply sound absorption at higher frequencies maybe. Other examples of the use of such acoustical artefact can be found in Swedish and Denmark Medieval churches, where the presence of pots like the one in Figure 2.7 probably helped to reduce low-frequency modes, sometimes together with the addition of ashes in the inside, which should have decreased the quality factor (Q) of the ceramic pots so to broad the frequency of its effectiveness. Nowadays, these principles have been reused with, for example, concrete acoustical blocks configurations with an open slot facing the closed cavity: a two-cell unit would have two slots. Sometimes, as it used to happen for the predecessors, additional materials were inserted in each cavity, like a metal divider, or in the slot inside the cavity, like a porous absorber [92]. Figure 2.8 shows idealized square bottles with tubular necks forming a perforated face resonator, where the bottle stacking increases the resonance aspect of such a device. So it is worth notice as well as Everest and Pohlmann attest that "*Consider a box of length L, width W, and depth H with a lid of*

thickness equal to the length of necks of the bottles. In this lid, holes are drilled having the same diameter as the holes in the neck. The partitions between each segment can be removed without greatly affecting the Helmholtz action." [52]

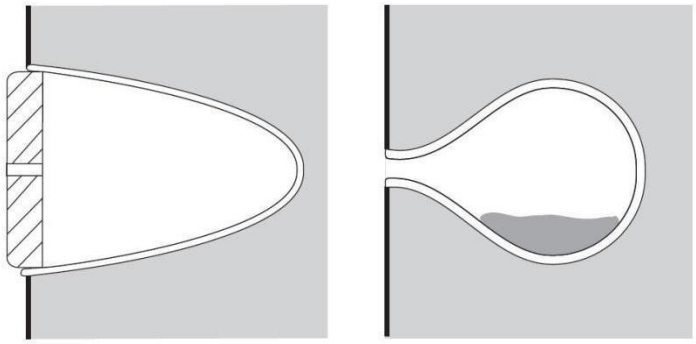

Figure 2.7 Pots embedded in medieval churches' walls in Sweden and Denmark served as Helmholtz resonators, absorbing sound. Ashes, found in some of the pots, may have served as a dissipative agent. (Brüel) [52]

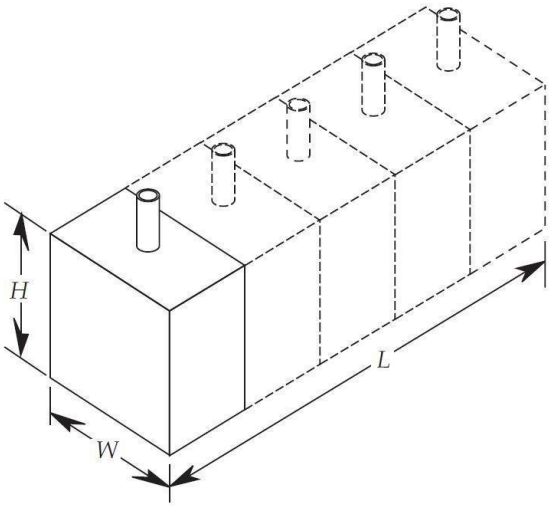

Figure 2.8 Development of perforated-face Helmholtz resonator from a single rectangular bottle resonator. [52]

There are several ways in which the Helmholtz resonators principle can be applied for architectural purposes, perforated panel absorbers, slat absorbers, and many others. However, the most evident thing they have in common is that they all use the holes built on their visible surface to simulate a Helmholtz resonator's neck. These systems generally perform at the maximum resonance when the sound impinges perpendicularly to the plane's face where the holes are situated since, in this way, all the tiny resonators are in phase.

The materials generally used for realising such devices are hardboard, plywood, aluminium, steel, or glass fiberboard (in the case of the slat absorbers), and the percentage of perforation (p) depends on the frequency of resonance (f_0, Hz) and the equations which define it is [52]:

$$f_0 = 200\sqrt{\frac{p}{(d)(t)}} \quad \text{[Hz]} \tag{2.5}$$

$$f_0 = 216\sqrt{\frac{p}{(d)(D)}} \quad \text{[Hz]} \tag{2.6}$$

where: f_0 = frequency of resonance, Hz

p = perforation percentage (see Figure 2.9)

= hole area divided by panel area × 100 (see Figure 2.9)

t = effective hole length, m, with correction factor applied

= (panel thickness) + (0.8) (hole diameter), m

D = depth of airspace, m

d = depth of airspace or thickness of slat, m

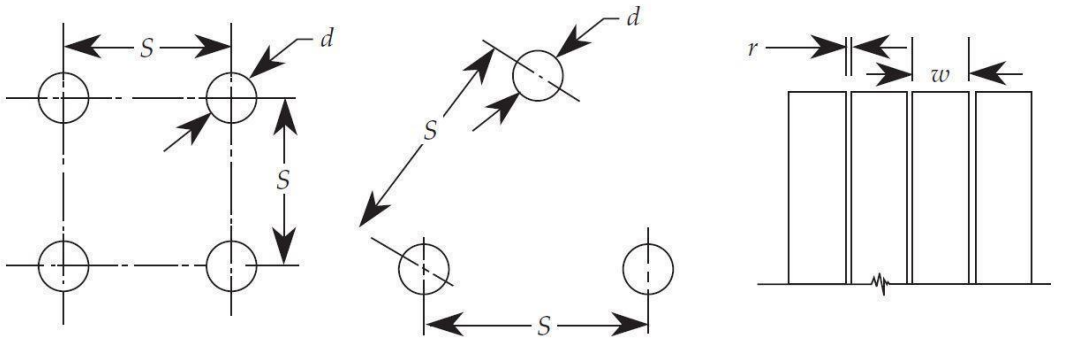

Figure 2.9 Formulas for calculating perforation percentage for perforated panel resonators, including slat absorbers. [52]

It is necessary to place sound-absorbing materials in distributed patches instead of a continuous area [37] to establish a rule on how to apply these materials for effective absorption and diffusion (such a sub-structuring approach will also be reflected in the following numerical analysis part). Moreover, according to Everest and Pohlmann, a system of multiple absorbers units is desirable, and it should be

split in a 3D dimensional spatial mode: using some of each type on ends, sides, and ceiling of the room. In this way, all three axial modes (longitudinal, transverse, and vertical) will come under their influence.

Moreover, besides the materials' placement, it is fundamental to remember that this kind of acoustically resonant device may perform with a relatively specific reverberation time. This may cause audio signal tuning changes, and so it should be controlled, from both electronic or acoustic systems, through the quality factor (Q, which describes the sharpness of tuning). Q is calculated from the expression $f_0/\Delta f$, and it is very short for Q factors normally considered (see Figure 2.10 and Table 2.1). Generally, the higher is the resonance peak, the larger is the absorption bandwidth. For example, as reported by Everest and Pohlmann [52], from a measurement campaign on a series of Helmholtz resonators-based slats, the reverberation time is related to the Q factor (that ranges between 1-100) through the resonant absorbers (see Table 2.1).

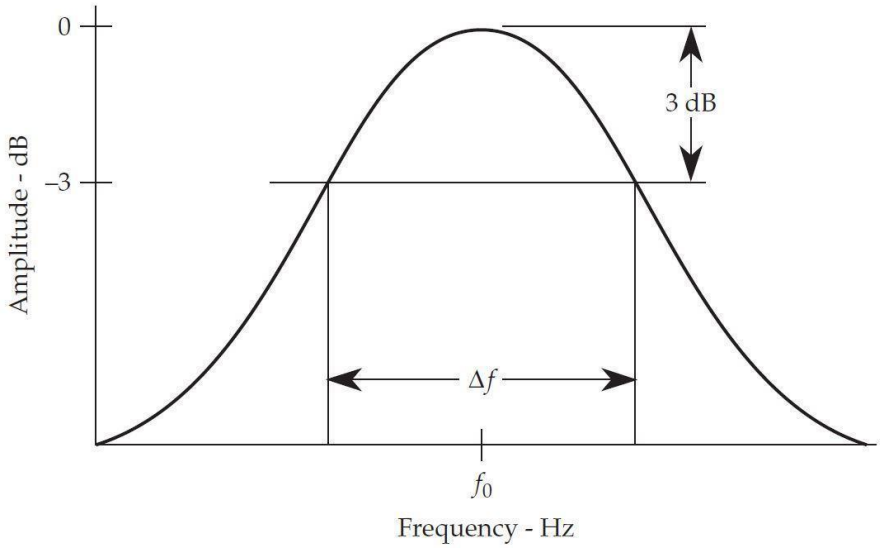

Figure 2.10 Determined tuning curve of a Helmholtz type resonant absorber [52]

Table 2.1 Sound Decay in Resonant Absorbers [52]

Q	Reverberation Time (sec)
100	2.2
5	0.11
1	0.022

*f_0 = 100 Hz

As the original sound absorbers or resonators, the metamaterial versions can modulate the incoming acoustic signal to reradiate it with an effective reduction in SPL and improved hemispheric diffusion. The new challenge of metamaterial absorbers and resonators simultaneously reduces the structure's geometric dimensions and increases the low frequencies related to states' density by finding good conditions to match the impedance to the background medium. This is a complex problem, but, in turn, there could be several advantages in perfectly absorbing an incoming wave field in a sub/wavelength material for applications such as in wave physics as energy conversion [93], time-reversal technology [94], coherent perfect absorbers [95], or soundproofing [96] among others. Some experimental attempts have shown that a metamaterial resonator can achieve absorption in the diffuse field of α_{diff}=0.93 calculated as $\alpha_{diff}=\int_0^{\frac{\pi}{2}} \alpha(\theta)\, 2sin(\theta)cos(\theta)\, d\theta$ [97] derived from Paris's formula $\alpha_s=\int_0^{\frac{\pi}{2}} \alpha(\theta)sin(2\theta)d\theta$ where α_s is the random incidence absorption coefficient, and $\alpha(\theta)$ is the absorption coefficient in the free field, at an incident angle θ .[98] This shows the quasi-omnidirectional behaviour of the absorption in this sub-wavelength structure, meaning that the absorptive capacity is perfect on a wide range of incident angles. The design is similar to the standard Helmholtz resonator (HR), even though the authors argue that the structure's thickness can be even reduced using coiled-up channels or embedding the neck into the cavity of the HRs.

Finally, Ma and Sheng [83] support that acoustic absorption is important for both noise mitigation and interior acoustics optimisation. Hence, two elements are fundamental for effective absorption. First is dissipation, of which friction is the most straightforward strategy. Therefore, materials with high porosity are commonly used as sound-absorbing materials (sponges, mineral wools, fibreglass, and cotton) [99]. Secondly, impedance matching aims at developing the optimal combination between incident acoustic energy and absorber, which can be developed through gradient index. The examples mentioned previously show effective absorption performance for a medium-wide frequency spectrum; however, they become less effective at low frequencies due to practical and fundamental reasons. For example, for linear response systems, dissipation is quadratic in proportions, so absorption can be enhanced by using many materials according to their thickness which should typically be set by order of several wavelengths; however, in low-frequency sounds (where wavelength can exceed 1 m), this is generally an impractical scenario.

Regarding their bulk modulus and the symmetry of the resonances, effective mass dispersion (in frequency) is generally associated with the displacement of the system's centre of mass; however, a compression-extensional motion could be involved in the deformation, which would make possible the stationarity of the centre of mass. This occurs in Helmholtz resonators, where the effective bulk modulus becomes frequency-dependent differently from the effective mass density.

Applying this theory to the concept of the membrane resonators, we can observe significant results reached so far, enabling the determination of the dynamic mass density $\bar{\rho}$ (defined when there are relative motions between the constituent components in a composite [84]). A special class of metamaterial that Ma and Sheng [84] chose to demonstrate the importance of the effectiveness of mass density and bulk modulus dispersions (and their underlying physics) are the decorated membrane resonators (DMRs). DMRs constitute a class of AMMs that can display both mass and bulk modulus frequency dispersions and specific frequency ranges' double negativity. Its effective frequency regime is included generally within the audible spectrum (50 to 2000 Hz); therefore, the thin and light membranes bring new application potentials. An example is shown in Figure 2.11a, where a flexible elastic membrane that is sub millimetres thick and several centimetres wide is fixed on a rigid frame. In order to provide a proper restoring force for the oscillations, a uniform prestress is applied. The membrane's centre is coupled with a rigid platelet. The platelet mass is customised according to the specific working resonant frequencies, representing a spring-mass oscillator (where the platelet is the mass and the membrane is the spring also with a small mass) [100].

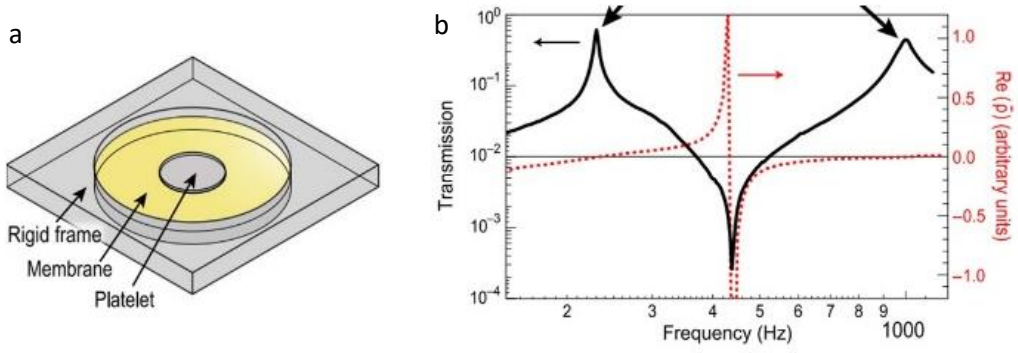

Figure 2.11 Single membrane with negative effective mass density. (A) A schematic drawing of a typical DMR [101].

In this context Ma and Sheng [84] highlight how $\bar{\rho}$ can be determined simply as:

$$\bar{\rho} = -\frac{1}{\omega^2 \underline{d}} \frac{\langle P \rangle}{\langle W \rangle} \qquad 2.7$$

Where $\langle P \rangle$ and $\langle \ddot{W} \rangle = -\omega^2 \langle W \rangle$ are, respectively, pressure difference on two sides of the membrane and acceleration averaged over the surface, and d is the mean thickness. Observing Figure 2.11b, it is possible to see how $\bar{\rho}$ has different signs but becomes zero at the DMR's eigenfrequencies. Near-zero $\bar{\rho}$ has also been utilized to achieve super coupling, to allow under normal incidence an almost-perfect transmission through small channels [102,103]. A negatively divergent $\bar{\rho}$ in the static limit is somewhat non-intuitive result. The reason of such result is that $\langle W \rangle \rightarrow 0$ due to the membrane's fixed

boundary condition, reproducing infinite inertia of the system under a quasi-static force. However, negative sign represents the opposite reaction to the applied force (Newton's third law), and such behaviour of $\bar{\rho}$ can also appear in other structures [104,105], some of which, specifically characterised by negative $\bar{\rho}$ on the low-frequency limit are arrays of flexible membranes modelled from liquid foam [106].

As previously mentioned, the membrane's small thickness entails a very high-frequency range for vibrations related to the membrane's compression and expansion along its thickness direction; however, since such vibrations are monopolar, they can cause anomalous values of $\bar{k}$. In this case, as explained by Ma and Sheng [84], coupling two membranes to form a new DMR, as shown in Figure 2.12a, could lower the monopolar resonant frequencies. This structure largely preserves the characteristics of $\bar{\rho}$ by having two dipolar eigenmodes similar to those of a single DMR and produce a new mode by creating an oscillation of the two membranes against each other. Figure 2.12b shows the vibration profiles of these three modes. The new mode entails compressive/expansive motions by the DMR (its volume is pulsating but keeping a stationary mass centre), leading to an effective bulk modulus *k* that is **frequency-dispersive** (Figure 2.12c, centre). At the monopolar eigenfrequency $\bar{k}$ reaches zero and turns negative on the higher-frequency side of this mode.

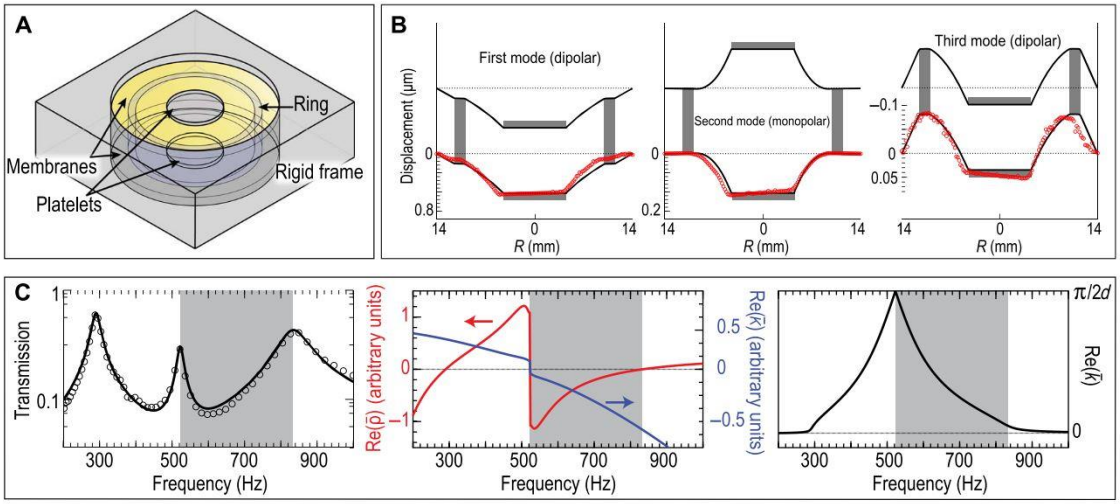

Figure 2.12 Coupled membranes giving rise to both mass and modulus dispersions. [84,100,101]

For our purpose of designing an origami metamaterial device within a window system to allow the natural air to flow and at the same time filter the acoustic wave propagation, it could be useful considering also the acoustic superlens strategy.

By following the optical metamaterial examples, a fundamental technique that creates perfect imaging known as "superlens" [61] emerged in the '70s from the electromagnetic waves research. According to this method, negative permittivity and permeability (meaning a negative index) material

could have several advantages over standard materials. If a negative index material is coupled with a standard material, it can be easily observed through Snell's law that an oblique incident wave on the side of the standard one, inside the negative index material, bends to the same side of the surface normal as the incident wave. It follows that this "negative refraction" may cause a reconvergence of diverging waves, generating two foci (hot spots) if a point source illuminates the flat slab of the negative index material: one focus inside the slab and another one on the other side of it [107]. This is presented schematically in Figure 2.13a (top). Zhang et al. [108] reported the first acoustic demonstration of negative refraction. Their study built a metamaterial interface through which a change from positive to negative was observed in the effective index. A focus (hot spot) was observed when a source was placed on one side of the interface.

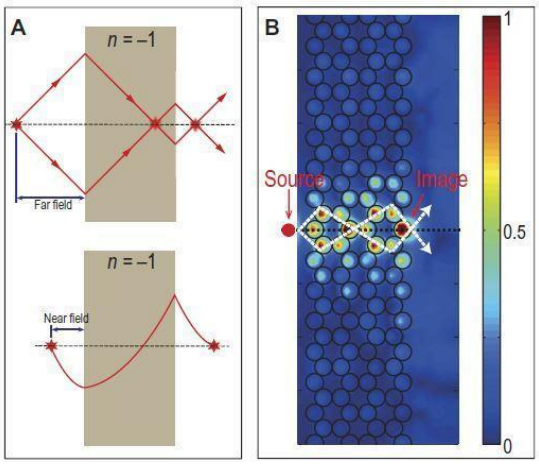

Figure 2.13 Acoustic realizations of superlens and hyperlens. [84,109]

Moreover, Ma and Sheng stress that when two eigenstates with the same eigenfrequency are coupled, they would show anticrossing and lead to two modes with opposite symmetries and different resonant frequencies [84]. Kaina et al., for example, developed two-dimensional lattices including in a unit cell a two coupled resonators dimer (Figure 2.13)[109], using resonators with Helmholtz-like cavities, which are known to have negative $\overline{k}$ values due to the related monopolar modes generation [110]. The coupled system is tunable by the resonators distance variation or eigenfrequencies mismatch introduction. Through this techniques, is indeed possible to tune consistently the dipolar modes' frequency and intensity, resulting in two resonators out of phase.

Another example of remarkable Snell's law application is provided by Xie et al. [111]. They use a 'driven' surface wave presented for the first time by Sun et al. [112] and design a metasurface based on a sequence of tapered labyrinthine metamaterials to convert efficiently free field propagating surface waves. Differently from propagating surface waves, the field of the 'Driven' surface wave remains localized to the incident field region. Through physic simulation, they demonstrated efficiently how

the structure (Figure 2.14) could represent a phononic crystal characterised by a lattice element made of inhomogeneous and dispersive metamaterial unit cells. In the one-dimensional case, isofrequency surface analysis can be used to predict the incident wave's diffractive properties. In our case, the origami system that could be investigated will not probably focus on diffraction or redirection but will be designed to filter the outdoor acoustic wave propagation with the indoor users' needs.

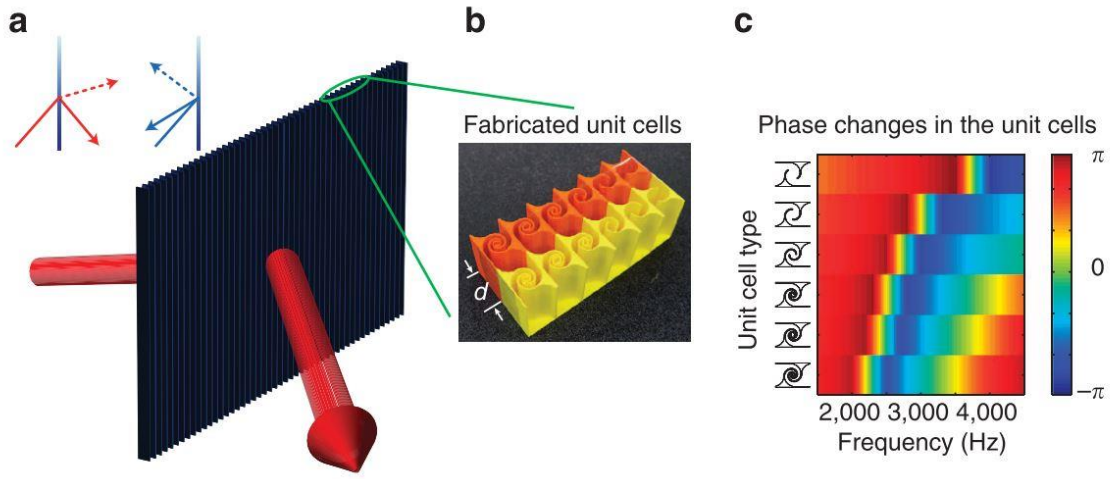

Figure 2.14 Wavefront modulating thin planar metasurface and its constituting elements. [111]

Liang and Li [113] have researched another way to solve the minimum space maximum sound absorbance. By aiming at large phase delays within a small space, they developed a complex, labyrinthine AMM with deep subwavelength cross-sectional passages. In this design, known as dubbed "space-coiling", the sound waves are essentially forced to propagate through channels that are much longer than their external dimension. Figure 2.15 shows this design where a large phase delay $D\varphi = k_0 L$ is caused by the coiled-up passage, where k_0 is the wavenumber through the background fluid, and L is the soundwave path. These structures are well known to be applied in bass woofers (also known as folded-horn speakers) [114]. So it is possible to tune the apparent phase and group velocity through the passage total length and, therefore, characterise the effective index and the dispersion relation accordingly. Recently, Cheng et al. developed a cylindrical unit cell with fan-shaped space-coiling segments [115], where the air passage generated a high effective index of the unit cell. Hence distinct angular momenta with multiple Mie-like resonances were allowed showing the feasibility of single negativity in $\bar{\rho}$ and $\bar{k}$. More practically, the strong resonant features of the AMM allowed a large scattering cross-section, generating high reflection independently from the random units position.

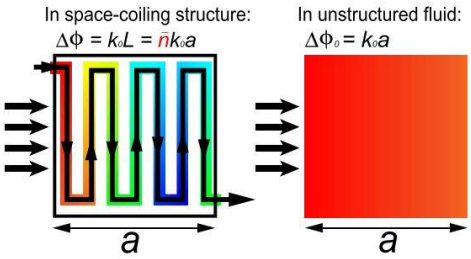

Figure 2.15 Space-coiling and acoustic metasurfaces. An example of the space-coiling structure and the relevant sound pressure field inside [113].

For all the acoustic resonators applications previously cited, sound absorption is fundamental and, due to noise exposure related health issues, is of high concern [116]. In these scenarios, lightweight, thin absorbers are strongly recommended due to their easy installation and wide frequency sound absorption, especially when a building needs to be distinctive for its architectural and energetic performance quality.

Indeed, in these cases, the main challenge is the materials innovation to improve the architectural impact and sound absorption, especially broadband, and many are the solution designed so far for this purpose [98]. For audible frequencies above 1 kHz to achieve this aim, it is preferable to use porous materials as thin as 10 cm [117]. When thin porous materials are inefficient, for example, in the presence of audible frequency below 1kHz (low-frequency regime, typically the most irritating noise), it is possible to use thin and low frequency absorbing materials made by sub-wavelength based structures. For example, it is possible to use Helmholtz resonator panels [118], a combination of Schroeder diffusers and perforated plates[90], perforated plates combined with tunable cavities [119] or Helmholtz resonators [120], sonic crystals slabs with resonant scatterers [82,121] or periodic groove structures [122] rather than using micro-perforations [123] instead of porous materials [124,125] or slow sound structures [126]. The general procedure is to design the unit cells in such a way as to overlap the frequencies of the resonant modes with respective absorption peaks close to 1.

2.2.2 Periodic lattices: auxetic and chiral metamaterials

The tessellation of a unit cell including beams or bars determines a reticulated cellular structure material called lattice [127] with multiple uses in the field of Engineering (for example sandwich beams, panels, and space trusses) [128]. The static and dynamic responses of such materials is determined by their geometric periodicity. There is comprehensive documentation on the elastic properties of 2D lattice materials and their relative density-dependence [127,129,130]. Lately, researchers have also studied the static elastic buckling and yielding phenomena of lattice materials [131], trying to understand as much as possible about their wave propagation behaviour.

To review the auxetic and chiral metamaterial concept, it is fundamental to introduce another factor: the Poisson's ratio. This is defined as the ratio of transverse strain to axial strain, $\nu = \delta_{\varepsilon\text{trans}}/\delta_{\varepsilon\text{axial}}$, and its effect is the phenomenon in which the material tends to expand in the perpendicular directions of the compression or compress in the perpendicular direction of the stretching. For example, the ν of a stable, isotropic, linear elastic material can variate between -1.0 and 0.5 due to the fact that Shear, Bulk, and Young's modulus must have positive values [132]. Specifically, the last one is used to calculate the dimension of a bar made of isotropic elastic material under tensile and compressive loads or to predict the deflection, which in a statically determinate beam can occur when a load is applied in a point in between the two beam's supports. Going back to the Poisson's ratio in the linear elastic regime, most materials are characterised by ν ranging between 0.0 and 0.5, where for example, materials like cork can have a ν of 0.0 (very little lateral compression when compressed), steel and rigid polymers can have a ν of 0.3 before yielding [132]. In contrast, after yielding, especially at constant velocity (v) as it happens to the rubber, they get a ν closer to 0.5 [132].

Materials such as polymer foams and origami are addressed as auxetic when they have negative ν. The term auxetic comes from the ancient Greek αὐξητικός (auxetikòs), which means "that which tends to increase" from the word αὔξησις (auxesis), which means increase. This term was coined by professor Ken Evans of the University of Exeter in an article in Nature in 1991 [133], and a representative schematic can be found in Figure 2.16. When stretched, auxetic materials become thicker perpendicularly to the direction of the applied force. This happens due to their particular internal structure and the way it deforms when the sample is loaded along the uniaxial direction.

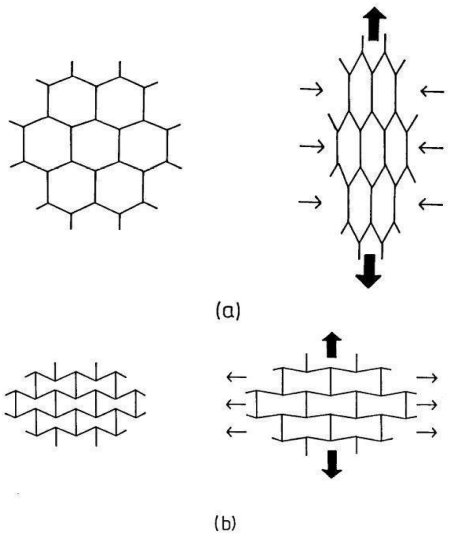

Figure 2.16 (a) A schematic diagram of a conventional hexagonal structure and how it deforms when stretched, producing a conventional positive Poisson's ratio. (b) A re-entrant honeycomb producing a negative Poisson's ratio [133].

Auxetic materials are characterised by mechanical properties such as high energy absorption and fracture resistance, useful to be applied, such as bullet/armour body, packing materials, knee and elbows pads, robust shock-absorbing materials, and sponge mops.

Lees et al. found that the first natural auxetic material was skin, several types that possess a negative Poisson's ratio, such as cat or salamander skin [134]. Since then, many areas of study have been investigating how to reproduce the negative Poisson's ratio artificially, where structural engineering, focusing on researched artificial behaviours, created a wide range of new metamaterials going from the molecular scale application of crystallising systems or chemical reactions [135] to the larger scales applicative scope for energy and sound damping structures, aerospace filler foams, and biomedical implants [136].

Among all the known methods for realising auxetic metamaterials, chirality is one of the most diffused due to the related deformation properties of such structures [137]. As introduced in the previous subparagraph of this Chapter, chirality comes from the ancient Greek χειρ, which means hand, indicating that a system/molecule is distinguishable from its mirror image, so it cannot be superimposed onto it. Körner and Liebold-Ribeiro observed specific 2D quadratic chiral lattice structures (eigenmodes of the lattices) showing auxetic behaviour (with negative Poisson's ratio) and analysed it from the totality to the unit cell. By classifying these eigenmodes of basic cellular structures characterised by triangles, squares, hexagons or cubes, (with periodic boundary conditions), it is possible to derive a criterion to identify auxetic structures based on eigenmodes analysis of simple unit cells [137] (see Figure 2.17). So it is possible to recognise immediately from the geometry if a metamaterial can be auxetic or not. Specifically, their study aimed to investigate why some eigenmodes show auxetic behaviour and others do not.

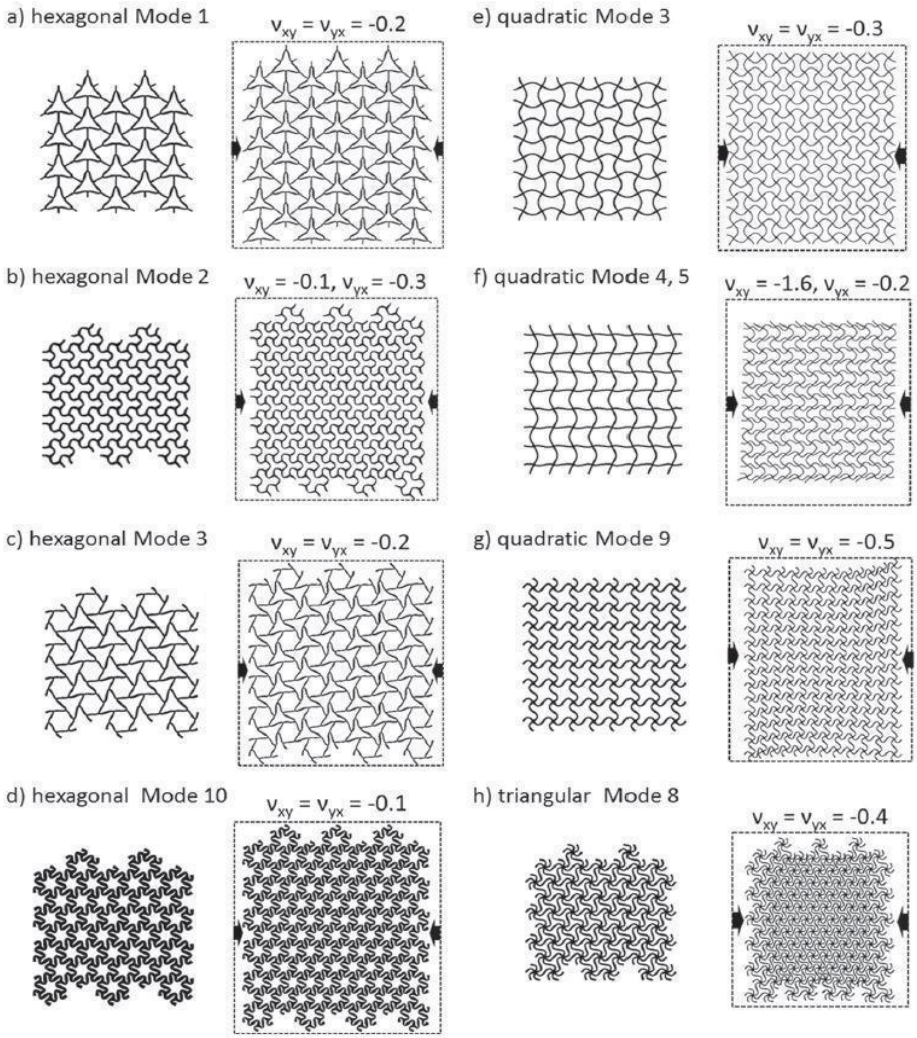

Figure 2.17 Periodic lattices that show auxetic behaviour [137].

Starting from the fundamental deformation mechanism of rotation for auxetic structures [138], it has been demonstrated that a systematic procedure can be obtained based on: 1) defining the simple unit cells as a space-filling unit cell, 2) analysing the unit cell's eigenmode with periodic boundary conditions, 3) identifying the eigenmodes with a high number of rotational centres expressing the symmetry of the lattice, and 4) assembling the eigenmode into a periodic lattice. Of course, as often happens for computer simulations and mathematical models, it is necessary to notice that the periodic boundary conditions (PBCs) give an approximation to a large (infinite) system by using a small part called a "unit cell", which is necessary to create an effective systematicity of the approach. It is demonstrated then that analysing basic structures' eigenmode and carefully selecting eigenmodes are effective to design auxetic materials [137].

As reported in the previous paragraph, the mechanism for auxetic behaviour is mainly identified as a simultaneous rotation of either nodal points or midpoints of struts, representing the lattice's symmetry for realizing full auxetic behaviour. Thus, for example, the rotation of cylindrical nodes and

the ligaments' bending characterises the deformation mechanism observed in auxetic chiral and anti-chiral honeycombs from Mousanezhad et al. [139] (see Figure 2.18). So, the structures contract in the transverse direction when subjected to uniaxial compressive loads [139]. This is the umpteenth demonstration due to which chirality is the only way to auxeticity, which we can find among the most studied topological features in natural structures [140,141] together with hierarchy [142–146], and the hierarchy of chirality [147,148].

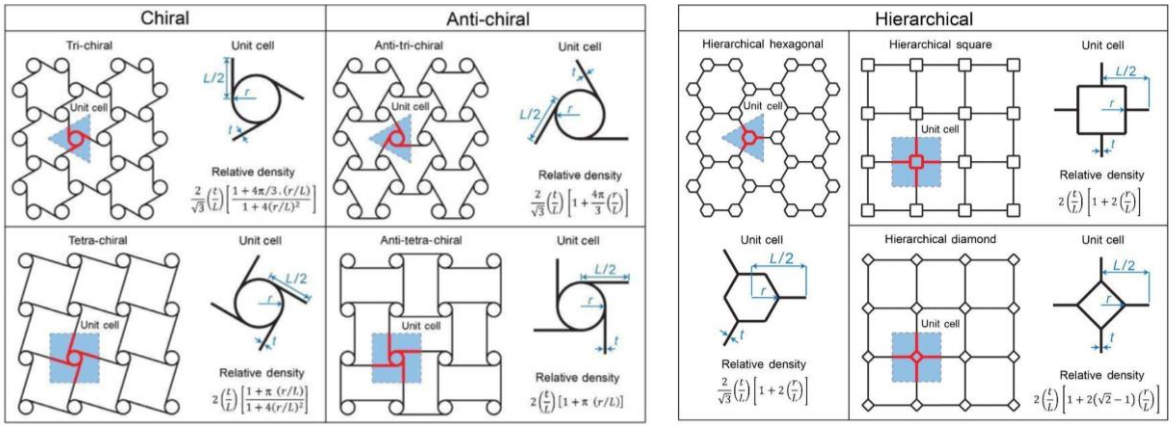

Figure 2.18 Schematic of the structure and the unit cell, and the expression of relative density for the chiral and anti-chiral honeycombs (left) and the hierarchical honeycombs studied by Mousanezhad et al. (right) [139].

From these topological indications, in recent years, several synthetic materials with ad hoc designed features have been proposed for novel applications such as dome-shaped panels [149,150] and high structural integrity foams [151]. Specifically, within honeycomb shape, it is overall known by experimental and numerical assessments that chiral honeycomb possesses a Poisson's ratio in the range of -1<ν< 0 [139]. Moreover, considering the enhancements in multiple parameters (introduced by Haghpanah et al.) allowing a tailored broad specific stiffness and strength thanks to the hexagonal lattice's higher orders of hierarchy [152], Mousanezhad et al. found that these structures' in-plane mechanical properties are affected by both chirality and hierarchy. However, considering similar values of hierarchy or chirality in separated structures (quantified by the *r/R* ratio), the first one determines higher stiffness and Poisson's ratio than the second.

Chiral networks are obtained by assembling circular elements (nodes) connected by ribs (ligaments) tangent to the nodes [153].

Table 2.2 Elastic constants of considered materials [153]

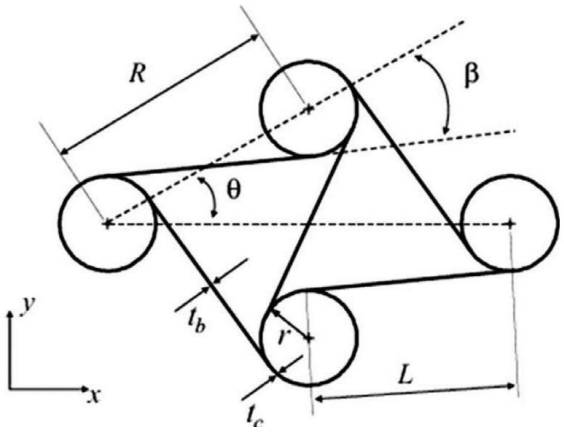

a.

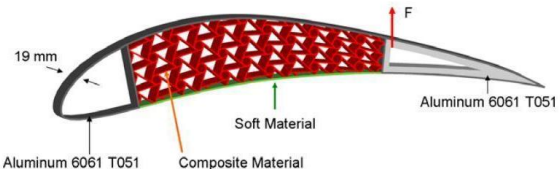

b.

Table 2

	Carbon-fiber CC90/ET443 SEAL	Aluminum Al 6061-T051
E_{xx}	56.6 GPa	68.9 GPa
E_{yy}	56.6 GPa	68.9 GPa
ν_{yx}	0.0514	0.333
G_{xy}	4.043 GPa	27.6 GPa
ε_{11max}	0.009	0.004

Figure 2.19 Chiral topology (a.), Chiral core airfoil (b.) [153]

R, L, β, t_b, and t_c, are the parameters defining the chiral geometry and represent respectively the distance between the node centres, the rib length, the angle between the imaginary line connecting the circles and a rib and the node and ligament wall thickness (Figure 2.19). The mathematical relationships between them are *tan β=2r/L, sin β=2r/R, and sin β= ½* [153]. Variation of *L/R* (*L/R = cos β*), here denoted as the ‘‘topology parameter”, alters the chiral geometry strongly and, in turn, in Bettini’s study significantly affects the mechanical behaviour of the truss-core airfoils. This kind of system, settled in a specific geometrical configuration, hexachiral honeycomb one, unlike other auxetic geometries, can tolerate transitional disorder considerably and possess the capability of retaining more or less the same Poisson’s ratio despite a disorder degree up to 90% [154]. This is a useful characteristic, especially considering the manufacturing processes.

2.2.3 Metasurfaces

Recently, an intense investigation has interested coiling up space due to the tuneable physical possibilities and multiple applications. In acoustics, waves can propagate within perforations of subwavelength dimension. Such perforation can be further coiled up, to allow the wave to propagate freely in the curled space [36]. Following the Helmholtz resonator principle, a significant innovation has been done in recent years by using perforated systems to be applied to the coiling concept and reducing the system's thickness. These systems are called metasurfaces, representing absorbers realised by coupling a perforated plate and a coiled coplanar air chamber [83,155]. Based on this method, the designed metasurfaces proved significant acoustic properties, such as high refractive index, double negativity, and near-zero index, while shrinking bulky structures into a deep subwavelength scale (which is a significantly relevant feature).

As Li and Assouar [155] have highlighted, acoustic absorbing systems are regarded as artificial boundaries characterised by normalized acoustic specific impedance $z_s = x_s + iy_s$. Here, x_s and $y_s$are respectively the acoustic special resistance and reactance normalized to the impedance of air $z_a = \rho_0 c_0 / S$ *with* ρ_0 and c_0 related to air mass density and sound speed, and S as the cross-section area of the unit cell (incident side). The absorption coefficient for this effective boundary is expressed by Li and Assouar as

$$\alpha = \frac{4x_s}{(1+x_s)^2 + (y_s)^2} \qquad 2.8$$

Moreover, Li and Assouar [155] suppose in their study that an incident acoustic wave propagating through the z-direction (Figure 2.20a) impacts the perforated system with periodic holes (period a) (Figure 2.20a) and then passes through the holes (diameter *d* and thickness *t*) towards the back cavity (length *l*) characterised by an hard boundary. At this point, thanks to the energy dissipation, a high sound energy absorption would result in the resonant frequency range. This dissipation is generated by the viscous friction on the wall of the perforated holes. This is due to the comparable since its geometrical size to the thickness of the viscous boundary layer, $d_v = \sqrt{2\mu/\rho_0\omega}$ with ω and μ referring to angular frequency and the coefficient of dynamic viscosity.

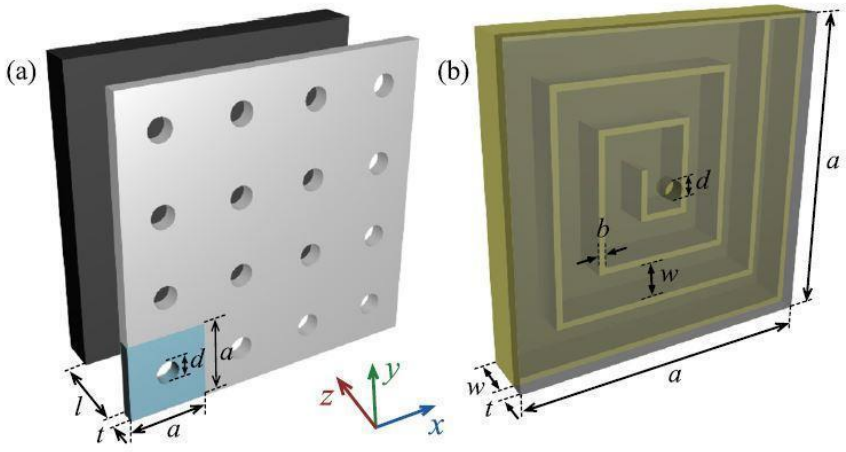

Figure 2.20 Acoustic metasurface-based perfect absorber with deep subwavelength thickness presented by Li and Assouar [155].

The results seem remarkable since, in some cases, the metasurface-based structures can totally absorb the incident acoustic energy at an extremely low-frequency range around 125 Hz [155], demonstrating that an effective absorption can be reached by, for example, the combination of perforated plates and coiled coplanar air chambers.

2.2.4 Origami metamaterials

Origami is a geometric folding technique well known for its artistic origin. The name comes from the Japanese 折り紙 (origami), which is made by the words ori (folding) and kami (paper). Through time, this art stepped from geometric folding algorithms and computational geometry to mathematical origami. Nowadays, scientific fields like architecture, physics, building and mechanical engineering have borrowed this artistic knowledge to apply it for their own purposes. The outcome has been a variety of different origami metamaterial solutions [141], especially in mechanical engineering the interest increased in studying and developing the different parts relative motion: orimetrics, rigid origami, action origami, kinematic origami, kirigami, with several applications such as folding\morphing structures, micro-electro-mechanical systems, etc. It is important to briefly report that the main origami techniques in the contemporary scenarios have been developed together with other procedures such as the 'snapology' one [142]. For the moment, the author will limit to describe it as a modular origami technique that has recently inspired the design of highly reconfigurable three-dimensional metamaterials assembled from extruded polyhedral.

The first attempt of effective origami metamaterial solution was developed using the folding system invented by the Japanese astrophysicist Koryo Miura and called 'Miura-ori'. This is a rigid origami fold, which means that it can be carried out by a continuous motion in which, at every step, all parallelograms are completely flat. This property allows it to be used to fold surfaces made of rigid materials from 3D spatial configurations to completely flat configurations changing the directivity of the system. For example, any electromechanical acoustic transducer , whether serving as a microphone or loudspeaker, is characterised by a specific directivity, exhibiting a sensitivity which varies spatially according to the radiation or reception of the sound wave. This property is critically affected by the transducer shape and acoustic wave frequency and, used in Miura-ori technique and combined with kinetic folding, gives the birth to a great versatility of material in functions and properties.

So origami reconfigurability is a fundamental characteristic that makes such technique attractive to design completely new acoustic devices, even if, relating to the Miura-ori and the star-shaped origami, this principle has been applied only on few examples. These include reversibly controlling the wave energy focusing by reconfigurable acoustic arrays design [156,157], redirecting the acoustic transmission and radiation pattern through reconfigurable origami waveguides made by three-dimensional tubes network [158], or guiding the reconfiguration of the associated arrays of inclusion via folding [159,160]. However, these previous examples highlight that the technology has been mainly used in middle-big scale applications, especially in terms of sound barriers. Hence, in this

research, suitable characteristics found in the Origami Metamaterials Literature Review will be investigated to understand if they are deployable in a new origami metamaterial system and filter the sound wave from the outside context according to the indoor needs, applying such device in windows technology.

USEFUL DEFINITIONS

To describe a more accurate origami metamaterials review, it is necessary to introduce some definitions presented by Turner et al. [161]:

- *Crease*, is a line (geometry) or mark made by folding or doubling any pliable substance, either convex (mountain) or concave (valley), and the collective of the creases is called *crease pattern*;
- *Vertex*, is where two or more creases intersect, and its *degree* is determined by the number of the creases emanating from it;
- *Folded state*, is the material configuration after one or more folding motions;
- *Pleat*, is a folding system that creates a relatively close and continual mountain-valley, and its reverse fold (valley-mountain) is called *crimp* (see Figure 2.21).

Regarding the material used for origami purposes, the choice of this component is clearly crucial. The bending capacity of the material in such a way that all the folded pieces are located and behave in an expected way is going to be at the base of our research to design an origami metamaterial allocated within the window frame and able to allow the natural air flowing, but mitigating/filtering the acoustic wave propagation. According to Turner et al., having a folding system that divides the shut-in triangular sections to build then the polyhedral 3D structures is the best folding path for engineering purposes since it is the one that covers each triangle only once, minimizing the overlap [161]. Hamiltonian refinements and Huzita-Hatori axioms are the most popular way to guarantee this, as the first one is the procedure with which it is possible to draw an ideal line that connects all the midpoints of each triangle (spanning tree), while the second defines rules for paper folds specifying the role of each of them through lines and points [161]. In particular, the axioms state that:

a. Given two points p1 and p2, a line connecting them can be folded;
b. Given two points p1 and p2, p1 can be folded onto p2;
c. Given two lines l1 and l2, l1 can be folded onto ‘2;
d. Given a point p1 and a line l1, a fold perpendicular to l1 can be made passing through the point p1;
e. Given two points, p1 and p2 and a line l1, a fold that places p1 onto l1 can be made passing through p2;

f. Given two points, p1 and p2 and two lines l1 and l2, a fold that places p1 onto l1 while placing p2 onto l2 can be made;
g. Given a point p1 and two lines l1 and l2, a fold perpendicular to l2 placing p1 onto l1 can be made.

These steps provide the basis of mathematical origami describing simple folds.

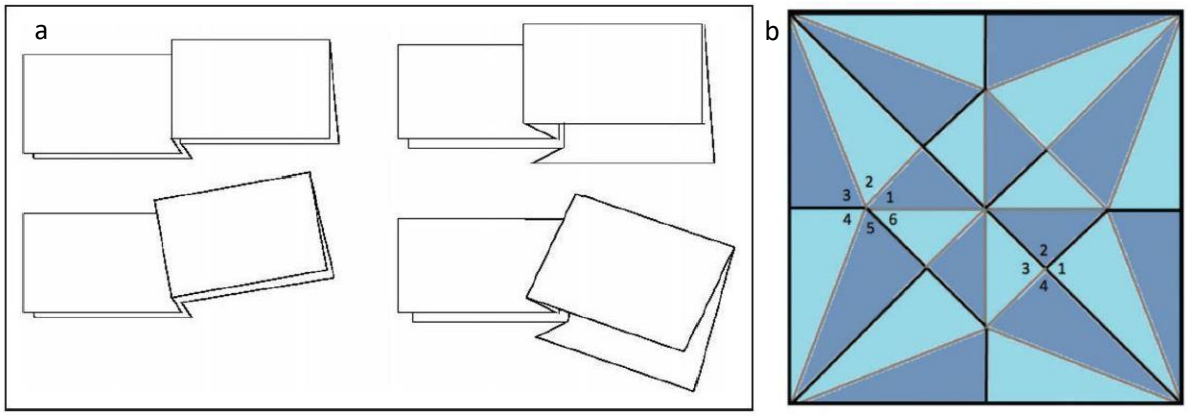

Figure 2.21 schematics of a) left: pleat folds and right: crimp folds [161], and b) flat-folding crease pattern (mountain and valley creases are black and grey respectively) [161].

Another important concept to understand origami design is the flat foldability, due to which for a flat piece of paper, there are n angles forming each vertex that all together compose the crease pattern and that the sum of these n angles must be equal to 360^{o}.

To realize a flat foldable origami configuration with a single vertex, the conditions to be satisfied are three, and they are mainly defined by the Kawasaki's and Maekawa's theorems, with a further generalisation of these made by Hull in order to globally investigate the foldability [162]:

a. According to Kawasaki's theorem, if numbering the angles in sequence, then the sum of the odd angles and even angles must be the same. From the labelled creases in Figure 2.21 this concept results clearly, as the sum of the angles 1,3, and 5 and one of the angles 2, 4, and 6 are equal to 180^{o}.
b. According to Maekawa's theorem, the number of mountains and valleys must differ by ±2. This is evident again from Figure 2.21, where in the crease pattern, mountains are coloured in black and valleys in grey.
c. Maekawa's theorem is satisfied only if the creases degree n is even so that for a complete multiple vertices origami design, each panel in the crease pattern must be colourable with only one of two colours without having the same coloured panel touching any of its borders. So this is another fundamental condition to obtain the foldability of multi-vertex designs together with each individual vertex satisfying the previous criteria.

INDICATIONS TO BUILD THE FOLDING PATTERNS DESIGN

The folding patterns of an origami model are generally designed by using the *tree method* to dictate a 3D structure. This helps to define the folding pattern starting from a uniaxial base and then projecting the crease structure in 2D as a shadow tree. Nowadays, the most common way to apply the tree method is using software like *tree maker* [163], which generates crease patterns to get a uniaxial base folded.

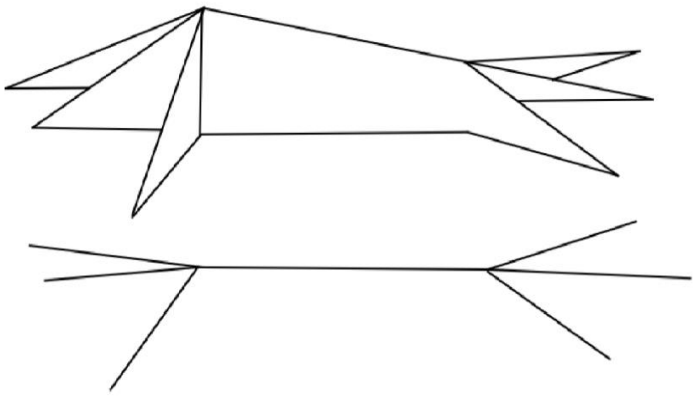

Figure 2.22 Top: uniaxial base. Bottom: corresponding shadow tree [161]

Observing Figure 2.22 from Turner et al. [161] and considering the represented animal folding model with the base consisting of a six limbs body (one head, one tail, and four legs), assuming that p_i and p_j are two points on the uniaxial base, and s_i and s_j are their projection on the shadow tree after the folding, to generate the crease pattern from the smallest piece of paper the condition $d_{pi\,pj} \geq d_{si\,sj}$ must be respected [161]. In this case, it is important to highlight that the shadow path is defined as *active* if s_i and s_j lie on the end of the limb so only one point in the paper represents the leaf on the shadow tree, so s_i and s_j are leaves, and $d_{pi\,pj=}\, d_{si\,sj}$. This definition is useful to understand how to fit the uniaxial base into a sheet of a specific dimension, and considering a scale factor λ so that $d_{pi\,pj} \geq \lambda d_{si\,sj}$, the scale optimization steps for the tree maker algorithm are: 1) maximizing λ; 2) driving the shadow path to become an active path (s_i and s_j are leaves and $d_{pi\,pj=}\, d_{si\,sj}$); 3) using the disk packing method to draw circles to design an efficient uniaxial base folding pattern; these circles must have diameters equal to the length of the limb on the base (for the folded state) and centred on the leaf edges, and define the maximum distance that can be possibly reached after folding from the point at its centre [161]. Nevertheless, from these steps, the more the shadow tree is shrinking, the highest is the uniaxial base.

Another important step for using origami techniques applied to metamaterials is to have a clear scheme of how each part is connected with the others. To understand how such linkages work in origami engineering, Turner et al. [161] recommend to have cleared the concepts of rigidity, linkage

configuration, and space, locked linkages (mathematically defined as those which have disconnected configurations space), chains and trees, unlocked configurations, and slender adornments:

- *Chain,* is a group of edges presenting one vertex and at least one other edge connected to it at each endpoint.
- *Tree,* is a group of edges presenting edges branches that end without reconnecting back into the inner group. It is not possible to lock 2D chains, differently from trees, and, on the other hand, it is possible to lock all 3D chains and trees [164].
- *Unlocked configuration,* is the one that can be folded into any other configuration.
- *Slender adornments*, are thicknesses or polygons formed arbitrarily and attached to links in a chain or tree-like configuration.

According to Turner et al. [161], it is also possible to use the glueing if the terminal parts of the unfolded future solid polygon are matching: this involves matching boundaries equal-length subsections of a 2D polygonal shape with one another to generate a polyhedron in 3D when connected or glued.

Folding and one cut is another technique due to which it is possible to realize a 2D shape by just folding a piece of paper and cutting it once (5 pointed star example, see Figure 2.23). It is demonstrated that through this method, any planar graph (or only straight lines based shapes) can be produced, even though it could happen that some of them would generate an impractical creases number to be achieved [165]. A method that is generally used to design origami is the “fold and one cut”, of which the foundation of the generative algorithm is explained in the Huzita-Hatori axioms [161] and consists of over positioning the overall final figure edges in one line and then cut there.

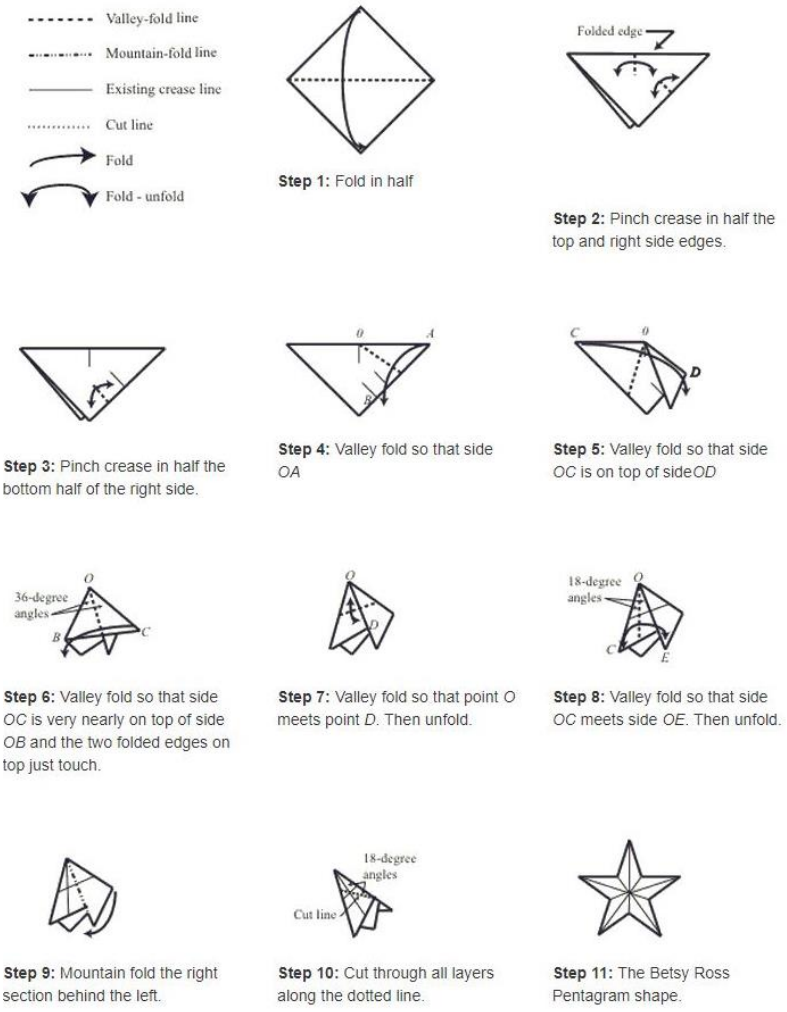

Figure 2.23 Folded and one cut 5 pointed star, produced by ten cuts on a folded square piece of paper It [166].

The most common rigid-foldable crease patterns described by Turner et al. [161] are:

- Waterbomb base (smart materials);
- Miura-ori pattern, with negative Poisson's ratio, parallelogram based structure, or trapezoids (that can achieve concave or convex structures). Both Waterbomb base and Miura-ori pattern can expand and contract in all directions;
- Yashimura pattern unfolds in a translational motion;
- Diagonal pattern unfolds in a rotary motion.

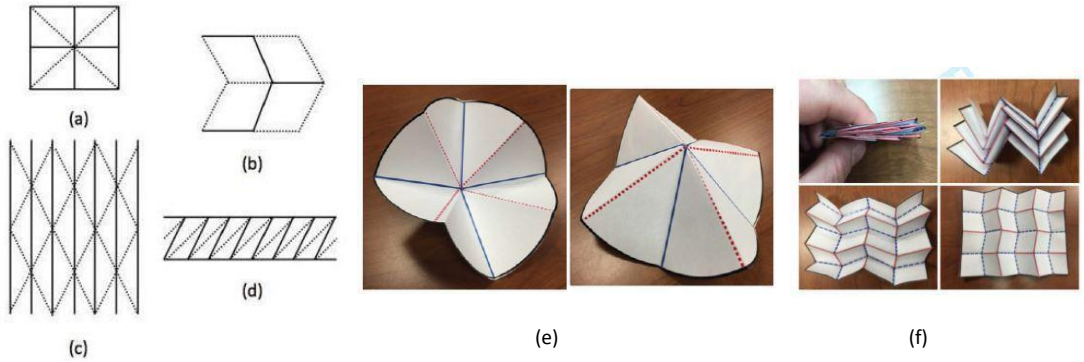

Figure 2.24 Common origami crease patterns (mountain and valley folds are indicated by dashed and solid lines), respectively (a,e) waterbomb base folding lines and in two stable equilibrium positions, (b,f) Miura-ori pattern, (c) Yoshimura pattern, and (d) diagonal pattern [161].

POSSIBLE APPLICATIONS

To apply origami engineering, Turner et al. [161] highlight the importance of taking into consideration a couple of simplifications applicable when using paper models:

a. Paper is flexible, and it is usefully described by the product of the maximum and the minimum curvature at any one point on a 3D surface (Gaussian curvature), which is negative for saddles, positive for convex cones, and zero surfaces which are intrinsically flat but never changes during folding. This consistently results in a form with zero local minimum curvature at every point;
b. Finite thickness of the real material, which is a major challenge from theoretical origami to engineering (see Figure 2.25). Moreover, materials less flexible than paper are generally used in engineering applications, so they are approximated as rigid.

The proposed solutions so far have regarded the adjustment to the hinges or creases. Folding edges can always be hinged together if positioned in valley creases. Using symmetry at each vertex is also possible to achieve workable designs (where there can be only a limited fold line at one vertex). Moreover, in the last case, if needed, trimming the volume of the edges on the valley side might be useful to increase the mobility facility (see Figure 2.24). This procedure might be helpful in case of relative thick soundproofing panels used to build the origami, even in our research study for the origami metamaterial to be placed within the window frame to allow the natural air flowing and filtering/absorbing selectively at the same time the acoustic wave propagation.

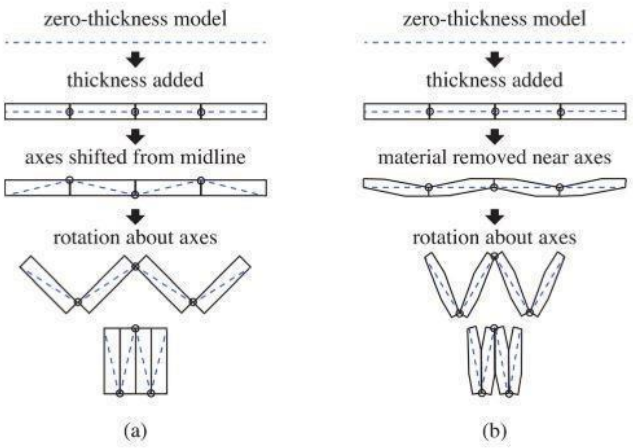

Figure 2.25 Two approaches for enabling origami with thickness, from Tach [167]: (a) Shifting rotation axis for the fold from the midline of the material to the material surface; (b) Removing the material near the fold line.

Other uses for origami techniques are, for example, packaging (like shopping bags or shipping containers/boxes), optigami (that can reflect light many times like mirrors creating high resolution, large aperture cameras with reduced thickness), space or biomedical devices, other storage applications (like cars airbag, lithium-ion batteries, flexible displays, stretchable circuits).

DEVELOPING THE MANUFACTURING

Those kinds of origami metamaterials that present a final folding system motion from their folded and/or unfolded state are called action origami, and they are separated from those that generally fold and unfold into static states. They can be *industrial origami* or *self-folding* and *self-assembly origami* [168]. In this second case, the printed circuits (PC) build a Micro-Electro-Mechanical-System (MEMS) where mesoscale structures fold due to lasers and magnetic fields [169] and Printed Circuit Board (PCB) are made by self-folding sheets of programmable matter actuated by shape memory alloys [170–172]. Moreover, lamination techniques generated by following PCB have shown several merits over standard fabrication processes for MEMS devices (for example, RF Switches) [173]. Another useful practice is designing single-use shaped memory polymers foldable towards the final structure design by absorbing light and heating through different coloured parts [174,175]. Finally, for origami-based stent-grafts, the Brounian motion simulation has been developed with significant results from the medical field [136,176].

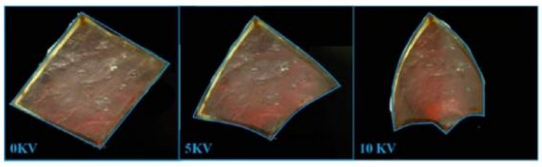

Figure 2.26 Dielectric elastomer folding actuator with a silver electrode and with VHB4095 as a substrate (a) at 0 KV DC, (b) at 5 KV DC and (c) at 10 KV DC [177].

Other *action origami* can be identified in the electrical devices made by origami metamaterials. They are low modulus electroactive polymers called Dielectric Elastomers (DEs) and prooved favourable physical foldable characteristics for the origami structures actuation [177] (see Figure 2.26). DEs generate mechanical motion of lightweight polymer after being electrically stimulated (causing then a Maxwell stress [178]). Moreover, as stressed by Turner et al. [161], DEs are characterised by high specific elastic energy density, wide strain response, fast response time, and high actuation stress and electromechanical coupling efficiency [179,180]. Finally, other *action origami* applications are used to exploit robotics for origami, specific mechanisms and pop-up mechanism for origami metamaterials.

POSSIBLE STRUCTURES

Depending on the purpose of the origami metamaterial design, there are many variations in terms of shape and structure. The advantages for the architectural applications, for example, are many: (a) a watertight continuous surface that gives much envelope freedom, (b) a purely geometric mechanism scale-independent since it is not reliable on the material elasticity and is not significantly affected by gravity, and (c) a smaller number of degrees of freedom, which controls the origami folding to the final configuration and enables semi-automatic deployment [181]. To analyse this kind of origami kinematics is possible to use both the unstable truss model and the rotational hinges model. Different existing examples of deployable structures are realised as cylindrical shells (which collapses under a torsional force/loading into a 2D plane, see Figure 2.27a) or as deployable membranes inspired by tree leaves (see Figure 2.27b). These natural structures indeed have biologically evolved using flexibility and rigidity in such a balance. Thanks to these folding characteristics, wind dragging damages are significantly reduced and the weight of the structure and occasional other loads can be supported simultaneously. The leaves veins and midribs link or support the flexible membrane panels and act as a stiffening member. This biological engineering system composed of tree leaves has been carried out in relation to the Miura-ori pattern [182].

Figure 2.27 Left: Foldable cylinder based on twist buckling. Right: Leaf patterns. Left: leaf-out. Right: leaf-in [161].

The energy absorption structures are another type of application for the origami metamaterial [183]. Compliant mechanisms origami-based can contribute to energy absorption and impact force distribution systems. Miura-ori design can also be efficiently applied in this case to use crushing or plastic deformation of its shape to achieve energy dissipation in static load conditions (dynamic load conditions have not yet been analysed significantly) [183]. The main reason is coupling one degree of freedom with a negative Poisson's ratio. These structural properties, in particular, might be useful for the object of our research to include an origami metamaterial system in a window frame, where of course, structural issues may be relevant. Moreover, a combination of honeycomb structures and kirigami can create sandwich structures that help avoid the humidity accumulation problem caused by a lack of ventilation and a positive Poisson ratio. As highlighted by Turner et al. [161], Kirigami has inspired an auxetic honeycomb core with higher density and averaged properties such as compressive modulus and strength [168].

Above all, the other additional applications for origami metamaterials based structures of particular interest to the acoustics field are the tuneable metamaterials. In this field, origami can be used, for example, to generate a range of resonance frequencies by adjusting the distance between each folded surface split-ring resonator [184].

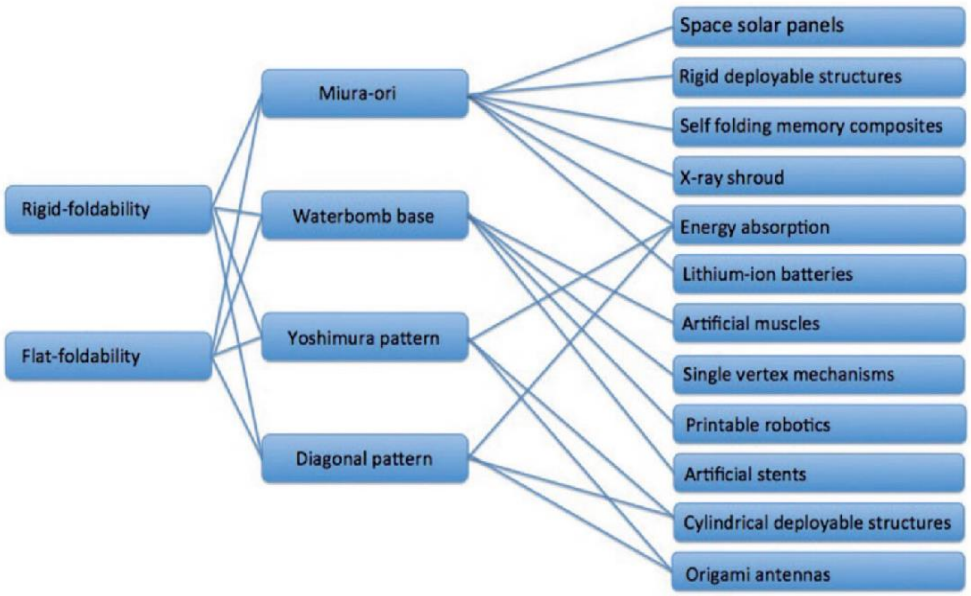

Figure 2.28 Relationship among fold properties, fold types and applications [161].

ORIGAMI-BASED DESIGN PROCEDURES

As depicted in Figure 2.28, there are several ways to go from the design stage to the realized origami metamaterial device. Four properties are useful to be considered to understand how to convert a folding pattern in a functional engineering system [161]:

a. Rigid-foldability is the property that allows the crease pattern to have more joints in the system, so more degrees of freedom, by either additional second crease to the original pattern, or a boundary material removal;
b. The surface must be uninterruptedly continuous, but in case there are no constraints regarding it, perforations can be used as well;
c. Strain energy is stored elastically in the creases and has some design constraints as different amounts of strain energy storage are desirable. This is necessary to improve the hinge behaviour and improve the strain energy storage for which materials like polymers and metals are preferable. Regarding this property, composites and sandwich membranes have been used [170], but probably for our research purpose, a monolithic material would be more suitable;
d. The manufacturing method is the last step after the material choice and, for a more flexible crease pattern design, the most common practice is to use a Computer Numeric Controlled (CNC) Method. CNC methods have been thoroughly discussed by researchers of this field [185], mentioning, for example, laser-cut, abrasive water jet-cut, plasma-cut, incremental sheet forming, and nibbling methods. In addition, various methods could be used to fold the final product, including robotic automated folding, using a robotics approach [186].

Apart from the techniques explained so far, Kinetogami is another origami building procedure, evolving from the kirigami combined with folded hinges along with Basic Structural Units (BSUs). BSUs are 3D empty volume structural polyhedral joints. Even though we are just naming this technique, that will not be further discussed; as for our origami metamaterial model, only layers folded in 2D and 3D minimal configurations will be used.

To simplify the designing and make the manufacturing process as efficient as several possible software are available: 1) Matlab, with its suite of functions written for rigid origami structures (Miura-ori); 2) Tree maker, which generates crease for origami patterns; 3)Organizer, the generator of crease pattern to be folded; 4) Freeform origami, quite significant because allow the alteration of crease patterns including flat foldability and developability; 5) Rigid origami simulator, that for specific crease pattern can replicate rigid origami designs; 6) E-Origami System (EOS), that is preferable in artistic origami

design and can define both the crease pattern folding and the mathematical origami folding; 7) Mathematica, which simulate the operation of paper folding; 8) Cad programs such as Solidworks, that is customizable with more materials options (generally metal sheets). Turner et al. stress how fundamental it is for the researchers in this area to implement and improve the understanding of folding algorithms related to gradually more intricated 3D configurations. More efficient cost-effectiveness solutions need to be achieved through the improvement of the mechanical folding efficiency, improving the effectiveness of the folding by new crease pattern design from the existing ones and defining a more formal and methodological approach for origami engineering.

2.3 Numerical computational methods

In recent years, programming development has introduced new perfectioned techniques of physical simulation. The cost-effectiveness of the testing procedure can be improved significantly with a solid numerical provisional method. This is why, nowadays, numerical methods are so popular among Engineering companies and researchers. Moreover, while previously calculating models had to be set up meticulously through software like Matlab, today, the commercial software available allows anybody with basic physical analytical and mathematical knowledge to set up a numerical study.

There are several methods developed and used among the Engineers or Architects community. In this Subchapter, we will explain the fundamentals of the most common ones: Finite Element Method (FEM), Finite-Difference Method (FDM), and Boundary Element Method (BEM) (see Figure 2.29).

When using numerical computation methods to solve a complex problem, we need to follow these steps:

1. Create the geometry (actual structure of a component in reality);
2. Define the material properties (if required by the problem);
3. Define boundary conditions including input and output physics characterisation (in acoustics, this could be the input soundwave pressure level or the characterisation of the output diffusion field, or in computational fluid dynamics (CFD) is the input/output flow velocity, rate, or pressure);
4. Mesh the structure (numerical representation of the geometry interested by the study);
5. Run the numerical analysis by using a specific method (a most common technique for acoustics FEM and BEM is the Galerkin method while for CFD is Reynolds-averaged Navier–Stokes also called RANS);
6. Visualisation.

After developing a mathematical model (i.e. governing equations, boundary conditions, geometry), the involved equations need to be applied to the geometrical domain and/or boundaries following different **discretisation** procedures. Each numerical methods abovementioned have a different approach to discretising the geometry interested in the problem. FDM approaches it through the discretisation of the problem geometry into a number of steps, where the value of each discrete point is approximated through the solution of algebraic equations, which contain nearby points finite differences and values. FEM divides the domain of interest into a finite number of subdomains (called finite elements) and uses the variational concept to construct an approximation of the solution over the domain collection. BEM solve the problem by analysing the response on the boundaries instead of analysing the domain itself.

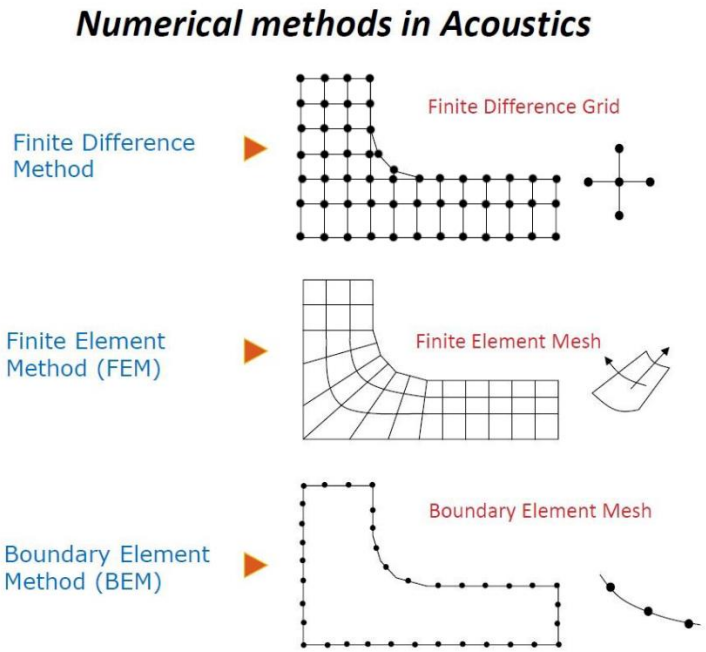

Figure 2.29 Schematics on the numerical methods generally used in acoustics. For FDM, the value of each discrete point is approximated through the solution of algebraic equations; FEM divides the domain of interest into a finite number of subdomains (called finite elements). BEM solve the problem by analysing the response on the boundaries instead of analysing the domain itself.

2.3.1 Finite Element Method

The Finite Element Method (FEM) is a numerical method used to find an approximate solution for complex problems by discretising the domain of interest into finite elements and approximating the solution over the domain collection using the variational concept. The origin of FEM are linked to research from applied Mathematics, Physics, and Engineering; however, significant development of FEM was made through Engineering research. The name was coined by R. W. Clough [187], and since

the 1960s, a great amount of research has concerned this technique which was initially developed on a physical basis for the analysis of problems in structural mechanics but was soon identified as applicable to the solution of many other kinds of problems.

Generally, in Physics, a mathematical model had to be selected to analyse a physical problem, so by solving the mathematical problem, the physical one was solved as well. This is achieved through a space discretization in 2 or 3 dimensions, implemented by creating a mesh of the object: a numerical domain for the solution with a finite number of points. The FEM formulation of a boundary value problem finally results in an algebraic equations system. The equations which define these finite elements are then included in a higher system of equations that models the whole problem. The FEM then approximates a solution by minimizing an associated error function by using variational methods from the calculus of variations [188].

FEM is used to solve highly complex mathematical models addressed on the main physical domain (rather than the boundaries) [188]. Geometrical domain reproduction can also be addressed through computer-aided design (CAD) within finite element analysis (FEA). BEM has been more popular for addressing acoustic-related problems, while FEM was preferred for structural vibration; However, recently FEM has been extensively used for acoustics and fluid dynamics studies [23,189,190] due to the topological potential of investigation. Through FEM, indeed, the physical analysis can be run at any point of the domain, either in stationary or non-stationary conditions and for this reason, FEM can increase the cost of the calculation.

At the base of the FEM method in acoustics, there is:

- the transformation of the original problem in an equivalent integral formulation (variable or weighted residues method). FEM can solve in straight forward way relatively complex problems, whereas the analytical solution is not readily available.
- the physical variables which must be accurately distributed within the domain (for example, the sound pressure in an acoustic FEM problem) and the geometry of the continuous medium, which must follow a specific shape function to define the most effective sub-domain (finite elements).

Generally, to obtain reliable results in a certain frequency range, it is necessary to divide the geometry using at least 6 (preferably 10) elements for every wavelength [188]. Overlooking every detail of numerical implementation, we can demonstrate that the non-homogeneous Helmholtz equation can be written again in terms of joint pressure as $([K_a] + j\omega[C_a] - \omega^2[M_a])\{p_i\} = \{F_a\}$ where $[K_a]$ is the acoustic stiffness matrix, $[M_a]$ is the acoustic mass matrix, $[C_a]$ is the acoustic damping matrix, and

$\{F_a\}$ is the external sources vector. The solution to this equation, setting some boundary conditions, let us determine the joints pressure from which it is possible to determine the acoustic pressure value in every point of the domain through the approximation $p(x,y,z) \approx [N]\{p_i\}$ where $[N]$ represents the shape functions set. For the computation of the resonance frequencies, it is proved that it is necessary to solve an equivalent system equation as $[K_a]\{\varphi_m\} = (2\pi f_m)^2[M_a]\{\varphi_m\}$ with $m = 1 \dots n_a$ and where f_m are the resonance frequencies and φ_m are the modal distributions at a certain resonance frequency [188]. In the end, is it possible to demonstrate that for the resolution of an acoustic problem like this, it is necessary to solve beforehand a more complex problem in which the FEM models are written for both the acoustic and structural case, and in which the fluid-structure interaction is assigned in terms of external strength. So $\left(\begin{bmatrix} K_s & K_c \\ 0 & K_a \end{bmatrix} + j\omega \begin{bmatrix} M_s & 0 \\ -\rho K_C^T & M_a \end{bmatrix}\right)\begin{Bmatrix} W_i \\ p_i \end{Bmatrix} = \begin{Bmatrix} F_s \\ F_a \end{Bmatrix}$ where K_s, M_s, and F_s are the stiffness matrix, mass and damping for the structural domain. The fluid pressure on the structure is proportional to the acoustic pressure (pressure continuity condition), and it appears as the connection matrix K_a, while the structure pressure that acts on the fluid is proportional to the acceleration (speed continuity condition), and it appears as a connection matrix $-\rho[K_c]^T$ [188]. Moreover, two key factors for the FEM prediction accuracy are 1) the number of elements and 2) the given shape functions' nature. Thus, the accuracy must improve along with the increase of the elements number to ensure convergence of the specific solution range towards the exact solution. The convergence is guaranteed when some conditions related to shape functions and weighting functions are satisfied. So another important aspect of FEM is the size of the mesh. This parameter follows different rules according to different physical problems. In acoustics, for example, the mesh size is determined according to the FEM criterion, where at least six nodes are used to simulate a wavelength in the air following the equation $c/6/F_{max}$ (so for a frequency range up to 5000 Hz, the maximum allowable element size is 343/6/5000 = 0.0114 m). For this reason, it is important to include a high number of room modes to cover a medium-high frequency range [188]. Indeed, element size for 3D FEM analysis can be very small, while number of degrees of freedom (n-DOF) is consequently high, causing excessively high computational costs, at the expenses of focus on AMM-based design and its optimisation; However, if the model results highly complex, but the results convergence is proved, mesh size simplification can be accepted. This method of mesh simplification has been already used in acoustics research field and validated by experimental measurements [59]. The FEM theory evaluates indeed comparisons between different meshes effectiveness by quantitatively estimating the convergence order of the FEM error on a sequence of progressively finer meshes obtained by uniform mesh refinement [191]. Systems such as the graphical user interface (GUI) of COMSOL can be used to determine the convergence of the results of the coarser minimum mesh

size, which allows to have a lower computational cost, while guaranteeing the convergence of the results [191].

2.3.1.1 Computational Fluid Dynamics method

In Computational Fluid Dynamics (CFD), the RANS method is commonly used in industry and for quicker and efficient approximation. RANS is moreover cheaper than other methods (such RANS-LES, LES, and DNS) and calculates and models larger turbulence scales; However, the Reynolds stresses it involves in the turbulence model in RANS add six additional unknowns to the system of equations while there remain four equations (essentially determining more unknowns than equations). For this reason, turbulence models are used to provide "closure" equations through which these additional unknowns are solved. Turbulence models are:

1. Spalart Allmaras (SA)
    - 1 equation, designed for Aerospace applications
2. K-ε
    - 2 equations, mostly used for internal flow, popular in the industry
3. K-ω
    - 2 equations, good for boundary layer predictions, poor performance in freestream flow
    - K-ω SST is a combination of k-ω and k-ε and is very popular in the industry
4. Reynolds Stress Model (RSM)
    - 2nd order model provides one equation for each Reynolds Stress
    - It is supposed to be superior to all others but very expensive to use

Another important parameter when considering CFD mesh problems is the turbulent boundary layer, which is necessary to model the behaviour of the CFD walls. A key parameter in this evaluation is y^+ which is the wall-normal coordinate normalized by the viscous length scale. This scale dominates the viscous sublayer region and hence is important in CFD (see Figure 2.30). To optimise the mesh calculation cost/effectiveness, most methods such as the K-ε allow defining a much coarser mesh where $y^+ > 5$ and a much finer mesh where $y^+ < 1$ (see Figure 2.30).

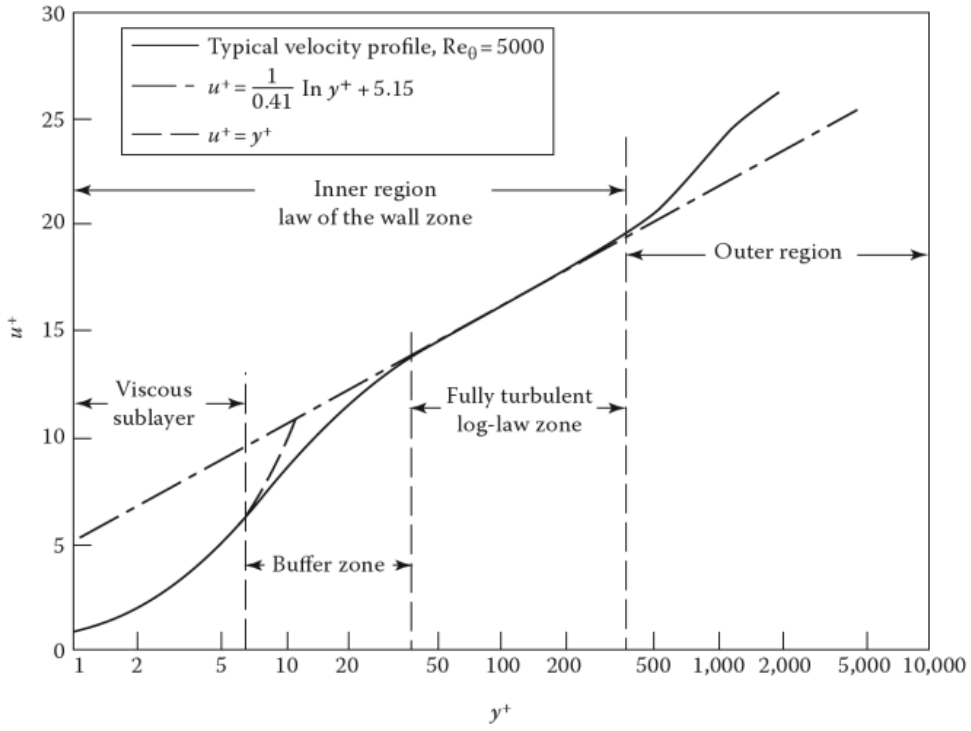

Figure 2.30 Schematics of turbulence boundary layer definition, according to the different velocity fields.

2.3.2 Finite-Difference Method

Finite-Difference Method (FDM) aims at solving differential equations by approximating derivatives with finite differences $\frac{\delta u}{\delta x}\Big|_{x_i} \approx \lim_{\Delta x \to 0} \frac{u(x_i+\Delta_x)-u(x_i)}{\Delta_x}$ or rate change of the function if there is a known function or a set of discrete data values from experiments. The spatial domain and, when it is applicable, the time interval are both discretised into a finite number of steps. Then the value at each discrete point is approximated through the solution of algebraic equations, which contain nearby points finite differences and values. FDM turns ordinary differential equations (ODE), also known as partial differential equations (PDE) and that could be nonlinear, into a linear equations system which can be solved through matrix algebraic techniques. An intuitive process to define the approximation is using the Taylor series expansion for $u_{j\pm1}$, and then to approximate geometrically by the improvement of the truncation error ($\mathcal{O}(\Delta x)$). This is possible through the application of the advection equation and the dissipation of the travelling signal (for acoustics) or flows (for CFD), expressed by the numerical artificial viscosity $\upsilon_S \equiv \frac{c\Delta x}{2} \sim \mathcal{O}(\Delta x)$ where *S* is the scheme of the derivative. *S* can be indeed either symmetrical or asymmetrical; however, in acoustic FDM, it is always better to use a symmetrical scheme to remove the complex part of the wavenumber *k*. Recently, these linear algebraic computations can be efficiently run by computers, leading to easier implementation of FDM in modern numerical analysis [192,193]. FDM is nowadays among the most popular approaches to PDE numerical

solution, together with FEM; however, it is less accurate than FEM and generally is used when the solution to a wider spatial range problem is required.

2.3.3 Boundary Element Method

The boundary element method (BEM) is used in fields including fluid mechanics and acoustics to solve linear PDEs formulated as integral equations (i.e. in boundary integral form) [123]. As depicted in Figure 2.31 BEM solves the problem by analysing the response on the boundaries instead of the domain itself (as for the previous two methods). So BEM is based on an integral equation over the boundary surface. Firstly the Helmholtz wave equation is considered $\nabla^2 p + k^2 p = 0$ and integration over the volume *V* is performed, followed by an integral equation over *V*. Through the Gauss theorem, the Helmholtz integral equation (HIE) can be performed over the surface of the geometry *S*: $C(P)p(P) = \int_S \left(p(Q)\frac{\delta G}{\delta n} + jk\rho c v_n(Q)G\right) dS$ where *P* and *Q* are points in space (HIE is fully dependent on these positions), *C* is a mathematical operator, *p* is the pressure, *G* is the Green Function which here is normalised over the direction *n*, and $jk\rho c v_n$ is the velocity boundary conditions (from Neumann). Afterwards, the surface geometry and the related variables are discretised and then a set of equations is solved to find the solution on the boundary and, secondly, the solution on the field points in the domain through another application of HIE.

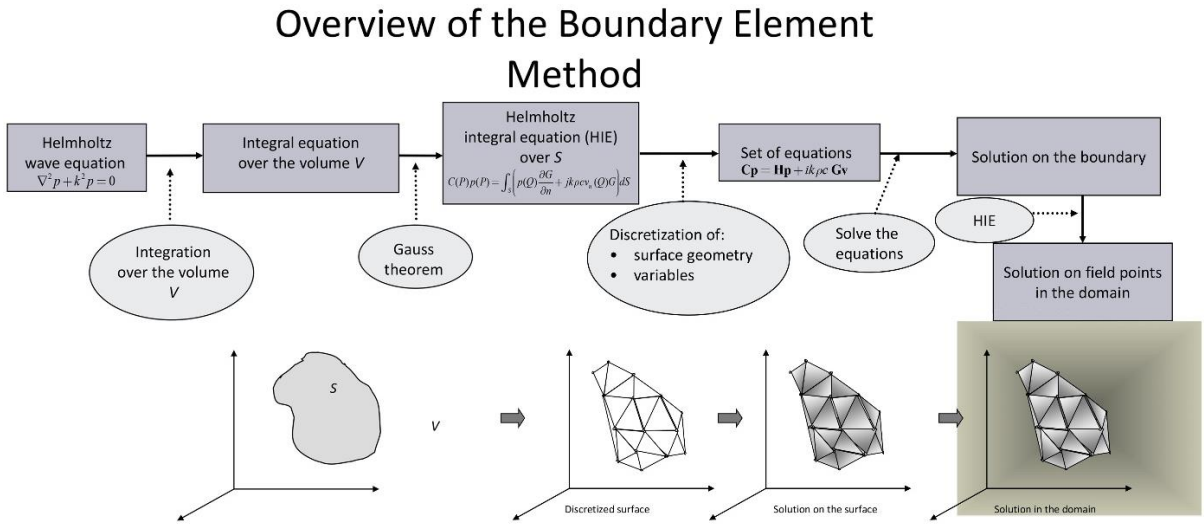

Figure 2.31 Schematic of the BEM overview

BEM provides accuracy in the problem's solution on the boundary domain due to its semi-analytical nature and use of integrals in the boundary integrated elements. It shows efficient meshing properties due to the reduction of dimensions, and it is good for stress concentration and infinite domain problems for modelling thin shell-like structures/models of materials; However, it fails on exterior

problems at certain frequencies and presents singularities in Green's function and near-singularities when the calculation point is very close to the boundary. Finally, BEM is currently a great tool to numerically analyse problems of acoustics or aerodynamics [194,195]; however, some limitations might appear. For example, BEM discretises only the boundary while FEM considers the exterior domain as a boundary (so it needs the support of perfectly matched layer = PML). Moreover, BEM are well suited for unbounded domains, and can well be used for arrays and other geometries; However, in FEM, there is a higher approximation in the vibroacoustics effect study in the internal domain [188], and so, in case of AMMs, resonant coupled systems and topic eigenmodes can be calculated most efficiently.

Overall, there are some cases where numerical analysis is efficient enough (i.e. physical implementation of a design process) and others where physical measurements are required for validating the numerical predictionsand and assessing the performance of the designed solution, considering uncertainties that are not necessarily modeled. In the next section, the most used techniques for experimental analysis in the acoustic field are presented.

2.4 Experimental assessment methods for acoustic properties of materials

In this section, we will define two main experimental assessment methods used in Acoustics. Through their detailed description, the suitability of one of them for the current research project will be highlighted.

2.4.1 Impedance tube

Materials' and Metamaterials acoustic properties (such as absorption coefficient and Sound Pressure Level) can generally be measured using these three experimental methods: the impedance tube, the reverberation room (diffuse field), and the anechoic or semi-anechoic chamber (respectively free field or free field over a reflecting plane), [196,197]. The first method involves a 100 mm diameter and a 30 mm diameter tube to cover different frequency ranges. The material sample is inserted at one end of the tube, while a loudspeaker is placed at the other to create a plane-wave sound field towards the sample. A movable system is used to detect sound pressure at any point. The absorption coefficient is determined from $\alpha = 1 - |R^2|$ [198] with $|R|$ as the magnitude of the pressure reflection coefficient in the tube, the ratio of the incident and reflected pressure (calculated from maximum and minimum

pressures). The distance to the first minimum of sound pressure can also be measured, and together with *R*, can be used to determine the normal impedance of the material at its Surface [197,198].

The impedance tube method is effective in demonstrating how plane-waves propagate and how they interfere upon reflection; However, this method has also a number of disadvantages:

1. The sample size is small, with 100 or 30 mm wide diameter; therefore, the derived properties may not be the same for a large sample.
2. The cut and instalment of the sample must be very accurate and careful for obtaining consistent results while avoiding vibrational interference.
3. The determination of α is on a single frequency-based; therefore, it is time-consuming.

This last limitation is nowadays overcome through the two-microphone method [199] for the sound field, where two closely spaced phase-matched microphones are coupled with broadband excitation of the tube. α is then calculated after the transfer function between them is defined by a digital signal processor. α can also be experimentally determined by the reverberation room method [200] from the difference in reverberation time in the room with and without the sample. This method allows the testing of larger material samples in the room, characterised by rotating diffusers, and a closer approximation of the diffuse-field α in terms of bounded space sound field. Nobile proposed one additional method more informative than the reverberation room by measuring α as a function of the angle of incidence of the spherical sound wave in a free field condition and using the above-mentioned two-microphone technique and a reflecting plane [201].

Since samples should be very small, sometimes impedance tubes are not the optimal measurements tool, so others should be considered, for example, anechoic chamber.

2.4.2 Anechoic chamber

The name of the anechoic chamber comes from the Greek "an-echoic" and means a space without echo, so it is designed for absorbing any internal sound wave reflection completely and is insulated externally from sound sources. The resultant simulation of a quiet open space of infinite dimension without depending on the outdoor influences is particularly useful. American acoustics expert Leo Beranek coined the term anechoic chamber, and it was originally used in acoustics (sound waves) to minimize a room's reflections[202]. More recently, anechoic chambers are being customised for testing antennas, radars, and interference from electromagnetic impulse in different radio frequencies [203,204].

Their size can cover a wide range of dimensions: from few cubic meters to ten thousand cubic meters. The two variables to determine the chamber's size are the tested objects' real size and the input signal frequency range. Scaled models can sometimes be used by testing at shorter wavelengths (higher frequencies). Figure 2.32 describes how the anechoic chamber structure minimises the impinging sound waves *I* reflection, thanks to a series of wedges *W* with height *H*. Therefore, *I* is reflected in a number of waves *R,* redirected randomly within the air gap *A* between the wedges *W* (delimited by dotted lines). During this process, such redirection may produce in A, a temporary wave pattern, characterised by the acoustic energy dissipation of *R* through the viscosity of the air, particularly in *C*. Moreover, an additional dissipation is generated by the foam wedges. The resultant soundwave *R',* which exits the gaps *A* on the propagation direction *I* away from the wall*,* is notably reduced. Overall, this bidimensional theory is also valid for 3D anechoic chambers structures.

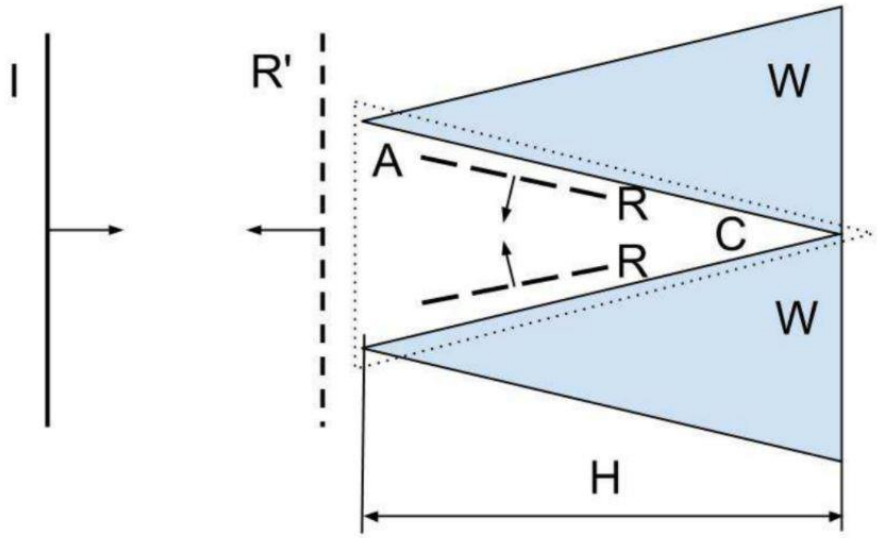

Figure 2.32 Minimization of the reflection of sound waves by an anechoic chamber's walls.

Overall, methodologies including metamaterials and numerical computational methods can count on established guidelines based on both Physics and Psychoacoustics [52] that they can use to define if the results they got from the simulations or the data acquisitions are effective or not, and this is so far an efficient solution. Moreover, most contemporary research in this field uses physic simulations or psych-based parameters to evaluate new architecture systems' impact on people's lives [47,59]. However, when these methodologies are applied to solve issues related to the built environment, the involvement of human perception and social function and interaction could be crucial. Users indeed evaluate the effectiveness of building's features (such as windows, balconies, walls) or environmental tools (such as absorbers, diffusers, and acoustic isolating materials) also through social meanings such

as the relationship they have with such system, the function of the room, and the outdoor environment characterisation [43]. Some researchers tried to apply social science-based practice within Industrial Engineering [41,205–207]; however, this is not a general practice for building's features made by AMMs that lack user experience consideration and contextualisation in their design phase. The increasing interest in involving human perception and social interaction to develop new architectural design systems should include social science-based methods to make the architecture as adaptive and dynamic as possible according to external inputs and indoor comfort needs. For these reasons, an extensive overview of human perception and interaction through the Social Sciences Method is included in the next section.

2.5 The Human Factors in the built environment

Human needs have always been central to the built environment evolution; however, the real contemporary evolution is based on the human perception and interaction with it [1,47,55,81]. The advances in materials, manufacturing, and construction technologies allowed Engineers and Architects to reach unbelievable results from the human interaction perspective while making Architecture as adaptive and dynamic as possible [80,208]. By focusing more on a customer-centred perspective rather than an enterprise-centred one, this trend eventually turned into what is generally known as Ergonomics. Ergonomics comes from the greek ἔργον, which means work or task, and νόμος which means law, custom or usage, and is the science that concerns the interactions among humans and other elements of a system (originally related to the work task but nowadays applied to any activity's tool design). In this discipline, "Human factors" are studied for optimising human well-being and overall environmental performance through theory, principles, data and design methods [209].

2.5.1 Human Perception-based methods

Human perception describes how the brain interprets and organizes the outside inputs captured by our senses [210]. Particularly significant in modern science has been to study how this process is formed and how it affects our memories [211–213]. This depends on the human sensory apparatus and many external factors, such as visual, thermal, acoustic inputs [214,215]. Moreover, most of the inputs perceived by humans are filtered through the built environment meaning, as people in contemporary time spend 80/90% of their time indoors [216]. Due to thermal, acoustic, luminous environments and indoor air quality, the indoor environment has a high impact on occupants' perception, health, and work performance [217–220]. Several international organisations intervened

on the topic: the United States Environmental Protection Agency (USEPA) ranked Indoor Air Quality (IAQ) as one of the top five environmental risks to public health [221], while noise distractions have been proved to lead to 66% drop in people's performance and concentration by World Green Building Council (WGBC) [222]. Thus, it is important to study such a topic from the users' perspective to increase public awareness of comfort and health and discover how they prefer the indoor environment using the latest energy-saving technologies according to their perception. Much research has further investigated how indoor environmental factors influence human perception or performance and vice-versa. Extensive investigation on environmental factors' relationship followed through quantitative research, namely simulations, questionnaire-based environments evaluation, and experimental requalification [223–227]. These works aimed and contributed to improve the working or living environment comfort; however, to optimally apply their findings to the built environment or its features, Ergonomics must be involved.

2.5.2 Ergonomics

Ergonomics comes from the greek ἔργον, which means work or task, and νόμος which means law, custom or usage. This science concerns the interactions among humans and other elements of a system (originally related to the work task but nowadays applied to any activity's tool design). In this discipline, "Human factors" are studied for optimising environmental performance and human well-being through theoretical principles, experimental data and design guidelines and methods [209]. This includes operational benefits of a product which include but are not limited to attachment and pleasure or fun [206,207]. External inputs, indoor comfort needs, and ergonomics have become a fundamental part of the design innovation process [38–41]; however, published works on the built environment and its features are still limited [43]. Only a few of these studies have indeed considered using social sciences methods to investigate such fields [44] involving, for example, focus group methods. Although many methods have been developed to test the physical or psychophysical effectiveness of window design investigation [2,9,45–49], there is still a need to better understand the interactions between people and windows to optimise building systems performance and human well-being through architectural and engineering design.

Participatory ergonomics can be useful for such a research gap, as it actively involves the users in implementing ergonomic knowledge and procedures in the environments they are used to [207,228,229]. A leading investigator supports these users' efforts to improve their living and working conditions and product quality. So collaborative methods of Social Sciences can be largely used in participatory ergonomics, which starts by organising a project team to solve the ergonomic problems

in selected environments. People who join the participatory ergonomics team are highly motivated by their participation in identifying human factors in familiar environments and finding solutions to problems [206,230]. The users know very well what kind of ergonomic problems there are in the environments they live and work in every day, and they become eager to solve them in terms of ergonomics. Therefore, they are willing to receive the redesigned environmental system because they have redesigned it and reformed their organisation for themselves and future generations [209].

Regarding the development of window design to improve the built environment, there are no indications derived from participatory ergonomics or the overall existent physical and psychophysical approaches. Therefore, it is not clear how people relate actively and passively to windows, how they perceive them as a means of communication between outdoor and indoor environments, and how they think they could be improved to make a better indoor environment. The previously cited window's design studies aimed and contributed to creating an ergonomic working or living environment; however, they do not fully capture the social meaning that those environmental qualities have for the users. This disconnection has led to a window design that does not consider how people possibly relate different window shapes or materials with indoor and outdoor environment function and with the degree of privacy. So it is necessary to fill this gap to improve the manageability of this fundamental tool from users' perspective by including more in Ergonomics Social Sciences based methods, especially using participatory techniques such as Focus Group.

2.6 Focus Group - Theory

Participatory methods, one of the examples is the focus group, have been initially related to business methods for product development, but in the last century, it has been increasingly connected to politics. The decision-making issue has evolved into a participatory democracy meant as a complementary dimension of representative democracy also applied to business reform governance [231]. Participation in politics and business generally involves people who belong to different backgrounds, including ethnicity, geography, culture, education, age, and gender. This gave rise to the fundamental debate related to non-scientists contribution to scientific output [231].

Patrimonial Management regards all the processes of collective management requiring negotiation among various individuals or collective involved (i.e. public stakeholders, representatives of public authorities, the financial world). It was natural that public governance came out with laws to manage it, giving positive results during its history. According to Ollagnon in France, for example, 'by creating consultative structures, by calling the users and the local authorities to negotiate,' 1964 French Water

Law 'considerably increased the efficiency of administrative action.' [232]. Non-scientists-participation can be directed and supported by researchers to make it useful to the ideas development process through several instruments: mixed groups (scientists and not) or supporting materials to read and watch (like documents or videos or tangible materials).

In the participatory method, a Focus Group is a small group of people, from 4 to 20 [233], with a moderator, whose main task is to present the study input most neutrally and facilitate an equal and fair discussion to develop points of view about preferences and opinions. Observing the interactions between group members reveals the variety of values and priorities regarding a specific topic. According to Wilkinson [234], in the focus group discussion, 'Collective sense is made, meanings negotiated, and identities elaborated through the process of social interaction between people'. So it is clear that, as she argues, this method opens up a new view on generally hidden and rarely penetrable processes. More than reaching a consensus or decision, this method investigates issues within *a priori* limited knowledge. Since an individual's opinion related to an issue can change during the discussion, it is fundamental for the researcher to focus on how the perspective changes and why. As Morgan suggests:' Focus groups are useful when it comes to investigating what participants think, but they excel at uncovering why participants think as they do'[235].

Furthermore, through focus groups, is it possible to obtain an added value. They provide an opportunity to generate data that, within the symbolic interactionist approach [236], which Seale [237] points out as an early version of the qualitative approach since they emphasized the active aspects of human social life, are open to analysis which highlights the active construction of meaning. Callaghan [238] argues that "carefully selected focus groups can access knowledge which embodies the "habitus" of the wider community". She mentions the 'habitus' coined for the first time by Bourdieu, who wanted to refer to 'dispositions' or filters through which individuals perceive the world, which is 'socially constituted' and 'acquired' [239]. Important hints for the design process can be included in this behaviour. It is important, therefore, to analyse individual voices within the discussion. This is why before the experiment is processed, some study and practice on human coding behaviours in group discussion would be recommended [233].

One of the most famous social research centres in London, the Tavistock Institute, asserts that during the 1940s, the most diffuse method was client-focused [240]. In this process, the company which had to realize a specified product for the client used to follow these phases:

1. Definition of the research topic by the client and following delineation of the problems by the company;
2. Initial troubleshooting;

3. Focus group with adequate classified samples of participants;
4. Call for an expert to address the issues identified from the focus group.

2.6.1 Setting limited a priori knowledge

A fundamental question is related to the method of conducting the focus group, discussing if the a priori categories setting is better than achieving those categories from the group's discussion. In the first case, it is possible to achieve a structured and linked discussion. All the categories are also defined and connected following the researcher criteria. In the second case, the categories generated by participants are analysed. So there could be the risk of finding data divided cleanly into separate categories but without any linkages. In this last method, it is possible to build a so-called 'grounded theory' approach to data analysis, used by many focus group researchers [241]. This phase is critical for the researcher due to the need to set a data analysis without setting a preconception regarding the research's aim. As Melia pointed out, it is necessary to understand the importance of stating the focus and the intents (from those used for the research proposal and funding and ethical approval) and how to use them to create a pragmatic version of grounded theory [242].

Moreover, it is generally preferable an active engagement with the participants from the moderator in discussing and processing a theory, directing each tentative and keeping the discussion close to any category. Udo Kelle describes such an approach as 'in-vivo' codes and 'theories of members of the investigated culture' [243]. In the latter, as Barbour argues, this approach should be seen as focusing on data set that belong to distinct categories which are completely disconnected [233]. This is generally a symptom of a stretched fitting data in available categories instead of deriving those categories from the data, cutting off an important part of the qualitative research, where every distinct transcript data is composite and can fit at the same time different categories of coding, possibly related to the different wide topic.

To allow participants to engage in a discussion, regardless of each different background, the researcher should introduce the topic discussion giving some brief information but not going in too specific details to let the discussion explore a possibly independent perspective. As Barbour assumes, presenting cuttings from tabloid newspapers or excerpts from TV shows can also work as icebreakers, especially in case participants may be introduced to the university environment for the first time. In this way, participants can be reassured of the discussion accessibility and offer a vast amount of resources through their daily lives and interests [233].

2.6.2 Determining topic guide and stimulus material

As has already been highlighted, it is important for a researcher approaching a focus group experiment to have a topic guide to follow. This should show a series of goals that the researcher aims to achieve during the experiment. The structure must be divided into blocks depending on the participation of the group members: passive (where the researcher spots some hot topic and ask open questions to them) and active (where the participants should actively build a discussion based only on a non-directed question as to the showing of pictures or other stimulus material). It is important to define every sub paragraph in each block, including the estimated time to conduct the discussion or to let the topic be sufficiently explored.

The researcher's general aim must be to conduct an in-depth study to anticipate the discussion and imagine the possible responses to his/her conversational gambits and then synthesize this whole process in a few key questions and images. For specific questions in the main research project, it is possible to use the pilot topic guides before making them. The questions should be open-ended since the task of the researcher/moderator is to ask participants to expand on or explain their comments or usage of a particular term and probe and invite them to theorize as to why sometimes they hold such a different view. It can also happen sometimes that the questions investigated and the input generated from the participants could be deeper and explore in a more sensitive way than those the researcher had decided to use.

In the end, the topic guide should be enough structured to allow the facilitator or the researcher itself to conduct the experiment, avoiding discussions too far from the main points. The topic guide's most important role is to accomplish a non-stop questioning and evaluation of the upcoming descriptive frameworks to protect the focus group researcher from slipping into using an imprecise method. So the data generated will reflect the brainstorming and the group's dynamics more than an accurate description of the individual’s opinions. Individual questionnaires could further explore this after the focus group. However, in the presented PhD project, the most important goal is to detect people's awareness of design issues in existing window systems and how they might collaborate to define a new approach to accomplish their necessities. This is another reason why the stimulus material will be shown and discussed between everybody to achieve an agreed ideal design prototype.

Two main alternatives can be considered to determine the criterion of the stimulus material. It can be, for example, a simplified building part of the discussed concept as several simplifications of window characteristics (e.g. different frame shapes, frame thickness, glazing colours or opacity degree proposal). Otherwise, it can be an example of an already built prototype as a different window typology with all the over cited characteristics already assembled. Stimulus materials can also be

extremely useful in breaking the ice and injecting humour [233]. Due to them, is it possible to stimulate the discussion and afford the potential for comparison across the groups. The importance of using stimulus material in this qualitative method research is the potential of interaction engaging as much directly as possible. Even since each group member will filtrate the material with their own experience, it will be easier for them to explain their feelings or present references related to their past. So it put them in a more direct connection in terms of discussing.

2.6.3 Setting the sample

Recruiting focus groups participants involves making several pragmatic and ethical decisions. Since there are no exact methodologies for conducting this phase of the study, it is fundamental to set the group composition coherently with the whole research structure and consistently throughout it. Barbour advocates using a topic guide and stimulus material to incite interaction and the definition of the group composition and simultaneously promote adequate experiences or perspectives variety [233]. This will, in turn, 'ensure that participants will have enough in common with each other to make discussion seem appropriate' and 'allow for some debate or differences of opinion' [233]. Regarding the purpose of qualitative sampling, Kuzel, Mays, and Pope all focus not on recruiting a representative sample but on reproducing the variety within the group or population under study [244,245]. This is a crucial stage since the researchers will make their comparisons and considerations using those data from it. For this purpose, it is important to draw up a sampling frame and leave the outline sufficiently open to make the most of any further researcher's intuitions or opportunities reached during the progression of the study. On the other hand, to carry out the systematic comparison, the data can be interrogated purposefully through purposive sampling. In this PhD project, for example, the sampling is quite open since the study's aim includes all the different kind of users of indoor spaces.

When setting the parameters of a focus group experiment, another important point is the number of participants since the bigger the number, the more difficult it is to analyse precisely each participant's behaviour within the group. This aspect traces the main difference between marketing and academic research. Most of the discussion is summarized in the marketing research approach, either verbally or in note form. In social sciences, research instead focuses on the whole verbatim transcript of the group discussion, which is the main document to be analysed systematically and in detail. This is why a larger group of eight participants could result in being too demanding for the moderator to guide and for the researcher to analyse. On the other hand, it is possible to hold a focus group discussion with three or four participants (which sets a minimum number of people in each focus group)[233]. Moreover, the room's size where the study will be conducted can also dictate the number of participants. Indeed,

it is generally advisable to visit the venue in advance so to ensure not only that there are the conditions to support a discussion (e.g. quiet place and size of the room), but also that there will not be any items that might influence the content of the discussion or even offend some of the participants. Finally, an inspection of the room and its accessibility is particularly advisable if any individuals with disabilities or restricted mobility will attend. Another aspect to consider is the involvement of a way to pay back the participants as money or food. Rewards and refreshments might be seen as a mystification of total volunteer participation in the experiment and a non-spontaneous interest from the individual participating in the research. On the other hand, it is worth considering providing a reward or supplying a refreshment during the focus group experiment since it can help create a relaxed atmosphere and show gratitude to the participants. In the case of refreshment, this should be planned to consider all the food restrictions given from individual's religions or ethnise, or people eating diseases or intolerances.

2.6.4 Relationship between researcher and researched

Should researchers as moderators try to engage in a discussion themselves with the participants, or should they open the discussion with a question or an example? Furthermore, in the second case, may they specify the context of the question/example or should it be left open to be explored by the participants? Focus Group could be intended as a maieutical process, so the approach to the participants should be to introduce the topic and then leave the participants to discuss it actively, redirecting them when the discussion goes far from the main aim. Indeed, according to Morgan's argumentation, if the moderator does not direct the discussion of the groups, they are not focused enough on the topic and cannot be called focus groups [235]. So, the researchers/moderators must have a clinical and mindful approach to the focus group, aware of the temptation to equate their disciplinary interests with the political interests of those they research without transmitting any personal perspective. However, what must be considered is the researchers' awareness of active contribution to the data they are generating: this concept is called reflexivity. Referring to this aspect of the research, Barbour summarise:

> "As with many other aspects of research design, there is no such thing as a perfect match between moderator and group. What is crucial, however, is that the impact of the researcher on the data is taken into account in the analysis, that this is used reflexively to analytic advantage." [233]

Puchta and Potter discuss the moderator's effort in 'working at' getting people to speak while not mining spontaneity [246]. The moderator has indeed a key role in keeping the balance between the importance of the participants to 'answer as spontaneously as possible' and the relevance of the discussion topic [246]. They continue: 'Put another way, it is a tension between the licence to give answers that are "neither right nor wrong" and demand participants actually to produce answers rather than "I-don't-know's"'.

At the latter qualitative research may generate a feeling of upset or distress in the researchers, even if it did not concern the relationship between them and the researched directly, and even where apparently there is no sensitivity to the topic. To ensure adequate support, Owen stresses that the researcher must have the availability of a 'supportive and experienced research supervisor or colleague: in order to discuss her/his thoughts and feelings after fieldwork exposure' ([247] p.657).

2.6.5 Using of focus group alongside quantitative techniques

It could be necessary to review window design examples to create stimulus material (e.g. making an images documentation analysed and grill to define windows elements categories). In this way, giving some pictures as references substitutes written description and gives the participants a direct sensorial input to represent reality. Moreover, it would be useful to observe specific keywords for each category at the transcript analysis stage. Indeed, it can happen that beneath the overall discussion, some particular words get repeated by several participants and so become keywords. It could be relevant not just to analyse how many times they have been repeated but also to define classes related to their qualitative acceptance. Unfortunately, no references in which this method was used have been found, so this is a first attempt of conducting in such a complementary way through keywords a qualitative and quantitative research method.

2.6.6 Guide lines for collecting the data

Data collecting can be done through several methods. The most common are note-taking, reports from moderators (that, in this case, will be the researchers themselves), and memory-based analysis. All these methods could be satisfactory for this academic research since the group's entity is reasonable, and the contents of the discussion will be regarding a tangible effect on an object as a built environment feature. After setting the focus group environment, the really important thing is to record all the experiments appropriately. This means choosing good quality recording equipment and placing it appropriately to reach all speaker voices but not in a too visible way because it will make

people feel uncomfortable about speaking in front of such a device if they feel its presence. Video recording could also be useful with this approach. The researcher can get all the behavioural expressions through speech and body language, giving the research some more input. However, even if this could be an efficient approach, it is not always the best option since it can increase participants' self-consciousness and discomfort. They will be stressed and so could act in a non-natural way. After this stage, the recordings must be transcripted, possibly through software that automatically does this. In this phase, it is extremely important to set everything with the aim of distinguishing individual voices. This is generally achieved by asking participants to introduce each other (observing common courtesies) and using people's names during the discussion to make this task easier [233]. Names that will be encrypted of course after this stage. It is also important not to go through the transcript analysis stage too far from the actual focus group to allow the researchers to recall as much as possible of the discussion, especially with the notes' aid. So researchers must be able to rely both on recordings' transcripts and notes as the first give the possibility to return to the data at a later date, perhaps to reanalyse them in the light of new insights gained from subsequent studies or through further reading. According to Kitzinger, it is recommended to read the transcripts whilst listening to the original recording and, using field notes aid, noting any significant gestures, emphases and expressions of participants voices [231]. So even if they are not following a rigorous conversation analysis approach, the researchers who analyse focus group data can generally learn much from the attention to detail and may include helpful notes on tone, interruptions and body language to aid analysis.

Moreover, the coding frame should be flexible enough to incorporate themes introduced by focus group participants on the analysis side. While identifying the broad themes, the researchers need to pay attention to provisionally allocate some other more specific themes to subcategories relating to these broad headings. It is worth then think about the linkages between them. According to Barbour, it is generally expected that no more than twenty broad themes would be generated for each experiment. In addition, at the end of each focus group, it is important to keep some time to debrief the group, allowing each participant to raise any queries or clarify any doubt about their participation in the experiment. Finally, participants must have the researcher's contact details if they wish to query or concern about anything.

2.7 Literature Review Highlights and Research Questions

In Chapter **2. Literature Review**, the relevant methods and fields were reported and discussed to show their importance within the PhD project and prove the relevance of the Research Question. From this chapter, windows are a key feature of physical connection with the outdoor environment, yet

standard windows cause discomfort when users must choose between natural ventilation and noise reduction. Modern technologies such as AMMs have a wide range of applications and could perhaps resolve the previous highlighted issue if implemented into the window system; However, so far, these technologies have been developed without considering human perception and ergonomics. So further research is needed to address the physical, perception and ergonomic issue of windows through AMMs to allow natural ventilation and optimised noise reduction. In particular, three research questions (see also Figure 1.1.2) should be answered by the end of this project to fill the actual research gap:

1. Which are the most relevant ergonomic principles to be followed when designing a new window system? Why is it important to follow ergonomic principles in an AMM-based window?;
2. What are the benefits of using AMMs over traditional window technologies? How is it possible to embed AMMs into ergonomic windows?;
3. Will an AMM-based window impact people' perception significantly and improve overall indoor comfort? How does this new AMM-based window relate to the ergonomic principles?

3. Participatory approach to draw ergonomic criteria for window design

The contents of this chapter have been published in the peer-reviewed journal *International Journal of Industrial Ergonomics* by the name of "Participatory approach to draw ergonomic criteria for window design" [4].

As Section **2.7 Literature Review Highlights and Research Questions** highlighted, the first research gap to be discussed and investigated is related to which are the most relevant ergonomic principles to be followed when designing a new window system. Literature review helped understanding how focus group theory and participatory design might contribute to improving the actual knowledge about the human factors in the built environment; however, no study has been clearly highlighting criteria or guidelines to follow when the ergonomic value of a building feature, such as the window, must be developed. It is logical then that this chapter reporting an experimental study and related discussion must be the first one presented in the thesis structure. Chapter 3 is indeed structured to explain the method followed to structure a focus group experiment, the Grounded Theory applied to derive each category of evaluation of the window's ergonomic value, and finally discuss the merit over previous studies about involving this specific participatory method to draw ergonomic criteria for window design.

3.1 Background

The first part of the project is based on a focus group-based experiment. While the theory and challenges of focus group experiments have already been exhaustively introduced in Section **2.6 Focus Group - Theory**, this experiment aims to study how participants relate the built environment openings with their perception of indoor spaces dynamics (according to multiple factors such as indoor function, outdoor environment, opening size, and geographical area). At this stage of the project, new criteria to improve windows design strategies using participatory ergonomics and the grounded theory method are investigated. Focus groups are used to investigate participants' reactions and discussions about the visual stimuli and their deduction regarding further employment of specific window design

techniques or uses. Results framework are established through the relevance of the relationship between 25 coded categories, grouped in 5 main macro-categories used to describe the value attribution of ergonomic window design from the users' perspective. Three design principles are highlighted: connection with the outside context to feel oriented, filtering glaze or techniques to mediate the outdoor stimuli towards the ideal indoor conditions, and manageability. Overall the method is validated and applicable to other architectural features design studies. For the designer or professional working on innovation and production in the Architecture and Engineering industries, these principles could be an efficient tool to improve the industrial appealability of a product.

3.2 Methodology

This part of the PhD study investigates the advantages and problematic aspects of window design experienced by general users, understanding its impact on indoor comfort and people behaviours, and optimising the ergonomic design process. Following the focus group method, visual stimuli were set at the beginning and a topic guide. The Focus Group method was used to facilitate a discussion about generic life scenarios involving a window system. Visual examples supported the single and collective awareness of window design influence on comfort perception. Participants were sought between the University's staff and students as well as people residing in Sheffield. A total of five focus groups were organised and performed in one of the University buildings. For each focus group, 12 tasks were assigned and completed, while the related visual stimuli were shown, according to the topic guide. The focus group method was more appropriate than individual questionnaires [248] since the awareness of the group more than just of the single person was one of the critical points for the research questions. Indeed, this methodology was concerned about whether people relate actively or passively to window design, how they perceive windows as means of communication between outdoor and indoor environments, and how they think this feature could be improved to create a better indoor environment.

After data were collected, Grounded Theory (GT) was used to analyse them. Generally, during this phase, the information was separated into smaller chunks through a word-by-word or line-by-line process called open coding [241]. A constant comparison method is indeed at the core of GT, which requires new codes to be compared to those already defined (like in our focus group study settings) or identified (along with the data analysis), focusing on similarities and differences. The continuous refinement theory was ensured by the constant reorganisation and redefinition of the thematic categories used to develop the theoretical constructs [241]. After having identified significant themes, the connections between categories in different parts of the data were explored in the so-called axial

coding [249], where their significance to the whole body of data was discussed. At the end of this study, 25 categories and 5 macro categories were elicited through GT. Moreover, three principles that drive the value attribution of ergonomic window design from the user's perspective were identified. Figure 3.1 shows the study workflow describing the passages between the initial settings, the processing, and the results.

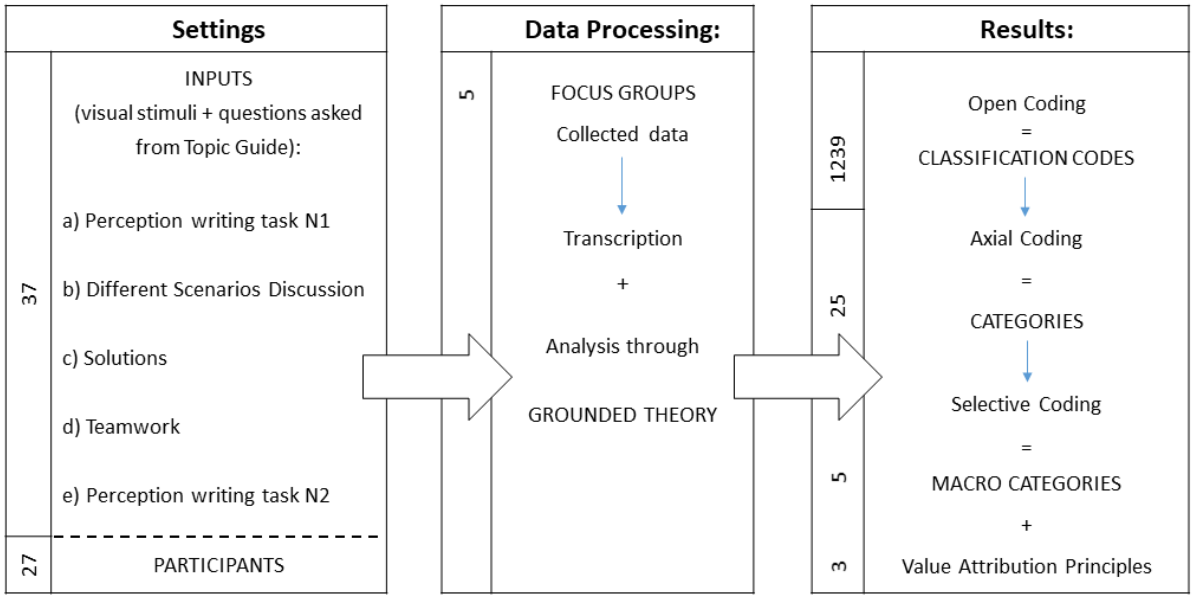

Figure 3.1 Workflow describing the passages between the initial settings, the data processing, and the results (the numbers indicate the elements used or elicited for each passage).

3.2.1 Procedure and questions asked

The procedure that was followed to gather the data from the focus groups was entirely designed from scratch. 9 from the Ethics Committee from the University of Sheffield was received before starting the experiment. The material used, as explained above, was a visual stimulus to start the discussion. As shown in Figure 3.2, the definition of passive and active role from the participants' perspective was drawn first to receive and process several pieces of information (passive role), and then discuss their opinion and elaborate as a group an ideal window design (active role). All the participants faced the same passive and active experimental parts simultaneously, which did not favour any group member compared to others. The experiment consisted of six parts:

0. Presentation of the study named 'Focus group: the relationship between spaces and openings experienced', consent form, and presentation of the participants to each other;
1. Negative/positive perceptions about window design expressed individually (written form): It

was asked to the participants to write what they perceived as being potentially negative or problematic and positive or beneficial about windows. This exercise was also repeated at the end of each focus group to understand if and how the study affected the way participants perceived the indoor environments depending on window design.

2. 'Different scenarios discussion': images of different contexts and different windows typology were presented to the participants to make them discuss it and highlight the actual knowledge and awareness on window design strategies owned by each of them. For instance, they were keen on explaining how they perceive the light's intensity, the dimensions of the openings and other similar characteristics. The scenarios were set to define offices (Figure 3.3,a-c), street views and spare time contexts (Figure 3.3,d-f) or home environments (Figure 3.3,g-i). The first part of this second stage was used to give the participants a universal base of the technical definition of different window's designable characteristics (parts or typologies) and different window design options. This stage, defined as 'passive', helped them create their vocabulary and strengthen their awareness regarding such aspects of window design to support their argumentations in the following parts of the study.
3. 'Solutions' phase: new images were shown to the participants to represent different methods that might have been used to solve some of the problems highlighted at the 'Different scenarios discussion' phase. This part, categorised as 'active', focused on observing the group's problem-solving techniques individually and collectively. The participants examined several methods in order to mediate the connection between the indoor and the outdoor environment in terms of visual contact, lightning, acoustics and thermal transmission, using the shapes of the opening, window's structure, and glaze treatments. As it is clear from the figures shown in the previous chapter, those methods were grouped depending on different shapes (Figure 3.3,j-k), overglaze printing (Figure 3.3,n-o), blurring (Figure 3.3,l), opaque (Figure 3.3,m), blinding and brises solei systems (Figure 3.3,p), reflective or mirror glaze (Figure 3.3,q-s), and coloured filters (Figure 3.3,t-v). After observing these pictures, the participants spotted different perceptive key points and discussed each solution system's feasibility and effectiveness.
4. 'Teamwork': a series of windows characteristics (Shape of the opening, Window inclusion or extrusion respectively to the wall, Frame thickness, Glaze opacity, Pane division) were presented to the participants through different systematic representations, with two, three or four options for each characteristic. They had to face a collaborative design stage [250,251], choosing a single option for every category step. The aim was to define a prototype of ideal window design through discussions and argumentations about their reasons, sometimes mediating their preferences and, in the end, finding compromises. The explicit formulation of

the questions asked to guide the participants in the discussion made them realise the importance of these two separate stages and helped them follow a clear structure of the debate. In this fifth and more active stage, the options within the categories that participants had to choose collectively were:

1. Shape of the openings: *rectangular - square - circular - polygon;*

2. Window inclusion or extrusion respectively to the wall: *included - extruded;*

3. Frame thickness: *minimal - thin - thick*;

4. Glaze opacity: *transparent - slightly opaque - strongly opaque;*

5. Pane division: *any - single - multiple.*

At the end of this exercise, the window design that resulted from their decisions was shown to make them understand the importance and the real effect of each characteristic's combination. These were not merely picking up or exclusion doing exercise but, after the previous information absorbing and brainstorming stage, it resulted as the expression in which all the window design awareness of the individuals and the group were condensed.

5. As at the beginning of the study, in the final part, the participants were asked to express if their perception of negative and positive window's aspects was changed and if their awareness of window design strategies had been affected somehow by that study. The majority of the participants (70%) were positive about the experiment's influence on their self-awareness on window design relationship and gave their feedback in written form.

Figure 3.2 shows the different parts of the study with their participants' engagement level (=P.E.L., active 'A' or passive 'P', which was the same for every participant in every phase), the purposes and the responsivity percentage of them (R%):

STUDY PARTS	P.E.L.	PURPOSES	R%
1. Perception writing task N1	A	Unconditioned perception of window's elements, characteristics, or presence	100%
2. Different Scenarios Discussion Work environment; Spare time activities in public and private places; Home environment	P	Raising of problematics related to different environments: private/public, exposed/non-exposed, crowded/lonely	90%
3. Solutions Different shapes; Blurred or opaque glaze; Over glaze printing; Brise soleil, Reflective glaze, or Mirror glaze; Coloured glaze or Filters	P	Giving possible solutions to the problematics raised in the previews part Setting common homogeneous knowledge and vocabulary regarding window design	80%
4. Teamwork Shape of the openings; Window inclusion or extrusion respectively to the wall; Frame thickness; Glaze opacity; Pane division	A	Discussion of the options and group choice of one option to be used in the final prototype	80%
5. Perception writing task N2	A	Perception of window influenced by the study process	70%

Figure 3.2 Chapter 3 study parts with relative participants' engagement level (=P.E.L., active 'A' or passive 'P'), the purposes, and the responsivity percentage of them (R%)

3.2.2 Setting of the visual stimuli

The methodology used for this study derives from the Focus Group method, where different typologies of users discuss together undergoing the same tasks in an informal environment, raising questions and problems regarding the specific themes proposed and supervised by a moderator. [252]

The two core parts of Chapter **3 Participatory approach to draw ergonomic criteria for window design** study were: (1) observing the participants' reactions to different scenarios and (2) understanding which strategies the participants would adopt to bring the indoor environment to an optimal setting. It was necessary to set a topic guide [233] to define key terminology better and help

the communication between the participants. The guide defined all the different stages of the study in terms of active and passive participant roles and organised visual stimuli (representing the *a Priori* Limited Knowledge [233]). It is important to stress again that all the participants experienced the same passive and active tasks simultaneously, without favouring any member of the group compared to others.

The *a Priori Limited Knowledge* to guide the focus group in parts (1) and (2) was presented as visual stimuli. A number of 21 pictures of different indoor and outdoor scenarios, including the feature window, were used for this scope. The main aim of this visual stimuli was to give the participants information about the terminology and characteristics of specific window's parts, following design concept modules (such as indoor function, outdoor connection, and others that will be presented in Section 3.1.4 *Categories Framework*) and considering which aspects customers prefer to have a voice in. [253] set a homogeneous basic knowledge to give all the participants the same possibility to discuss their ideas on window design. Moreover, by using *a Priori Limited Knowledge,* it was possible to achieve a structured and linked beginning of the discussion. With this method, all the categories are defined and connected following the researcher criteria. Of course, since the focus group is a method of open possibilities nature, the list of categories defined in the topic guide had to be updated and expanded due to participant interaction and autonomous collective constructions. *A Priori Limited Knowledge* was appropriate for setting Chapter **3 Participatory approach to draw ergonomic criteria for window design** study; however, GT was introduced in the analysis part to define the window's qualification categories from the group discussion, added then to the topic guide for the sake of completeness.

More than reaching consensus or decision, this mixed methodology aims to investigate issues within a priori limited knowledge. Since an individual's opinion related to issues can change during the discussion, it was fundamental for the researcher to focus on how the perspective changed and why it did. Thus, even if individually the shown figures were limited under many aspects (such as outdoor scenarios and different light conditions), they were chosen for their simplicity of input. The number of elements and number of dominant window design characteristics were contained, and all together, the pictures gave overall complete information about the window's components and scenarios. In Figure 3.3, all the pictures involved in the study are presented. They show different scenarios with a significant amount of characteristics that the participants could use for each different study stage. With these instruments, a fairer discussion was guaranteed especially when, during the teamwork phase (the one for constructing the ideal window design), the group managed to accomplish the task with less help as possible from the moderator. For this reason, this was evaluated as an effective mixed methodology.

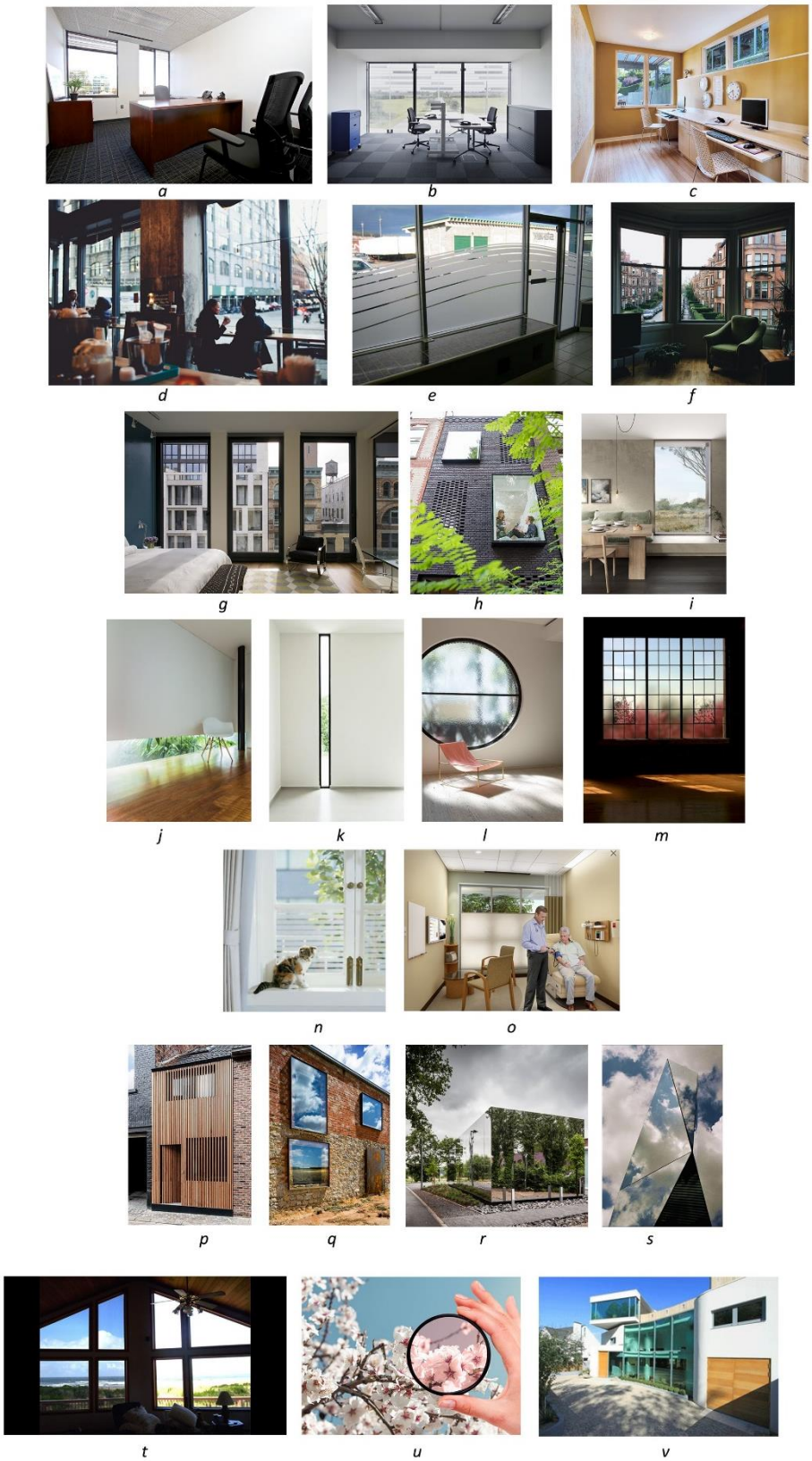

Figure 3.3 Different Scenarios Discussion figures: offices (a, b, c), spare time contexts (d, e, f), home environments (g, h, i); and Different Solutions Discussion figures: different shapes (j, k), blurring systems (l), opaque systems (m), overglaze printing (n, o), blinding and brises solei systems (p), reflective or mirror glaze (q, r, s), coloured filters (t, u, v)

3.2.3 Participants

In this project, the sampling is quite open since the study's aim includes all the different kinds of users of indoor spaces. As previously explained in Section **2.6.3 Setting the sample**, it is necessary to set a sampling strategy since, as Macnaghten and Myers argue, 'Whatever the dangers for the research of a rigid scheme of categorization of identities, it is useful in planning the groups, because it pushes researchers beyond the voices that are most familiar, most obvious, most articulate, or easiest to recruit' [254]. Due to this principle, the recruitment for the focus groups experiment was done through the University of Sheffield students and staff and Sheffield's residents. More than in the sampling before the experiment, the most important action was taken after the participants' enrollment, ensuring that there was at least one architecture background individual in each group. This was set to give each group the possibility to have an "expert" voice to support the discussion and give deeper background hints. The study sample was set as optimal with 5/6 participants per group [186], and the number of focus groups was retained as enough once the data gathered were saturated [190].

The whole group of participants included 27 individuals, of which 20 females and 7 males, with ages between 24 and 44 years old, hailing from Europe and North Africa (33%), Asia (45%), and America (22%). It is essential to highlight that the study focused on the different backgrounds that would have defined correspondent factors under contextual experience (demographical, space usage, and psychological). [255] Hence, window design investigation is still at a global environmental stage in terms of history/heritage, ethnicity, geography and economic situation.

Moreover, to make the methodology as effective as possible, it was fundamental to have a moderator (the author) guiding the discussion without influencing it, checking and putting the discussion back on the main topic when the participants started to deviate from it.

The following graphs (Figure 3.4a-d) show the participants' characteristics in terms of gender, age, and nationality.

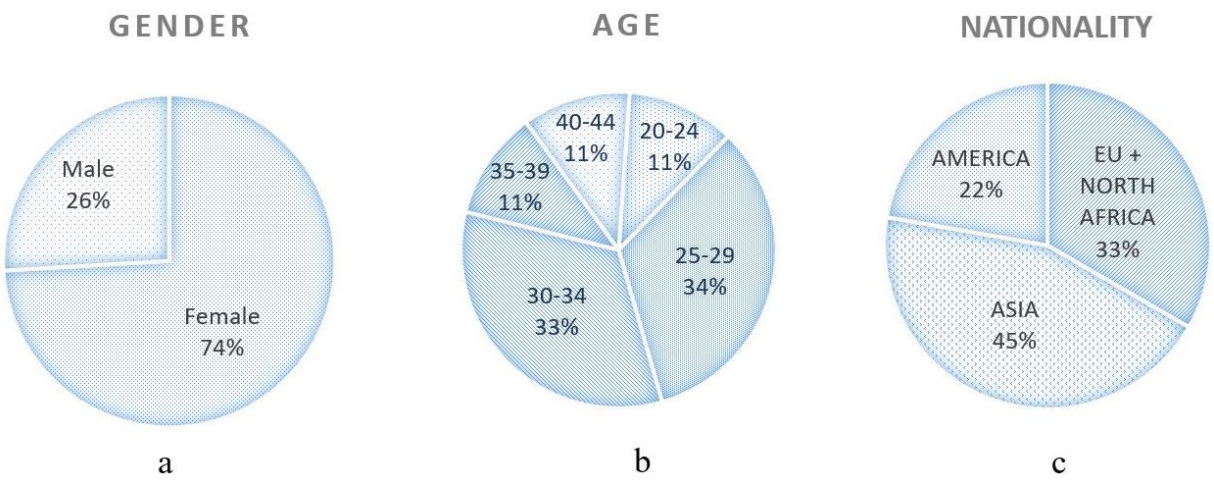

Figure 3.4 Background of the participants: (a) gender, (b) age, and (c) nationality.

3.2.4 Categories framework

A categories framework was defined during the analysis part through a technique used frequently in the GT qualitative research method. The GT aims to explain the processes characterising the observations collected rather than merely describe the phenomenon. The theoretical saturation and full development of the categories elicited from participants' choices (which should account for minimum and maximum variability in the data) ensure the theory's validity and states the end of the data collection [241,249]. The study's completeness and rigour are more important than the number of focus groups or interviews conducted. The main influencing factor is represented by the presence and epistemological position of the researcher moderating the study. For these reasons, negative effects deriving from any personal bias were neutralised, and the only interference was related to strictly follow the topic guide in the specified amount of time. Moreover, due to the importance of including in the study each participants' tone or behaviour within the group discussion, before the experiment was processed, a thorough study and practice on human coding behaviours in group discussion were performed during the project of Farley et al. [196] at the Information School of the University of Sheffield. Thus, the author experienced both academic training and practice from experts in the field.

During the focus groups experiment, it was useful to observe for the transcript analysis stage which specific keywords were used at any point of the topic guide. Indeed, it can happen that beneath the overall discussion, some particular words got repeated by several participants, and so they become keywords. In this way, it was possible to group them into noticeable categories and observe how they were related to each other by the participants. Following Barbour theory [233], it was also important not to go through the transcript analysis stage too far from the actual focus groups and then read the

transcripts while listening to the original recording. This procedure allows the author to recall as much as possible of the discussion, especially noting any significant peaks and expressions of participants voices.

The coding frame started from setting the *a priori* knowledge and was expanded during the analysis, incorporating GT themes introduced by the participants' discussions. So, from the set *a priori* knowledge, the first analysis categories were:

a. Indoor function, when the participants reflected on a specific function of the indoor space;
b. Outdoor Connection, when they focused on the importance of the various outdoor scenarios;
c. Time amount of use, related to a particular long or short term activity influencing the evaluation of the window design;
d. Frame shape;
e. Inclusion or extrusion off the wall;
f. Frame thickness;
g. Glaze treatment, intended as any possible colour or filtering, mirroring or reflective, blurring or opaque, overglaze printed and screening variation;
h. Panel division;
i. Wideness of the opening;
j. Blinding system;

These categories had been defined to be applied to each relevant point raised from the topic guide. Moreover, during the analysis, the GT coding added new categories and the relative belonging to different context groups (or macro-categories), elicited from the open, axial, and selective coding (showed in the results section).

At the end of the analysis stage, 25 categories and 5 macro categories were coded. Even if this is part of the analysis stage, it can be considered a fundamental achievement for its methodology. So it is included and fully explained in the results part.

3.3 Results

3.3.1 Categories' properties and dimension determined through Open Coding

After the verbatim transcription of the focus groups' audio recording, the software NVivo Pro 11 for qualitative research was used to code the files. The researcher broke down the data into chunks,

examining, comparing, conceptualising, and categorising the emergent concepts. The first phase, called open coding, consisted of analysing the text line by line, focusing on the mental constructs and the vocabulary related to them. Next, the objective and reflective sphere of their expressions was evaluated simultaneously to understand the participants' views on their relationship with window design and the possible improvement on the already known window system. A total number of 1239 classification codes were used to determine the Window Design categories by properties and dimensions qualitatively. In Table 3.1, an example of open coding workflow is showed. In some cases, the chunks of statements could be coded in two separate parts, and different categories would have been derived.

Table 3.1 Example of open coding workflow with relative processing parts: Statement, Chunks, Codes, Categories, Dimensions.

Statement	Chunks	Codes	Categories: properties	Dimensions
They have different functions: the one on the right (Figure 3.3,o) needs to be fully private because there is some medical stuff happening and the one on the left (Figure 3,n) it just gives you enough privacy so people can see what you are doing but not clearly.	They have different functions:	functions	Indoor Functions	range
	the one on the right (Figure 3.3,o) needs to be fully private because there is some medical stuff happening	privacy	Degree of privacy	high
		medical use	Indoor Functions	defined
	and the one on the left (Figure 3.3,n) it just gives you enough privacy	privacy	Degree of privacy	sufficient
	so people can see what you are doing but not clearly.	outdoor relationship	Outdoor Connection	possible neglectable
			Effectiveness	small
I think the bottom one (Figure 3.3,f) is the only one we choose so we can have some control on it. We can open it for some ventilation.	I think the bottom one (Figure 3.3,f) is the only one we choose so we can have some control on it.	control	Manageability	good
	We can open it for some ventilation.	control	Manageability	good
		outdoor relationship	Outdoor Connection	possible
Maybe in my country for example this type of window would work, in contrast with the UK, because the thermal comfort is important as the privacy. So we need this type of design (Figure 3.3,k)."	Maybe in my country for example this type of window would work,	functionality	Life Experience Connection	direct
	in contrast with the UK,	comparison	Life Experience Connection	direct
	because the thermal comfort is important as the privacy.	comfort	Amount of Lighting	good

		privacy	Degree of Privacy	high
	So we need this type of design (Figure 3.3,k).	usefulness	Frame Shape	necessary

The additional categories and the determination criteria were:

a. Floor level;
b. Degree of Privacy, observing how much a specific characteristic of the window design changed the perception of being observed or not from the outside and how comfortable or uncomfortable this made the participants feel about;
c. Costs, considering participants concerns on the window maintenance and effort;
d. Effectiveness, meaning how significantly supportive was the window design towards the ideal indoor comfort condition;
e. Life Experience Connection, coded when the participants related a specific window characteristic to a direct/indirect experienced or known/studied condition;
f. Manageability, when the participants expressed a particular comment related to the window design control;
g. Amount of lighting;
h. Comfort;
i. Safety, coded when the participants related a part of the window design or a qualitative configuration as creating a safe environment or not;
j. Anxiety, considering the relation of some windows characteristics to stressing situations;
k. Ventilation;
l. Design;
m. Listening, elicited when participants expressed the specific will to have a connection with the outdoor environment in a sonic way;
n. View;
o. Architecture.

3.3.2 Categories connection through Axial Coding

After the preliminary coding, closer attention was paid to those categories which were recurring during the text. With an increased organisation level, the categories were studied and divided depending on their dimensions and properties. As Glaser et al. [256] indicate, to be efficient, the analysis had to be done "around one category at a time in terms of the paradigm items". In the axial

coding, this category becomes the reference axis concerning which other categories building is performed. Figure 3.5 shows a schematic of the axial coding, explaining the connections between the 25 elicited categories. The size of the name font represents the importance of each category in terms of spoken iterations number.

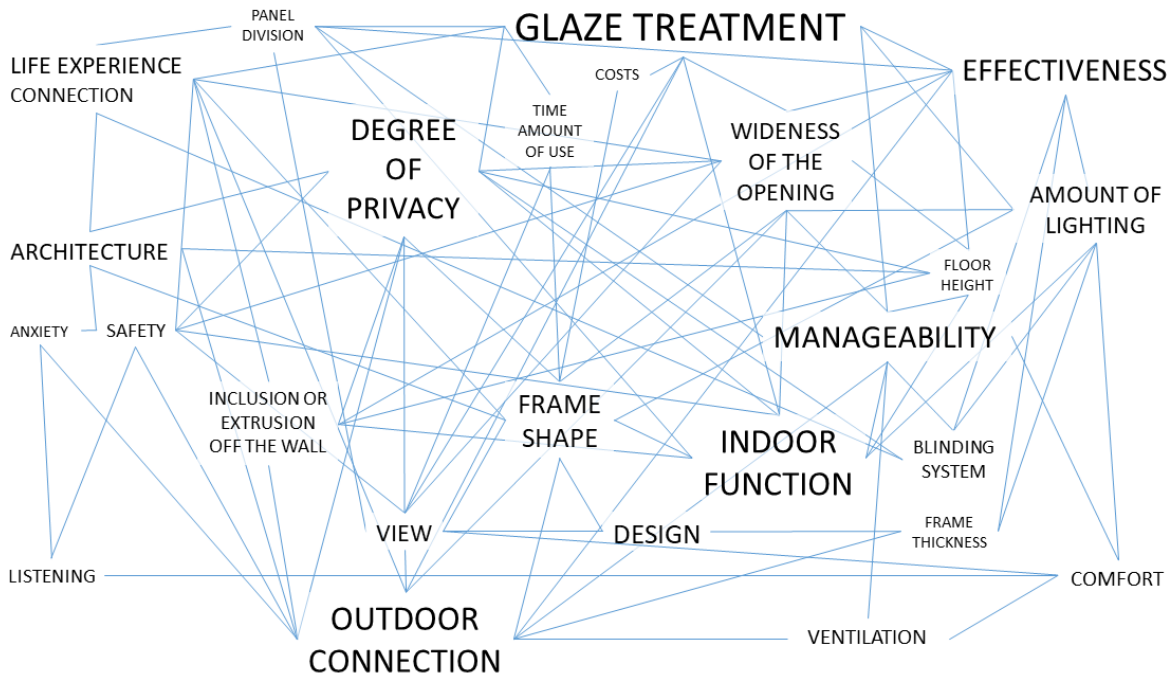

Figure 3.5 Schematic of axial coding phase with the macro-level categories connection

3.3.3 Definition of Value Attribution of Ergonomic Window Design from the users' perspective with Selective Coding

The participants perceived the window design, whose aspects are positive or negative for their judgmental system, and how they would like to be entitled to modify what is not optimal. The topic guide and the visual stimuli were found very useful in this stage. Indeed, the categories already identified helped the participants to support their discussions. From the topic guide structure, they managed to explore new categories elaborated autonomously by the groups. After the axial coding defined the connections between the elicited categories and their relevance in the focus groups discussions, selective coding was applied.

The selective coding individuated and connected themes relevant to the central phenomenon's description (in this case, represented by the value of ergonomic window design from the users' perspective). This is identified as the core category of the theory and can be connected with all the other ones. The 25 categories were assigned to five macro-categories (see Table 3.2): Affective Impact,

Contextualisation, Filtering Outdoor Stimuli, Manageability, and Architectural Inclusion. Figure 3.6 represents how the macro-categories are related to each other and which principles the users followed to establish the core category: Value of Window Design. This was defined by the participants through the formulation of relationships between macro-categories which highlighted 1) Importance of the Outdoor Connection to feel oriented, 2) Filtering the information from the outdoor without changing the meaning of it, and 3) Controlling the window system behaviours within physical boundaries. These three principles have been found at the base of all the focus groups discussions of the study, and they are fundamental for the Value of Window Design from the participants' perspective. Researchers and designers could use them when investigating window design optimisation or improving the engineering product proposal towards window purchasers or selectors in the market.

Table 3.2 Categories and Macro Categories from the codes that describe qualitatively the Window Design

ERGONOMIC WINDOW DESIGN				
AFFECTIVE IMPACT	**CONTEXTUALISATION**	**FILTERING OUTDOOR STIMULI**	**MANAGEABILITY**	**ARCHITECTURAL INCLUSION**
Outdoor Connection		Glaze treatment	Manageability	Frame Shape
Degree of Privacy	Indoor function	Amount of lighting	Effectiveness	Design
Life Experience Connection	View	Wideness of the opening	Time amount of use	Inclusion or extrusion off the wall
Safety	Blinding system		Costs	Frame thickness
Anxiety	Architecture	Panel division	Ventilation	
Comfort	Listening		Floor level	

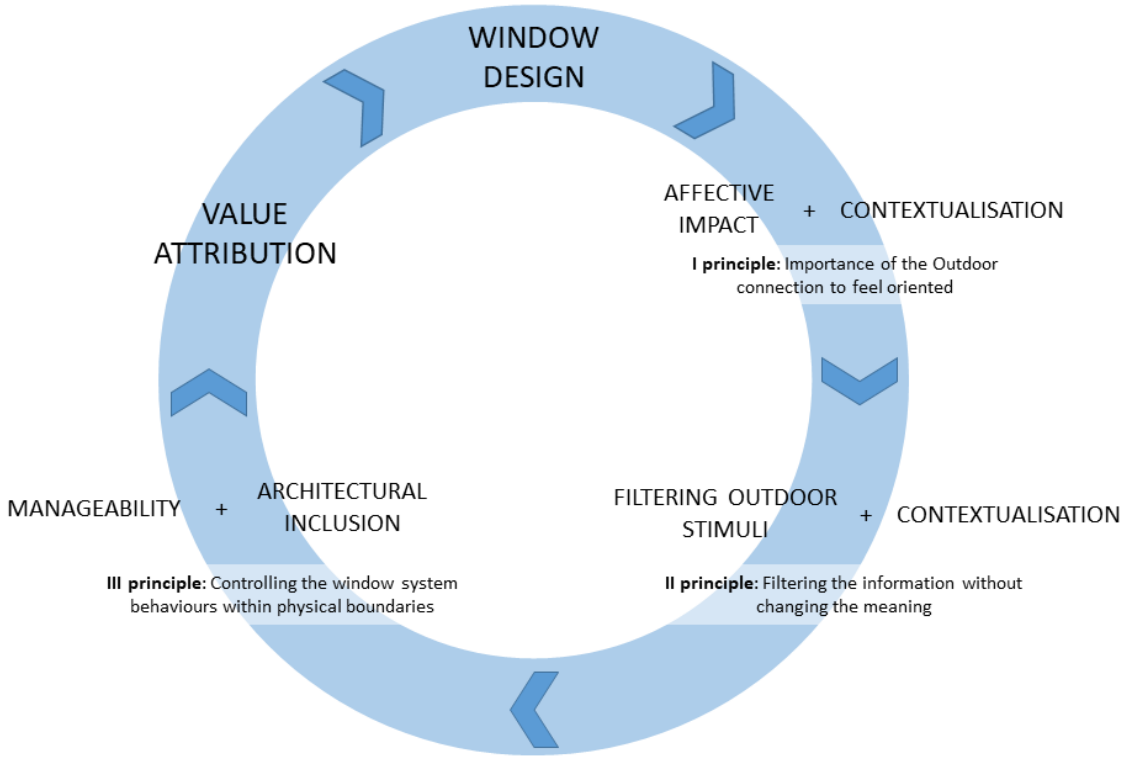

Figure 3.6 The attribution of value to Ergonomic Window Design built by the relationships between macro-categories and their three fundamental principles.

3.4 Discussion

The importance of the relationship between particular macro-categories and the three fundamental principles that drive them towards the Value of Ergonomic Window Design (from the participants' perspective) is further discussed in this section with the available Industrial Ergonomics literature [40,41,205,229,257–259]. The importance of the relationships between the elicited macro-categories is underlined once more to highlight the significant impact of the principles they follow within the whole focus group experiment. The workflow coding supports this discussion (see Table 3.2 and Figure 3.6) and examples of focus groups excerpts (presented in Table 3.3-7) expressing the degree of interest and the emphasis used by participants to support and argue their ideas.

3.4.1 AFFECTIVE IMPACT and CONTEXTUALISATION: Importance of the Outdoor Connection to feel oriented

From Figure 3.5 and Figure 3.6, it is possible to observe how the participants need contact with the outdoor; nevertheless, the outdoor conditions could be non-optimal for indoor comfort. Frequently,

such affective impacts and user's satisfaction over a specific design have been studied by researchers to develop a method to integrate the modelling attractiveness factors of productions based on user psychological needs (Singh and Tandon [41], as well as Wang and Zhou [205] for example). The first researchers established a list of values for the evaluation model, including 'emotional values' such as Inspiration, Joy, Belongings, Care, Concern, Fun, Culture, Ease. A series of categories and their properties that reflect those emotional values have been coded within our study. Through them, the 'Affective Impact and the Contextualisation' principle was determined. The second researchers presented interval hesitation time value as a key factor for users' satisfaction when investigating and developing a product design system. Unlike Wang and Zhou, in the presented PhD study, a series of auto determining factors such as those described within the categories and macro-categories (see Table 3.2) were considered to attribute value to the window design by the users themselves in a collaborative, constructive environment. A focus group approach is indeed at the base of a method that can serve researchers or designers to reach a more comprehensive analysis related to an architectural feature or product such as a window. A series of excerpts from participants' discussions now follow to highlight how the auto determining collaborative approach adds meaning to the principle of being affectively impacted by a window design and the importance of the outdoor connection to feel oriented.

Table 3.3 Statements from the Focus Groups Discussion to support the Discussion on the first principle: AFFECTIVE IMPACT and CONTEXTUALISATION

	Statements from the Focus Groups Discussions
a	"Even the view in front of me in Figure 3.3,c gives me some kind of privacy because it is like a private garden, but I'm just wondering if it was a street or if I can be seen from the outside, maybe is not going to be comfortable. However, being open to that view and being in contact with that relationship it will help me overcome the boring times.".
b	"Even if it is not a view that works. It helps me get oriented, and a part from the fact that such a light makes you feel tired, it's also the moment you want to look at the window and you can't, you won't think it at that time, but it's another factor that don't let go your mind and relax for maybe some moments…"
c	"I think very big advantage to have a window is to feel the outdoor so you can feel relaxed, and having this very narrow window it makes you feel the opposite, so you feel trapped in a place.".
d	: "because you know, windows are there to create a connection with life for me, this is how I feel in my home.";
e	"Honestly it is such a pleasure as it has the playful aspect, and I remember one man was just saying hello to people that were coming by. Moreover, you know looking at that playful childless aspect, and how they are using the windows like some kind of Connection rather than sitting on a plastic chair or the step at the porch, he is just at the window, not very high, but he looks relaxed and comfortable. So it is quite nice even though it was not designed for that.".

From *Different scenarios, discussion* participants highlighted concepts like the statement in Table 3.1.a. *The Importance of the Outdoor Connection to feel oriented* has been defined by the participants also mediating the *Outdoor Connection* category with the *Degree of privacy, View, Comfort,* and some time

with *Wideness of the opening*. This principle applied to window design helps users feel orientated and more aware of the outdoor situation in real-time, visible from the excerpts in Table 3.3.b,c. Overall, it is clear that the users need to connect with the surrounding outdoor environment even if sometimes this would not maximise the comfort. They sporadically expressed this need, for example, in the *Teamwork* phase, by choosing one large panel completely transparent. This highlights the design *Effectiveness* and *Manageability* of the *Outdoor Connectio*n on the user's *Comfort* even through a *Life Experience Connection,* as is visible from the statements in Table 3.3.d,e.

Overall the principle of the *Importance of the Outdoor Connection to feel oriented* establishes a first guideline to the Value Attribution of ergonomic window design from users' perspective. Furthermore, it demonstrates that the first approach of participants towards this architectural feature concerns their subjective impressions of the indoor and outdoor context. From this point, in combination with the following principles, it is possible to define an accurate Value Attribution of the window design.

3.4.2 FILTERING OUTDOOR STIMULI and CONTEXTUALISATION: Filtering the information without changing the meaning

The window system represents a feature of connection between the outdoor and indoor physical conditions. The study's results seem to acquire even more functional value when associated with various glaze treatments such as those presented in this research to the participants (see Section **3.2.1 Procedure and questions asked**). During the outlining stage of this value's attribution, different window characteristics' compatibility to slightly alter the outdoor stimuli was considered following a scaled approach for manufacturing and customising the product in the focus groups experiment: the window. Recently, Realyvásquez-Vargas et al. [257] provided a model to measure macroergonomic compatibility of macroergonomic elements, factors, and work systems. Their research underlined that compatibility relies on the product ability to adapt its capabilities, limitations, and needs of another object to perform a specific function. Realyvásquez-Vargas et al. applied then this concept to a macroergonomic sphere, consisting of a perception based measurement of different macroergonomic practices. In our experiment, such an approach is transferred to users perceived compatibility of windows to adapt to human needs through a series of integrated design criteria such as light filters, glass colours, opaque glass treatment, indoor function, degree of privacy requirements, and outdoor connection. On the other hand, researchers such as Shankar et al. [254] discussed the importance of non-functional requirements (NFR) over functional ones, demonstrating that NFRs drive the most design decision-making process and constrain how the product functionality is realised. In their study,

functionality is approached from an environmental and stimuli point of view, and the product function is described by its action with or without external stimuli while it is being used. In our experiment, we confirm Shankar et al. theory, and we also highlight NFRs as leading characteristics in users' discussion about the optimal window design to pursue the same functionality highly affected by the outdoor stimuli that Shankar et al. were discussing; however, this study also highlights how the window functionality should adapt to the outdoor stimuli from the users' perspective. As in the previous section, a series of excerpts from participants' dialogue are reported to support the second principle discussion.

Table 3.4 Statements from the Focus Groups Discussion to support the Discussion on the first principle: FILTERING OUTDOOR STIMULI and CONTEXTUALISATION

	Statements from the Focus Groups Discussions
a	"..there are certain filters of which the colours are very tented, and you can't really feel what colour is it, but it will only compromise the amount of light getting inside, and this is one of the genius things of technology that works to compromise the light getting inside without compromising your emotions and affecting your positivity inside.";
b	"Cause even if you think that opaque part was a wall (Figure 3.3,o), you would have felt less connected if the window was only on the upper. So I think the size of the translucency is actually still connecting the outside with the inside. Cause you can feel the atmosphere. You are aware of what's happening outside.".
c	"I think that if the filter is not too extreme it can really make you understand the light from the outside is different, so it could be a good solution but it's necessary to make a study of what filter is best depending on each specific condition. However, once that you have established it's going to improve the environment, so I will use them.";
d	"Or maybe it could be, like for me changes if it's an office or if it's my house. Like an office, I don't care if they have red, blue, or whatever (glasses) because I'll go back home after. But if it's in my house, I think it will bother me to see like blue like the third picture (Figure 3.3,v) windows all around my house, and I would see blue everywhere that would bother me after a while.".
e	"We use this in our country, reflective glass, to maintain privacy. But it doesn't work after dark.";
f	"We need this especially in summer in UK (Figure 3.3,t-v). The sun raises till ten o'clock, I need my children to go to bed. (general laughing) Because they feel it's still early and they don't want to go to sleep. Their biological clock is type of that.";
g	"Yeah also, there's probably glass glow or something. And then that's typical top right (Figure 3.3,e) of a store or like you know where you want people seeing but not completely. So like maybe as at the hair dressers, nobody wants to be seen whilst their hair is being cut, but also they want some light to be able to work. So let's say it's for privacy, it's very commercial, it's not very necessarily pleasant, but probably necessary."
h	"I think it's applicable in clinics or in places where you need extreme privacy but still need some connection. It's better than a wall, that's sure. I mean imagine to have a wall and have this top window, it will make me feel really claustrophobic.".

According to the users' point of view, the filtering effect should be as natural as possible, as they want to achieve an *Outdoor Connection* while allowing an ideal indoor condition related to the function. Specifically for the *View* contribution and the *Amount of lighting,* this is supported by excerpts like the ones in Table 3.4.a,b. Furthermore, during the discussions, the participants highlighted the

effectiveness of filtering the outdoor environmental conditions accordingly with the *Indoor Function* as the passages in Table 3.4.c,d attest.

Emphasised connection of *Filtering Outdoor Stimuli* categories with the *Indoor function* and participants' *Life Experience Connection* occurs, also considering the consequent *Degree of privacy*. From the participants' point of view, the window has to be organic and adaptable to human needs after those specific outside stimuli and indoor environments have been established. This demonstrates that the user's first approach with window design is through Outdoor Connection and Affective Impact research, followed by a necessity of adaptation of the outside stimuli. Consequently, this principle turns to be also connecting with the *Affective Impact* macro category, as is visible from excerpts in Table 3.4.e-h. The excerpts also demonstrate a significant connection between the categories of *View, Listening, Comfort, Outdoor Connection* and *Glaze treatment*.

The second principle (*Filtering the information without changing the meaning*) introduces an additional value to window design when, in the case of non-optimal outdoor conditions, the connection with the outdoor is not neglected but adapted. It is essential to stress further that the previous principle is related to the connection, while this establishes how this connection should be supported according to the users' perspective.

3.4.3 MANAGEABILITY and ARCHITECTONICAL INCLUSION: Controlling the window system behaviours within physical boundaries

From the previously explained principles, the participants' need to define which degree of connection with the outside they want to have according to several outdoor and indoor conditions is clear. This final principle determines users' need to control the window system to finalise the previous principles' application. In recent years, researchers within the Industrial Ergonomics field have systematically increased their focus on participatory ergonomics processes based on the manageability of a product [40,229,258]. Naweed et al., for example, included in their study a console to control environmental conditions such as lighting [229]. A virtual management practice was highlighted as fundamental to identifying a proposed case study's design limitations and then optimising it through the user-based control system. Following the same approach, in each focus group's final stage, the participants were presented with several before-after real case studies of indoor architectural design, including windows. After having evaluated the 'before' examples, they were enabled to decide how to modify them through a series of design options offered by a virtual system built by the authors (see Section **3.2.1 Procedure and questions asked** at 4. Teamwork part). So through this immediate simulator, they were

able to talk about the different options and then choose as a group the one they felt more comfortable with, according to how they wanted to manage the presented 'before' real case study. This method using participatory ergonomics and transdisciplinarity gave a unique perspective of the group underpinning simulated window design by substantive values and qualities, which sometimes naturally lead to a collective function. On the investigation of the maintenance evaluation method, also Zhou et al. presented valuable solutions [258]. They specifically focused on describing the effects of ergonomics in product design, formulated evaluation criteria based on ergonomic requirements, and evaluated applications of such criteria on real design maintenance cases. Finally, in the literature available, Pereira Pessôa and Jauregui Becker adopted an approach that is the most similar to ours [40]. Their findings presented the 'System lifecycle management' as one factor that directly impacts the design-engineering process of products. They also underline that Product Lifecycle Management Systems solutions should be dynamically adaptable and reflect the constantly changing working environment and organisation according to human needs. In our experiment, the same approach is highlighted from the focus groups discussions, where participants clearly expressed the need to be in charge of managing different window functional configurations to adapt the outdoor conditions to indoor comfort. A series of excerpts from participants' discussions now follow to support the discussion on the third principle.

Table 3.5 Statements from the Focus Groups Discussion to support the Discussion on the first principle: MANAGEABILITY and ARCHITECTONICAL INCLUSION

	Statements from the Focus Groups Discussions
a	"But sometimes I open the windows to hear the street, I prefer that otherwise you are locked inside. So sometimes, just hearing the street, and if it is a pleasurable street, of course, it depends on the amount of noise in the outside. However, if it is set in a nice local street, I would rather open it. So you get some sense of the street.".
b	"For me, they are just different materials of the façade, and if you consider it as a window, you have to open it. Otherwise, I do not think it is a window."
c	"I think the bottom one (Figure 3.3,f) is the only one we choose so we can have some control over it. We can open it for some ventilation."

Users often associate the *Manageability* macro-category with the *Architectural Inclusion* one (through *Frame shape, Design, Inclusion or extrusion off the wall, and Frame thickness* categories connections). However, they also have associated *Manageability* and *Architectural Inclusion* macro-categories with Affective Impact, Contextualisation, and *Filtering Outdoor Stimuli* (through categories connections with *Outdoor Connection, Anxiety, Listening, Glaze treatment,* and *Panel division)*. This means that the third principle is applied within the previous two principles decision-making process about the Value Attribution of ergonomic window design from the users' perspective.

The importance of the window control is supported by excerpts like the one in Table 3.5.a. Alternatively, statements like Table 3.5.b show the crucial role of window settings' manageability to maximise or minimise the outdoor connection.

On the other side, high interest was expressed in visualising the window system functionality as part of a higher architectonical composition where this is placed. In particular, they commonly relate categories like the *Ventilation* with *Frame shape, Design, Frame thickness and Inclusion or Extrusion off the wall.* According to the participants, the connection between these categories identifies the window as a functional part of the building. It also defines the opening of its external boundaries towards the outdoor context (see Table 3.5.c). This third principle draws the final relationships between the macro-categories and the Value Attribution of Ergonomic Window Design from the users' perspective.

3.4.4 Implications of the three Principles for research and practice

The three principles discussed in the previous sections can establish essential guidelines for both researchers in the Architectural or Building Engineering field as well as designers and professionals who work on the window design optimisation process. For the researcher in these fields, it is fundamental to consider the importance of users' control over the window system due to various outdoor and indoor contexts and different degrees of connection. In this part of the PhD study, a correlation between the expression of increasing people's comfort and their awareness of being in charge of actuating window-related mechanisms (such as natural ventilation and natural lighting) has been demonstrated. Further study could consider, for example, specific cultural or geographical scenarios or conditions and develop window design studies focusing on specific macro-categories. For the designer or professional in window's innovation and production, these principles could be an efficient tool to improve the product's appeal in the Engineering or Architectural market. This study demonstrates that people feel more comfortable when they are in control of the window's functions, specifically if the technologies allow them to use more natural sources and limit the artificial ones saving energy and money and increasing their well-being. Nowadays, product sustainability is one of the most competitive fields in building engineering and architectural innovation. [260] The principles derived from this part of the PhD study could be used to improve the window design and production not just from an ergonomic point of view but also an energy efficiency perspective towards a more sustainable building system.

3.5 Conclusions

In this PhD study section, a new approach for window design methodology was investigated involving a participatory approach. The main aim was to understand the principles that define the value attribution of ergonomic window design from the users' perspective. Focus group and Grounded Theory methods have been used to study and code participants' discussions by the degree of interest in the selected visual stimuli and the employment of specific window design technologies to modify the window's settings and adapt outdoor inputs to indoor comfort.

The results framework has been established through the relevance of the relationship between the 25 categories, grouped into 5 main macro-categories. The macro-categories relationships were then used to describe the principles that drive the value attribution of ergonomic window design from the users' perspective. The three principles defined were: 1) Importance of the Outdoor Connection to feel oriented, 2) Filtering the information without changing the meaning, and 3) Controlling the window system behaviours within physical boundaries.

It was highlighted that participants perceive the window as an essential mediating instrument between the indoor and the outdoor of a building. Through this feature, they feel connected to the outdoor environment. Despite the non-optimal conditions (such as noise pollution, impulsive or disruptive sounds, neighbours chatting or kids playing too loud) through the window, they feel oriented which makes them perceive affectively the indoor environment. In the second place, participants expressed a relevant interest in the glaze treatments or window technology to be able to mediate outdoor physical inputs (such as thermal mitigation, lighting adaptation, and noise reduction). According to them, the application of such technology must follow specific principles to keep the perception of the outdoor as authentic as possible. Finally, the participants wanted to be involved actively in window management according to their specific needs based on the relative contextualisation.

This chapter aims to draw a new methodology for window design, which considers users' preferred aspects and combines them with specific window's technologies. As a result, the methodology could be used by Engineering and Architecture researchers to investigate the optimal building feature design ergonomically according to the users' perspective. Moreover, the final categories could be applied to study real scenarios and help other researchers better investigate some of the categories or support designers or window's companies to develop a more refined proposal for a specific window's application. Finally, the three main principles related to window design requirements from the users' perspective outlined in this study could be used as a guideline for optimised ergonomic window design for both building engineering and architectural research or professional application. Through the use

of these principles, there could be a significant improvement in terms of window innovations. It could be possible, for example, to draw a windows design prototype depending individually on the macro-categories and categories (as highlighted from the analysis stage) defining specific optimal window requirements. The window design would become, then, not only the mediator between the outside inputs and the indoor comfort, but it could even modulate the first one to optimise the second.

In the next chapter, the investigation on a set of acoustic metamaterials will establish which is the optimal type to be applied in window design for natural ventilation and noise reduction simultaneously.

4. AMM for natural ventilation window

Users have set the window design criteria through the focus groups study (RQ#1). Another fundamental paradigm of this project must be investigated: acoustic metamaterials for natural ventilation and noise reduction. The contents included in this chapter have been published in the Proceedings of the 10th International Conference on Computational Methods (ICCM – Singapore 2019) [261] and the 23rd International Conference of Acoustics (ICA – Aachen 2019) [262], and in the peer-reviewed journal Applied Acoustics by the name of "Development of metacage for noise control and natural ventilation in a window system" (2020)[263].

Ventilation window is one of the critical elements in sustainable building development, although outdoor factors such as environmental noise can frequently limit their use. Therefore, it is necessary to develop windows with both natural ventilation and noise mitigation functions. To improve window performances in reducing the noise and allowing for air exchange, most current approaches (Explained in Section **Sound insulation** and **2.1.4 Air insulation**) focus on techniques such as double glazed and ducted designs, generally leading to bulky designs, visually non-optimised, and with narrow-banded frequency. These limitations to traditional double glazing and duct designs have been so far addressed by the development of window systems based on the local resonant stopband of acoustic metamaterial (AMM) to achieve dual functions of noise reduction and natural ventilation. AMMs set indeed a new trend in solving physical challenges related to sound wave control, which can find their applications in the ventilation window.

4.1 Acoustic Metamaterials Broad Investigation

4.1.1 Background

Conventional acoustic techniques control sound wave propagation for a limited range of frequencies due to the device shape and bulky configuration [8,54]. Metamaterials can be versatile thanks to their advantages in acoustic properties related to their physical size [59,84]. Two specific kinds of metamaterials are particularly of interest from their geometrical deployability perspective: origami and bistable auxetic metamaterials. The first metamaterial changes the spatial and the acoustic range of efficacy while assuming different folding physical sizes. The second metamaterial has the capacity

of keeping a permanent, consistent volume, which may allow openings thanks to their well-known negative Poisson's ratio [37,264]. Recent studies have associated such techniques with acoustic performances for mechanical devices improvement [158,265]. However, contemporary research is still seeking a significant impact on the combination of noise reduction and natural ventilation, in addition to architectonical sustainable solutions [84].

This section presents a novel acoustic design approach based on two acoustic metamaterials, enabling natural air ventilation while significantly reducing noise transmission. The two mechanisms (origami and auxetic) are applied to already tested acoustic structures to increase the dynamicity in noise reduction and ventilation capacity [84]. A metacage will be implemented by an origami system, while a metasurface will be implemented with an auxetic mechanism. These designs allow expansion and compression of the geometries, surrounding (Design 1 in Figure 4.1) or facing (Design 2 in Figure 4.2) a sound source. FEM simulations are performed with a frequency range between 100 and 5000 Hz to test the designs' effectiveness. In the first case, two extreme configurations are tested (unfolded and folded configuration). The possibility of using a transparent material to realise both the models give hints for also achieving natural lightning.

4.1.2 Methodology

4.1.2.1 Geometrical Settings

FEM simulation is employed to investigate the acoustic characteristics of both models. The boundary conditions and simulation set-ups are detailed in this section. Two design models are proposed to enable noise reduction and natural ventilation between two separate spaces. For the origami metamaterial (Design 1), the acoustic performance is tested with a monopole sound source inside the mechanism, aiming to screen the radiation towards outer space. In the bistable metasurfaces (Design 2), the acoustic mechanism works with a surface sound source facing the structure, reducing noise propagation towards the space behind it. In both cases, the sound wave and the air are meant to pass through a duct characterised by a number of connected cavities. This mechanism properly customised through a parametric study, is supposed to create a resonance effect and significantly influence the sound wave propagation and the TL within in the most sensitive frequency range for human's hearing system (50-5k Hz) [266].

The geometry in Design 1 is mainly composed of a deployable system that can achieve two configurations: unfolded and folded (respectively Figure 4.1.a and Figure 4.1.b). Indeed, the origami structure allows the valley and mountain folds to go from a circular shape of 0.256 m diameter to an

eight-point star shape (with 0.025 m length of each point's side). Internally, each point is characterised by an opening of 0.052 m each long (52% of perforation ratio of the entire boundary structure) and two cavities with 0.008 m depth created by three layers built starting from the perimeter surface of the metacage. These layers are modelled to leave at the centre of the point a resulting duct width of 0.008 m, allowing the air and acoustic wave to flow freely. Since in the unfolding, the main resonant structures (with the embedded cavities) are considered rigid, when the system moves to assume the unfolded configuration, they have a direction perpendicular to the centre with an angular difference of +30° (see Figure 4.1).

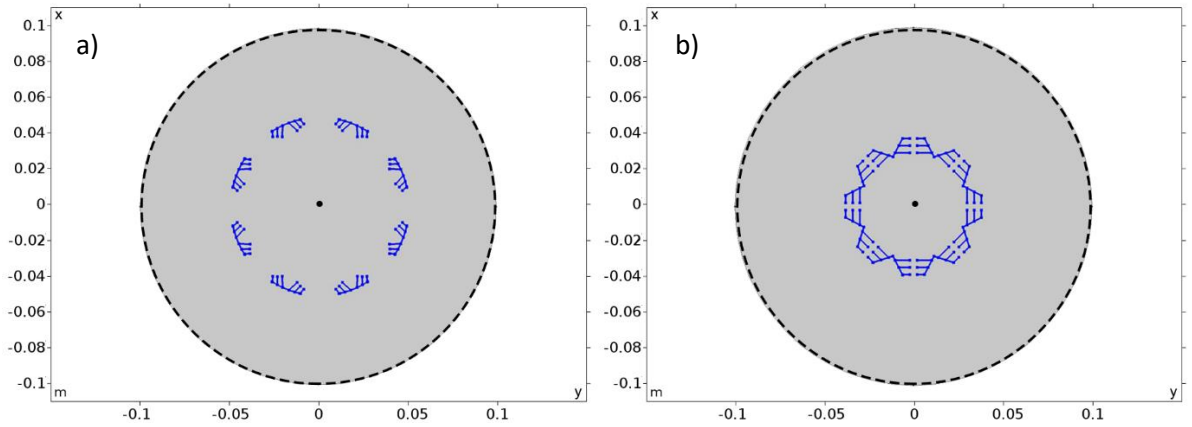

Figure 4.1 Geometrical configurations of Design 1 unfolded (a) and folded (b) and boundary conditions: central point source, interior sound hard boundaries (blue), and cylindrical free wave radiation (dashed line).

Design 2 is an auxetic metasurface generated from the coupling of two layers, each made by the repetition and connection of 4x4 basic squared units (each 0.01 m^2 wide and 0.02 m thick). Figure 4.2 shows how this unit is repeated and connected with the others through hinges applied on each one's four edges. In this case, the apertures through which air and soundwave pass have been reproduced by a statical hinge rotation effect on the perpendicular direction of the air and soundwave of 5° and 10° compared to the closed configuration (see Figure 4.2.c). This mechanism is used to study the relationship between the metasurfaces opening and its noise reduction potential. Moreover, the single resonant units (each rotating perforated cube) follow a displacement which globally can be identified with a negative Poisson's ratio material. When a stretching force is applied in one direction, the metasurfaces expand perpendicularly to the force application, and this is why the structure can be defined as auxetic. So, apertures are generated between the units thanks to global negative Poisson's ratio displacements of the metasurface structure, allowing the air and sound waves to propagate through them. Each opening has a 50% of perimeter surface removed, so, as in the previous case, a certain number of cavities face each opening, working as resonators (see Figure 4.2.c). The apertures which result from the negative Poisson's ratio effect (see Figure 4.2.a-c) leads to an opening ratio of 30% for the 10° configuration (see Figure 4.2.a) and 15% for the 5° one (see Figure 4.2.b).

Design 2 is characterised by two layers (four cavities facing the aperture, two per two of the blocks composing it). At the end of this section, further investigation of Design 1 and 2 will be explained, involving the relationship between TL and the models' thickness. For Design 1, two bigger models will be analysed, having respectively 0.4 and 0.8 m diameters in the folded configuration (the original one is 0.2 m). At the same time, Design 2 thickness effectiveness in terms of TL will be investigated by comparing the 2-layer basic configuration with a 4-layer or 8-layer one (having a total metasurface thickness of respectively 0.08 or 0.16 m).

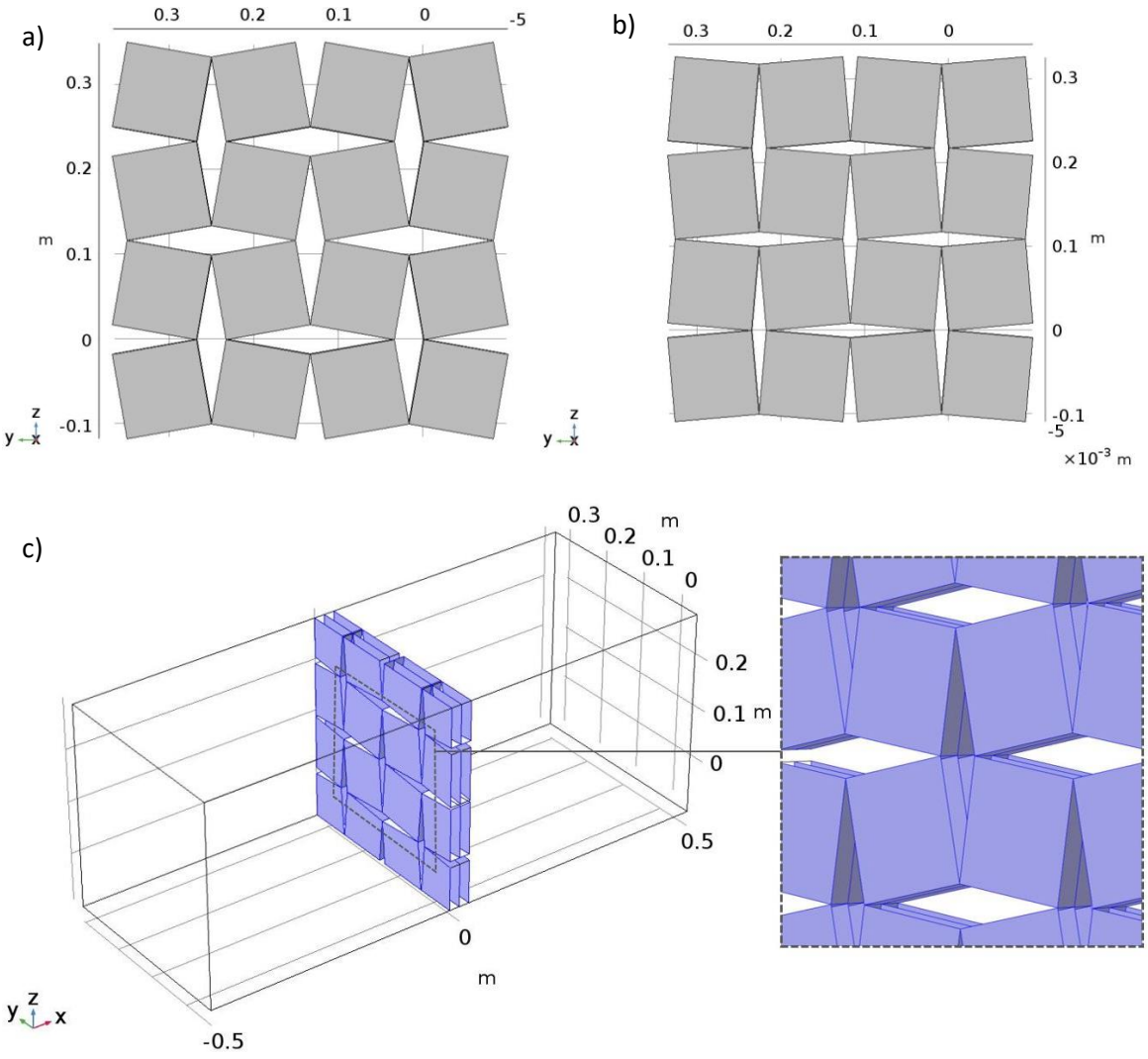

Figure 4.2 Geometrical configurations of Design 2, frontal view of a) 10° configuration and b) 5° configuration. c) Schematic of interior sound hard boundaries, highlighted in blue.

4.1.2.2 Boundary Conditions and Study Settings

The Acoustics module of a commercial FEM software, Comsol Multiphysics, is used to implement the numerical model. This software was chosen for its simplicity in managing differential equations related

to different geometry components and boundary conditions. Moreover, the multi-physical study capacity can be very useful and straightforward. For Design 1, a monopole point source is placed at the centre of the origami metacage with a volume flow rate is 0.01 m^2/s. At the outer boundary, cylindrical wave radiation is defined to simulate free outgoing waves without reflection. The simulation domain is filled with air, where air density and sound speed at room temperature are used. The metacage and material cells' walls are set as interior sound hard boundaries, as depicted in Figure 4.1. Sound transmission through walls of the metacage and possible viscous-thermal effect in the narrow resonator channels are neglected in this study, in order to approximate the worst resonating possible condition. Moreover, a numerical viscous-thermal acoustic model resulted too computationally expensive for the preliminary parametric study held in this phase. In Design 2, a plane wave radiation is applied to one of the ends of the 3D boundary volume (incident pressure = 1 Pa). This is a parallelepiped centred with the analysed geometry, having a length of 1 m (x-axis) and a width and depth of 0.38 each (y and z-axis). The opposite end of the boundary volume is characterised by air impedance. For both Design 1 and 2, the two displaced configurations were reproduced statically to focus the use of FEM only for the acoustic problem.

For Design 1, the TL is calculated mathematically within the simulation software, from the averaged SPL at the outlet boundary (dashed line in Figure 4.1) and the monopole source SPL (=130 dB), to compare the acoustic response in the unfolded and folded state. In Design 2, TL is calculated by the reduction of sound power through the metamaterial interface (in decibel). An increase in the TL curve will thus indicate less efficient sound transmission because sound energy is more confined in the two systems (Design 1 and 2). The mesh size is determined according to the FEM criterion, where at least six nodes are used to simulate a wavelength in air. The dimensions and the complexity of the geometric problems have defined two different frequency ranges of application. So for Design 1, to reach 5000 Hz, the maximum allowed element size is thus 343/6/5000=0.0114 m. Indeed, the study is a frequency domain analysis from 100 Hz to 5000 Hz with a step size of 10 Hz. The meshes characterisation of Design 2 instead has a maximum allowed element size of 343/6/3000=0.0114 m. Although this model results very complex and, since the convergence of results is proved, simplification is needed. So the maximum allowed element size is increased at 343/6/2000=0.0285 m. The study has a frequency domain that goes from 100 Hz to 3000 Hz with a step size of 10 Hz. In the results, the TL and SPL distribution are shown linearly and superficially within the simulation frequencies.

4.1.2.3 Parametric studies

The acoustic effectiveness of different metamaterials is tested through a parametric study in both models. Following the principle of resonant cavities used in quarter wavelength resonator [267] and acoustic black hole theory [268], 2D parameters such as 'cavities thickness' and 'duct width' have been investigated. These parameters have been studied throughout a number of configurations ranging between 0.006 configurations for the first one (a= 0.006-0.008-0.010 m) and three for the second one (b= 0.006-0.008-0.010 m). In Design 1 each side has two cavities positioned towards the centre (upper section and lower section), delimited by layers that start from the sides and extend towards the middle of it for respectively 0.008 m, 0.012 m, and 0.016 m, and cavities width as 0.08 m (see Figure 4.3). In Design 2, the parametrization is performed with straight sides and geometry defined by cavities width and layers length. In this case, the layers' length is set the same for all, respectively 0.04 m, 0.06 m, and 0.08 m, and cavities width as 0.01 m, 0.02 m, and 0.03 m (see Figure 4.3). The parameterisation is set to see if there are any significant correlations between the cavities or the duct's width and the consecutive *TL* behaviour.

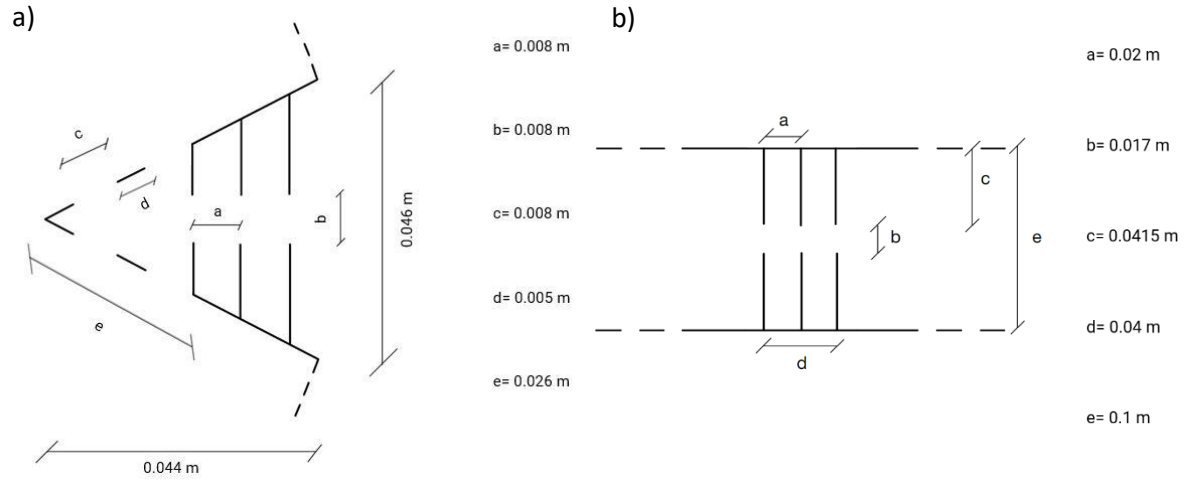

Figure 4.3 Schematic and dimensions of the metamaterial unit formed in the folded state for a) Design 1 and b) Design 2.

4.1.3 Results of the Origami Metacage analysis (Design 1)

4.1.3.1 Numerical Results of Origami metacage

Figure 4.4 first shows the simulation results of Design 1 in the folded and unfolded state. The *TL* is between 8 dB and 30 dB, where some variations can be observed due to the circular enclosure's resonance. From the *TL* graph (Figure 4.4.a), both the unfolded and folded configuration effects are analysed. For the folded one, the *TL* performance is significant at low frequencies (average of 20 dB

of *TL*), while at medium frequency, it loses efficacy, and from 2500 Hz to go on, an increasing sinusoidal behaviour starts, with a *TL* average of 18 dB and a *TL* peak of 22 dB at 3900 Hz. Figure 4.4.b and Figure 4.4.c highlight the confinement effect of the *SPL* at the different *TL* peak frequencies for both unfolded and folded configurations. Both graphs show how the unfolded state has a slightly higher acoustic impact on the sound wave confinement.

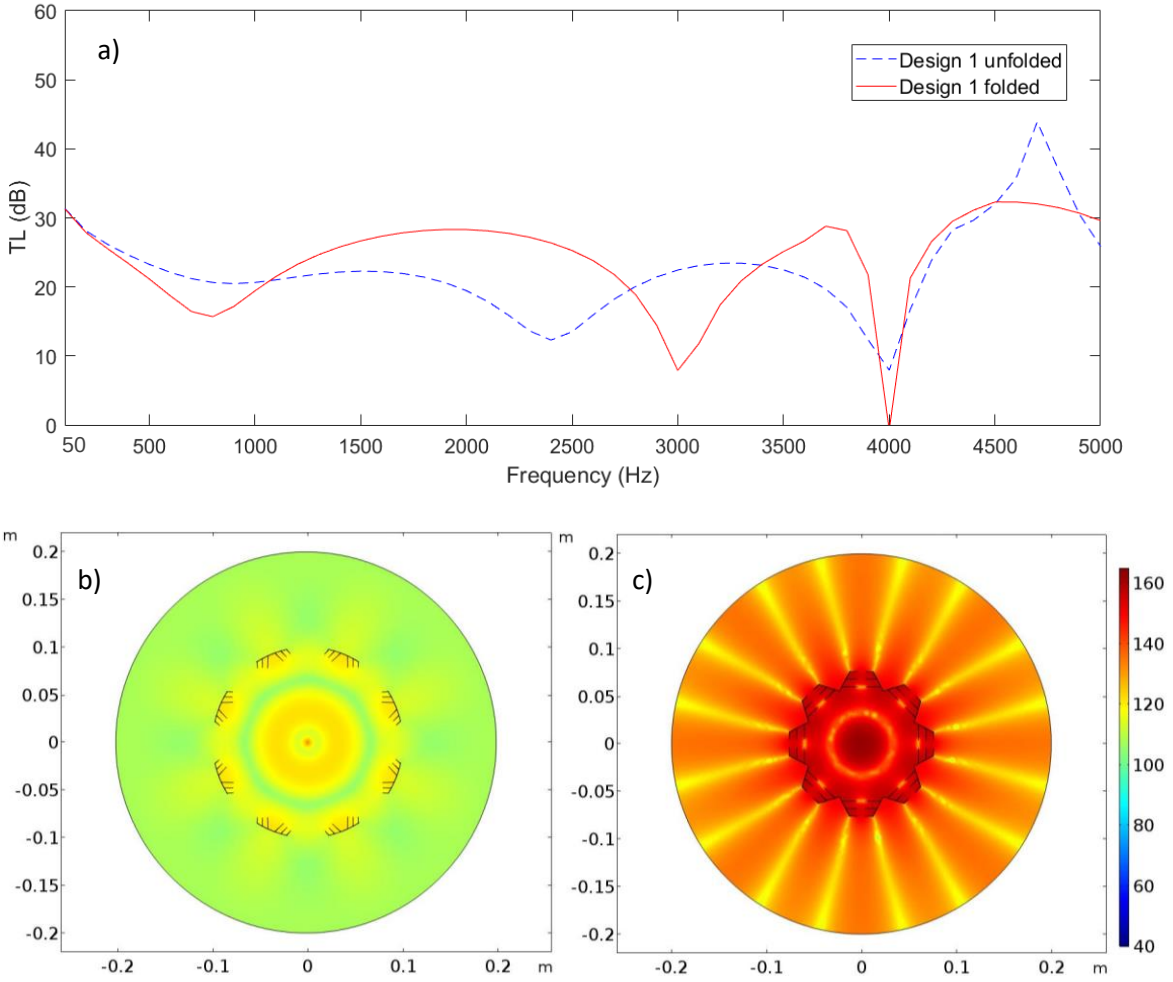

Figure 4.4 a) Schematic of the Origami Metacage's TL (unfolded and folded configuration), and SPL distribution graph for 0.2 m Design 1 at b) 3000 Hz of the unfolded and c) 3900Hz of the folded configuration.

4.1.3.2 Parametric study on cavities' dimensions' ratio

Figure 4.5 shows the average behaviours according to two parameters: cavities thickness and duct width. From the nine combinations of the three per three options of two different variables (see schematic in Figure 4.3), these variables were considered: a_1=b_1=0.006 m, a_2=b_2=0.008 m, a_3=b_3=0.01 m. The results show that either the cavities or the central duct width change do not affect the acoustic metasurface performance. So the configuration a_2 and b_2 can be set as standard (a_2=b_2=0.008 m) to

guarantee a significant sound reduction performance and sufficient ventilation at the same time. Indeed, the acoustic and airwave propagation from the inside to the outside of the metacage and vice versa is guaranteed by the resulted duct of width 0.008 and cavities total thickness of 0.016 m.

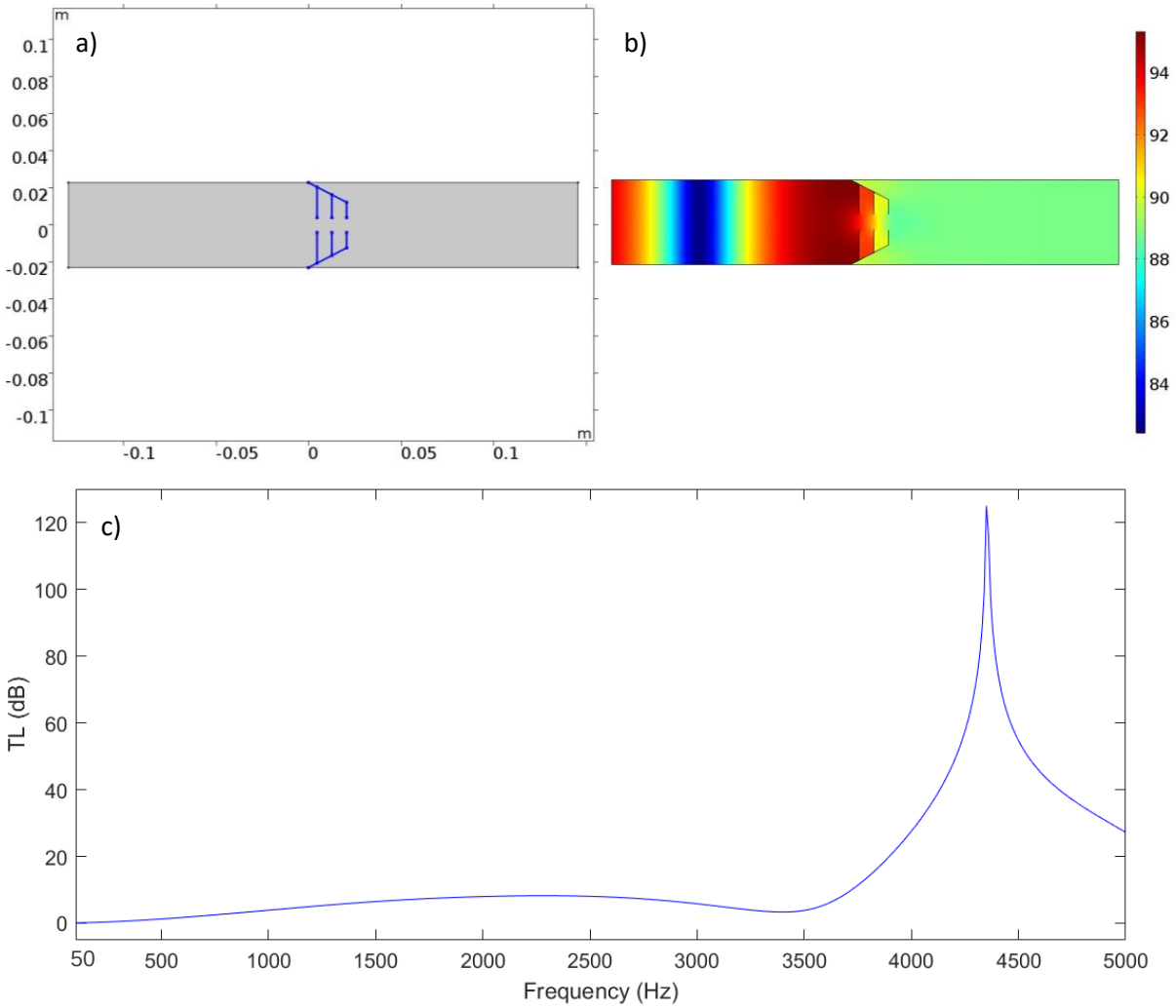

Figure 4.5 TL Parameterisation for conical duct as the one in Design 1: a) geometrical setting (internal boundary in blue), b) SPL distribution at peak frequency 4400 Hz, c) TL.

4.1.3.3 Comparison of the Different Scaled Models

The *TL* increase is correlated with the dimension of the device. For the sake of completeness, wider samples of Design 1 are built and analysed through the same acoustic simulation settings. So results will be presented, comparing the original model's performance with those of diameter equal to 0.4 and 0.8 m. From Figure 4.6, it is clear that, as expected, the increasing of the dimensions (two and four times bigger in this case) causes a shift of the *TL* peak towards lower frequencies. In particular, for the folded configuration, in the 0.4 m model, the peak is at 4000 Hz (Figure 4.6.a) with a *TL* of 83dB. This phenomenon happens consistently and progressively with the increasing of the models, and it is

demonstrated by the following study, with dimensions ten times bigger than the original ones. For the 0.8 m models, the peak is at 2000 Hz, where *SPL* is 89dB (see Figure 4.6.b).

From Figure 4.6, the effectiveness of the origami metacage is demonstrated in the selected frequency range, and the contribution of the folded configuration in this process is proved.

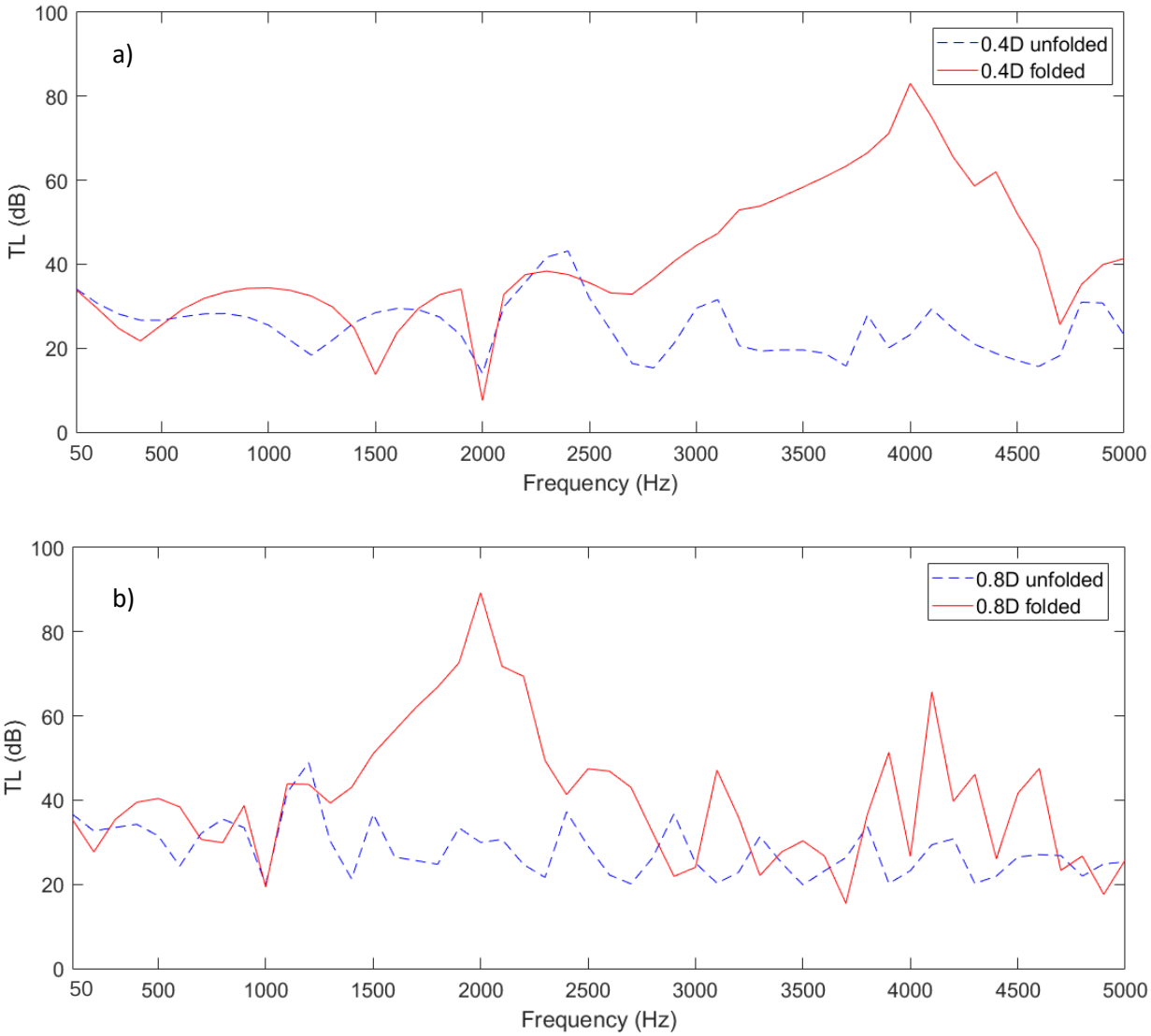

Figure 4.6 TL comparison of Design 1 (unfolded and folded) with different diameters dimensions: a) diameter = 0.4 m, and b) diameter = 0.8 m).

4.1.4 Numerical Results of Acoustic Bistable Metasurface (Design 2)

4.1.4.1 Numerical Results of the Acoustic Metasurface

Figure 4.7 shows the simulation results of Design 2. A slice graph representing the SPL distribution is placed at the middle of the metasurface height to compare the two models' effect (with 10° tilt and

5° tilt). The *TL* behaviours are very similar in both configurations (10° and 5° rotating angles) but shifted on lower results for the 10° one. Overall, the *TL* is between 0 dB and 51 dB, where some variations can be observed due to the resonance of the cavities facing the duct's openings. The *TL* has a sinusoidal behaviour at low-medium frequencies (500-1500 Hz, average of 7 dB), while in the upper-medium frequency range (1500-3000 Hz), it increases in efficacy, with a *TL* average of 23 dB and a *TL* peak of 51dB at 1700 Hz. Figure 4.7.b highlights the confinement effect of the *SPL* at the *TL* peak frequency for both 10° and 5° tilt configurations.

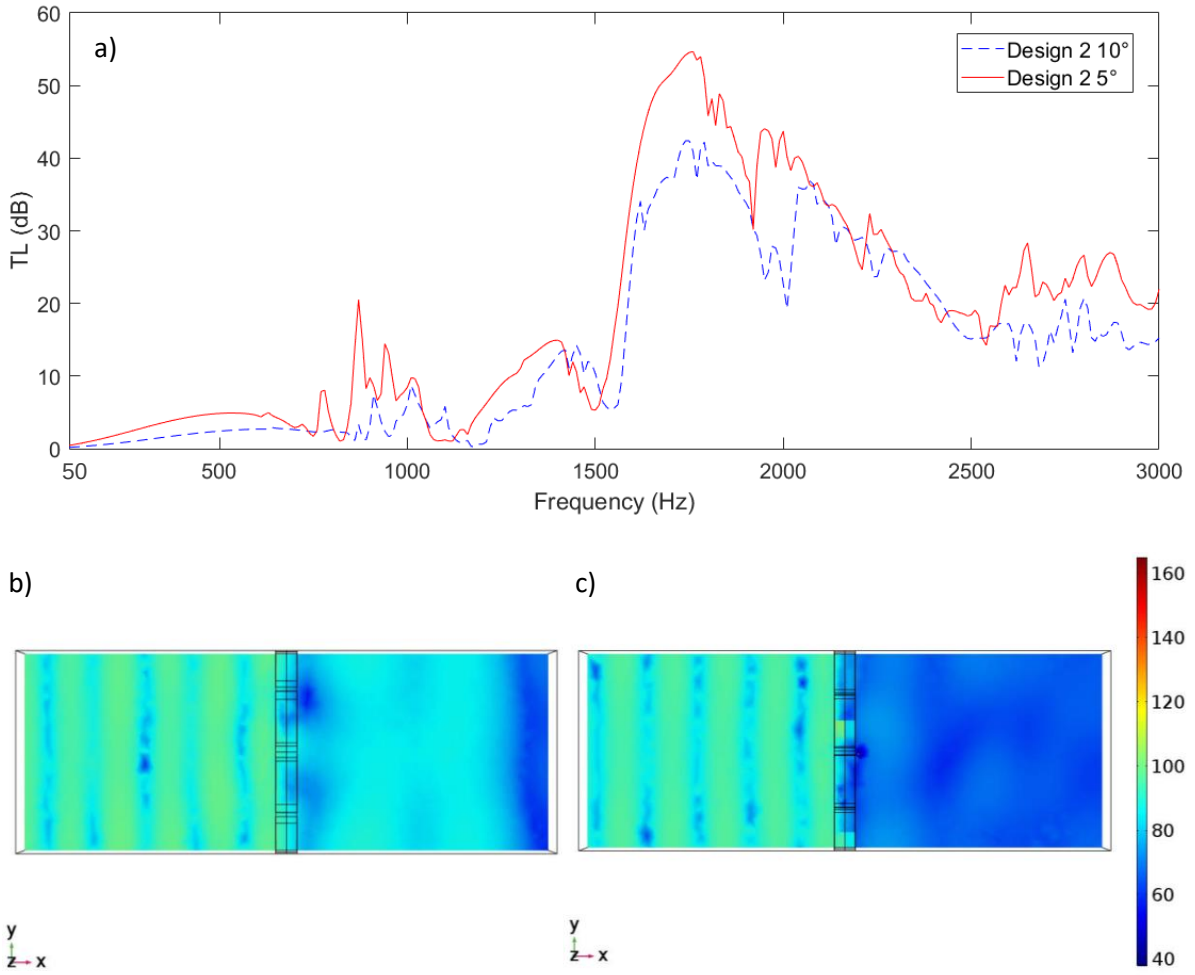

Figure 4.7 a) Graph representing TL and SPL distribution graph for b) Design 2 with 10° tilt at 1800 Hz and c) Design 2 with 5° tilt at 1700 Hz.

4.1.4.2 Parametric study on cavities' dimension's ratio

Figure 4.8 shows the average behaviours according to the two variables considered: cavities thickness and duct width. From the nine combinations of the three per three options of two different variables (see schematic in Figure 4.3), these variables were considered: $a_1=b_1=0.01$ m, $a_2=b_2=0.02$ m,

a_3=b_3=0.03 m. The results show that either the cavities or the central duct width change do not affect the acoustic metasurface performance. So the configuration a_2 and b_2 can be set as standard (a_2=b_2=0.02 m) to guarantee a significant sound reduction performance and sufficient ventilation at the same time (see duct formed by the coupling of the cavities in Figure 4.8.a,b). Indeed, the acoustic and airwave propagation from the inside to the outside of the metacage and vice versa is guaranteed by the resulted duct of width 0.017 and cavities total thickness of 0.04 m.

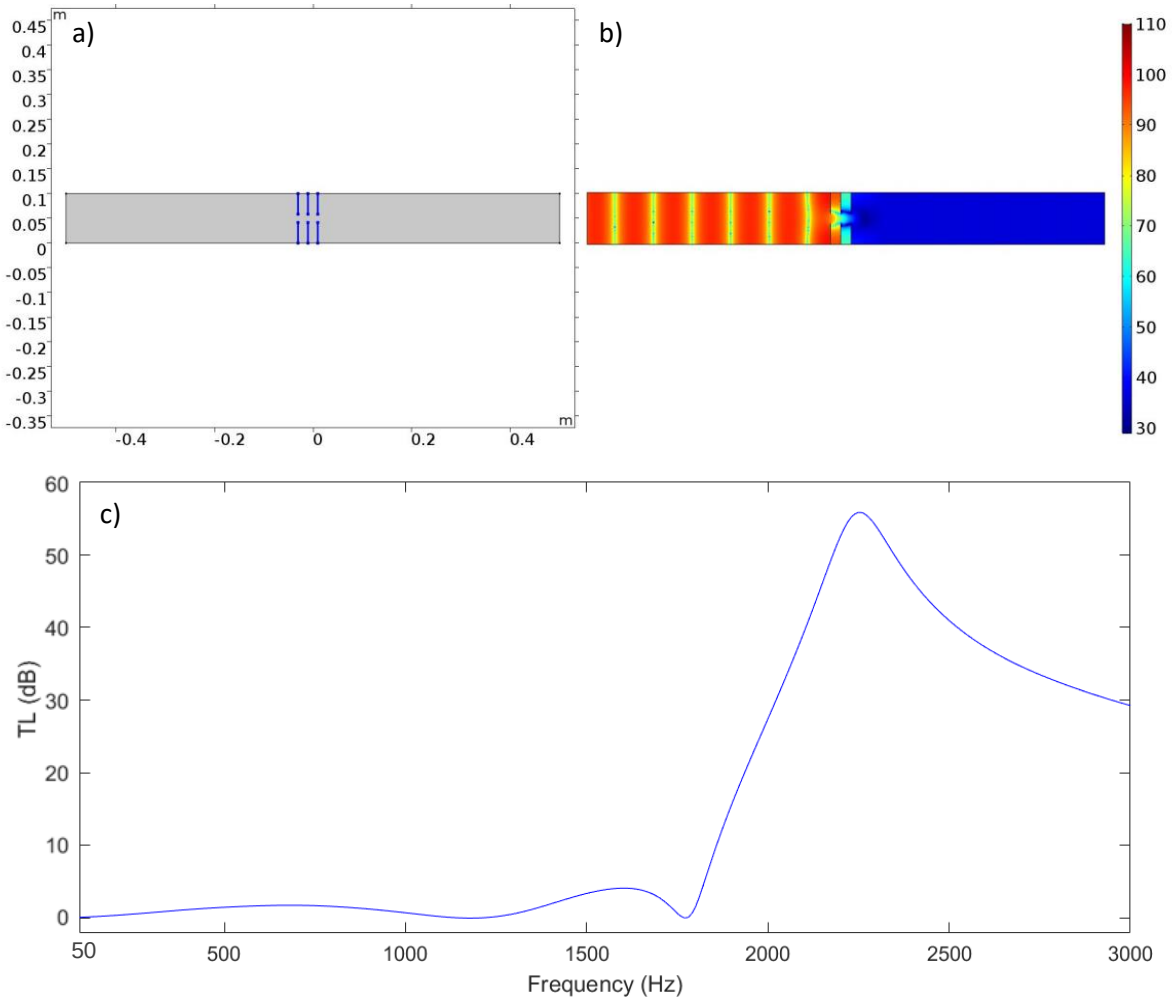

Figure 4.8 TL Parameterisation for straight duct reproducing the one in Design 2: a) geometrical setting (internal boundary conditions in blue), b) SPL distribution at peak frequency 2300 Hz, c) TL.

4.1.4.3 Comparison of the Different Scaled Models

Differently from Design 1, the TL increase is not significantly correlated with the dimension of the device. For the sake of completeness, thicker samples of Design 2 are built and analysed through the same acoustic simulation settings. The results are presented in Figure 4.9 and allow us a comparison

between the original model's performance and those of overall thickness equal to 0.08 and 0.16 m. From Figure 4.9, it is clear that there is no shift of the *TL* peak while increasing the metasurface thickness. In particular, a significant result is the different tendencies of the 10° and 5° tilt configurations. While the *TL* associated with the first one decreases its amplitude around the peak frequency range (1500-2500 Hz), the second increase significantly. The peak is always around 1700 Hz, but the amplitude is different. For the four-layer models, the *TL* peak is indeed 67dB (1760 Hz) for the 5°tilt configuration, and it is averagely 38 dB for the 10° one (much spread and less concentrated than the previous one). The eight-layer model *TL* peak is lower again for the 10° tilt configuration (averagely 40 dB) while increases with a maximum peak of 77 dB for the 5° tilt model at 1740 Hz.

Generally, from Figure 4.9, the auxetic metasurface's effectiveness appears not to be connected significantly with the thickness increase. Excluding the isolated most evident peak, the graph shows a similar overall TL behaviour related to the model with 2, 4, and 8 layers of Design 2; However, for the sake of completeness, quantitative approach is also used to compare these Design 2 configurations. So, with the aim of quantifying the discrepancies between each configuration (with different opening degree and thickness), the root mean square (RMS) deviations has been calculated on the overall frequency range (50-3kHz): 0.35 between 4 Layers with 10° and 5°, 0.24 between 4 and 8 Layers configurations with 10° of rotation, 0.31 between 8 Layers with 10° and 5°, 0.18 between 4 and 8 Layers configurations with 5° of rotation. From these values, it is confirmed that the rotation angle (10°, 5°) seems to affect the results more than the layers' number (4, 8 layers). This means that, differently from Design 1, a two-layer model might be enough to allow natural ventilation and reduce noise on a broader frequency band.

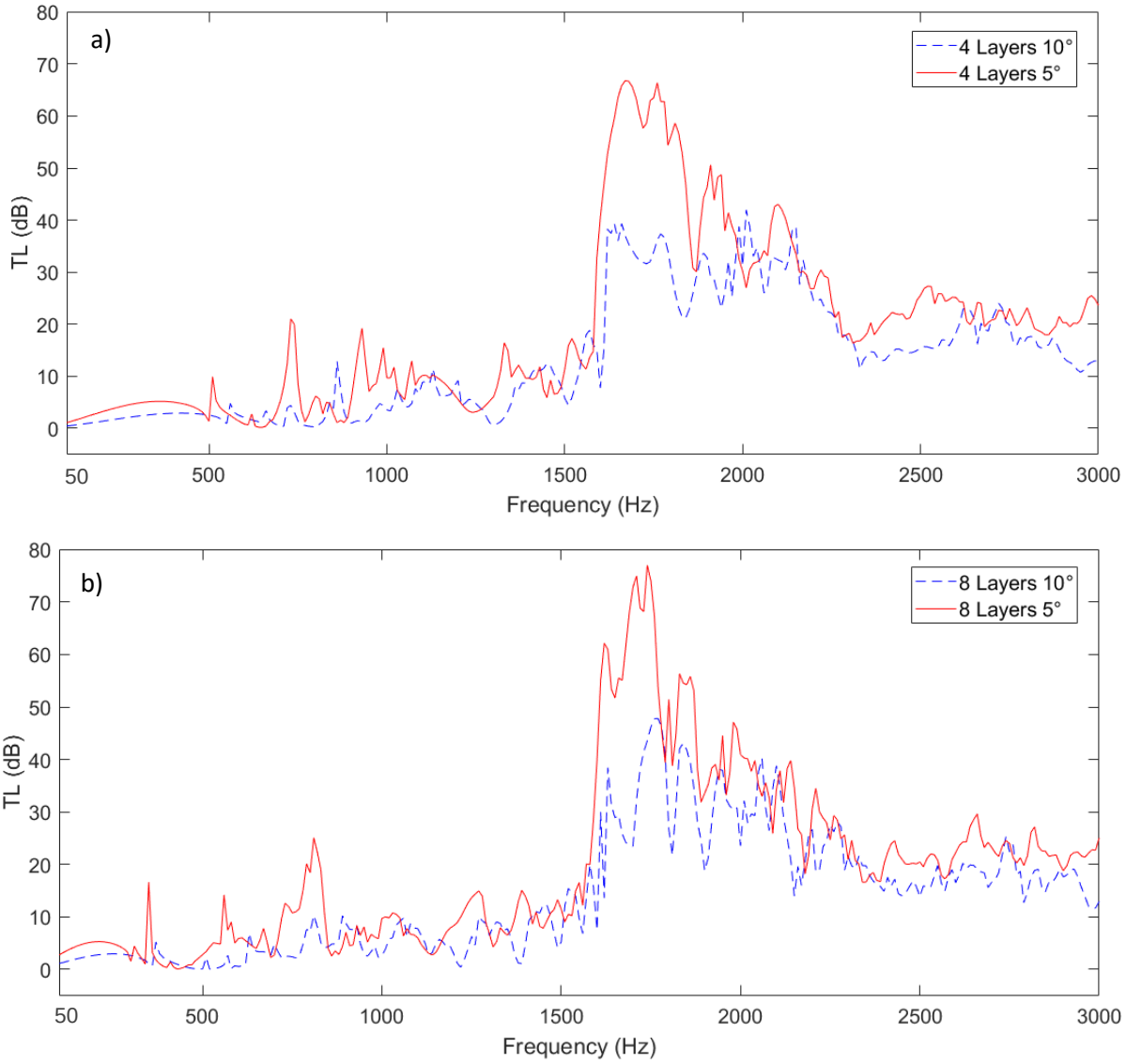

Figure 4.9 TL comparison of Design 2 (with 10° and 5° tilt) with different thicknesses: a) thickness = 0.4, and b) thickness = 0.8 m.

4.1.5 Discussion on design applications

This chapter study's main aims are achieved, and further numerical improvement or experimental study on the model will give more completeness to the research. So now, new possibilities are open for devices' design which aim noise reduction together with natural ventilation. The proposed geometry may be embedded in a window design. The resulting *TL* broad peaks of 54, 67, and 77 dB (two, four and eight-layer model) might impact a situation where the application area is affected by high-level noise. Design 1 could embed a system of origami metacage ducts in window frames or use the structure itself with increased width and a transparent back panel to allow light exchange between two environments. The structure of Design 2 could be used as a transparent panel for windows

enclosures. A further parameterisation and validation work will follow to test the actual building feasibility of the prototypes and determine whether the use of transparent materials might affect their performance or allow a new generation of tunable window systems.

4.1.6 Conclusions

In this project section, the proposed acoustic metamaterials' characteristics with a unique reconfigurable mechanism have been investigated. Different configurations with specific ventilation designs have been tested to assess the noise reduction and estimate the ventilation volume between the two areas separated by the devices: the inside and the outside for Design 1 (52% of opening ratio) and front and back for Design 2 (from 15% to 30% of opening ratio). Both models show high peaks in the *TL* due to each metamaterial unit's effective silencing effect in front of the ventilation apertures. In different effective ways, the effective region's frequency and bandwidth are related to the geometric parameters and scales of the systems. The potential of the proposed devices to be used in ventilation window systems is proved since natural ventilation is possible without any additional elements. Better ventilation and noise reduction in the desired frequency range can be achieved by developing further numerical models for optimising the devices in terms of size and shape.

Due to the findings highlighted in Chapter **Participatory approach to draw ergonomic criteria for window design**, noise reduction, and natural ventilation are as important as the outdoor environment's visual connection to make the user feel oriented. For this reason, the Origami metacage seems to perfectly suit this aim due to the availability of a plain central panel. In the next section, its deployability and parameters are further optimally investigated both analytically and numerically.

4.2 Origami Metacage deployability

In this chapter, one of the previously investigated AMMs, the Origami Metacage, is investigated, particularly focusing on its deployability. A system with foldable origami metamaterial which allows noise reduction and natural ventilation is presented. The proposed device allows air exchange between the interior and exterior domains, and it forms an omnidirectional acoustic metacage in the folded state. The design concept of the proposed device and the important design parameters were elaborated in this second phase. The sound reduction performance was investigated using FEM simulations again. The numerical method developed in this work can facilitate the optimisation of origami metamaterial for real window designs, starting from a circular enclosure and then adapting it

in a more ergonomic or geometrically standard way. The main aim of this part of the study is indeed to corroborate the numerical-parametric investigation method, while ergonomic adaptation will follow in the next chapters.

4.2.1 Background

As mentioned in Section **Sound insulation**, conventional acoustic techniques allow controlling sound waves within a limited range of frequencies. Noise control devices are bulky to operate in the typical airborne noise frequencies [8,54,59,269]. Acoustic metamaterials are versatile due to their excellent properties related to their physical size [37,270]. Particularly, origami metamaterial greatly extends the tuning ability and design range of existing metamaterial benefiting from its unique geometric flexibility. Recent studies have shown that origami folding can be combined with appropriate acoustic and mechanical design to improve performance in many regards [84,158,264]. Based on the origami concept and the encouraging results, metamaterial window design with a specific aim to achieve both noise reduction and ventilation can be further improved.

This section presents the second phase of the study of AMMs for natural ventilation window design. First, the conceptual design of a novel origami acoustic metacage, of which the performances are tunable during the reconfigurable process, is investigated. The working principle for noise reduction is similar to the acoustic metacage structure proposed earlier [271], while origami enables a unique mechanism to effectively vary the acoustic and ventilation characteristics in the folded and unfolded state. Starting from the metacage concept, a design to allow expansion and compression of circular boundary surrounding a sound source is developed, as illustrated in Figure 4.10. Unique structural design on the boundary forms a couple of metamaterial units in the folded state, controlling sound wave radiation to the exterior domain through the ventilation apertures. Two types of ventilation conditions are considered in this study. According to Figure 4.10, Design 1.a has distributed perforations along the perimeter, while Design 1.b has ventilation apertures and a much larger ventilation volume. In the first case, the open ratio (open surface/total perimeter) is 32%, while in the second is 52%. The folded and unfolded configurations of the two designs are compared in Figure 4.10. As a preliminary study, only the two extreme configurations (completely folded and unfolded) are tested using 2D Finite Elements Method (FEM) simulations, to demonstrate the dramatic change in the acoustic property resulted from the origami metamaterial.

This section aims to demonstrate the effectiveness of this novel metamaterial for window applications. This model can be used at different frequency ranges (100-10000Hz), and several dimensions (0.2, 1,

and 2 m in diameter) are tested to show the shift of working frequency as the system size changes. Thus, the device can be incorporated into a window without obstructing natural lighting from the outdoor environment. An inversely proportional correlation between shifting the most affected frequency range and the model dimensions are expected. This phenomenon should be accompanied by a Sound Pressure Level (*SPL*) dip, in accordance to the metamaterial's resonator nature.

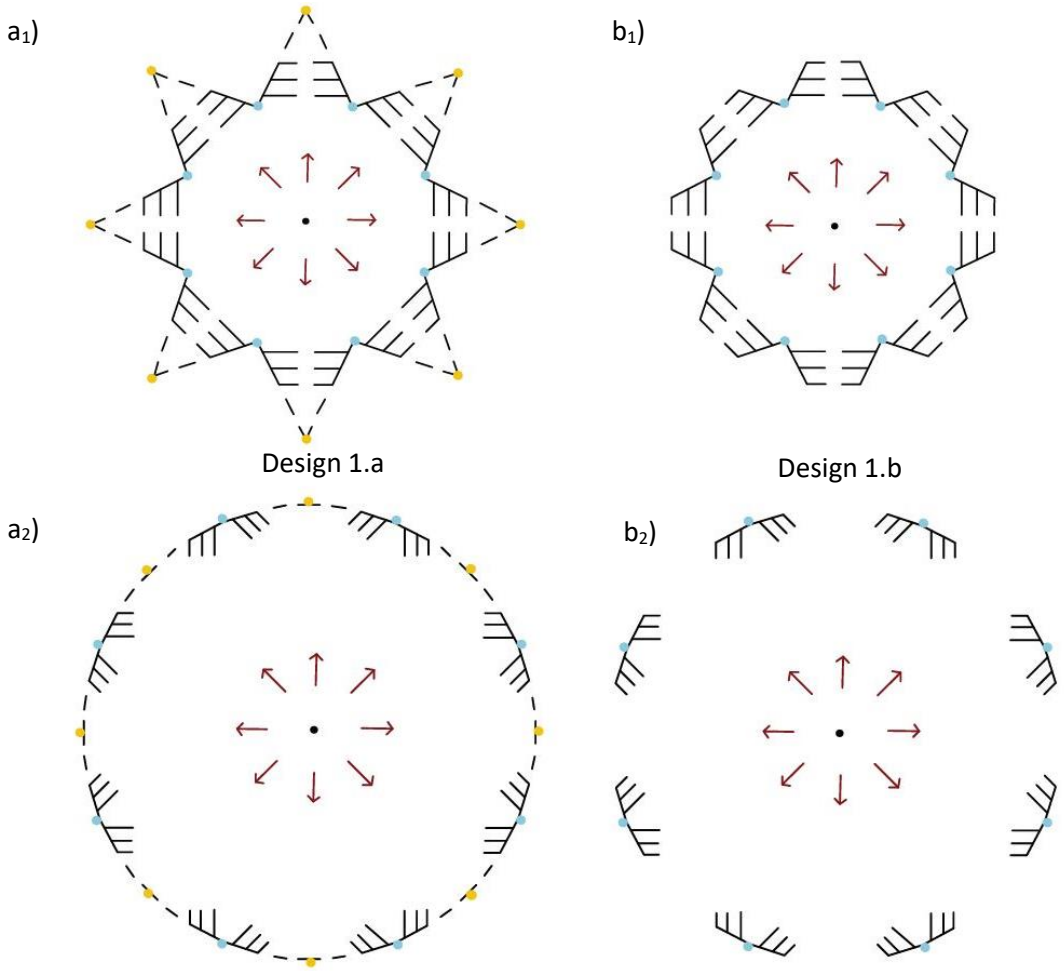

Figure 4.10 Schematic of a1) Design 1.a (Origami metacage with perforations) and b1) Design 1.b (Origami metacage with apertures) in the folded and a2,b2) unfolded state. The yellow and light blue dots denote the folding points' movements along the boundary: valley folds (light blue) and mountain folds (yellow).

4.2.2 Methodology

4.2.2.1 Geometrical Setting

The acoustic wave propagation is set to be originated from the interior of the origami metacage and radiates out through the distributed ventilation holes along the surface. Thus, the actual 3D system

can be viewed as a protrusion from the 2D plane, where each cross-section has the same geometry. For this reason, 2D simulation is carried out for the sake of computation efficiency. The 2D FEM model represents the origami metacage, and the folded and unfolded configurations are illustrated in Figure 4.11. The diameter of the metacage (refer to unfolded state) is 0.2 m and 0.4 m for the circular outer boundary. This diameter ratio of 1:2 is kept the same for all the simulation cases with different scales, which will be tested later to understand the effect of system size on the frequency range.

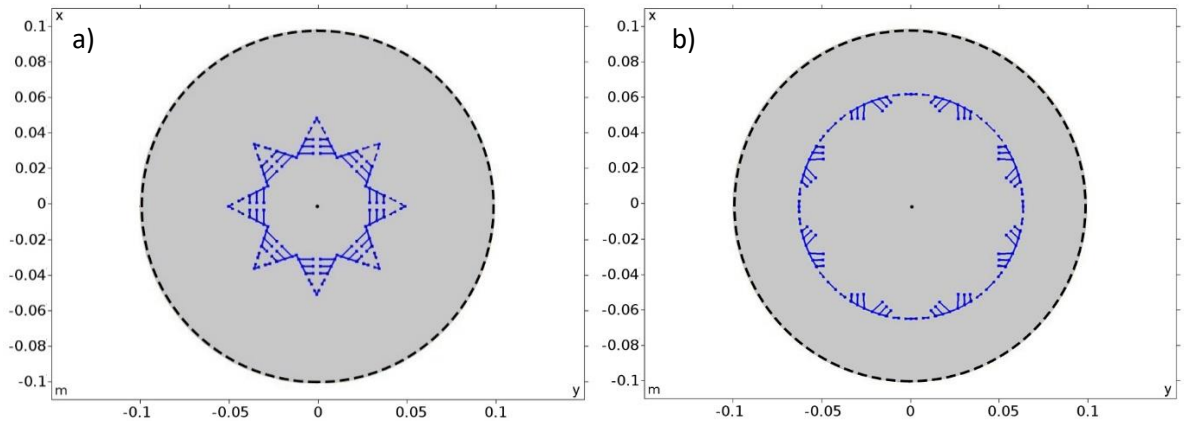

Figure 4.11 Geometrical configurations of Design 1 (a) folded and b) unfolded) and boundary conditions: central point source, interior sound hard boundaries (blue), and cylindrical free wave radiation (dashed line).

The folded configurations represent a 2D octagonal star (eight points) with a 0.05 m length on each side. In each of these extremities, two cavities are positioned towards the centre of the triangular point, delimited by layers that start from the sides and extend towards the middle of it for respectively 0.008 m, 0.012 m, and 0.016 m, and cavities width as 0.008 m (see Figure 4.11). A parametric study, done to see an acoustic effectiveness difference while changing those components dimensions, supports the setting up of both cavities and central duct's dimensions (see Figure 4.12). The parametric study took in consideration three width configurations for the cavities (a= 0.007, 0.008, 0.009 m) and three for the central duct (b=0.007, 0.008, 0.009 m). The results show that the cavities width change does not affect the metacage performance, so that the a_2 configuration will be used for the next parametric study. The next results show that the central duct width change does not affect the metacage performance in the considered terms of dimension changing. So the configurations a_2 and b_2 can be set as standard, as explained before. The resulted duct of width 0.008 m and the four holes of 0.008 m length each on the point guarantee the acoustic and airwave propagation from the inside to the outside of the metacage and vice versa. When the geometric configuration passes from the folded to the unfolded one (see Figure 4.11), each extremity's sides open and generate a circular perimeter shape. The holes rotate with the sides, and the layers that constitute the cavities rotate until they are oriented towards the centre with displacement from the direction perpendicular to it of 30° (see Figure 4.11).

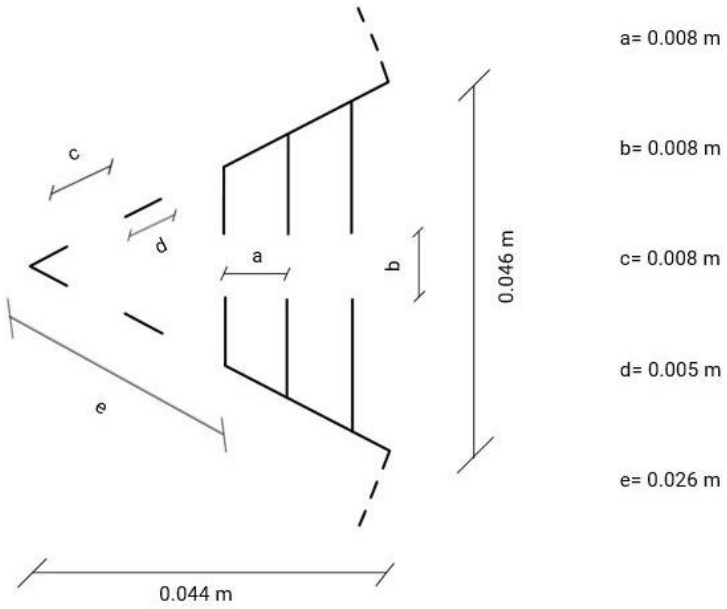

Figure 4.12 Dimensions of the metamaterial unit formed in the folded state for Design 1.

4.2.2.2 Boundary Conditions and Study Settings

The numerical model is implemented using commercial FEM software Comsol Multiphysics under the Acoustics module. A monopole point source is placed at the centre of the origami metacage with a volume flow rate of 0.01 m2/s. At the outer boundary, cylindrical wave radiation is defined to simulate free outgoing waves without reflection. The simulation domain is filled with air, where air density and sound speed at room temperature are used. Finally, the metacage and material cells' walls are set as interior sound hard boundaries, as depicted in Figure 4.11. Sound transmission through walls of the metacage and possible viscous-thermal effect in the narrow resonator channels are neglected in this study.

The SPL is averaged at the outlet boundary (dashed line in Figure 4.11) to compare the unfolded and folded state's acoustic response. A decrease in the SPL curve will thus indicate less efficient sound radiation because sound energy is more confined in the metacage. The mesh size is determined according to the FEM criterion, where at least six nodes are used to simulate a wavelength in air. The maximum allowed element size to reach 10000 Hz is thus 343/6/10000=0.0057 m. The study is a frequency domain analysis from 100 Hz to 10000 Hz with a step size of 100 Hz. In the results, the SPL radiation is shown linearly in the simulation frequencies.

4.2.3 Design 1.a Results

Figure 4.13 first shows the simulation results of Design 1.a in the folded and unfolded state. The averaged SPL at the radiation boundary is between 40 dB and 120 dB, where some variations and peaks can be observed due to the circular enclosure's resonance. The SPL radiation graph (Figure 4.13.a) shows that both the folded and unfolded configuration effects are analysed. For the folded one, the SPL radiations reduce significantly at low frequencies (average of 106.6 dB of SPL), while in medium frequency, it loose efficacy, and from 2500 Hz and above, an increasing sinusoidal behaviour starts, with a SPL average of 90 dB and a SPL dip of 48.7 dB at 8100 Hz. Figure 4.13.b and Figure 4.13.c highlight the confinement effect of the SPL at the different dip frequencies for both unfolded (dip at 4700Hz) and folded (dip at 8100 Hz) configurations. In both graphs, it is evident how the folded state has a higher acoustic impact on the sound wave confinement.

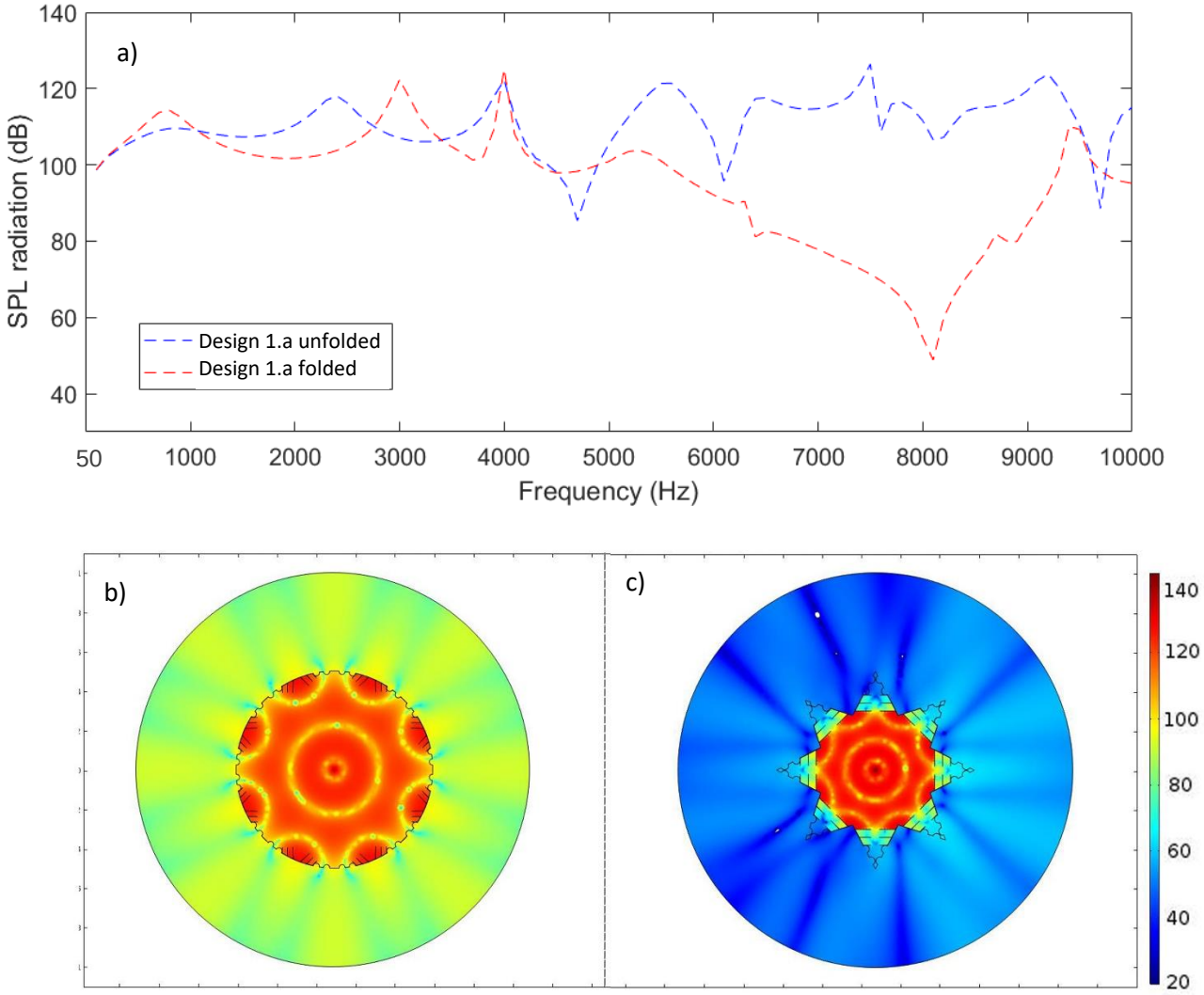

Figure 4.13 Graph of a) SPL radiation and schematic of SPL distribution for 0.2 m Design 1 at b) 4700 Hz of the unfolded and c) 8100Hz of the folded configuration.

4.2.4 Design 1.b Results and Comparison with Design 1.a

In the next section, the results of Design 1.b are analysed and compared with Design 1.a. The graphs in Figure 4.14.a and Figure 4.14.d show that the two samples' acoustic behaviours are the same. This conclusion is visually supported by the SPL distribution graphs in Figure 4.14.b and Figure 4.14.c, which shows how similar the distribution of the colour is. For Design 1.b, both graphs show clearly how the folded state confine the sound wave in the internal part with more effectiveness. This comparison result (between Design 1.a and Design 1.b) is significant to understand how the design can allow a better ventilation condition without affecting the device's acoustic performance. As explained in the introduction about purposes, this improvement is needed to have proper ventilation of the contained mechanical or physical system.

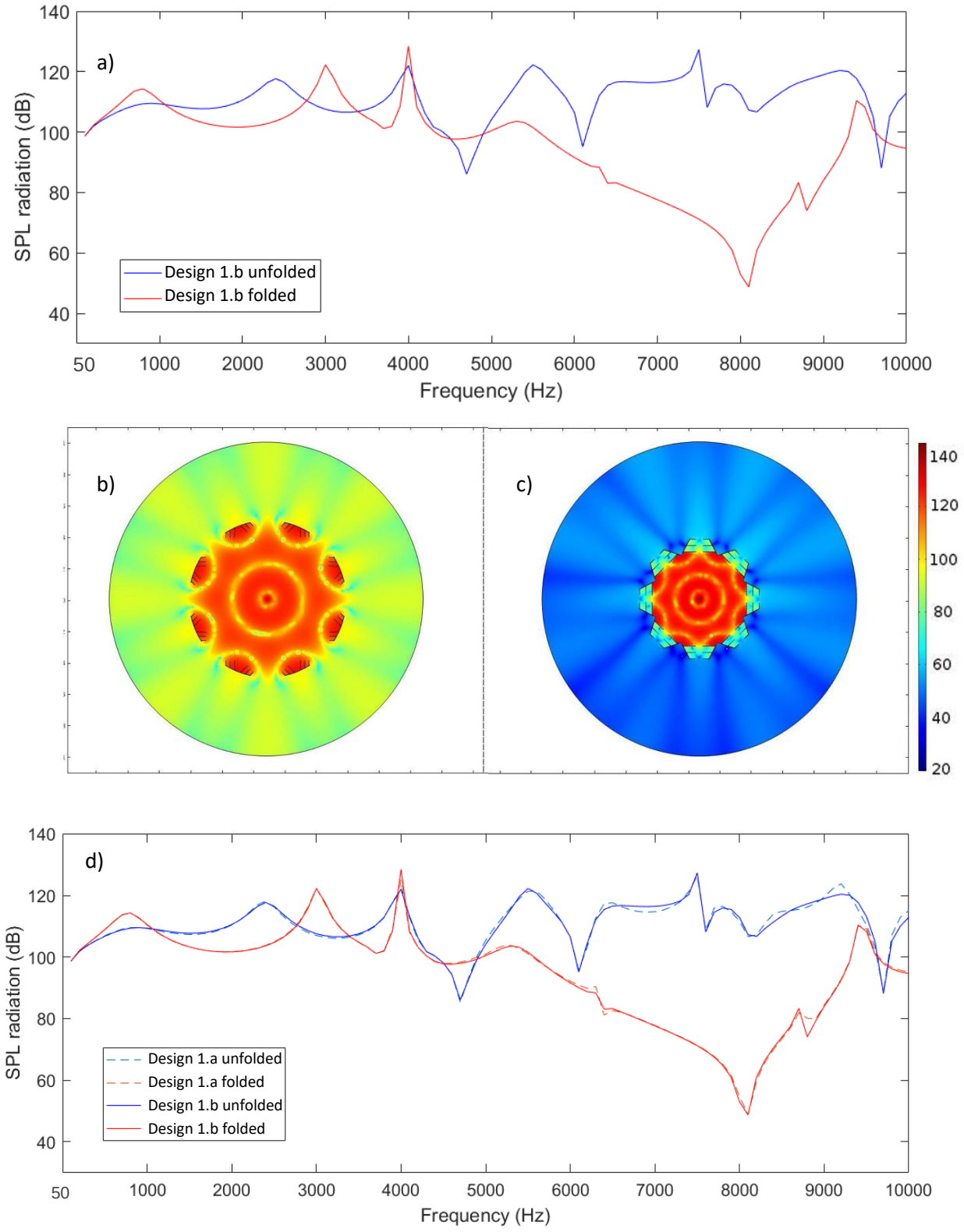

Figure 4.14 Graph representing a) the SPL radiation and schematic of SPL distribution for 0.2 m Design 1.b at b) 4700 Hz of the unfolded and c) 8100Hz of the folded configuration. d) Comparison between SPL radiation of Design 1.a and Design 1.b.

4.2.5 Comparison of the Different Scaled Models

This section focuses on the correlation between the device's dimension and its *SPL* reduction effect. In order to investigate the general relation between the models dimension (here called 'diameter' to easily refer to wideness of the circular enclosure) and the acoustic performance, bigger samples of both Design 1.a and Design 1.b are analysed through the same acoustic simulation settings. Although, since the performance of Design 1.a and Design 1.b is mostly identical from the folding point of view, and since the second one allows a more direct air flow inside-out the model, it can be reasonable to consider only the second one to further investigate the relationship between the enclosure diameter and the acoustic performance. So for the sake of simplicity, only results related to Design 1.b will be presented, comparing the performance of the original model with those of diameter equal to 1 and 2 m.

From the results, it is clear that, as expected, the increasing of the dimensions (five and ten times bigger in this case) causes a shift of the *SPL* reduction peak towards lower frequencies. In particular, for the folded configuration, in the 1 m model, the dip is at 1600 Hz (Figure 4.15) with a *SPL* of 38.25 dB. This phenomenon happens consistently and progressively with the increasing of the models, and it is demonstrated by the other study with dimensions ten times bigger than the original ones. For the 2 m models, the dip is at 800 Hz, where SPL is 31.95 dB. From Figure 4.15, the effectiveness of the origami metacage is demonstrated in this frequency range, and the contribution of the folded configuration in this process is proved.

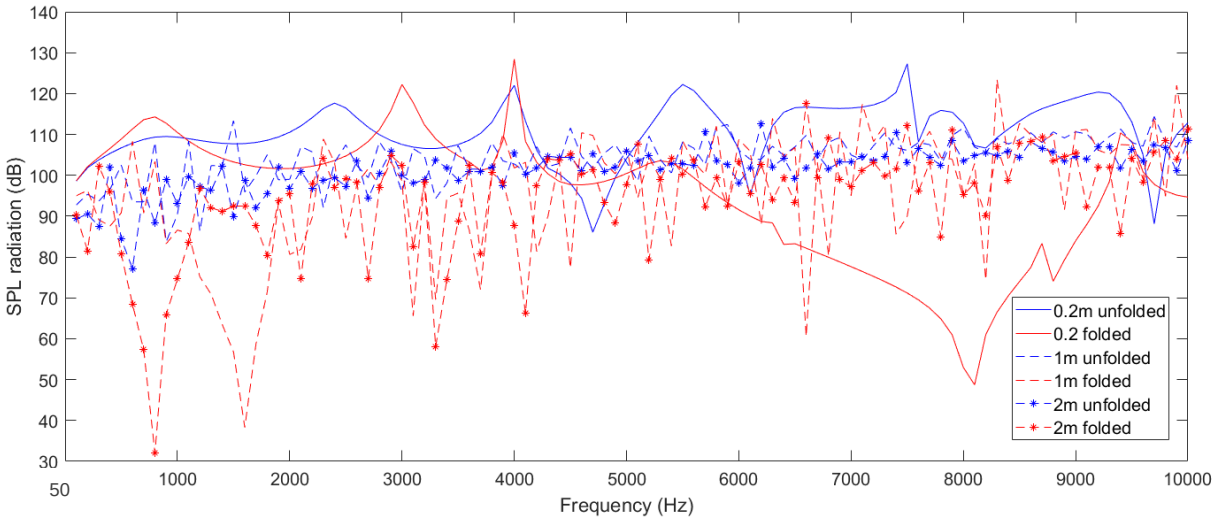

Figure 4.15 SPL radiation of Design 1.b with 0.2, 1, 2 m diameter.

4.2.6 Discussion on design applications and Conclusions

The main aims of this second phase of this project on AMM investigation for natural ventilation window design are achieved, and further numerical and experimental study will give more completeness to the research. So now, new possibilities are open for devices' design which aim noise reduction together with natural ventilation. Furthermore, applications can interest private and public spaces, which are affected acoustically by the co-existence of different activities or infrastructures. For these reasons, windows systems might be taken into account. For example, the proposed geometry may be embedded in a window design built on an external wall of a private or public building such as a house, a school or a hospital. The resulting *SPL* broad dips of 38.25 and 31.95 dB (1 and 2 m diameter model) might impact a situation where the area surrounding these buildings is very crowded or overlapping activities might create high-level noise. An example could be embedding a system of origami metacage ducts in window frames or using the structure itself with increased width and a transparent back panel to allow light exchange between two environments. A validation work will follow to test a prototype's actual building feasibility and determine whether the transparent back panel might affect its performance or allow a new generation of tuneable window systems.

This study has investigated the acoustic characteristics of a proposed origami acoustic metacage with a unique reconfigurable mechanism. Two configurations with different ventilation designs (perforations/apertures) have been tested to assess the noise reduction and estimate the ventilation volume between the inside and the outside of the origami metacage (from 32% to 52% of the opening ratio). The folded metacage shows a profound dip in the radiated SPL due to the excellent silencing effect provided by the metamaterial unit in front of the ventilation holes. The frequency and bandwidth of the effective region are related to the system's geometric parameters and scales. Natural air ventilation is possible without any additional element, showing the proposed device's potential to be used in ventilation window systems. The developed numerical model can be further employed to optimise the device's size and shape to improve ventilation and noise reduction in the desired frequency range.

In the next section, the acoustic metacage model will be further developed in 3D and investigated analytically and numerically to overcome the aforementioned limitations 3-dimensionally. For this reason, a more in depth parametric study will be run, specifically to determine the optimal design of AMM unit cell, and understand how this system might be customisable according to different frequency ranges. Moreover, a preliminary ventilation analysis will be included as well.

4.3 Development of metacage for noise control and natural ventilation in a window system

In this section, a metacage for noise control and natural ventilation in a window system was developed in 3D, and its effectiveness was tested analytically and numerically through several configurations. In this third study, FEM was used to study and optimise the acoustic performance of the metacage window. It is worth noticing that the point source used in the 2D study has been adapted in 3D as a plane wave radiating perpendicularly to the former setup plane. This adaptation is also due to the real window noise condition approximation, where the source of noise is not a point but rather similar to a plane wave radiation from the outdoor environment. The ventilation was evaluated simultaneously, following predefined guidelines related to the window's opening ratio and air-flow directivity. Finally, the metacage window structure was proved to reduce the noise transmission with a mean value of 30 dB within a frequency range of 350–5000 Hz while having an opening ratio of the 33% compared to the whole system surface. The front panel gives a mean high frequencies TL contribution of 17 dB (2000–5000 Hz). Additional lateral constraints and cavities increase the TL performance up to 70% on a wider lower frequency range (350–5000 Hz). Thanks to the cavities, the resonant unit cells among the acoustic metasurface (AMS) significantly suppress sound from exiting the structure in broadband frequencies and allow a bigger opening on the lateral side. This significantly contributes to the natural ventilation potential of the metacage window, which in the long term becomes equally effective to the conventional open windows.

4.3.1 Background

Natural ventilation is an energy-efficient approach [272,273]. People spend over 70% of their day indoors in modern times, emphasising the importance of a comfortable indoor environment [3,274]. However, indoor comfort through natural ventilation is frequently limited by outdoor inputs, such as noise sources. Different noise mitigation windows can reflect or absorb the incident acoustic energy. Active noise control can be used to create low-frequency stopbands [15,54]. Rolling shutter boxes are shown to be a reasonable noise control passive system [9]. An increased thickness is usually needed for either active or passive systems to obtain a wideband attenuation in the frequency range between 350 and 5000 Hz [269,275]. These methods do not guarantee the required airflow, precluding their usage in applications where ventilation is required.

A brand new diversity of manipulating the sound wave has come up because of the development of acoustic metamaterials (AMMs). Metamaterials' subwavelength structure determines more effective acoustic properties according to their structural shape rather than their constitutive materials. Acoustic metamaterials for wave-front modulation [111,276], sub-diffraction imaging [79], and acoustic cloaking [277] have been demonstrated and may be considered for building uses. [271,278] In the mechanical engineering research area, acoustic metamaterials have inspired a series of acoustic ducts for noise reduction [12,23,46,279,280], the applicability of which may be extended in buildings structures. Their inherent large spatial footprint of duct limits their versatility and flexibility during implementation. For these reasons, improvements are needed to align ventilation and noise control targets to the buildings (and so windows) requirements in a broader range (350-5000 Hz).

Natural ventilation is generally meant to be performed according to three window parameters: the opening size (or opening ratio), the air-flow directivity, and the time addressed for the ventilation. [281,282] For the first parameter, generally bigger opening induces larger air mass flow, higher air change rate (*ACR*) and CO_2 removal rate. [272] Secondly, the normal direction of the air-flow towards the window wall (horizontal pivot or turning window) has been proved to be the best solution for obtaining an efficient ACR in a short amount of time [273,281], while lateral air-flow direction (such as in tilt or awning windows) requires a longer amount of time to reach the same *ACR*. Ventilation time as the final parameter determines the indoor environment's exposition to the inputs (such as harmful noise) of the outdoor and vice-versa according to the window characteristics. By combining these parameters, it is possible to achieve window design for different indoor functions. In a perforated panel, for example, [12] sound waves and airflow are blocked according to the orifice size. Smaller perforated holes and perforation ratios will yield better sound insulation while poorer ventilation.

Although several previous works attempted ventilation and noise reduction through AMMs [23,281], it is still rare to see the substantial potential for window application in a wide frequency range. For this reason, this section aims to 1) proving sound reduction and ventilation performances of a tunable AMM structure to be used for window design and 2) investigating which are the determinant factors for such vital features. Following the sub-structuring approach of Yu et al. [37], and starting from the concept of AMM, ventilated unit cells with local resonant cavities are chosen to allow better ventilation and sound reduction, ideally offering high flexibility for geometric tuning and subsequent acoustic optimization. The geometry is fixed through some preliminary analyses of the proposed unit cell's acoustic properties, and its sound attenuation in *TL* is characterized. Afterwards, an array of unit cells is analysed as acoustic metasurface (AMS), which, folded into an octagonal shaped acoustic

metacage [271] creates the AMM. Different geometrical configurations of the AMM are then compared in terms of *TL* and *ACR* to establish which is the optimal one.

4.3.2 Acoustic unit cell characterisation

4.3.2.1 Design of acoustic unit cell

The AMM window is based on a hierarchical geometry based on a unit cell. Let us consider the schematic in Figure 4.16, which is composed of two symmetric resonant parts characterised by inclination α and several cavities decreasing in lengths along the z-axis and open towards a central duct. The tailoring of the inner structure creates local resonances in order to form a stop-band. The unit cell can be considered a waveguide attached to periodic scatterers in the lateral direction for flow exit. This specific system is based on the theoretical wave propagation and the existence of stop-band related to both constant and linear structures such as the AMMs based on the resonant tubular array and the acoustic black hole (ABH). [268,283]

Table 4.1 Geometric variables involved in the acoustic unit cell characterisation process.

(α) Rotation angle	**(n) Cavities Number**							
	4	**5**	**6**	**7**	**8**	**9**	**10**	
	(a) Cavities Width							(b) Unit cell height
45°	0.016	0.013	0.011	0.009	0.008	0.007	0.006	0.066
55°	0.019	0.015	0.013	0.011	0.009	0.008	0.007	0.077

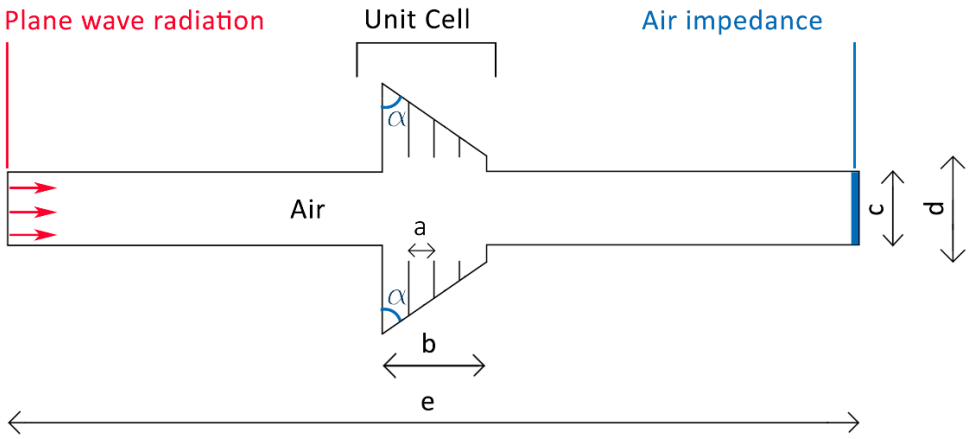

Figure 4.16 Geometrical settings and boundary conditions for the particular of the acoustic unit cell with cavities width (a), tip height (b), tube width (c), smaller tip base (d), tube length (e), rotation angle (α).

In order to suppress sound waves, the resonators lined along the duct in a unit cell provide locally resonant stopbands while exerting minimal airflow interruption. Table 4.1 shows the three parameters that define the structure and which are investigated: the inclination of the unit cell's lateral sides ('rotation angle'), number of cavities, and width of the cavities. The tube used for this

parametric study has a length of 0.6 m and a width of 0.05 m (Table 4.1 and Figure 4.16). The smaller unit cell base ('d' in Figure 4.16) is 0.055 and 0.080 m when the rotation angle is respectively 45° (Figure 4.17.a) and 55°(Figure 4.17.b). A number of rotation angles have been tested in this parametric study (20°-80°, with a step-angle of 5°); However, 45° and 55° have been chosen as example of optimal balance between duct width (for ventilation purpose) and acoustic performance.

4.3.2.2 Numerical study on the acoustic unit cell

Two-dimensional simulations are carried out by COMSOL Multiphysics, Pressure Acoustics Module, in order to understand the *TL* characteristics of the unit cell. A plane wave incidence is applied to the left end of the 2D tube (incident pressure = 1 Pa), and the walls of the tube and resonant cavities are set as a sound hard boundary. The tube outlet surface, is characterised with air impedance to simulate sound waves free radiation condition, meaning that sound can propagate through it with no back reflections. The mesh size is determined according to the FEM criterion, where at least six nodes are used to simulate a wavelength in air. The maximum allowable element size is 343/6/5000=0.0114 m in order to reach 5000 Hz. The frequency-domain analysis covers a frequency range from 350 Hz to 5000 Hz with a step size of 100 Hz. The frequency range between 350 and 5000 Hz is chosen to be a realistic approximation of the average environmental noise. [284] The averaged incoming sound power at the inlet boundary and outgoing sound power at the outlet boundary are used to calculate the *TL*, following the equation $TL = 10\log_{10}\left(\frac{w_{in}}{w_{out}}\right)$ [dB]. An increase in the *TL* curve will thus indicate less efficient sound transmission because sound energy is more confined in the cavities.

This methodology has been already proved several times by Yu et al., showing the effectiveness of such numerical predictions validated efficiently by experimental tests. [23,37] So, it is reasonable to consider that the numerical study is an efficient instrument for accurate acoustic performance prediction with similar boundary conditions and simulation settings. Further experimental validation could improve the methodology but is not a fundamental part at this stage.

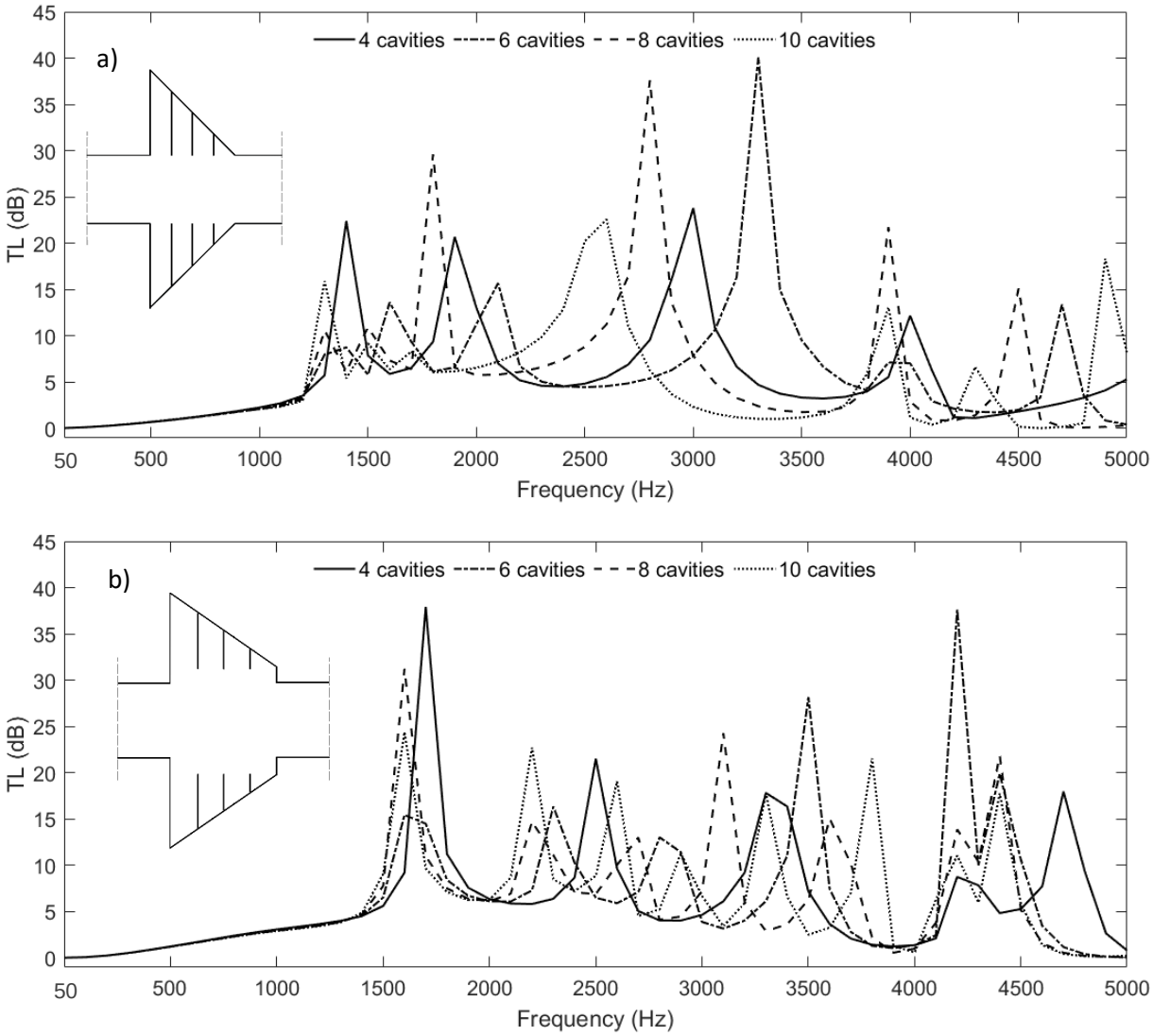

Figure 4.17 Transmission Loss related to (a) α= 45°, and (b) α= 55°, for the sake of simplicity, only even numbers of the cavities parameterisation results, are shown.

The parametric study highlights significant correlations between the cavities and the duct's width and the consecutive *TL* behaviour. Figure 4.17 shows the *TL* results for 4, 6, 8, and 10 cavities number combinations. From these graphs, it is observed that as the inclination angle increases, the peaks are higher since the cavities are more prolonged, producing a more substantial resonance effect. In this case, a broader average *TL* is achieved. At the same time, the *TL* peaks rise when the cavities number is less. Generally, the frequencies with effective sound attenuation are shown to be significantly affected by the resonator geometry.

This part of the study shows how the unit cell geometry is characterised and which parameters combination is best for ventilation potential and noise reduction. So the system with the angle α= 55°, and n= 4 (see Figure 4.17.b) is considered in the further numerical analysis due to broad *TL* capacity combined with a wider central duct (so higher *ACR* potential).

4.3.3 Resonance-induced localised modes in the AMM: Physics principles behind the acoustic metacage window

Figure 4.18.a shows the transversal section of the developed metamaterial. The model has an axisymmetric configuration concerning the directions passing through the centre of the metacage window o with a pace of kπ/4 with a transversal uniform thickness of t (x-direction). For the sake of simplicity, the use of a second axial reference such as z'y' is necessary to study the wave propagation in a radial reference system (see Figure 4.18.b). In this reference system, z' is each direction passing through the centre o with a pace of kπ/4, starting from the axis z, and y' is the perpendicular direction. The incoming pressure (P_{in}), the density (ρ_0), and the velocity in the medium (air) (c_0) are considered uniform in the transversal section (Figure 4.18.a). Therefore, a specific impedance and refractive index can be assigned to the different geometrical areas of the metacage window. Region 1 (approximately $r< r_1$, Figure 4.18.b) is characterised with an acoustic impedance of Z_1 and refractive index of n_1 and region 2 ($r_1 <r <r_2$) has an acoustic impedance of Z_2 and refractive index of n_2. Due to the contrast in refractive indices of the two regions, while the sound wave travels through towards the unit cell, in Region 1 it remains in a continuum state (we assume the reflection on plane xy like a constant). On the contrary, when the sound waves travel through Region 2, it interacts with the relative resonance-induced localised modes. After it passed Region 2, it will result in an out-of-phase condition. The incident acoustic wave travelling through the metacage window will enter Region 2, having a small phase shift, with a consequent destructive interference on the transmission sides of the metamaterial unit cell (Figure 4.18.b).

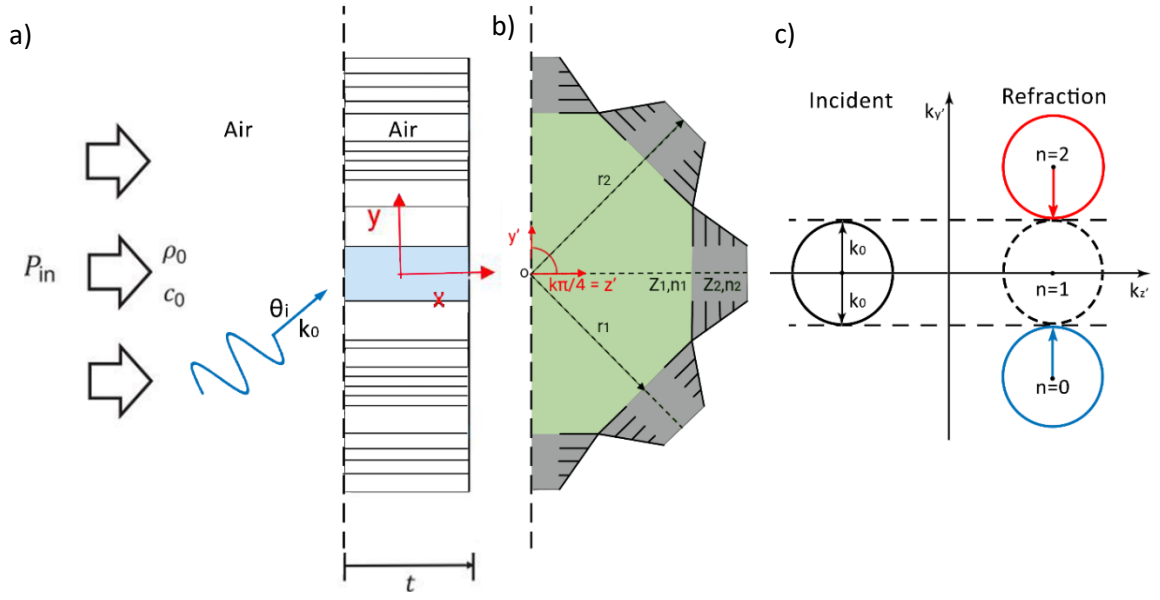

Figure 4.18 Schematic of the physical characteristics according to the metacage window geometry: (a)Transversal section of the whole structure (plane xy), (b) particular of the frontal section of the AMM (plane zy), highlighting different gradient metamaterial grating with both sides of the AMM that are air, (c) iso-frequency contours for ξ = G = 2k0.

In this case, the grating order should be considered as in the generalised Snell's law for metasurfaces.[285] The studied system comprises one internal cavity with eight unit cells with four cavities (sub-unit cells) in one period p, which corresponds to r1 and r2. The relative wave with the angle of incidence ϑ_i and the refraction angle ϑ_t can be calculated using the generalised Snell's law [111]

$$(\sin\theta_t - \sin\theta_i)k_0 = \xi + nG \qquad 4.1$$

Here k_0 is the wavenumber in free space, $\xi = d\Phi/dz' = 2\pi/p$ is the phase gradient along the surface (along the z'-direction in Figure 4.18.b) on the right outgoing interface, n is the integer representing the order of diffraction (or grating order), and $G=2\pi/p$ is the reciprocal lattice vector (depending by the reciprocal lattice of the cavity and the unit cells). It is noted that only when the period is comparable with the wavelength λ the term nG appears [111] for large angles of incidence. Comparing the unit cell system with the supercell developed by Quian et al., the physics related to both can be studied through the example case of $p = \lambda/2$ by assuming that the period is less than half the wavelength ($p \leq \lambda/2$).[286] Since in this case equation

$$\xi = G = 2\pi/p = 2\,k0 \qquad 4.2$$

can be rewritten as

$$\sin \theta_i = \sin \theta_t + 2(1+n) \qquad 4.3$$

The iso-frequency contours for $\xi = 2 k_0$ in Figure 4.18.c are employed to study the importance of different incident angles on the propagation character of the incident wave impinging on the unit cell (solid circle). As demonstrated by Quian et al., if $\xi = 0$, there are no phase shifts introduced along with the interface (black dashed circle in the refraction part of Figure 4.18.c). Consequently, a black dashed circle displacement of $\xi = 2k_0$ appears when phase shifts are introduced along with the interface. So in Figure 4.18.c the lower blue circle corresponds to $n = 0$ in eq. 4.3, while the red circle corresponds to $n = 2$ in eq. 4.3. Generally, the incident wave couples more easily with such two propagation orders ($n = 0, 2$) rather than higher ones. The incoming wave to couple into propagating modes has a critical angle expressed as $\vartheta c = \sin^{-1}(1 - \xi / k_0)$ for 0th order diffraction (i.e., $n=0$). When p is a minimal value, i.e., $p < \lambda/2$, then $\xi = 2\pi/p > 2 k_0$. For this reason, and since $|1 - \xi / k_0| > 1$, the critical angle ϑc becomes an imaginary number, meaning that the propagating mode for an arbitrary angle of incidence ϑi and $n=0$ is not allowed through the AMM. On the other side, for the arbitrary non zero value of n+1 (n is an integer), the mode-coupling method can interpret the transmission coefficients. [271] The nth-order diffracted wave (recalling that $\xi = 2\pi/p$) has a y component of the wave vector defined by the equation $k_{y',n} = \sqrt{k_0^2 - \left[k_{z'} + \frac{2\pi(n+1)}{p}\right]^2}$, where k_x, is the component of the wave vector on the x axis. Since $p < \lambda/2$ for an arbitrary non zero value of n+1, we shall have $\left|k_{z'} + \frac{2\pi(n+1)}{p}\right| > \frac{2\pi}{\lambda} = k_0$ (note that $|k_{z'}| < \frac{2\pi}{\lambda}$), meaning that $k_{y',n}$ becomes imaginary for any non-zero value of n+1. For this reason, the transmitted waves are evanescent and decay exponentially along the z' direction on the plane z'y'. Nevertheless, since $k_{y',n}\left(k_{z'} + \frac{2\pi(n+1)}{p}\right)$ is still a real number, it is essential to stress further that the propagation of surface waves in the y' direction is still possible. For n=-1, although the propagating waves are allowed, their transmission is minimal due to destructive interference [271]. In conclusion, the transmission through the AMM for $p < \lambda/2$ is small regardless of the angle of incidence for any value of n, and the AMM design can be used as an omnidirectional sound barrier for all-angle incoming waves.

4.3.4 Development of the metacage and the acoustic performance

4.3.4.1 Sub-structural design of the acoustic metacage window

As depicted in Figure 4.19, an array of 8 unit cells can be considered an Acoustic Metasurface (AMS) [37], where identical unit cells with the same resonance and phase properties can allow a homogenous sound isolation effect. The AMS can be folded into a ring shape to realise an acoustic metacage [271] to confine acoustic transmission in all directions. Based on the chosen unit cell geometry, 8 unit cells form an octagon-shaped metacage applied to separate two acoustic domains, as shown in Figure 4.19.b. The domain with incoming waves is denoted as the "noisy" side, and the transmission side is denoted as "quiet". The octagonal opening of the metacage opens fully to the noisy side, allows air to enter with sound waves. The metacage front facing the quiet side is closed with a rigid panel, which forces sound to exit through the eight lateral unit cells, thus interacting with the resonant cavities. For this reason, the original soundwave (propagating along the axis x) affected by the reflection of the front panel and diffraction and resonance within the metacage inner volume (without considering the AMM unit cells) is considered as a new modified soundwave entering the AMM unit cell (see Figure 4.19.b). Analytical and numerical analyses are performed to investigate the system effectiveness according to each part contribution in terms of *TL* (configuration without the metacage window, configuration with only the front panel, configuration with lateral constraint, configuration with cavities). Finally, in the discussion, the ventilation capacity of the final model is compared with other ordinary window models to address the ventilation parameters mentioned above. The efficiency of the opening ratio combined with the noise reduction is analytically and numerically demonstrated, and a new technique for long term consistent ventilation and noise reduction on the middle-high frequency range (350-5000 Hz) is defined.

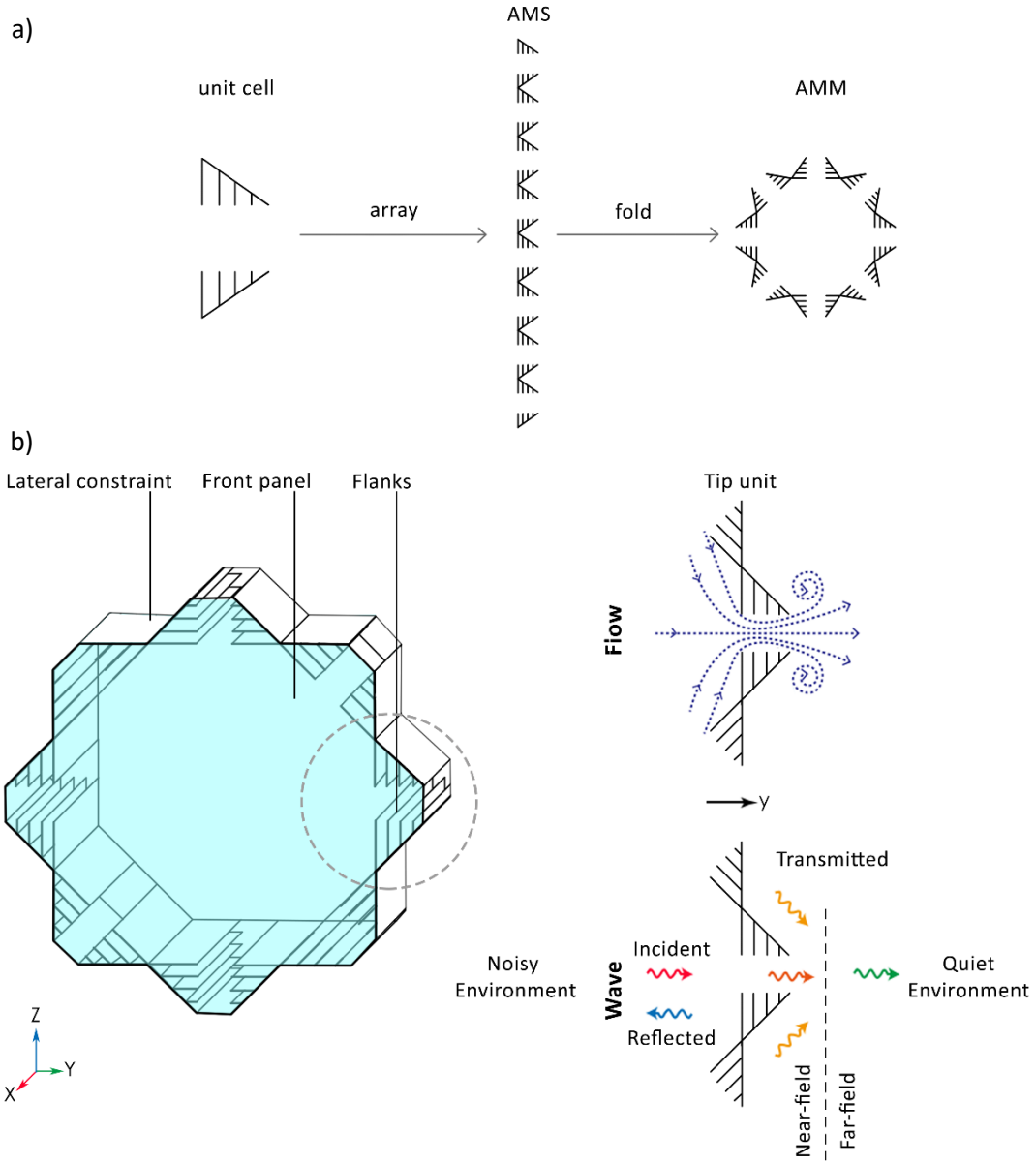

Figure 4.19 Metacage window system: (a) AMM geometrical concept and (b) schematic of the flow and the wave propagation

4.3.4.2 Numerical analysis: unit cell, AMS, and AMM

After the analytical analysis of the AMM structure, the 3D simulation is defined as semi-infinite acoustic conditions are applied to the spherical geometrical boundaries as depicted by Figure 4.20. The overall boundary sphere has a diameter of 0.7 m and is centred with the analysed geometry. The metacage window has a total height of 0.6 m (maximum distance between two opposite unit cell tips). The background pressure field is defined on the noisy side as incoming waves, while the entire semi-sphere surfaces are assigned with free wave radiation conditions (see Figure 4.20.b). The walls of the metacage and material cells are set as interior sound hard boundaries. Sound transmission through walls of the metacage and possible viscous-thermal effect in the narrow resonator channels are

neglected in this study. The 3D domain is filled with air, where air density and sound speed at room temperature are used. *TL* is calculated by the reduction of sound power through the metamaterial interface (in decibel). Regarding the mesh size for the 3D study, this model results are very complex and, since the convergence of results is proved, simplification is needed. So the maximum allowed element size is increased at 343/6/2500=0.0228 m. In the results, the *TL* and *SPL* distribution are shown linearly and superficially within the simulation frequencies.

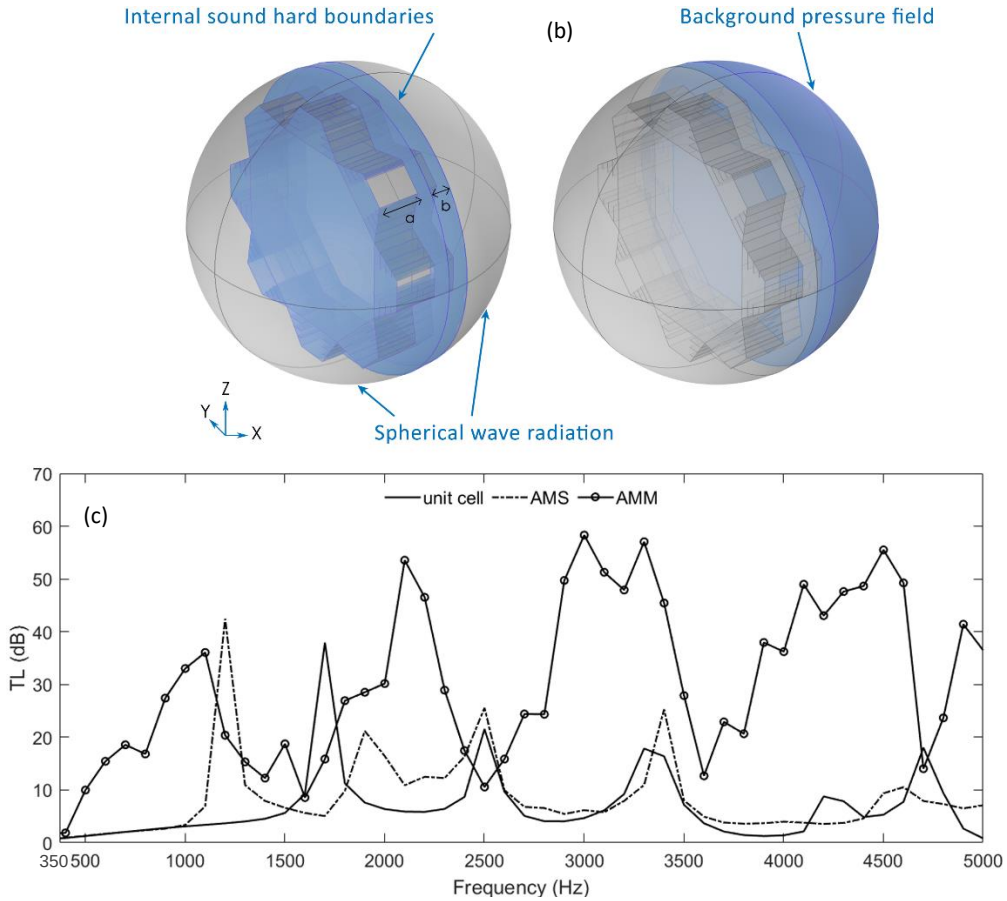

Figure 4.20 3D boundary conditions in the FEM settings: (a) internal sound hard boundary, (b) background pressure field, where a=0.1 m, and b= 0.05 m; and (c) TL results of the unit cell, AMS, and AMM for a frequency range of 0-5000 Hz expressed in dB.

Results of *TL* related to the unit cell, AMS and AMM are presented in Figure 4.20, where the array of 8 unit cells considered as a metasurface is investigated with the same 2D physical boundary condition of the unit cell. The unit cell *TL* analysis shows peaks at 1700, 2500, 3300, and 4700 Hz (Figure 4.20). The AMS determines a higher *TL* in the lower frequencies with peaks at 1200, 1900, 2500, and 3400 Hz, and the mean value of *ΔTL*=2dB compared to the unit cell mean *TL*. Finally, by folding the AMS in a loop (generating the AMM), a broader increase of the *TL* is achieved (mean value of ΔTL=22dB compared to the AMS *TL*). This phenomenon is probably due to the three-dimensional configuration characterised by a front panel (Figure 4.19) that contributes to reflecting the sound wave backwards. This and other AMM configurations contributions need to be further investigated. Comparing them

can give insights into the sound attenuation mechanism and reveal the critical parts determining the overall system's effectiveness.

4.3.4.3 Numerical analysis: different AMM configurations comparison.

As a comparison, four configurations are studied, as illustrated in Figure 4.21.a-d. The first configuration (Figure 4.21.a) includes only the opening between the two acoustic domains. The second configuration (Figure 4.21.b) inserts a rigid frontal panel, but sound can still exit freely from the lateral side. The third configuration (Figure 4.21.c) includes the structure with nozzle shaped unit cells, but the resonant cavities are missing. This is quickly done by removing the interior flanks inside the unit cells. The last configuration (Figure 4.21.d) is the proposed 3D acoustic metacage window design. The *TL* curve in Figure 4.21.e shows that for Configuration 1, there is no significant *TL*. This is typically between 0-3 dB and sets a reference value for other configurations. Note that if the front and back panels of the metacage are both opened, the acoustic effect is similar despite the presence of any unit cell elements. For the other three configurations, the *TL* results in Figure 4.21.e show a dome-like behaviour, typically appearing in the *TL* pattern of expansion acoustic ducts [279]. Since the expansion ratio and unit cell volume characterized by the primary dimension is almost the same, the tendency of the slopes in the three configurations is similar, with peaks appearing near 1100, 2100, 3000, 3300, and 4500 Hz. The amplitude of *TL* is, however, different due to reasons to be discussed later. For example, as stated in the previous analytical considerations, the comparison between curves 1 and 2 in Figure 4.21 shows the crucial importance of the front panel for sound reflection. As showed by Figure 4.22.a, when the acoustic wave interacts with this part of the metacage window, it is partially reflected back and partially passes through the lateral space between the front panel and the division towards the quiet environment. The barrier performance of the second configuration is only effective by cutting the direct “line of sight” between source and receiver. [14] The results also show that, along with the common knowledge, high-frequency sounds are more inclined to be attenuated by the front panel than low-frequency sounds due to their low wavelength. A longer wavelength sound will easily pass through the barrier by diffraction (Figure 4.21.e).

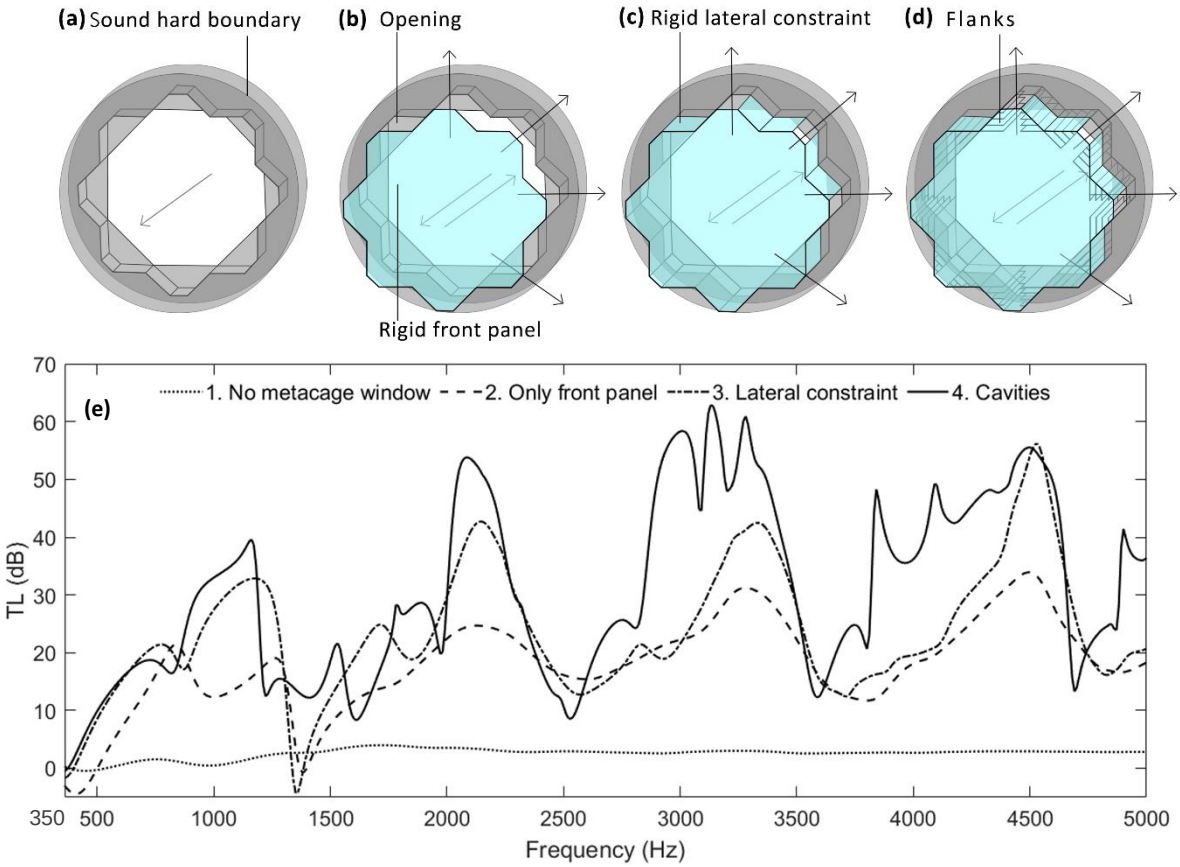

Figure 4.21 Geometrical settings of 4 different internal boundary configurations: No Metacage (a), Only front panel (b), No flanks (c), Metacage (d); and Transmission Loss related to these configurations (e).

Although the front panel plays a fundamental role in noise reduction, the *TL* can be further improved by adding the lateral geometrically designed constraints. Indeed, a significant *TL* step-up is made on the system's acoustic performance when the lateral part is added. This particular feature differentiates the metacage window from the previous window technology attempt [14]. Thanks to the cone shape of the unit cells, their acoustical responses become exponentially divergent when they propagate in the narrowing area direction [287]. As a result, the *SPL* results confined in the internal geometry and within the quiet environment results much lowered (Figure 4.22.b), although significant lateral *SPL* concentration may interfere in the metacage window performance. The final improvement of the model comes with the cavities (Figure 4.21.d and Figure 4.22.c), which, as proved before, at specific frequencies, function as resonators. As depicted in Figure 4.21.d, the TL has a much broader dome-like behaviour with this configuration with considerably higher peaks and slightly lower depths. The frequencies of effectiveness are still the same (1100, 2100, 3000, 3300, 4500 Hz) since the thickness and distance from the division is still kept the same (0.1 m). The slopes' behaviour slightly varies for higher values of *TL*, probably due to simulation imprecisions, for which correction through mean value might be performed. As stated in the previous analytical analysis section, the dimension of the folded AMM period makes it more suitable for middle-high frequencies (1000 – 5000 Hz).

However, if paired with the front panel and the lateral constraints, it can cover a broader frequency range even at lower frequencies (350 – 1000 Hz). As showed by Figure 4.22.c, when the acoustic wave interacts with this part of the metacage window, it is drastically reduced by the destructive interference between the central duct and the lateral resonant sides of each unit cell. As a result, the overall *SPL* in the quiet environment results as reduced and more uniform than the previous configurations.

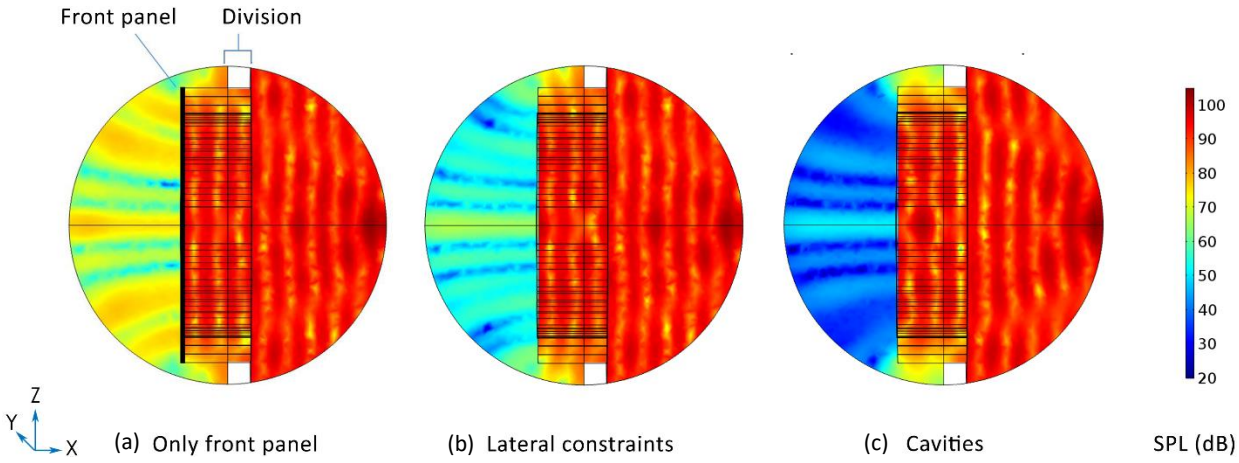

Figure 4.22 SPL related to the configuration with (a) only the front panel, (b) with the front panel and the lateral constraints, and (c) with the front panel, the lateral constraints, and cavities involved in the noise reduction through the opening. The colour legend refers to dB as a measuring unit, and 3300 Hz is the analysis frequency.

4.3.5 Basic ventilation analysis

As mentioned in the introduction, natural ventilation is a central feature of the AMM here presented. The technique used is buoyancy, which only requests the presence of one or two openings on an external building wall, placed systematically to create a natural airflow system. In particular, buoyancy ventilation results from the difference between interior and exterior air density. This change causes the warm air to rise above the cold air and create an upward air-stream, of which the ventilation rate can be calculated as:

$$q = AC_d\sqrt{\frac{\Delta T\ g\ h}{(T_I+273)}} \quad (\mathrm{m^3/s}) \qquad 4.4$$

where A is the area of each opening (m^2), C_d is the discharge coefficient (typically 0.6), T_I is the internal temperature (°C), ΔT is the difference between internal and external temperature (°C), g is the gravitational force (m/s^2), and h is the height between openings (m). According to Bayoumi [282]

(where the thermal comfort and heating and cooling energy demand are also considered), natural ventilation would occur by an opening in the building when the outdoor temperature is within ±3 °C of the indoor temperature (i.e., within +3 °C in heating; within −3 °C in cooling). So this technology is widely applicable in most environments (from a temperate climate to a slightly cold or hot climate).

Besides this, Von Grabe et al. [281] accurately investigated natural ventilation in buildings through buoyancy and the flow directivity according to the window opening features. The tested window types are several: double vertical slide window, turn window, tilt window, awning window, horizontal pivot window and vertical pivot window. Different opening rates were included for each window test to allow a more extensive comparison, and the windows performance is evaluated according to various criteria such as the mass flow and the air change rate and the CO^2 removal rate. In their study, Van Grabe et al. highlighted how the horizontal pivot window is the best performing type of window.

Due to the lateral airflow of the metacage window, this can be compared with the tilt or awning windows. In the optimisation process of combining natural ventilation with noise reduction, it was considered that lateral airflow, such in tilt or awning windows, is quite lower than the horizontal pivot window, the double vertical slide window, and the turn window. These last two are meant to be better due to allowing faster air exchange since, in their design, the attenuation of outdoor inputs such as noise sources is not guaranteed. So natural ventilation is generally meant to be performed in the shortest amount of time to avoid indoor contamination with negative factors such as outdoor noise [281]. However, from the metacage window acoustic effect combined with 33% of the opening rate, a perpetual opening can be guaranteed in several outdoor noise conditions. So if we compare the effects of the horizontal tilt window in the short term with the one of the metacage windows in the long term, they are equally valid.

4.3.6 Conclusions

In the presented study, a new metacage window that allows natural ventilation and noise reduction was developed through the principle of Snell's Law for AMS and investigated through the semi-infinite FEM Method. A parametric study first assessed the geometry to determine which combination between rotation angle, cavities number, and cavities width would have been optimal for the scope. Afterwards, four acoustic configurations were analysed to understand the impact of each part of the metacage window.

From the acoustics point of view, unit cells, AMS, and AMM have been evaluated through a sub-structural approach. Overall the metacage window design allows a *TL* with a minimum of 8 dB and a

mean value of 30 dB within a frequency range of 350-5000 Hz. The final opening rate of the metacage window was 33%. The ventilation capacity was proved to be good enough to allow buoyancy ventilation in the conditions considered by Bayoumi [282], and the flow directivity discussed and investigated by Von Grabe et al. [281] Indoor comfort was guaranteed by the perpetual opening of the window supported by the noise reduction effect. The lateral ventilation was not the most efficient in the short term [281]. Nevertheless, in the long one, it became equally effective.

Many factors influence the overall performance of the acoustic metacage window. For example, regarding the optimal combination for the unit cell structure, its constraints total dimension were certainly a limit in terms of noise reduction wavelength. However, combined with the lateral metacage constraints and the front panel, they performed significantly in the high frequencies (2000-4500 Hz). The unit cell array (AMS) proved to be equally efficient in the same frequency range. An additional improved performance was observed between 1000-2000 Hz. The acoustic effectiveness increased by folding the AMS into an octagonal closed shape and adding a front panel. Each part of the AMM demonstrated to give different *TL* contributions. The front panel gave a mean power reduction of 17.5 dB with a peak value at high frequencies. At the same time, the additional lateral constraint and the cavities increased this performance by respectively 31% and 70%, with a significant contribution at middle-low frequencies. The cavities of the unit cell played a vital role in the resonant stopband, so they improved the previously considered configuration by 30%. The *TL* peaks frequencies were due to the thickness of the AMM. Indeed, they were the same for all the configurations.

The significant results in the acoustic part set a new AMM generation with various merits over traditional windows, including effective long term natural ventilation combined with customised noise reduction. However, in the next chapter, further optimisation steps that might clarify if this mechanism can be adapted to multiple and more conventional window's shapes are investigated through numerical and experimental analysis.

5. AMM adaptation to real window design

The contents included in this chapter have been published in the peer-reviewed journal *Applied Sciences* (MDPI) by the name of "A Metawindow with optimised acoustic and ventilation performance" (2021).

In this chapter, the ergonomic criteria highlighted in Chapter **3. Participatory approach to draw ergonomic criteria for window design** are considered to adapt the acoustic metacage system investigated in Section **4.3 Development of metacage for noise control and natural ventilation in a window system**. Chapter 3 highlighted that 1) participants perceive the window as an essential mediating instrument between the indoor and the outdoor of a building; 2) through this feature, they feel connected to the outdoor environment; and 3) despite the non-optimal conditions, they feel oriented and perceive an improvement in the indoor's affective impact. These three design criteria were followed as guidelines when adapting the acoustic metacage to an ergonomic design. This project indeed aims to draw a new methodology for window design, which considers users' preferred aspects and combines them with a specific window's technologies. The window design would become, then, not only the mediator between the outside inputs and the indoor comfort, but it could even modulate the first one to optimise the second.

5.1 Background

Outdoor noise façade insulation, provisions for ventilation, and overheating mitigation have been commonly considered disconnected in building design developments. Consequently, strategies to control these different systems have been developed with entirely separated approaches involving building features [2]. Conventional windows, for example, allow visual connection with the outdoors, natural ventilation, and the partial acoustics isolation when closed; however, the way these mechanisms work forces the users to choose one function and to exclude the other and, of course, neither choice is conducive to indoor comfort [3–5]. So far, researchers have used several methodologies to overcome both problems by using, for example, mechanical ventilation [6], active or passive noise control systems [7–15]. These last ones consume less energy and can be built through

several features within the window, such as perforated and microperforated panels [8,16,17,123], porous materials [19–21,92], or acoustic metamaterials (AMMs) [23–28].

AMMs, in particular, are artificially engineered composite structures with unique acoustic properties derived from the use of modern engineering and physics, which are unlikely to be found in natural materials. Their range of applications includes sound absorption [26], noise attenuation [29], acoustic wave manipulation [30], as well as asymmetric acoustic wave propagation[31], acoustic energy harvesting [32], acoustic holography [33] and topological acoustics [34]. Among these, applications to combine noise control with air transmission have received considerable attention from acousticians. Recently they focus on methods such as resonant based acoustic meta-absorbers [16,35], evolving into subwavelength coiled channels metamaterials [36,37], and a combination of labyrinthine AMMs with porous materials such as foam and cotton[25]. However, due to their bulky and visually invasive geometrical nature, complex geometries, or relatively narrow bandwidth, they sometimes limit architectural choices, such that the design of thin and visually pleasant metastructures embedded in window systems remains a challenge.

In this project chapter, an acoustic metawindow (AMW) unit for broadband noise control (50 to 5000 Hz) and natural ventilation is presented, and its performances are examined numerically and experimentally. Firstly, since our previous study numerically tested the feasibility of a metacage [263], the ergonomic window adaptation is investigated in order to determine the most regular window shape [4] with the closest noise control properties to the previous model [263]. This is not of immediate determination since the previous paper highlighted that acoustic properties are strictly related to the 3D geometry [263]. In this model, the AMM system is incorporated in the window frame space for noise reduction and ventilation, while the central area allows a visual connection between the outdoor and indoor environment. Secondly, the acoustic performance of the AMW unit is investigated experimentally to show the validity of the design. Through the experimental results, our developed numerical model is validated. Thirdly, the influence of geometrical components and parameters is investigated to determine the optimal design set-up for the AMW unit in a wider frequency range. A combination of multiple perforations-cavities of different configurations further leads to realising a higher bandwidth noise control range. So, finally, the ventilation performance of the AMW unit needs to be investigated, including the acoustic optimised models. FEM is used for the acoustic and CFD analysis while experimental measurements are set to validate the 3D printed unit's acoustic performance.

5.2. Materials and Methods

The AMW unit's validity is first numerically determined and then experimentally investigated to demonstrate if the AMW unit design is performative from an acoustic perspective. The window prototype's experimental measurements have been run in the anechoic chamber of the acoustics laboratory in the Department of Mechanical Engineering of the National University of Singapore (NUS).

5.2.1 Analytical considerations on the geometrical adaptation

This part of PhD work focuses on an AMW unit consisting of a cubic main body of volumetric dimension of 0.4mx0.4mx0.13m with an embedded AMM system in the window frame space, as shown in Figure 5.1a. Each unit cell consists of *N* number of resonance cavities. The air gap *g* and length *l* of each cavity is dependent on the inclination α (Figure 5.1.b). The tailoring of the inner structure creates local resonances in order to form a stopband. The unit cell can be considered a waveguide attached to periodic scatterers in the lateral direction for flow exit. The theoretical wave propagation in this specific system generates an acoustic stopband related to the resonant tubular array and inspired by the acoustic black hole effect [268]. More details about the simulation results and theoretical analyses can be found in our previous publication [263]. The adaptation to a more ergonomic and common design is required for real application as a building feature. Following the analytical analysis from the previous acoustic metacage model [263], a specific impedance ($Z_{1,2}$) and refractive index ($n_{1,2}$) related to the different geometrical areas (Region 1 = R_1 and Region 2 = R_2) of the AMW unit are considered (see Figure 5.1.b). Due to the contrast in refractive indices of the two regions, the sound waves passing through the AMM unit cell experience an out-of-phase condition, and this phenomenon is proved regardless of the sound wave angle of incidence for any value of n. This physical principle is verified for the AMW unit, and the preliminary numerical analysis confirms it: the AMW unit design can be used as an omnidirectional sound barrier for all-angle incoming waves.

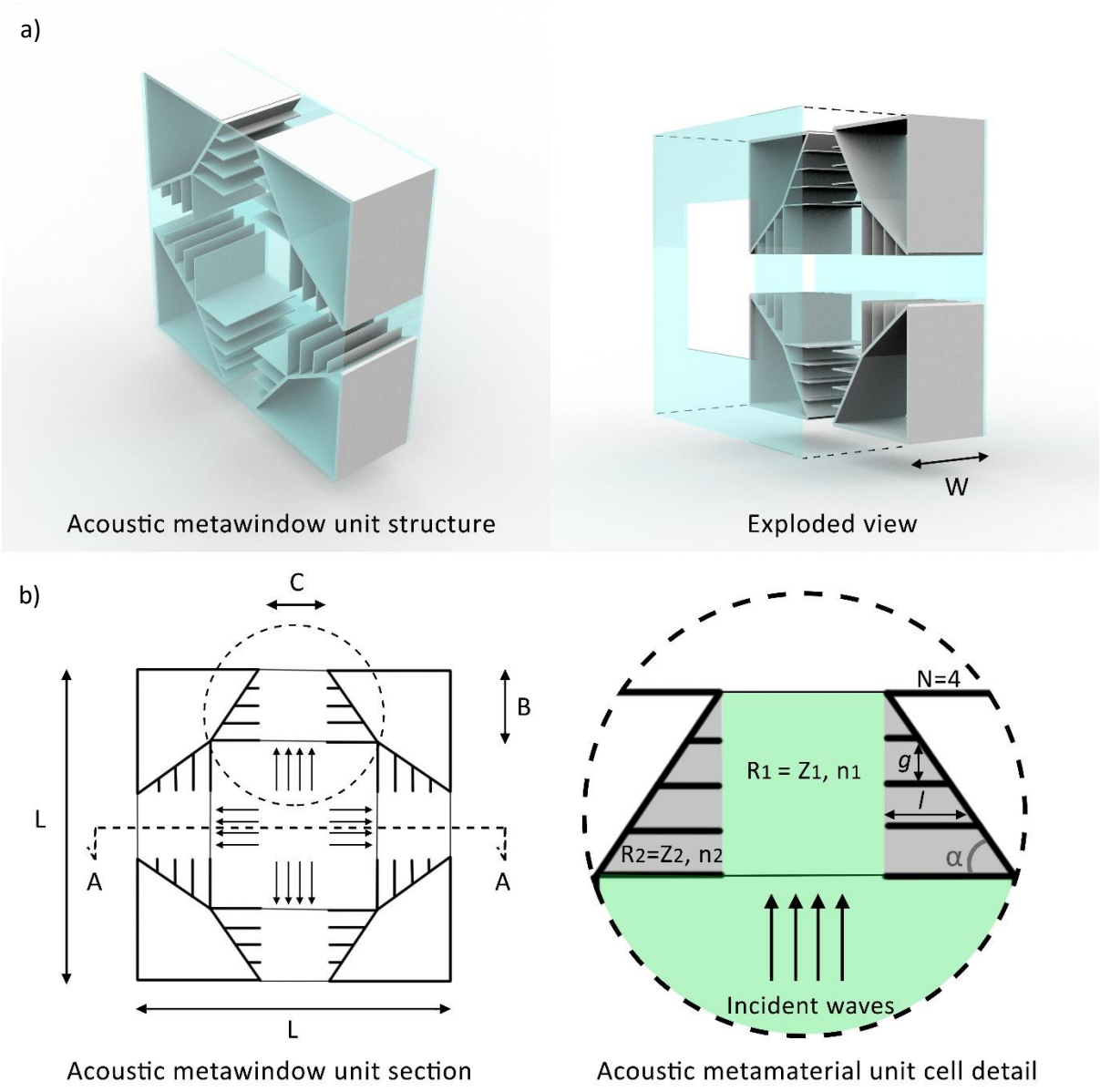

Figure 5.1 (a) Schematic representation of the acoustic metawindow structure (left) with an exploded view (right) where W is the AMW width (W=0.13 m). (b) Details of the AMW unit and a unit cell, including their geometries and dimensions. Here, L (L= 0.4 m) and W are the AMW constants, lengths, and width, respectively. The characterising measures of the ventilation cavities are respectively B = 0.095 m and C = 0.067 m. Other geometrical parameters are the number of space cavities N, length of each cavity l, rotation angle α, and channel air gap g (e.g. Distance between one flank and the other), their dimensions are: N = 4; l = 0.066 m, 0.05 m, 0.033 m, 0.016 m; α = 55°; g = 0.024 m. This geometrical configuration of the AMW unit and the related measures specified here were used for numerical and experimental analysis.

5.2.2 Numerical analysis set up

For the first stage, namely the numerical simulation, the FEM model was used. The 3D domain is filled with air, where air density (ρ=1.215 kg/m³) and sound speed (c=343 m/s) at room temperature (T=20°C) are used. The outdoor boundary is characterised by a plane wave radiating towards the receiving environment with a pressure amplitude of 1 Pa and an airspeed of the sound of 343 m/s, as

shown in Figure 5.2.a. The simulation study was performed using frequency domain analysis covering from 300 to 5000 Hz with a step size of 100 Hz. Such step size was considered the optimal arrangement for lower computational cost and general wide frequency range analysis. Of course, in case a more in depth analysis on a specific frequency range will be run, the step size of the frequency range must be modified accordingly. The lower bound of the frequency range is limited by the anechoic chamber's cut-off frequency at 300Hz used in the experimental analysis. As it can be seen from the geometrical characterisation and measures in Figure 5.1, the 3D model is complex, and the required mesh size to reach 5000 Hz is $343/6/5000 = 0.011m$. Such fine mesh results in very computationally intensive models. For this reason, a coarser minimum mesh size of 0.023 m was used, which showed no problem to meet the convergence criterion. SPL RMS deviation between the standard and coarser mesh FEM models resulted to be averagely 0.081, so the mesh simplification can be considered as effective. Moreover, the FEM theory evaluates indeed comparisons between different meshes effectiveness by quantitatively estimating the convergence order of the FEM error on a sequence of progressively finer meshes obtained by uniform mesh refinement [191]. In this case, the graphical user interface (GUI) of COMSOL was used to determine the convergence of the results of the coarser minimum mesh size, which allowed to have a lower computation cost, while guaranteeing the convergence of the results. The simulation accuracy was later validated experimentally.

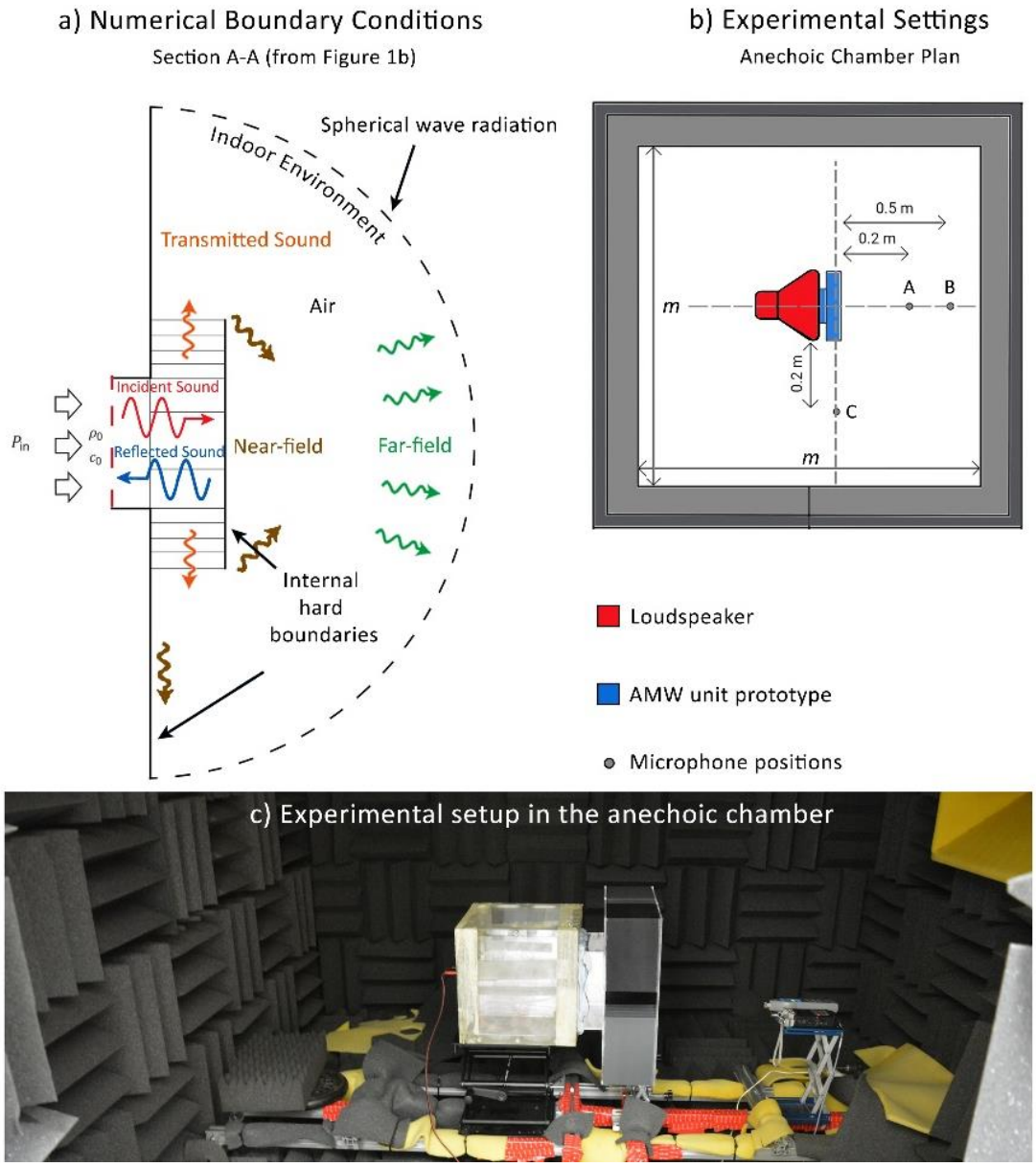

Figure 5.2(a) Schematic of boundary conditions used in numerical acoustics simulations; (b) 2D representation of experimental settings with m= 2m is the length of the anechoic chamber's inner area; (c) photograph of the experimental set-up in the anechoic chamber.

The acoustic performance is evaluated by measuring insertion loss (*IL*) at three receiving points A, B, C, respectively, where A and B are normal to the AMW unit surface (0.2 and 0.5 m far), and C is on the side of it (0.2 m far) (Figure 5.2.b). The choice of these three specific points instead of a wider spatially-averaged pressure level on the radiating side is mainly due to the lack of sound power measurement equipment.

The *IL* is calculated by the difference between the sound pressure level (*SPL*) at each of these points with and without the AMW unit applied. So, the *IL* of the AMW unit is calculated as:

$$\boldsymbol{IL_{AMW} = SPL_{woAMW} - SPL_{wAMW}} \quad \text{(dB)} \qquad 5.1$$

where:

- SPL_{woAMW} = *SPL* of experimental configuration without the AMW unit (dBA)
- SPL_{wAMW} = *SPL* of experimental configuration with the AMW unit (dBA)

5.2.3 Experimental set-up and Equipment

The AMW unit was fabricated following the same dimensions of the numerical analysis model (Figure 5.1) by using 3D printed Polylactic Acid (PLA, material properties; *E*= 1.28GPa, *ρ*=1210 kg/m3, and *n*=0.36), with fused deposition modelling technology (3D printer Fortus 350) (white geometry in Figure 5.1.a). Moreover, a FusionPro laser cutter (by Epilog Laser) was used to cut transparent acrylic panels (of thickness 5mm and 2mm) to build the rest of the AMW unit (transparent part in Figure 5.1.a). The unit is placed at the centre of a small-size anechoic chamber (inner dimension is 2mx2mx2m, cut off frequency is about 300 Hz). The AMW is attached on the outdoor side with a VISATON loudspeaker coupled with a power amplifier FRS 10 WP 8 OHM No. 2101 by VISATON (frequency range from 90 Hz to 19000 Hz and input power of 25 W) connected to the computer of the laboratory as shown from Figure 5.2c. The model is fixed to the loudspeaker to avoid any sound leakage from the two systems junction. The *SPL* measurements were performed at the same three positions, A, B, C (Figure 5.2.b), using a sound level meter with a built-in FFT analyser (Aihua AWA6228), and reproducing white noise signal from the loudspeaker. *IL* was calculated following Equation

$$\boldsymbol{IL_{AMW} = SPL_{woAMW} - SPL_{wAMW}} \quad \text{(dB)} \qquad 5.1$$

.

5.2.4 Acoustic numerical optimisation

The further broadband numerical analysis concerning acoustic optimisation follows the same boundary conditions described before. The numerical characterisation study of the AMW unit is performed due to the numerical and experimental methods agreement for *IL* calculation of such an AMM window system and the need for acoustic performance improvements on the lower frequency range. The AMM units' resonance volume is extended through the AMM unit cells' lateral panels perforation, and its impact on the AMW unit broadband performance (10-5000 Hz) is investigated. Perforation was chosen as it allows to have a further resonant effect to be coupled with the one related to the flanks, which results more effective than the simple removal of the lateral panels (this will be further discussed and proved in section 5.4 Broadband potential optimisation of the AMW

unit's acoustic performance). The AMM unit cells inner panels are perforated according to two different perforation ratios and two perforated panels positions, and the related *IL* is compared to the original AMW unit. The perforation ratio is calculated with the ratio between the whole inner panels' area and the perforated area. The single perforation hole has a diameter of 0.006 m. Moreover, to define the additional contribution of such perforations and the consequent increase of the resonating volume behind the AMM unit, we run a series of additional numerical analyses, which demonstrated the impact of such perforations over the lack of panels at the same position within the AMM unit.

The final numerical computational fluid dynamic analysis on the ventilation potential of the AMW unit and its optimised versions follow the same geometrical set-up for the acoustic analysis, and more details can be found below.

5.2.5 Computational fluid dynamic (CFD) analysis set-up

The numerical ventilation analysis is used to assess the AMW unit: its initial geometrical model (the one also tested through experiments) and its acoustic-optimised versions. A turbulent flow is set on the commercial software Comsol Multiphysics using the Rans method with k-ε turbulence model to calculate the environmental pressure drop (Δp) caused by the different airflow velocities passing through the AMW unit models. The k-ε turbulent flow is used to simulate mean flow characteristics for turbulent flow conditions. The Δp is calculated considering the wall where the AMW unit is positioned and the AMW unit itself, which are considered respectively as wall and interior wall with no slip. The 3D domain is filled with air, where air density (ρ=1.215 kg/m^3) is used at room temperature (T=20°C), while the inlet velocity is set from the inlet surface and characterised by with a maximum of 1.132 m/s and a minimum of 0.5 m/s. The inlet surface is the same which before was representing the loudspeaker (or outdoor environmental noise) role, and the maximum normal wind velocity flow is set according to Asfour and Gadi criteria [288], depending on the height above the ground (20m) and the room height (3m). As our current study only focuses on sufficient natural ventilation under low Mach-number flow (typically below 0.1), the flow-induced noise is considered weak [289] and should not deteriorate the overall sound reduction performance. Moreover, due to the AMM unit cavities dimension (g=0.024 m and l = 0.066 m, 0.05 m, 0.033 m), the condition for the development of Rossiter tones may only develop on the shallowest cavity, since $g/l \geq 1$ [290]. Outlet flow conditions with 101.325 Pa pressure are assigned to the indoor environment semi-spherical boundary to simulate the standard environmental indoor pressure. The geometric boundaries are the same as the acoustic FEM model, excluding the sphere radius, which is 0.72 m (1.44 m of diameter) within the assumption of 3 m room height for Asfour and Gadi criteria [288]). Regarding the mesh size for this 3D study, this is

characterised by a maximum element size of 0.115 m and a minimum element size of 0.0144 m, with more refinements for the regions where the turbulences are expected to happen (especially applied for corners refinement within the AMW unit structure and in its proximity). The study is run by a stationary solver, for which the CFD analysis is dependent on pressure (*p*) and velocity (velocity, *u*, and velocity field components *u,v,w*).

5.3. Acoustic performance based on experimental measurement

5.3.1. AMW unit performance according to different user position

Figure 5.3 shows the experimental study results, highlighting significant correlations between the microphones' position and the consecutive *IL* AMW unit performance. For example, from Figure 5.3.a, it is observed that the *IL* graph shows a dome-like behaviour, typical of the sound reduction pattern of expansion acoustic ducts [279]. In addition, the peaks become lower as the position axis angle goes from perpendicular to parallel to the AMW unit application plane (see Figure 5.2.b) for spatial reference). This, in turn, reduces the *IL* from a mean value of 11.9 dB at point A and 10.8 dB at point B to a mean value of 2.7 dB at point C. This difference is noticeable in the high-frequency range (2000-5000 Hz). A smaller difference of average 1.1 dB is also shown between the *IL* results of points A and B, showing that the AMW unit performs better when the user is placed on the perpendicular axis (e.g. in front of the window) rather than on the parallel one.

5.3.2 AMW unit performance on the lower frequency range (500-1000 Hz)

It is also necessary to notice that in the frequency range below 380 and between 700-900 Hz, the *IL* related to point B goes below zero. Since the sound wave that passes through the AMW unit is then refracted through the four openings on the window frame, such configuration might originate new noise sources characterised by a different mode that varies in the space. So *IL* dips measured in Points B and C are probably due to a superposition of the sound wave's low-frequency component when it exits from the four openings on the window frame. For this reason, while in point B measurements, there is such a low dip between 700-900 Hz, from the graph of *IL*(A), this is much higher (*IL*(A-B) =10.6 dB). Generally, excluding the frequency range of 700-900 Hz for *IL*(B), the sound wave pressure level

on a broad frequency range from 300 to 5000Hz is shown to be significantly affected by the AMW unit system.

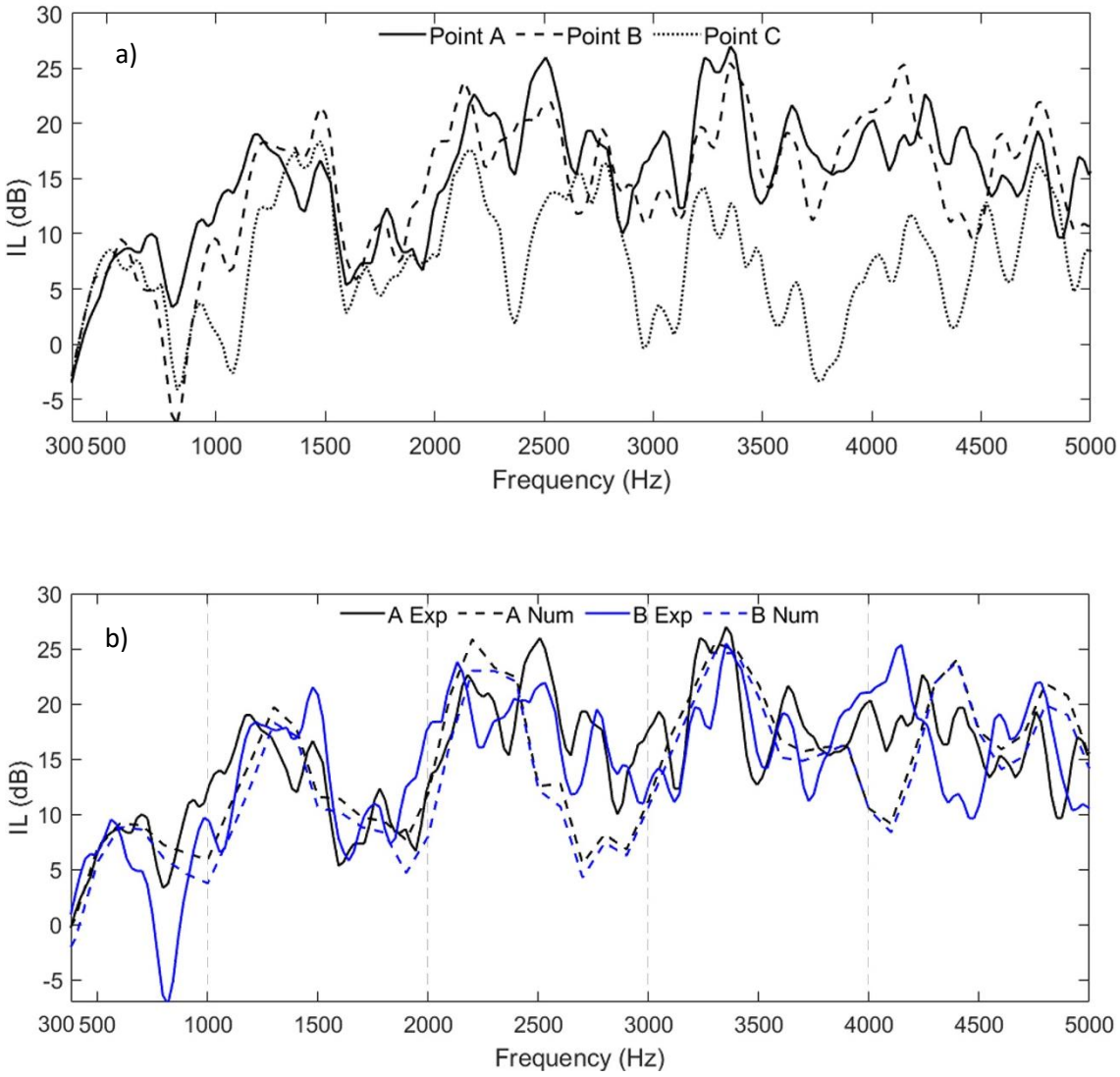

Figure 5.3 (a) Experimental analysis results in terms of IL related to measurement points A, B, and C; (b) Comparison of IL results related to the numerical and experimental studies on point A and B: six peaks are distributed along with the overall range, where the first is between 300-1000 Hz, the second between 1000-2000 Hz, the third between 2000-3000 Hz, the forth between 3000-4000 Hz, and the fifth and the sixth between 4000-5000 Hz.

Table 5.1 CV value calculated between the numerical results values and the experimental results values of specific frequency ranges.

	Frequency ranges (Hz)				
	300-1000	1000-2000	2000-3000	3000-4000	4000-5000
CV (A)	36.34 %	28.05 %	39.55 %	22.63 %	28.62 %
CV (B)	89.45 %	33.07 %	32.97 %	21.80 %	39.92 %

5.3.3 Determination of the coefficient of variation for the validation of numerical method through the experimental results

The numerical method is validated through experimental results in terms of *IL* and about each measurement point. *IL* slopes are observed with their characterising peaks and dips in terms of coefficient of variation (*CV*) according to the frequency range:

$$\boldsymbol{CV} = \frac{\boldsymbol{RMS_1}}{\boldsymbol{RMS_2}} \times \mathbf{100} \quad (\%) \tag{5.2}$$

where the Root Mean Square (RMS_{1-2}) express the measure of the magnitude *IL* values and is used to determine standard deviation and mean between the numerical and experimental results values:

$$\boldsymbol{RMS_1} = \sqrt{\frac{\sum_{i=1}^{N}\left(\boldsymbol{IL_{Num,i}} - \boldsymbol{IL_{Exp,i}}\right)^2}{\boldsymbol{N}}} \tag{5.3}$$

where:

- RMS_1= RMS to determine the standard deviation.
- $IL_{Num,i}$= *IL* calculated from the numerical method. (dB)
- $IL_{Exp,i}$= *IL* calculated from the experimental method. (dB)
- N = sample size.

$$\boldsymbol{RMS_2} = \sqrt{\frac{\sum_{i=1}^{N} \boldsymbol{IL_{Exp,i}}^2}{\boldsymbol{N}}} \tag{5.4}$$

where:

- RMS_2= *RMS* to determine the mean.

The CV is the standard deviation ratio to the mean and shows the variability of the population's mean. So, the higher the *CV*, the greater the dispersion RMS.

Figure 5.3.b compares *IL* results at points A and B obtained from the experimental measurement and numerical simulation. From the graphs, six peaks distributed along the frequency range are possibly highlighted (see Figure 5.3.b). The simulation curve can capture the main variation trend and the occurrence of *IL* peaks well. The *CV,* as defined in Eq. *5.2*, is used to evaluate the correspondence between experiment and simulation. Table 5.1 shows the values of *CV* in the sub-divided frequency ranges. A generally good agreement between numerical and experimental results can be found within

the broad frequency range: *CV* is always below 40%, excluding the *CV* (B) at low frequencies (300-1000 Hz).

The discrepancies between experimental and simulation curves can be possibly attributed to a few reasons. First, the frequency step size adopted by the simulation is much wider than that used in the experiment, mainly limited by the heavy computation cost. Therefore, simulation captures IL's magnitude and variation behaviour while neglecting the frequency fluctuations. Second, the experimental set-up slightly differs from the numerical model, mainly in the sound source condition and the *IL* evaluation points. In the numerical simulation, a plane wave is assumed to impinge on the AMW, partially reflected back and partially transmitted through the structure. The *IL* is then calculated from the results with/without the AMW. While in the experiments, the AMW is attached to a loudspeaker, which forms a much more complicated system than the assumed plane wave incidence. The reflected waves cannot exit freely from the inlet duct, and the measured *IL* can possibly couple with some loudspeaker characteristics such as the resonances of the membrane, cavity, and so forth. Meanwhile, the *IL* is evaluated at two selected points, although ideally, *IL* could be measured by the overall reduction of radiated sound power level, which could further improve the correlation accuracy. Third, the AMW prototype made of acrylic panels may vibrate during *IL* measurement, and the simulation does not consider this structural sound transmission path. The relatively small anechoic chamber and geometric imperfections during prototype fabrication may also lead to some errors. Generally, the simulation and experiment's general correspondence is acceptable, which allows using the model for some parametric studies.

5.4 Broadband potential optimisation of the AMW unit’s acoustic performance

A further broadband potential optimisation of the AMW unit’s acoustic performance is investigated next. The numerical characterisation study of the AMM unit is indeed performed due to the numerical and experimental methods agreement for *IL* calculation of such AMM window system and the need for acoustic performance improvements on the lower frequency range. The resonating volume extension through AMM unit cells panels perforation is investigated to reach a resonance that affects low-frequency bandwidth wavelength. The study this time is performed between a frequency range of 10-5000 Hz. As a comparison, three models with different perforating percentages and dispositions are studied and compared to the *IL* performance of the original frame model concerning point A measurements. Only the frame’s corners' inner sides are modified accordingly with a 14 or 7 %

perforation ratio (where the percentage is calculated with the ratio between the whole inner panels' area and the perforated area). As illustrated in Figure 5.4.a, configuration A (with 14% of perforation of the area of the overall panels) has a resonating volume of 13,85 x 10^{-4} m^3 (see Figure 5.4.a). Configuration B has 7% of perforation on the panels belonging to 2/4 of the same AMM units, while configuration C has 7% of the overall panels' area's perforation applied on one panel of each AMM unit. In these two last models (B and C), the resonating volume reaches 15.40 x 10^{-4} m^3, and the perforated panels within the AMW unit geometry are placed differently to investigate if the perforation position is a determinant parameter for the AMW IL.

Figure 5.4.b shows that the *IL* performance of the acoustically optimised configurations B and C improves from 50 to 5000 Hz with an average increase of 11 dB from the original frame window model. This is because the resonant volume is increased significantly and can control the wavelength of lower frequency bandwidths. On the other hand, the *IL* curve in Figure 5.4.b also shows that for Configuration A, there is no significant difference with the normal frame performance except for a significant average improvement of 5 dB in the frequency range 700-1200 Hz. Consequently, such small resonance volume addition does not improve the AMW unit performance significantly on broadband. So configuration B and C work more efficiently when compared to either the original configuration or configuration A because they allow the AMM unit to have the biggest resonating volume, showing that the perforation percentage is a crucial factor for the design of such AMM window, especially at low frequencies (50-800 Hz) where they reach an average of 15 dB of *IL*. On the other side, it is important to note that the perforated panels' disposition does not seem crucial, meaning *IL*'s most influencing parameter is the additional resonant volume (so the panels' perforating percentage).

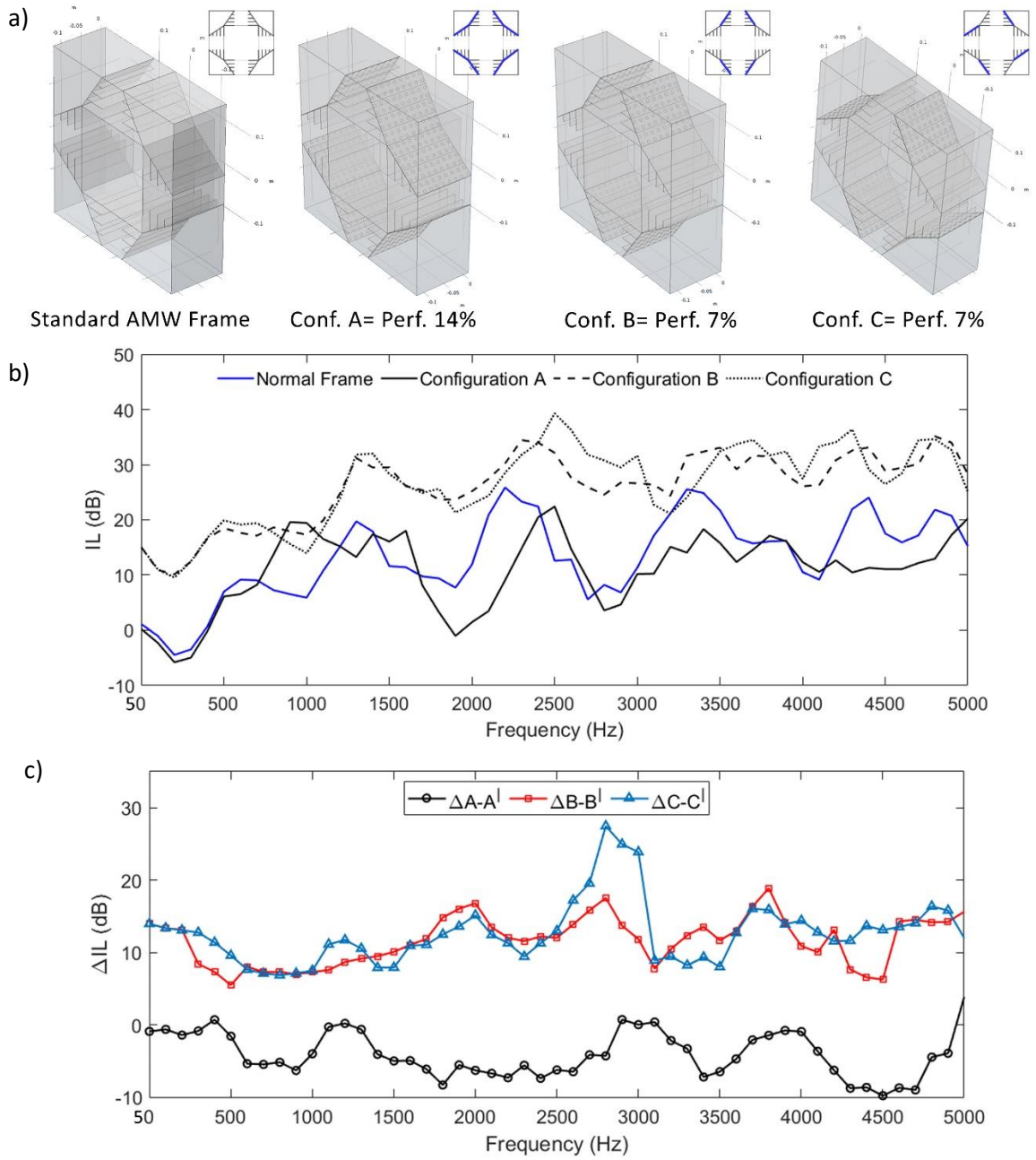

Figure 5.4 (a) Sketches of the AMW unit upgraded models through the perforation of the AMM unit frame side panels (the position of the perforated panels is shown in the section schematic with blue thicker lines); (b) IL numerical comparison between the original AMW unit model and the perforation characterised ones (A-C); (c) flanks contribution assessment in combination with the resonant volume extension (through perforation).

Furthermore, since an additional characterisation of the geometry has been introduced in the AMW unit, it is fundamental to assess that the contribution of the original AMM unit cell (see Figure 5.1.b), especially focusing on the cavities is still in place. For this reason, another numerical analysis is conducted by removing from the internal sound hard boundaries the unit cells panels interested by the perforation for each configuration (A, B, and C) and calling them A', B', and C'. Then the difference between the *IL* of the configurations A, B, and C, and the *IL* of A', B', and C' is calculated as $\Delta A - A' = ILA - ILA'$ and so on, (see Figure 5.4.c). This schematic proves that resonance coupling of flanks and

corners is especially visible for Δ B-B' and Δ C-C', where *IL*'s positive value shows an efficient combination of the two acoustic techniques where the contribution of the flanks is still visible.

5.5 Integrated optimisation of acoustics and ventilation

The proposed configurations' ventilation performance is finally numerically investigated through a FEM computational fluid dynamic (CFD) model. In the numerical analysis, the air was set to flow through each configuration, and the corresponding responses were analysed for different inlet velocities and different ventilation opening percentages. Figure 5.5.a shows the pressure drop against inlet air velocities for different AMW configurations, while Figure 5.5.b shows the same parameter results for configuration B for different airflow and a different percentage of the ventilation opening values. An increase of the required pressure differential across the AMW is observed proportionally to the increasing flow rate. Moreover, a higher pressure drop is resulted from an AMW with 13% of ventilation opening, demonstrating that the smaller ventilation openings offer high airflow resistance, as the static airflow resistance. This is because the static airflow resistance σ_f is indirectly proportional to the ventilation opening ($\sigma_f = 8\eta/\psi(0.5d_v)^2$, where η is the dynamic viscosity of the fluid, ψ is the percentage of the opening, and d_v is the opening diameter). [12] It is evident that as d_v becomes smaller, σ_f increases rapidly, and due to buoyancy forces results in a high pressure drop ($\Delta P = -\sigma_f v_a$ where v_a is the airflow velocity) across the AMW unit. [291] Consequently, most of the AMW configurations are suitable for natural ventilation, and a dynamic tuned ventilation capacity can be achieved for particular ranges by adjusting the models' ventilation opening.

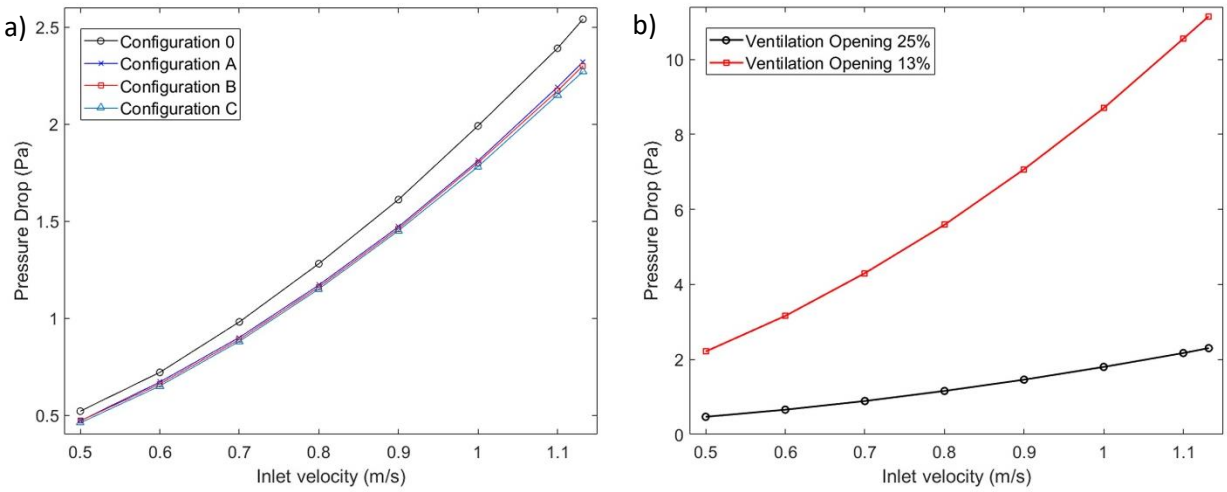

Figure 5.5 Pressure drop against inlet air velocities (a) for different AMW configurations and (b) for configuration B with different per-centage of the ventilation opening values.

It is worth mentioning that this study is intended to present a preliminary evaluation of the ventilation and acoustic performance of the AMW unit, where the effect of flow-induced noise is neglected. As the AMW structure comprises cavities along the flow path, Rossiter tones may occur aerodynamically. Previous studies have investigated the effect of low Mach-number flow (below 0.1) on a similar system comprising cavities and perforations, which found that the maximum deviation between no flow and Mach 0.1 is around 10 dB, mainly at the attenuation peak [292]. Therefore, as ventilation only requires very low flow speed, the current simplification by neglecting aerodynamic noise is considered to be reasonable. The results in the absence of flow could also set a baseline for future comparisons with the flow.

5.6 Conclusions

In conclusion, in this project chapter, we designed a metawindow unit system and examined the acoustic and ventilation performance numerically and (for the acoustic part) experimentally. Both numerical and experimental results showed a significant *IL* within a frequency range of 300 to 5000 Hz, and the agreement between them was proved. Acoustic optimisation was numerically investigated by extending the resonant volume until including the whole corners' areas. Two of the new configurations (B and C) showed to significantly reduce noise on a broad frequency range of 50 to 5000 Hz. They are specifically more effective on a low-frequency range within 50-1000 Hz, where they improve the original model's performance of averagely 15 dB. They also seem to be acoustically improved from configuration A, making the perforated panels' percentage crucial. The ventilation performance was also assessed, and it proved that most of the AMW configurations are suitable for natural ventilation and that the ventilation capacity can be tuned according to different ranges by adjusting the window's ventilation opening.

While the significant results in the acoustic and ventilation analysis showed advantages over the standard ventilation AMMs (such as effective long term natural ventilation combined with customised broadband noise reduction), further optimisation steps might clarify if this mechanism can be applied to different window's shapes and dimensions, or wider environmental settings with different inlet flow conditions and room characterisation.

6. AMW unit effect on the human perception

The contents included in this chapter will be submitted for publication in relevant international peer-reviewed journals. Part of section **6.3 Psychoacoustic effect of the AMW unit** has been published in the peer-reviewed journal *Building Acoustics* (Sage) by the name of "Design of urban furniture to enhance the soundscape: A case study" (2018) [47].

In this chapter, the model of the AMW unit investigated in Chapter **5 AMM adaptation to real window design** is going to be validated through the psychoacoustic and human perception spheres. In this way, the alignment of the AMW unit ergonomic development with the ergonomic criteria explained in Chapter **3. Participatory approach to draw ergonomic criteria for window design** will also be tested. The ergonomic criteria are: 1) participants perceive the window as an essential mediating instrument between the indoor and the outdoor of a building; 2) through this feature, they feel connected to the outdoor environment; and 3) despite the non-optimal conditions, they feel oriented and perceive an improvement in the indoors affective impact. If these criteria are respected, this chapter of the PhD study will represent a first experimental application of the ergonomic design criteria explained in Chapter 3. The window design would become, then, not only the mediator between the outside inputs and the indoor comfort, but it could even modulate the first one to optimise the second.

6.1 Background

AMMs have lately opened up a wider range of applications in building acoustics, also related to the simultaneous natural ventilation/thermal regulation [23–25,27,28,189,263]. In addition, these materials play a key role in the regulation of indoor comfort from the users' perspective through building features[16,26,35]. Ergonomic design criteria related to some of these features, such as the window, have been drawn recently [4]; however, there are no clear guidelines on how to assess the effectiveness of an AMM based feature design from a psychoacoustic and human perceptional point of view.

In this part of the PhD thesis, a new method for evaluating AMMs based on human perception is presented. Starting from several definitions of psychoacoustic parameters and soundscape descriptors [49,293], the effect of the AMM based window is applied to a number of ordinary

environmental acoustic scenarios [225]. Through a mixed experimental methodology, human preferences and perceptions regarding each filtered acoustic environment are investigated. As a result, customisable AMM-based window design could be applied to specific indoor functions following the previously established ergonomic design criteria [4].

This study aims at validating the presented AMW unit model from a human perception point of view. Moreover, the methodology used could be integrated and also used for other AMMs based architectural features design. Therefore, experimental parametric and experimental questionnaire methods are carried out synergically to determine an optimal way to investigate such a multidisciplinary research question. Through such a new methodology, the impact of the AMW unit on the environmental indoor human perception would be assessed, creating a new paradigm for AMM based systems for natural ventilation/heating control combined with noise reduction systems.

6.2 Materials and methods

The AMW unit's effect on seven soundscape recordings is first experimentally recorded and then analysed in terms of psychoacoustic parameters. Furthermore, on a second stage of the study, the AMW unit effect recordings are presented randomly and in a non-identifiable way to 85 participants. Their perception is investigated through an experimental laboratory and online questionnaire. The window prototype's experimental recordings and measurements have been run in the anechoic chamber of the acoustics laboratory in the Department of Mechanical Engineering of the National University of Singapore (NUS). The experimental laboratory questionnaire was conducted in a controlled environment room at the University of Perugia (IT).

6.2.1 Experimental setup for the input signals

The AMW unit was fabricated following the same dimensions of the numerical analysis model (Figure 5.1). The same procedure was explained in Chapter **5 AMM adaptation to real window design**. 3D printed Polylactic Acid (PLA, material properties; E= 1.28GPa, ρ=1210 kg/m3, and n=0.36), with fused deposition modelling technology (3D printer Fortus 350) (white geometry in Figure 5.1.a) was used for the internal parts. FusionPro laser cutter (by Epilog Laser) was used to cut transparent acrylic panels (of thickness 5mm and 2mm) to build the rest of the AMW unit (transparent part in Figure 5.1.a). The unit is placed at the centre of a small-size anechoic chamber (inner dimension is 2mx2mx2m, cut off frequency is about 300 Hz). The AMW is attached on the outdoor side with a loudspeaker coupled

with a power amplifier FRS 10 WP 8 OHM No. 2101 by VISATON (frequency range from 90 Hz to 19000 Hz and input power of 25 W) connected to the computer of the laboratory as shown from Figure 5.2.b,c. The model is fixed to the loudspeaker to avoid any sound leakage from the two systems junction. The *SPL* measurements were performed at the same three positions, A, B, C (Figure 5.2.b), using a sound level meter with a built-in FFT analyser (Aihua AWA6228). *IL* was calculated following Equation

$$\boldsymbol{IL_{AMW} = SPL_{woAMW} - SPL_{wAMW}} \quad \text{(dB)} \qquad 5.1$$

.

6.2.2 Experimental setup for the laboratory human perception questionnaire

NEXT.ROOM is a laboratory facility specifically designed to perform multi-domain human comfort studies. The facility (4x4x2.7 m) is located inside the laboratories of the Engineering Campus of the University of Perugia (Italy, Cfa Köppen-Geiger climate class [294]).

The test room indoor conditions are thermally controlled through both air conditioning and a radiant system. During the presented experimental campaign, all the surfaces were conditioned at the same temperature to provide a homogeneous thermal environment. The NEXT.ROOM lighting system comprises four LED panels presenting constant luminous flux (3200 lm) and Correlated Color Temperature (4000 K). These were the only light sources during the present experimental campaign.

According to the standards [295], internal conditions are continuously monitored for assessing thermal, visual, and air quality status. No specific audio systems are currently installed in the NEXT. ROOM and the presented experimental campaign provided acoustic stimuli through wired noise-cancelling headphones (model WH-1000XM4, by Sony).

The internal background noise level was mapped through a sound level meter (model SOLO SLM, by 10dB) on a 9-points grid at 1.10 m height (which corresponds to the average height of a sitting person auditory system) in order to capture the background noise contributed by different fan speed settings of the mechanical ventilation (MV) system (Figure 6.1.a). The acoustic measurements were carried out under five internal conditions (MV off and MV operating at the four available levels of inlet flow). Figure 6.1 shows the measured background noise with MV off (off in Figure 6.1.b). MV could also operate at the second and fourth levels of inlet flow. Overall, as expected, the sound level of internal

background noise increases directly with the MV's intensity. Sound pressure level (*SPL*) peaks are highlighted at a low-frequency range (below 500Hz).

a)

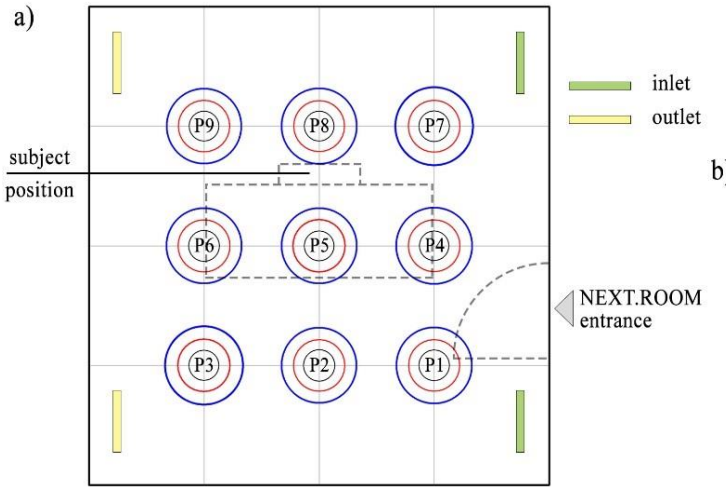

b)

Grid point	Ventilation speed level [db(A)]		
	Off ■	L2 ■	L4 ■
P1	23.7	39.8	58.6
P2	24.3	39.7	57.9
P3	23.3	40.4	60.2
P4	22.8	39.9	59.0
P5	23.1	40.3	58.1
P6	23.9	40.1	58.2
P7	23.7	40.0	60.1
P8	23.1	39.3	58.1
P9	22.9	39.7	57.8

Figure 6.1 NEXT.ROOM background noise level analysis considering the MV system off and operating at second (L2) and fourth (L4) levels of inlet flow. The sound level meter was placed at 1.1m of height at each measurement point.

Each subject listened to and evaluated seven different environmental sound recordings comprising the following categories: #1 Beach, #2 Woodlands, #3 Quiet Street, #4 Pedestrian Zone, #5 Park, #6 Shopping Mall, and #7 Busy Street. The following eight soundscapes descriptors are considered in this study: pleasant, chaotic, vibrant, uneventful, calm, annoying, eventful, monotonous [296,297].

The questionnaire-based study was set through Gorilla, an online platform. The questionnaire was developed through 15 questions. The first was open reply-based, while the other 14 were based on a 5 point Likert scale.

The comprehensive list of questions was:

1. While listening, please write down in the following tab any sound sources you can identify in this sound environment (please separate each sound source with a comma).

2. How did you hear the following four sounds? (Not at all; A Little; Moderately; A lot; Dominates Completely) (each sound source is here addressed with a different letter from A to D):

2.A Traffic Noise (cars, bus, trains, aeroplanes, etc.)

2.B Other noise (e.g. sirens, construction, industry, loading of goods)

2.C Sounds from human beings (e.g. conversation, laughter, children at play, footsteps)

2.D Natural sounds (e.g. singing birds, flowing water, wind in vegetation)

3. For each of the 8 scales below, to what extent do you agree or disagree that the outdoor public space you heard is... (Strongly Agree; Somewhat Agree; Neither; Somewhat Disagree; Strongly Disagree) (each soundscape descriptor is here addressed with a different letter from A to H)

3.A Pleasant

3.B Chaotic

3.C Vibrant

3.E Uneventful

3.F Calm

3.G Annoying

3.H Eventful

4. Overall, how would you describe the outdoor public space you have just heard? (Very good; Good; Neither bad nor good; Bad; Very bad)

5. How loud would you say this environment was? (Not at all; Slightly; Moderately; Very; Extremely)

The complete Questionnaire structure is shown in **Appendix A - Online Questionnaire related to experiment described in Chapter 6**.

6.2.3 Participants

In this project, the sampling is quite open since the study's aim includes all the different kinds of users of indoor spaces. Approval from the Ethics Committee from the University of Sheffield was received before starting the experiment. For this AMW unit human perception experiment, the recruitment was done through the University of Sheffield, the A*STAR and University of Perugia students and staff, and Sheffield's, Singapore's and Perugia's residents. The whole group of participants included 85 individuals, of which 39 females, 43 males, and 1 non-binary with age between 20 and 60 years old, hailing from Europe and North Africa (77%), Asia (19%), America (4%), and Australia (1%). It is essential to highlight that the study focused on the different backgrounds that would have defined correspondent factors under contextual experience (demographical, space usage, and psychological). [255] Hence, window design investigation is still at a global environmental stage in terms of history/heritage, ethnicity, geography and economic situation.

The following graphs (Figure 6.2, a-c) show the participants' characteristics regarding gender, age, and nationality.

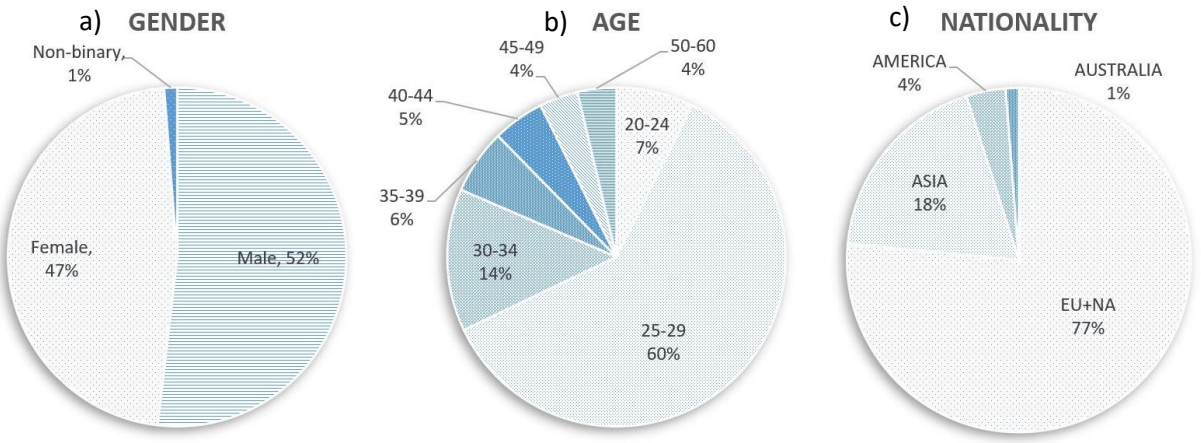

Figure 6.2 Background of the participants: (a) gender, (b) age, and (c) nationality.

6.3 Psychoacoustic effect of the AMW unit

Following the EU Directive on Environmental Noise [116], certain noise levels during the day and night time must be ensured to guarantee the people a limit of exposure to sounds in public spaces, which kept increasing during the last 50 years due to the wild urbanization worldwide. According to WHO the 30% of the EU population is exposed to noise levels exceeding 55 dB(A) during nighttime [298]. However, since Schafer [280] defines the soundscape concept, a new methodology more focused on people's psychoacoustic perception of spaces has entered modern acoustics. Simultaneously, new soundscape inspired descriptors focused on people perception in specific soundscape environments (called psychoacoustic parameters) were added to the standard ones (as the *A-weighted SPL*) [47,49,299,300]. The use of such new parameters is also encouraged by the International Organization for Standardization, which defines soundscape as 'the acoustic environment as perceived or experienced and/or understood by a person or people, in context'.[301] Therefore, it is clear how this new acoustic approach put more effort into enhancing the more pleasant sounds rather than the mere reduction of the noise level. [302]

Psychoacoustic parameters have been selected to study the capability of the AMW unit prototype to facilitate the perception of desirable sounds coming from the outdoor, which can be considered one of the most important features which influence the global assessment of public and private indoor spaces quality [225]. The selected parameters have been used to evaluate the recorded data from the anechoic chamber tests through a descriptive analysis of the effectiveness of the AMW unit on the

user performed through the HEAD Artemis 11.0 software. The present research has been developed through the study of a physic parameter, such as *SPL*, and psychoacoustic parameters such as loudness (*N*), roughness (*R*), sharpness (*S*) and fluctuation strength (*FS*), to evaluate the effect of the AMW unit in the seven experimental acoustic environments. Perception of sounds involves a complex chain of events to interpret the information contained in sound signals emitted from sound sources [303]. While sound parameters (such as *SPL* and Insertion Loss, that is, the difference in *SPL* measured with and without the AMW unit) can help in the study of the physical tolerance of the human organ of auditory perception, psychoacoustics is the science of sound perception, investigating the statistical relationship between acoustic stimuli and hearing sensations. This section examines the variations of the analysed parameters expressed as arithmetic averages over all the values related to different soundscape recordings. The obtained values are expressed with respect to the two different configurations (with and without the AMW unit), the seven different environmental recordings and the three positions of the microphone.

In order to verify the efficiency of the AMW unit in improving the user acoustic comfort conditions, it is necessary to detect the minimum differences in these metrics which are subjectively perceived: just noticeable differences [304], *ΔMIN*, for each parameter used for the analysis: 3 dB for *SPL*, 32 phon for loudness, 17% asper for roughness, 0.04 acum for sharpness and 17% vacil for fluctuation strength.

Moreover, for the sake of simplicity, the microphone position is labelled with letters from a to c as it changes in terms of distance from the point where the source is perpendicular to the AMW unit and 0.2m and 0.5m far perpendicularly (respectively measurement point a and b) and 0.2m far laterally (measurement point c) (see Figure 5.2.b). Environmental recordings are labelled by numbers from 1 to 7 as described in the introduction of this chapter: beach (#1), woodlands (#2), quiet street (#3), pedestrian zone (#4), park (#5), shopping mall (#6), and busy street (#7).

For each psychoacoustic parameter, the value *ΔX* has been considered as the difference of the parameter *X*, evaluated with and without the AMW unit interposed between the source and the microphone. Then each *ΔX* value has been divided by each specific *ΔMIN* to determine how perceivable is the AMW unit contribution in terms of psychoacoustic parameters (*Eff(X)*). Below is shown an example with (*Eff(N)*):

$$Eff(N) = \frac{\Delta N}{\Delta MIN} \tag{6.1}$$

where

$\Delta N = N_{without} - N_{with}$

ΔMIN= just noticeable difference from a human hearing system in terms of each psychoacoustic parameter [304]

Figure 6.3 shows the effectiveness of the AMW unit contribution according to different environmental recordings (#1-7) and different measuring points in the anechoic chamber (a-c). Loudness (*N*) is effectively reduced according to the analytical analysis. Specifically for a perpendicular distance of 0.5 m, the user can perceive an average of 3 times the *ΔMIN* in terms of sone. So the AMW unit reduces the N component consistently in most of the recorded environments. A significant decrease of Roughness (R) is also perceived in terms of *ΔMIN* through the application of the AMW unit. As in the *N* case, soundscape 1 and 7 are those where its contribution is more perceivable. This is probably due to the high pitch components of the recordings (see Figure 6.8, and Figure 6.14). Differently from the *N* perception, the *R* seems to be reduced sensibly through the model also in measurement point c, showing an overall significant impact of the AMW unit on this psychoacoustic parameter. Sharpness (*S*) is influenced by the AMW unit consistently overall for all the measurement points. It is useful to observe that, especially in measurement point b, soundscape 1, 4, 6 are influenced the most from the AMW unit. These recorded acoustic environments are also those with middle-high frequency peaks reduction (100-4500 Hz) (see Figure 6.8, Figure 6.11, Figure 6.13). Finally, Fluctuation Strength (*FS*) *ΔMIN* is also perceived through the application of the AMW unit. However, the contribution is mostly negative in this psychoacoustic parameter. This is inversely related to S, and it is highlighted in recording #6 (Shopping Mall), where *FS* seems to be amplified by the model in measurement point b. All parameters are not effectively changed in the measurement point c. The reason is probably due to the directness of the sound wave towards point c, which is also the closest to the ventilation openings.

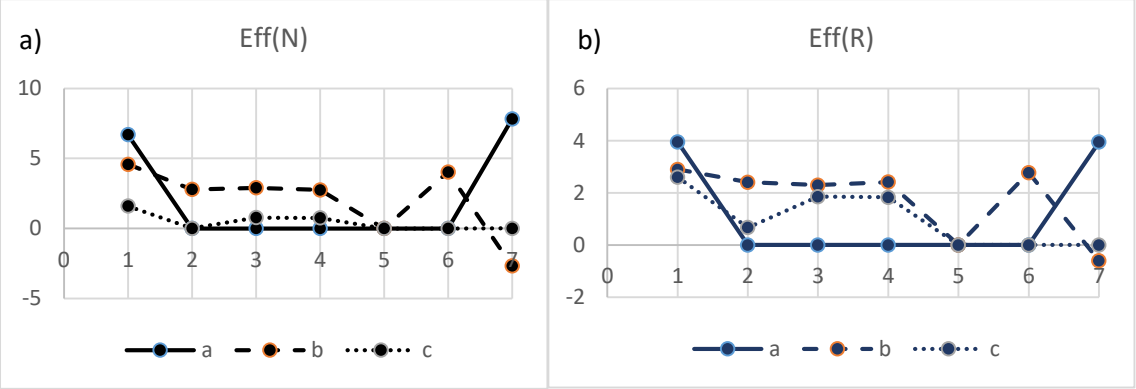

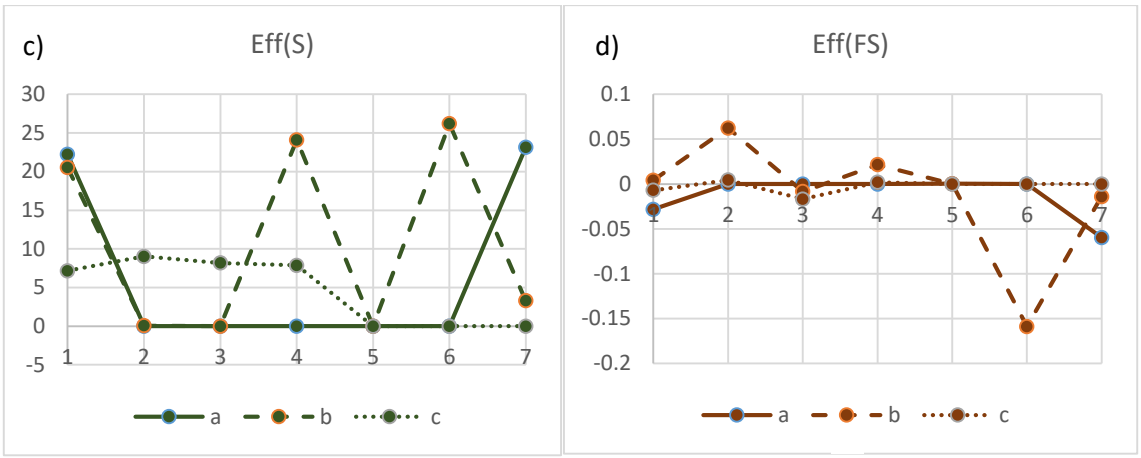

Figure 6.3 Effectiveness of the AMW unit (EffX) according to four psychoacoustic parameters: a)Loudness (N), b) Roughness (R), c) Sharpness (S), and d) Fluctuation Strength (FS). The graphs show data gathered from the three measuring points showed in Figure 5.2.b. X axis represents the recorded sound environments, ordered from the most natural to the most artificial one: beach (#1), woodlands (#2), quiet street (#3), pedestrian zone (#4), park (#5), shopping mall (#6), and busy street (#7).

6.4 AMW unit effect on human perception

First of all, results from the human perception over the AMW unit contribution will be discussed broadly (including laboratory and online experiments). Since there is no available methodology to conduct such an experiment on an AMM based design, a new method had to be drawn, and so, even if the focus of this PhD thesis is to demonstrate the effectiveness of the AMW unit, a discussion on the robustness of the method is needed. In a further section, the robustness and limitation of such a method will be discussed.

6.4.1 AMW unit effect through soundscape descriptors

Through the laboratory and online questionnaire, the seven proposed soundscape recordings with and without the effect of the AMW unit (14 recordings in total) were evaluated qualitatively by the participants. The recordings were presented randomly. Soundscape descriptors helped the participants to describe each listened recording in terms of the following adjectives: eventful, vibrant, pleasant, calm, uneventful, monotonous, annoying, and chaotic[297,299]. The scale used to rate the 14 recordings were based on five votes: strongly agree, somewhat agree, neither, somewhat disagree, and strongly disagree. During both the laboratory and online questionnaire, the participants did not have a time limit to evaluate each listened recording and replay it as many times as possible. This section will analyse the overall participants' evaluation according to each soundscape and compare the recordings with and without the AMW unit. Due to their 5 point Likert scale nature, a ponderation

was performed to allow clearer visualisation of different soundscape recordings evaluation. Participants' responses for each soundscape recording were multiplicated times 0 to 4 according to the participants' rate. Respectively, 'strongly disagree' rates were multiplied times 0, 'somewhat disagree' rates were multiplied times 1, 'neither' rates were multiplied times 2, 'somewhat agree' rates were multiplied times 3, and 'strongly agree' rates were multiplied time 4. Through this ponderation process, the overall soundscape descriptors showed in Figure 6.4 were calculated as:

$$Total\ ponderated\ vote = \sum X_0 \cdot 0 + X_1 \cdot 1 + X_2 \cdot 2 + X_3 \cdot 3 + X_4 \cdot 4 \qquad 6.2$$

where

X_0= total 'strongly disagree' votes for specific soundscape recordings

X_1= total 'somewhat disagree' votes for specific soundscape recordings

X_2= total 'neither' votes for specific soundscape recordings

X_3= total 'somewhat agree' votes for specific soundscape recordings

X_4= total 'strongly agree' votes for specific soundscape recordings

Figure 6.4.a shows the overall participants evaluation of the first six soundscape recordings: #1 Beach (without and with the AMW unit), #2 Woodland (without and with the AMW unit), and #3 Quiet street (without and with the AMW unit). Overall the original three soundscape recordings (without the AMW unit) are perceived much more eventful and vibrant than the other configuration (with the AMW unit). On the other hand, the AMW unit effect increases the monotonous and uneventful component significantly (20% more), especially for the #1 Beach and #3 Quiet street. Furthermore, #2 Woodland is negatively affected in terms of pleasantness, 17% less than the original one.

The participants' evaluation of soundscape recordings #4 Pedestrian zone and #5 Park are showed in Figure 6.4.b. Also, the participants perceive an overall significant decrease in eventfulness, vibrancy, and pleasantness. These two soundscapes recorded with the effect of the AMW unit are judge sensibly more monotonous and uneventful than the original recordings (especially #5 Park_w, 26% more monotonous and 22% more uneventful). They are showing then a general neutralisation of the heard environment through the window prototype.

Figure 6.4.c shows the overall participants evaluation of the last six soundscape recordings: #6 Shopping Mall (without and with the AMW unit) and #7 Busy street (without and with the AMW unit). Overall the configuration with the AMW unit is perceived as less chaotic and eventful. However, in the

case of #6 Shopping Mall, this configuration is perceived as slightly more annoying. According to Di Blasio et al., this could be because, in this soundscape, there are many "talking sources" that include music playing, people chatting, and radio advertisement [305]. As explained by Di Blasio et al. and also Haapakangas et al., our brain tends to pay much more attention to these sorts of sources, rather than music or natural sound sources, because it naturally tries to understand the message they are communicating [305,306]. Therefore, since the application of the AMW unit tends to neutralise each specific sound source, including the "talking" ones, participants naturally feel slightly annoyed because its message cannot be easily elaborated. So this is probably why they judge the recording as more annoying than the original one.

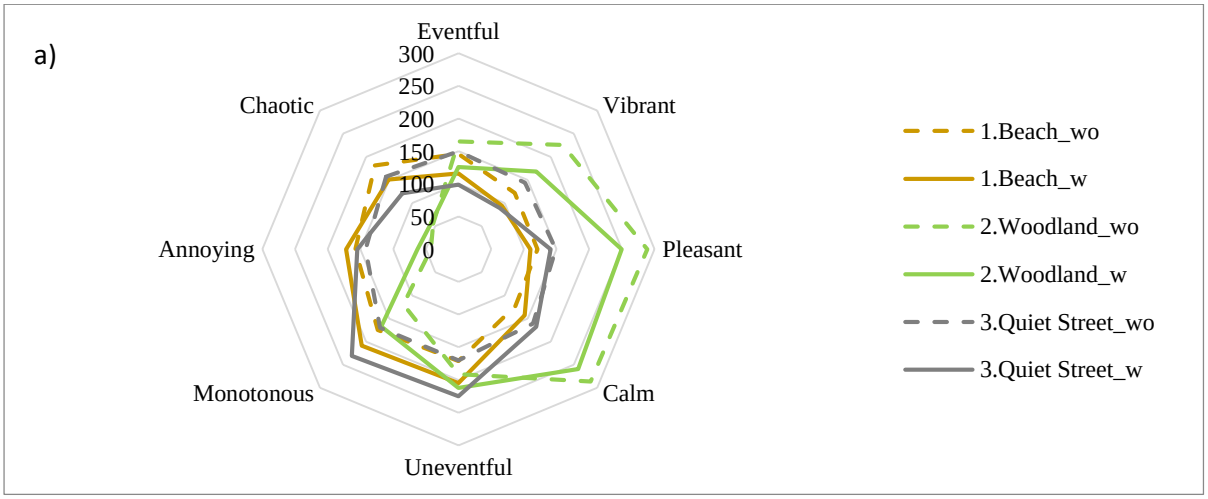

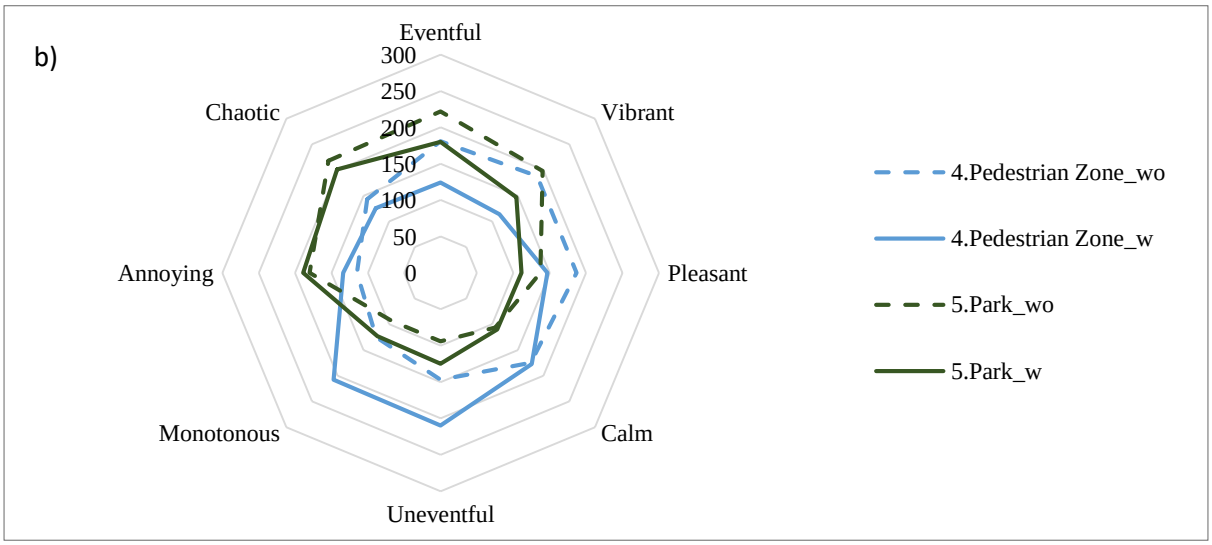

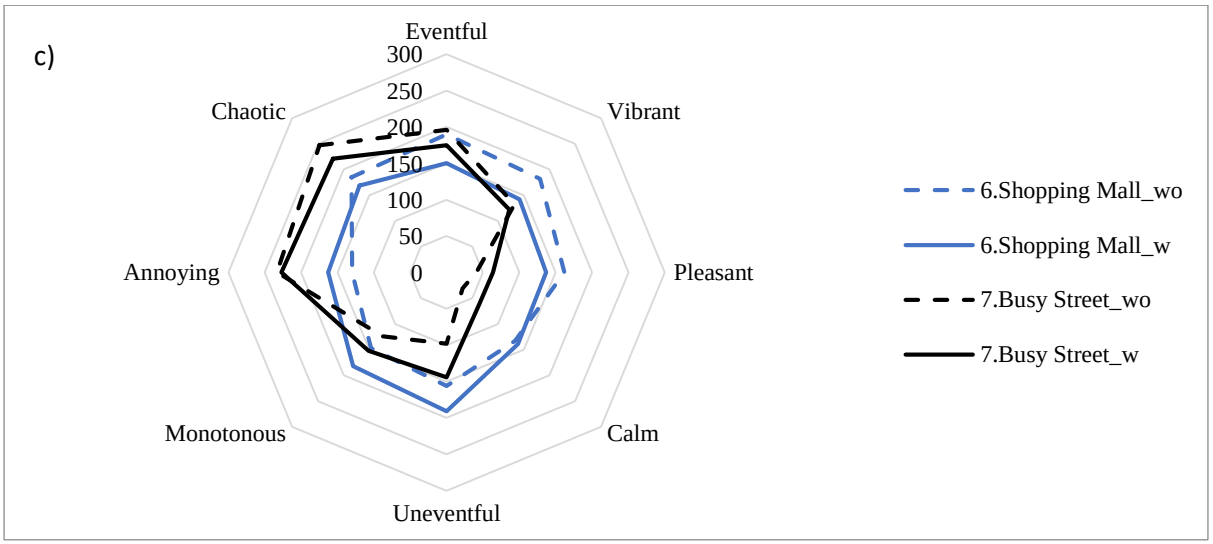

Figure 6.4 Overall participants evaluation of the 14 soundscape recordings: #1 Beach (without and with the AMW unit), #2 Woodland (without and with the AMW unit), #3 Quiet street (without and with the AMW unit), #4 Pedestrian zone (without and with the AMW unit), #5 Park (without and with the AMW unit), #6 Shopping Mall (without and with the AMW unit), and #7 Busy street (without and with the AMW unit).

6.4.2 AMW unit effect on Loudness through psychoacoustic analysis and human perception evaluation

The loudness of a soundscape is crucial for both human wellbeing and comfort [296]. Hong et al. demonstrated how perceived loudness could directly influence the soundscape quality and so the physical stress that a person may develop from it. At the same time, Hong et al. argue that higher Loudness can be an expected and so pleasant component in specific recreative environments such as concerts and recreational activities. In this study, Loudness has been analysed analytically through the HEAD Artemis suite (representing the magnitude of an auditory sensation and calculated according to ISO 532-1 [307]) and experimentally through the participants' evaluation. It is important to compare the loudness of the soundscape recordings, from the psychoacoustic analytical analysis and the human perception point of view, to define how standardised the questionnaire results can be. If they do correspond, then maybe the method used is validated from the psychoacoustic evaluation side.

The two Loudness (Psychoacoustic and Perceived) are compared in Figure 6.5 with two different evaluation scales highlighted on the left. Psychoacoustic Loudness is expressed as determined by Equation 1.17. In contrast, Perceived Loudness evaluated all the soundscape recordings by the laboratory and online experiment participants with a 5 Likert scale (Not at all Loud, Slightly Loud, Moderately Loud, Very Loud, and Extremely Loud). The results compared in this schematic should be evaluated as inversely proportioned, which means that a higher level of *Eff(N)* corresponds to a lower

rate of Perceived Loudness. From Figure 6.5, a correspondence can be observed especially referring to the Loudness related to soundscape #1 and #7. Both analyses show significant results in terms of Loudness reduction through the application of the AMW unit. For soundscape #2-#6, a less perceivable change of Loudness is highlighted from both Psychoacoustic analytic and Perceived analysis. However, the second one does not draw as defined results as the first one. Of course, some limitations related to the headset set-up might be the reason for that, so this variable should be investigated in the next section.

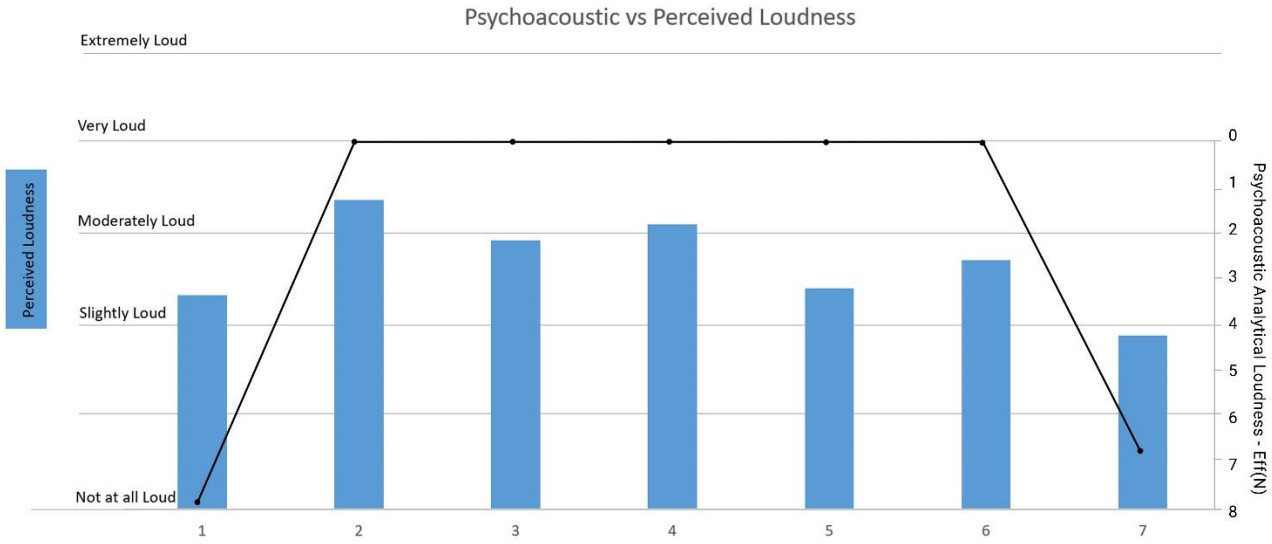

Figure 6.5 Comparison of psychoacoustic analytical results (solid black line) and experimental perceived results of Loudness in each soundscape recordings in the configuration with the AMW unit applied (bar graphs): #1 Beach, #2 Woodland, #3 Quiet street, #4 Pedestrian zone, #5 Park, #6 Shopping Mall, and #7 Busy street.

6.4.3 Spontaneous and directed sound sources detection

When considering the analysis of questionnaire-based soundscape evaluation, it is fundamental to analyse the perception of specific sound sources. This can be done through either a spontaneous or directed detection process. The participants are asked to report any particular sound sources they can detect within a specific soundscape or soundscape recording in the first case. In the second case, a number of sound sources options or categories are given as an example, and the participants have to rate how much they perceive a specific component within the soundscape or soundscape recordings (generally on a five-point Likert scale). These two methods have been widely used separately [296,308]. However, both were used for each soundscape recordings with and without the AMW unit effect in this study.

Figure 6.6 shows a comparison of the ponderated results for both spontaneous and directed sound sources detection. The first one was an extended written form where a comma separated each sound source. The second one was based on a five-point Likert scale which included the following categories:

1) Traffic Noise (e.g. cars, bus, trains, aeroplanes, etc.), 2) Other Noise (e.g. sirens, construction, industry, loading of goods, etc.), 3) Sounds from human beings (e.g. conversation, laughter, children at play, footsteps, etc.), 4) Natural sounds (e.g. singing birds, flowing water, wind in vegetation, etc.). Due to their different report nature, a ponderation and alignment of the results scale had to be performed, followed by a percentage transformation in order to compare them. For the directed votes, the ponderation was performed as in equation *6.2*. The percentage expression was then calculated considering the sum of the total votes for all the sound sources categories (Traffic Noise, Other Noise, Sound from human beings, and Natural sound) as the 100% of sound sources TOT_{ss}. So each sound sources percentage (SS%) of Figure 6.6 was calculated as:

$$SS\% = \frac{(SS_{votes} \cdot 100)}{TOT_{SS}} \qquad 6.3$$

Where

SS_{votes}=overall votes for specific sound sources

TOT_{ss}= overall sum of all the votes for all the sound sources for each spontaneous or directed based rate

From Figure 6.6, it is highlighted that some SS are most likely to be detected by the participants through the directed rate rather than the spontaneous one: Traffic Noise overall +6% and Other Noise overall +13%. The other two SS tend to be less detected on a directed based rate: Sound from human beings overall -14% and Natural Sounds overall -2%. Participants tend to neglect negative noises spontaneously, while they recall them once they are directly asked to detect them. In terms of results analysis through the effectiveness of the AMW unit, participants detected more Traffic Noise SS overall +8%, and less Natural sounds overall -5%. Because of this phenomenon, there is a potential for change in the results, so this should be taken into account for future studies and needs further investigation related to the robustness of the soundscape investigation approach to assess AMM based technologies. Another further research could be, for example, related to different environmental sound recordings.

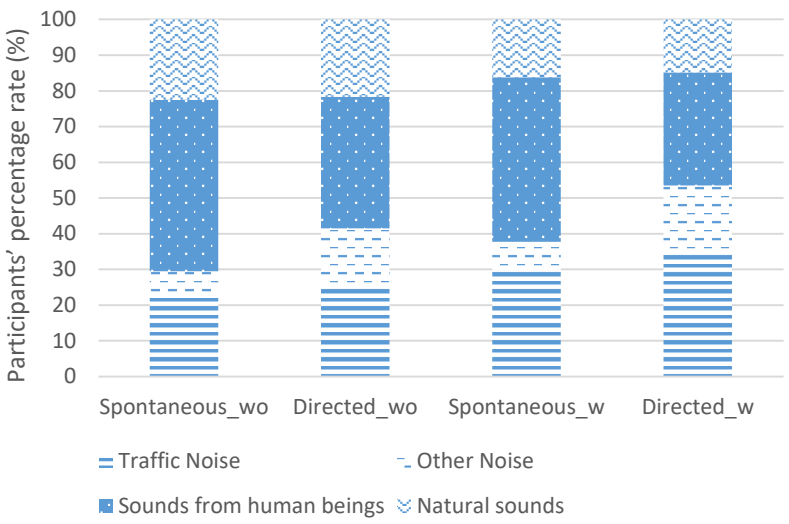

Figure 6.6 Comparison of the ponderated results for both spontaneous and directed sound sources detection in the soundscape recordings without and with the AMW unit effect and evaluated through 4 categories of sound sources: . 1) Traffic Noise (e.g. cars, bus, trains, aeroplanes, etc.), 2) Other Noise (e.g. sirens, construction, industry, loading of goods, etc.), 3) Sounds from human beings (e.g. conversation, laughter, children at play, footsteps, etc.), 4) Natural sounds (e.g. singing birds, flowing water, wind in vegetation, etc.).

6.5 Discussion

6.5.1 Robustness of the method

This study aimed at investigating the human perception of the AMW unit effect on soundscape recordings. Even if analytical and numerical studies have been run to investigate AMMs effectiveness in terms of *SPL*, *IL*, and *TL* (which are all physical parameters), the psychoacoustic or human perception related effectiveness of such materials has not been addressed consistently so far. Therefore, the method presented in this chapter has been developed by merging soundscape based questionnaire strategies and AMMs based input recordings for the beforementioned questionnaire. Moreover, the current pandemic situation provided an excellent opportunity for this project to expand the knowledge on the online questionnaire methodologies. People are indeed getting significantly used to online exercise everywhere in the world. If the study was limited to the laboratory tests, the sample would have had mostly the same geographical and cultural background, which might have biased the experiment's output. So the online experiment was included; however, the robustness must be assessed since this mixed (laboratory and online) methodology has not been used widely before.

6.5.1.1 Robustness of Online 1 method through the laboratory results

The laboratory method is characterised by constant headset set-up and background noise conditions. When conducting the questionnaire online, these parameters may variate slightly or strongly. In this part of the study, the robustness of the online questionnaire method will be discussed by comparing it with laboratory one through their results. First of all, the laboratory and online test results related to the same participants (16 in total) were compared. All the online tests (here referred to as Online 1 test for simplicity) were run with a three-week time difference to ensure that the laboratory answers would not bias participants. Results were compared in terms of 1) difference in the answer between the Laboratory and the Online 1, 2) approximation of the Laboratory answer, and 3) headset through which the Online 1 test was taken. The first parameter is defined as $\Delta rate = rate_{Laboratory} - rate_{Online\ 1}$ and it goes from 0 (in case the answer is the same for both Laboratory and Online 1 rate) to 4 (in case there are 4 points of rate in between the Laboratory rate and the Online 1 one). The second parameter determines how neutralised is the Online 1 rate compared to the Laboratory one. In this case, the answer for each question could be a) neutralised (when the Online 1 rate is closer to the neutral rate), b) Extremer (when the Online 1 rate is more extreme than the Laboratory one), and c) Opposite (when Online 1 rate is the opposite of the Laboratory one). The third parameter considers wired headphones, wired earphones and wireless (or Bluetooth earbuds) as headset setup of the Online 1 test. It is worth focusing on analysing the results according to the different headsets as they could lead to a different audio quality of the soundscape recordings without or with the AMW unit effect.

In terms of the second parameter, overall (without considering the different headsets), the participants' rates of the soundscape recordings without or with the AMW unit effect have been Neutralised in the 48% of the cases, Extremer in the 33% of the cases and are the Opposite to those they gave in the laboratory test for the 19% of the cases. The difference in the participants' rate of soundscape recordings between the Laboratory and the Online 1 ($\Delta rate$) is shown in percentages and according to the overall (TOT= total) and each specific headset in Figure 6.7. Overall there is a good correspondence of the Online 1 rating with the Laboratory ones. The 44.6% of the answers are indeed the same, followed by 37.8% with 1 rating point of difference, 15.3% with 2 rating points of difference, 2.0% with 3 rating points of difference, and 0.3% with 4 rating points of difference. From the headset setup point of view, all the Online 1 used systems result reliable in causing the same Laboratory response. The majority of perfect correspondence (*Δrate* = 0) is related to the wired headset. However, 29% of it is linked to wireless reproducing systems. Even more equal proportion is found in results with a *Δrate* equal to 1, meaning that the overall headset setups are also good at approximating the Laboratory set-up. A big difference in the headset acoustic quality reproduction starts to be

highlighted from *Δrate*= 2, where Bluetooth systems turn to cause responses less compatible with the Laboratory ones (same is highlighted for *Δrate*= 3, even if this has an overall percentage of 2%). Furthermore, even if the overall percentage is very low (0.3%), it is worth noticing that only wired headphones caused the most extreme and opposite response in the participants' Online 1 test. As it could be expected, *Δrate* related to the Bluetooth earphones/earbuds is the worst at approximating the laboratory perceptional judgements of the participants. This will be taken into account in the next stage of analysis: the one of the Online II questionnaires.

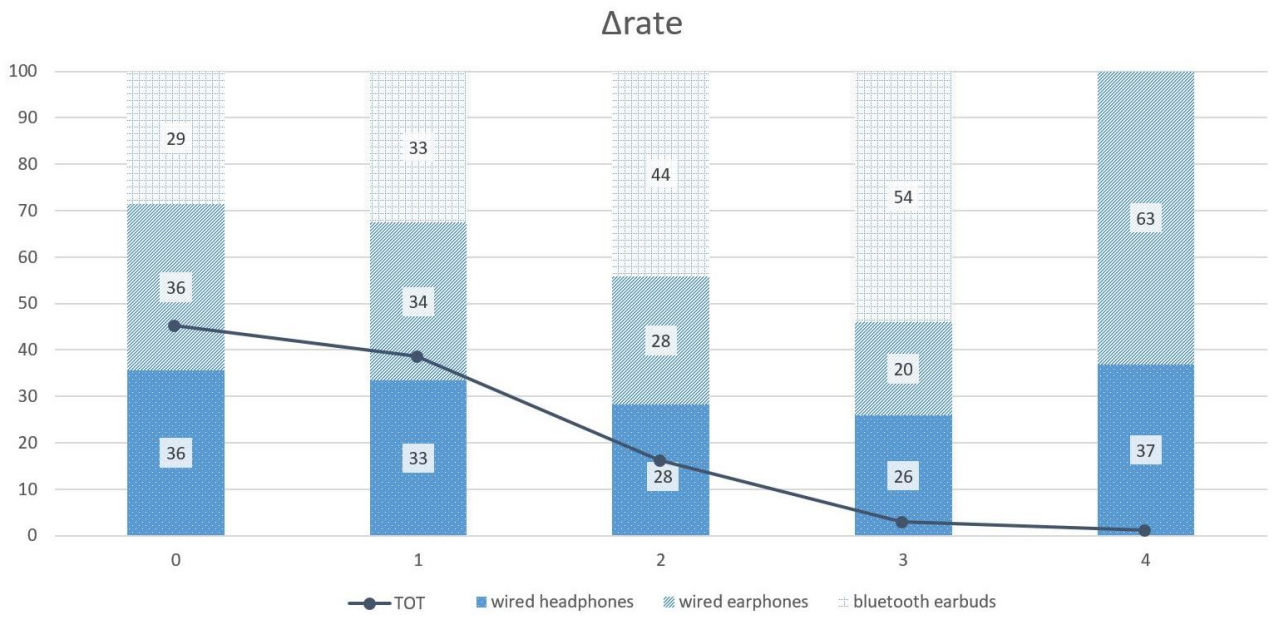

Figure 6.7 Difference in the participants' rate of soundscape recordings between the Laboratory and the Online 1 (Δrate) according to the overall (TOT= total) and each specific headset (expressed in percentages).

An Intra-Rater Reliability evaluation has been performed to understand if there was any significant influence of the different headset set up on the same participants' response to the auditory perception questionnaire. Intra-rater reliability based on the five-points Likert scales questions was obtained from Cronbach's alpha calculation. Appropriate and reliable measures to assess soundscape comfort have been identified in previous research (e.g. using psychoacoustic parameters); However, the reliability of individuals' judgement of soundscape comfort according to different environmental and experimental settings (i.e. headset setup intra-rater reliability) needs to be further investigated. Within the ambience scale in nursing homes context, for example, Kosters et al. [309] highlighted that, between individuals of the same experimental group, the overall physical and social features effect of a perceived environment relies differently on their feelings, moods, behaviour, actions, and reactions. Hoerzer et al. suggest that, intuitively, most individuals should have high intra-rater reliability when the mechanical, neurophysiological, and psychological factors that may influence a specific comfort

remain constant; however, they also highlight that this has not been tested specifically [310]. Following Hoerzer et al. suggestion in the acoustics sphere of research, a poor headset setup intra-rater reliability would generate inconsistent soundscape evaluation upon consistent questionnaire judgment. Thus, the acoustic perception impact of the AMW unit might not be effectively assessed. Therefore, assessing soundscape through poor reliability would be potentially misleading when investigating the effectiveness of AMMs based building features on human indoor comfort, while inaccurate evaluations of product development might also damage the window manufacturers. Intra-rater reliability investigation of different headset setup-based soundscape assessments is then crucial for identifying individuals with low reliability and developing strategies to account for this issue in the analysis stage.

In this chapter study, intra-rater reliability concerning the laboratory results (headset quality benchmark) was calculated by the intra-class correlation coefficient (ICC) [311]. ICC is a single index calculated variance that partially overcomes the popular correlation coefficients limitations. It is obtained by partitioning the total variance into between and within-subject variance (known as analysis of variance or ANOVA). Thus, both degrees of consistency and agreement among rating ICC are shown. However, this coefficient does not compare units through different studies of reliability. Therefore, to determine the reliability quality, researchers established thresholds [312,313] which helped the authors to classify the participants according to high or acceptable reliability (ICC ≥ 0.7) and or low or not acceptable reliability to assess soundscape with different headset setups (ICC < 0.7). In this study, particularly, Cronbach's alpha was also used to assess further the intra-rater reliability related to the five-point Likert scale questions (Cortina [314]), where a Cronbach's alpha value ≥ of 0.7 is considered as acceptable reliability (Cortina [314]) as for the ICC. Both parameters were calculated through SPSS Statistics, and, as a result, inter-rater reliability was proved for all the 16 participants with an ICC ≥ 0.7 and Cronbach's alpha value ≥ 0.7 (minimum α=0.723, maximum α=0.875), assessing the robustness of the online method used for the questionnaire on AMW unit soundscape impact assessment.

6.5.1.2 Robustness of Online 2 method through the laboratory results

In the Online 2 questionnaire, the soundscape recordings have been evaluated through the same questionnaire method but with different headsets (recorded by the system for further evaluation) and different background noise conditions. Thus, participants were able to do the test independently and in any place it was most convenient for them. The only requirement was to conduct the test in a relatively quiet environment using a set of headphones they already had available. So for accuracy, and due to the previous consideration in Section 6.5.1, different headsets results will be compared

with the laboratory results to show different used headsets in the Online 2 method affects people perception tendency.

Figure 6.8 shows the perception of participants regarding the #1 Beach environmental recordings. From a frequency point of view, the AMW unit does not effectively reduce SPL from 5000Hz above. Whereas, from 2000 to 5000Hz, there is a good filtering capacity and a significant neutralisation of the signal (most *SPL* peaks disappear). This filtering capacity is still visible from 2000Hz below; however, some resonance peaks appear, meaning that the overall neutralisation is less effective. *SPL* peaks are visible at 1600, 1100, 850Hz. Below 300Hz, the AMW unit seems to increase the environmental noise recordings. This limitation is also highlighted in Section **5.3.2 AMW unit performance on the lower frequency range (500-1000 Hz)**. This, in turn, results in a human perception response to the Beach environmental recordings less eventful and vibrant but calmer (less chaotic). From a different online headsets point of view, participants who used wired headphones and earphones seems to have the same answers' tendency as those who participated in the Laboratory test (same constants headset conditions). Slightly more eventfulness and vibrancy were detected from these two online headsets rather than the Laboratory one; however, wired earphones response seems more neutralised. Wireless headphones and earbuds disagree a bit more with the Laboratory headset response, according to 5/8 soundscape descriptors (Eventful, Vibrant, Calm, Uneventful, Annoying).

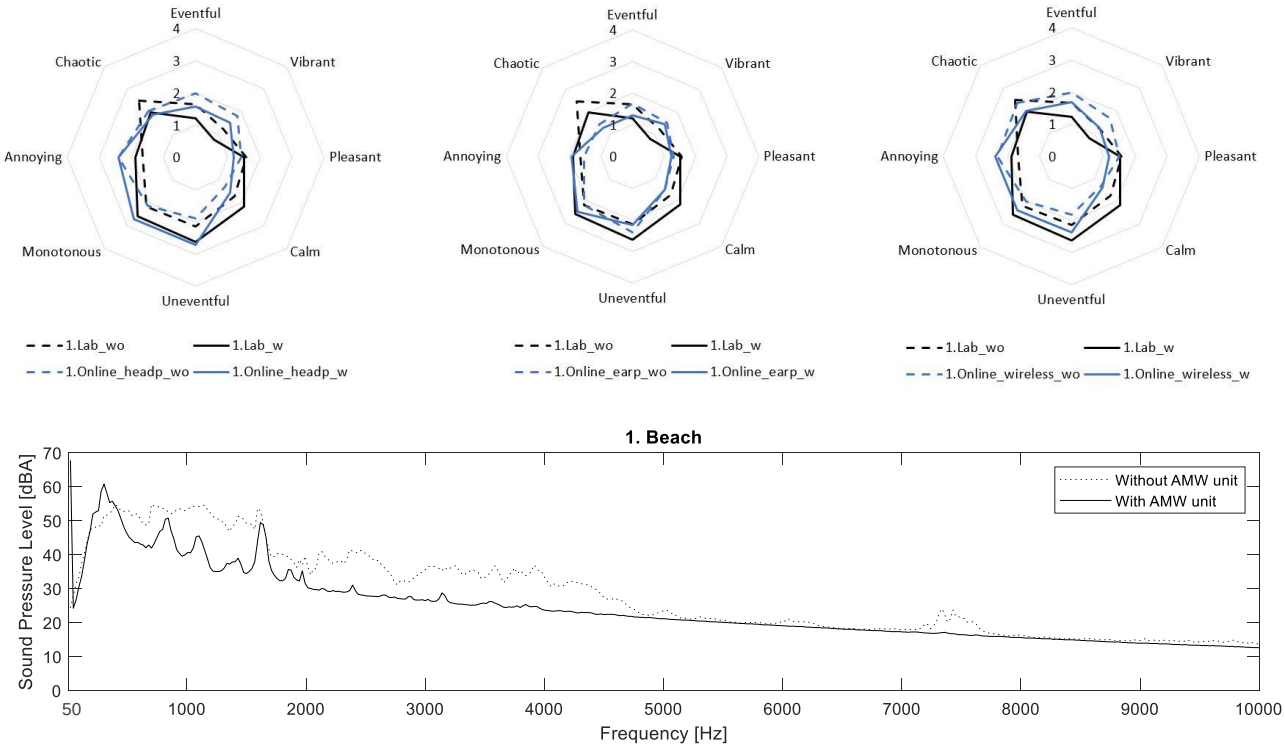

Figure 6.8 Schematics of the soundscape recording #1 Beach (without and with the AMW unit) through a) Laboratory and Online 2 participants evaluation (with wired headphones, wired earphones, and wireless headphones and earphones), and through b) SPL analysis of the soundscape recordings.

Figure 6.9 shows the data related to the #2 Woodland environmental recordings in the frequency domain and as perceived by the participants. The same phenomenon described before (Recording #1 Beach) was observed above 5000Hz, so the AMW unit performs no evident filtering capacity. The environmental noise component of the Woodland, which is mainly focused between 2800-5000Hz, is again significantly filtered out by the AMW unit. In the lower frequency, another resonance peak appears at 200Hz but is less amplified than the #1 Beach-related. Also, for this environmental sound recording, the human perception response is less eventful and vibrant but calmer (less chaotic). From a different online headsets point of view, wired headphones and earphones set up have the same answer tendency as the Laboratory one; however, they all highlight a generally not chaotic and not annoying component. They also highlighted a more monotonous component of the recording with the AMW unit, probably due to a more variable but overall lower acoustic reproduction quality. Wireless headset slightly disagrees with the online response tendency; however, the answers fall into a ± 8% compared to the Laboratory ones.

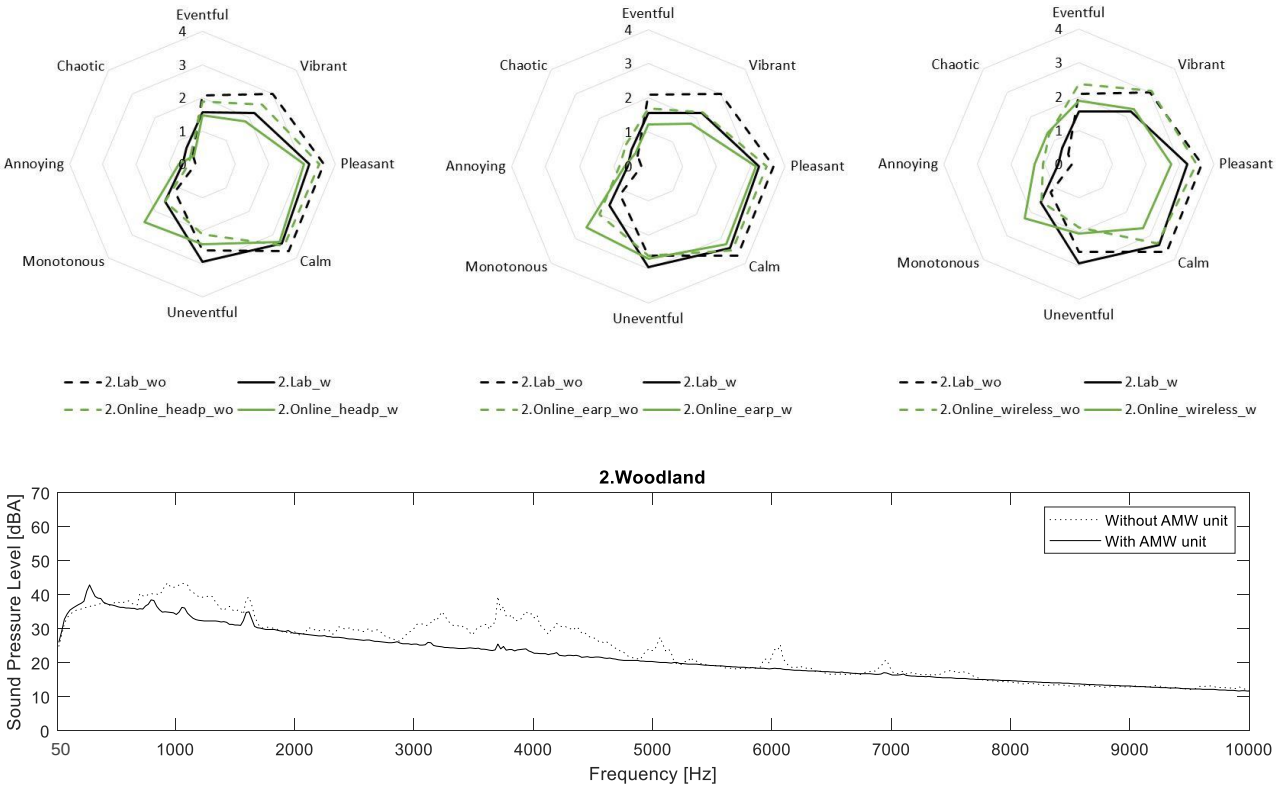

Figure 6.9 Schematics of the soundscape recording #2 Woodland (without and with the AMW unit) through a) Laboratory and Online 2 participants evaluation (with wired headphones, wired earphones, and wireless headphones and earbphones), and through b) SPL analysis of the soundscape recordings.

Figure 6.10 represents the perception of participants regarding the #3 Quiet Street environmental recordings. Overall from a frequency point of view, the AMW has the same effect as for the previous two environmental sound recordings. In this case, the separation between the first and second range of effectiveness is significantly reduced, and a continuous *SPL* reduction can be observed from 400 to 5100Hz. Some resonance peaks are still visible at 1600, 1100, 850Hz (as for recordings #1,2). The lower frequency peak (200Hz) is present yet still lower than the one of recording #1. The human perception response, in this case, is affected similarly to the #1 Beach environmental recordings (less eventful and vibrant but calmer), even if uneventfulness is slightly neutralised either for wired earphones and wireless headset setup. For the rest of the soundscape descriptors and headset setup used by the Online participants, the overall answers fall into a ± 8% of the Laboratory ones.

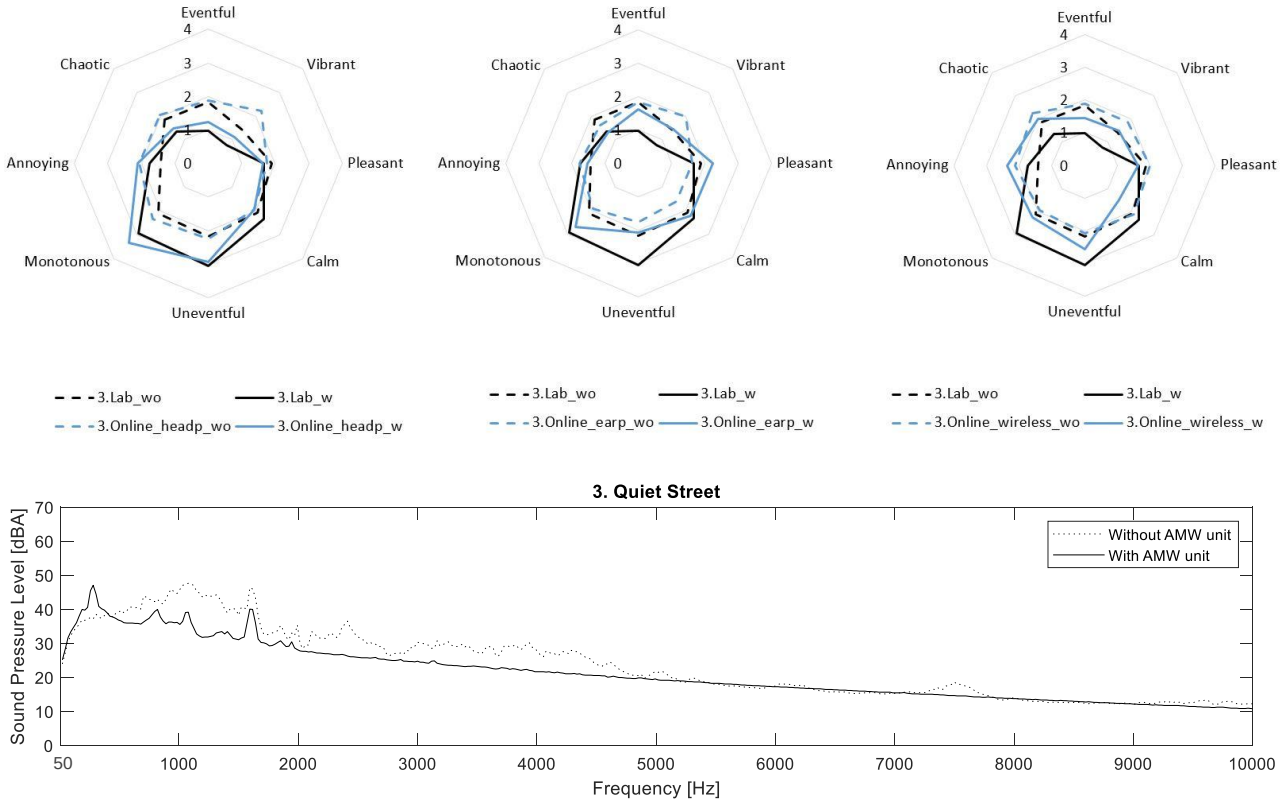

Figure 6.10 Schematics of the soundscape recording #3 Quiet Street (without and with the AMW unit) through a) Laboratory and Online 2 participants evaluation (with wired headphones, wired earphones, and wireless headphones and earphones), and through b) SPL analysis of the soundscape recordings.

Figure 6.11 shows the data related to the #4 Pedestrian Zone environmental recordings in the frequency domain and as perceived by the participants. *SPL* analysis highlights the same impact of the AMW unit application over the environmental sound recordings: overall good filtering capacity is visible from 300 to 5000Hz (with low resonance peaks at 850, 1100, and 1600Hz) while a high resonant

peak appears at 200Hz. These specific environmental sound recordings allow observing a good approximation of the first two online wired headsets again. At the same time, the wireless one shows a higher disagreement (up to 10% of the difference in terms of soundscape descriptors scale) especially highlighted for annoying and calm descriptors.

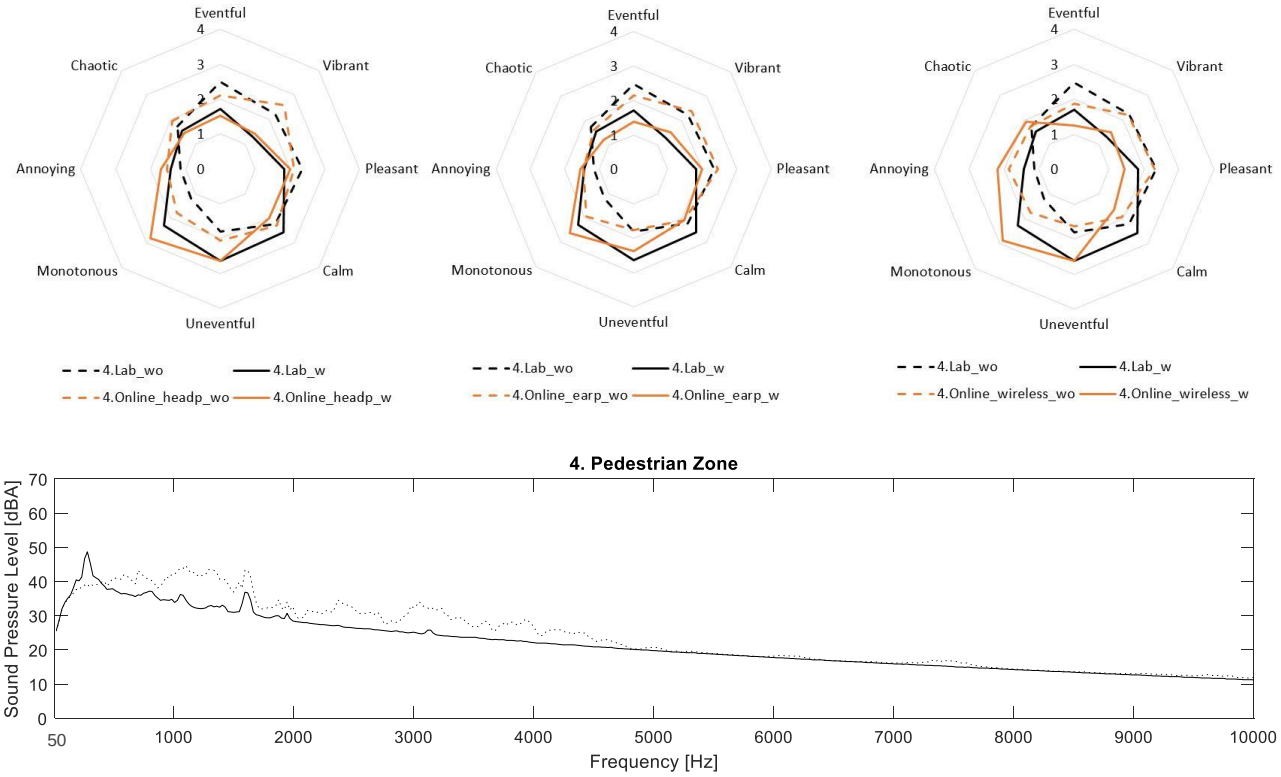

Figure 6.11 Schematics of the soundscape recording #4 Pedestrian Zone (without and with the AMW unit) through a) Laboratory and Online 2 participants evaluation (with wired headphones, wired earphones, and wireless headphones and earphones), and through b) SPL analysis of the soundscape recordings.

Figure 6.12 shows the data related to the #5 Park environmental recordings. The same phenomenon described above was observed above 5000Hz, so the AMW unit does not show any evident filtering capacity. The environmental noise component of the Park, which is mainly focused between 100-5000Hz, is this time strongly characterised by the influence of high pitch human voices (adults screaming and kids playing). For this reason, the overall middle-high frequency component is sufficiently filtered by the AMW unit impact; however, the resonance peaks between 300-3200Hz increase visibly. New peaks appear at 1400, 1800, and 3100Hz. This performance surely impacts the overall human perception; however, online participants tend to perceive a more vibrant soundscape through the wired headset and sensibly less eventful and calm soundscape with a wireless headset.

Overall wired headset slightly disagrees with the online response tendency (± 5% of the Laboratory ones) while wireless response falls into an overall ± 9% compared to the Laboratory headset response.

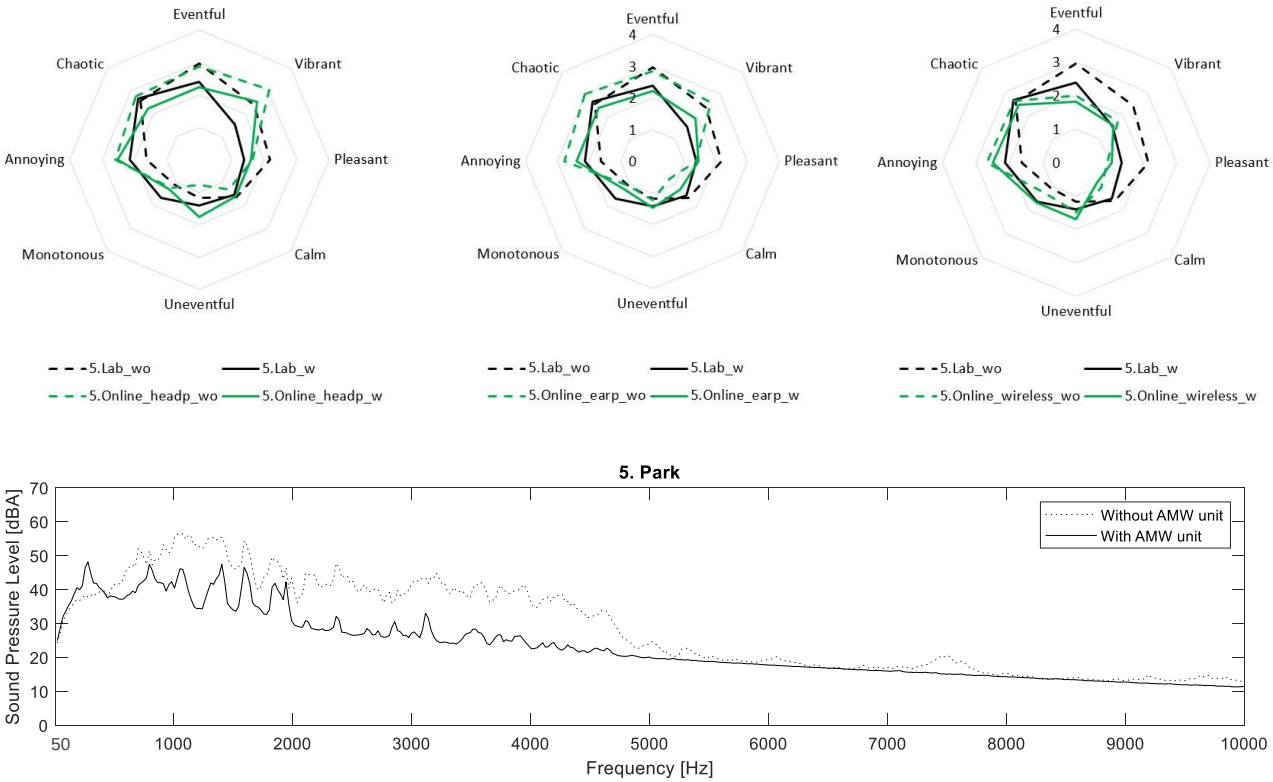

Figure 6.12 Schematics of the soundscape recording #5 Park (without and with the AMW unit) through a) Laboratory and Online 2 participants evaluation (with wired headphones, wired earphones, and wireless headphones and earphones), and through b) SPL analysis of the soundscape recordings.

Figure 6.13 shows the data related to the #6 Shopping Mall environmental recordings in the frequency domain and as perceived by the participants. In this case, *SPL* analysis highlights a consistent new filtering effect between 7000-8000Hz and 9500-10000Hz. The *SPL* of this environmental sound recording without the AMW unit effect presents an increase in these ranges, probably due to the human voices and loudspeakers playing music in the background. The same overall good filtering capacity is visible from 300 to 5000Hz (with low resonance peaks at 850, 1100, and 1600Hz), while a significant high *SPL* peak appears at 200Hz as for the previously described recordings. Through recordings of #6 Shopping Mall it is highlighted a good correspondence of responses with those related to the Laboratory headset setup and an agreeing attribution of Eventful (with an overall error of 6% over the Laboratory response), Vibrant (overall 4%), Pleasant (overall 4%), Calm (overall 2%), Uneventful (overall 5%), Monotonous (overall 7%), Annoying, and Chaotic (overall 9%).

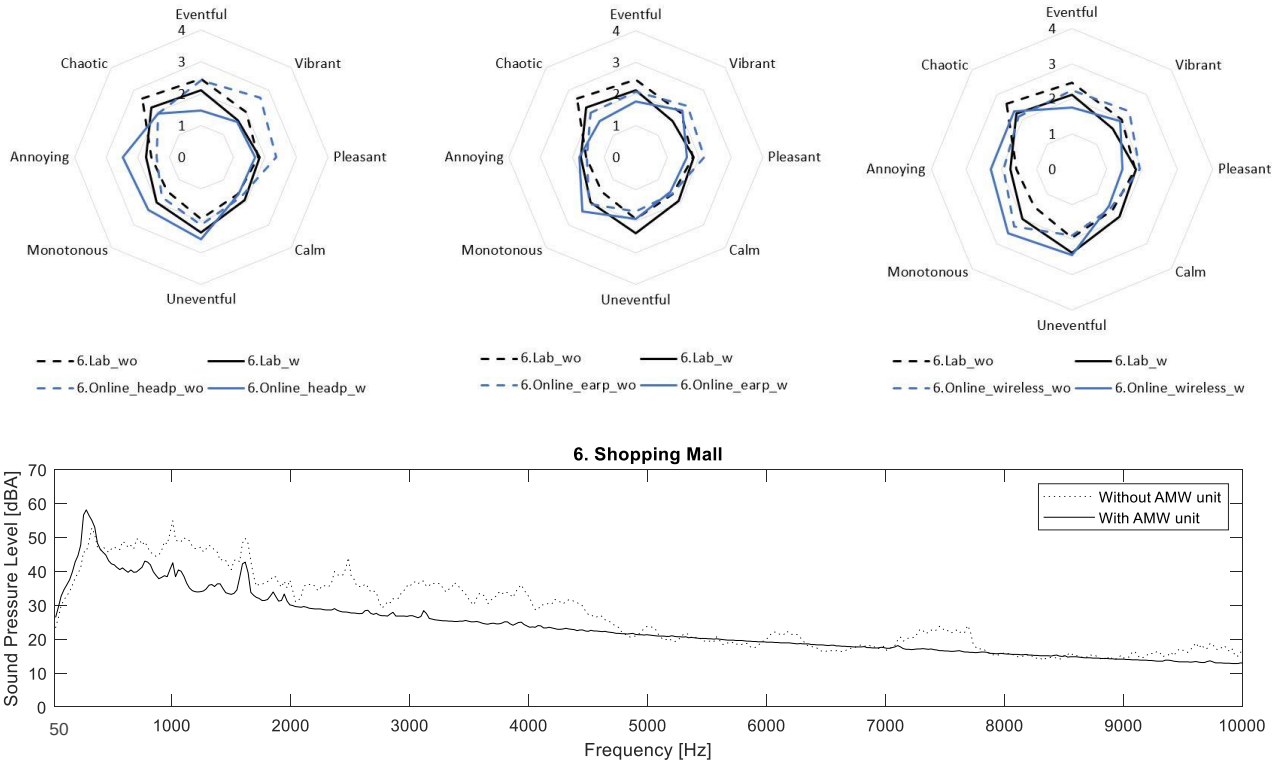

Figure 6.13 Schematics of the soundscape recording #6 Shopping Mall (without and with the AMW unit) through a) Laboratory and Online 2 participants evaluation (with wired headphones, wired earphones, and wireless headphones and earphones), and through b) SPL analysis of the soundscape recordings.

Finally, in Figure 6.14, data of #7 Busy Street environmental recordings are displayed. The effective filtering frequency of the AMW unit is confirmed here to be between 300-5000Hz. Even if filtering, resonance peaks are also highlighted from 500 to 2000Hz (with the same frequencies as the previous analysis). The higher and more isolating headset quality influences here the perception of a significantly less vibrant and eventful (and in turn more monotonous and uneventful) soundscape through wired headphones over a more neutralised one for wired earphones and wireless headsets. In the general online headset case scenario, the responses fall into a ± 10% compared to the Laboratory ones.

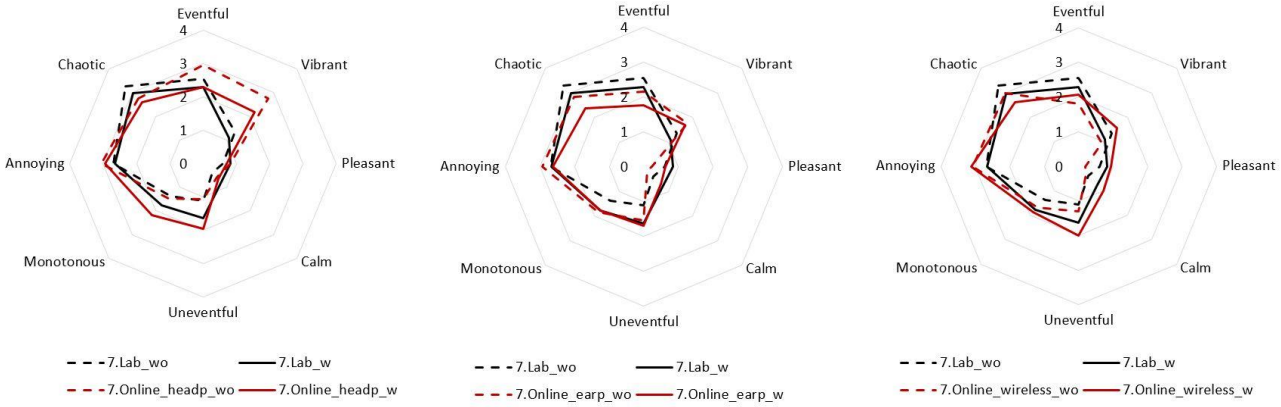

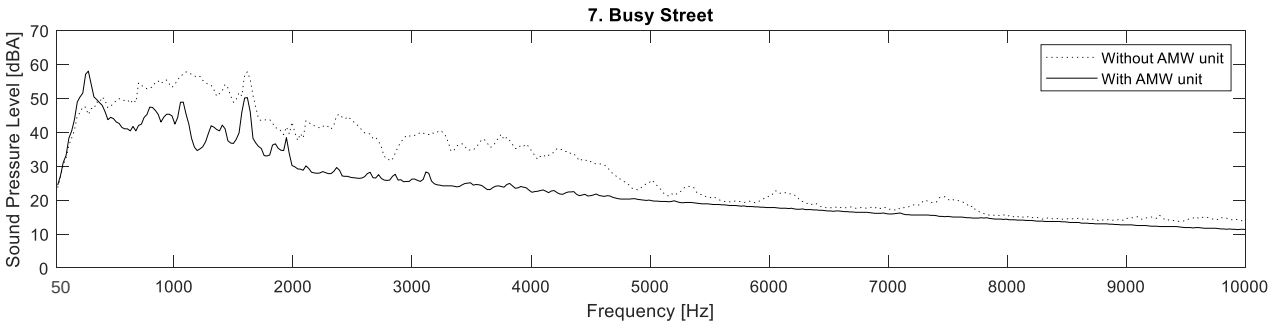

Figure 6.14 Schematics of the soundscape recording #7 Busy Street (without and with the AMW unit) through a) Laboratory and Online 2 participants evaluation (with wired headphones, wired earphones, and wireless headphones and earphones), and through b) SPL analysis of the soundscape recordings.

Overall, as shown in Figure 6.8 and Figure 6.14, wired headphones tend to give more agreeing responses in terms of soundscape descriptors, whereas they seem to result in a more vibrant, more annoying and less calm human perception when compared to the Laboratory conditions (and so results). This is mostly related also to the noisier background noise (as stated in the 80% of the participants who used this headset setup). Wired earphones have the same effect. However, responses seem more neutralised as negative discrepancies are also highlighted in terms of how chaotic and uneventful each environmental sound recording is perceived. Wireless headphones and earbuds result on the other side a bit less agreeing with overall Laboratory responses. Moreover, in this case, the background noise component has not been highlighted by the participants (only 20% of the wireless-based Online 2 participants reported it). For this reason, results from the Online 2 test confirm that wireless headsets reduce the overall response tendency agreement with the Laboratory one, and it should be so avoided in future AMMs human perception online questionnaires.

Differences between Laboratory and Online 2 tendencies are always within a ±8%, which mean that the Online 2 method shows a satisfactory agreement with the initial laboratory test. Of course, as highlighted in this section, attention must be paid to a different headset, as they might slightly change the results.

6.5.2 AMW unit Impact in the window's Ergonomic value

Since the Online method has a good agreement with the Laboratory one, and their soundscape response over the same environmental sound recordings is similar, the filtering capacity of the AMW unit was not specified. However, this data could specifically draw a frequency range of application for the actual AMW unit configuration. As different environmental sound recordings are affected differently by the AMW, the filtering capacity should be calculated for all the 7 recordings: #1 Beach, #2 Woodlands, #3 Quiet Street, #4 Pedestrian Zone, #5 Park, #6 Shopping Mall, and #7 Busy Street.

Moreover, to demonstrate the characterisation of real sound sources over a broadband source, the filtering effect over a white noise was also considered. In both analysed recordings, the AMW unit Amplitude filter was calculated as:

$$AMW\ unit\ Amplitude\ Filter = \frac{SPL\ (with\ AMW\ unit)}{SPL\ (without\ AMW\ unit)} \qquad 6.4$$

Figure 6.15 shows different filtering capacities of the AMW unit according to the sound input characteristics, where values below 1 highlight a filtering capacity while values equal to or over 1 indicate no filtering effect. Overall a good filtering performance is clear from 300 to 5000Hz from 7000 to 8000Hz, and from 9000 to 10000Hz. These results confirm what has been highlighted in the previous *SPL* related analysis. The filtering ability of the AMW unit decrease at 5000-7000Hz and 8000-9000Hz, and at 50-300Hz, all the studied files are affected by a magnification of the signal culminating at 280Hz. Unfortunately, as also highlighted in the results of Section **5.3.2 AMW unit performance on the lower frequency range (500-1000 Hz)**, the AMW unit noise reducing capacity has a limitation over a lower frequency range. In that specific section, an acoustic broadband optimisation was investigated and numerically demonstrated; however, due to the current pandemic situation, the AMW model used for these experiments was the basic one (without broadband optimisation).

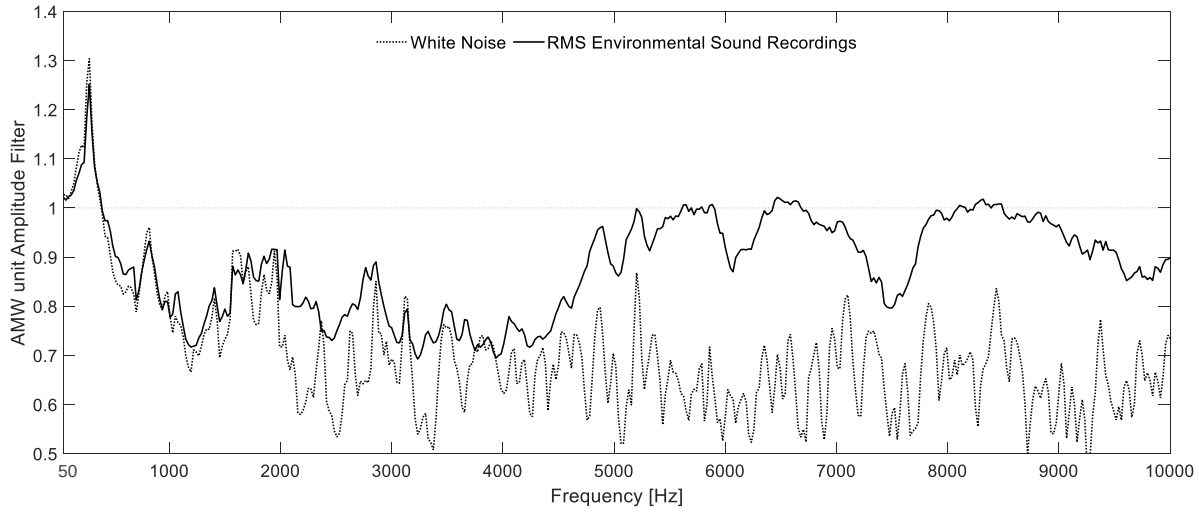

Figure 6.15 schematics of AMW unit Amplitude filter of white noise and the RMS of the AMW unit Amplitude Filter related to the 7 environmental sound recordings: #1 Beach, #2 Woodlands, #3 Quiet Street, #4 Pedestrian Zone, #5 Park, #6 Shopping Mall, and #7 Busy Street.

Finally, the AMW unit was tested both from a physics and human perception point of view while following the Ergonomic Principles highlighted in Chapter **3 Participatory approach to draw ergonomic criteria for window design**. This process allowed the AMW unit to

1. Have a significant acoustic filtering capacity over the most frequently heard noise sources frequency range (by using a customised AMM system) while allowing natural ventilation;
2. Mediate between the indoor and the outdoor of a building: acoustically (through the AMMs), visually (through possible filtering effects applied on the central panel), and from a ventilation point of view (by regulating the opening of the window);
3. Put the users in connection with the outdoor environment: acoustically (by filtering the incoming noise without changing the meaning), visually (through the transparent frontal panel), and from a ventilation point of view (by regulating the opening of the window);
4. Make the users feel oriented and perceive an indoor affective impact improvement, despite the non-optimal conditions (acoustically by filtering the noise sources but keeping them recognisable.

6.6 Conclusions

In this chapter, the effectiveness of the AMW unit was investigated through human perception based laboratory and online questionnaires. The results highlighted a significant reduction in terms of vibrancy, chaos and eventfulness, showing a general neutralisation of the perceived soundscapes through the window prototype. Furthermore, according to the preliminary psychoacoustic analysis, participants sensibly perceived an acoustic difference in the soundscape recordings with the AMW unit effect. Results also demonstrated a perceivable Loudness reduction in the heard acoustic environments when the AMW unit is present from a psychoacoustic and human perception point of view.

The combined methodology (environmental sound recording evaluation through human perception questionnaire based in laboratory and online) resulted effectively consistent, and robustness was proved for the online part. The customised mixed methodology has highlighted potential over an exclusive online-based questionnaire rather than the standard laboratory one. If appropriately customised, the use of this online-based methodology for AMMs human perception experiments could lead to a broader and less biased sample for the investigation.

Regarding the actual AMW unit prototype, the effect of neutralisation of more chaotic and loud soundscapes recordings has been proved as well as the significant filtering capacity combined with natural ventilation. Therefore, this customisable AMM-based window design could be applied to specific indoor functions (requiring different soundscape indoor characteristics at different degrees) and following the previously established ergonomic design criteria [4] with significant improvements over standard windows. Moreover, as it has already been proved numerically [189], future studies

might implement prototypes of AMW in order to overcome the lower frequency range limitations and experimentally prove the broadband effectiveness of such window design.

7. Development of a full-scale AMW

The contents included in this chapter have been published in the 2020 Inter-Noise Conference (Seoul - Korea) proceedings by the name of “Full-scale metamaterial window for building application”.

In this chapter, the ergonomic criteria highlighted in Chapter **3. Participatory approach to draw ergonomic criteria for window design** are considered to develop further the acoustic metawindow unit system (AMW unit) investigated in Chapter 5 AMW unit effect. Chapter 3 highlighted that 1) participants perceive the window as an essential mediating instrument between the indoor and the outdoor of a building; 2) through this feature, they feel connected to the outdoor environment; and 3) despite the non-optimal conditions, they feel oriented and perceive an improvement in the indoor's affective impact. These three design criteria were followed as guidelines when adapting the AMW unit to a full-scale window design. This project indeed aims to draw a new methodology for real window design, which considers users' preferred aspects and combines them with a specific AMMs based window's technology. Then, the window design would become a real scale system to modulate outside inputs to optimise indoor comfort.

7.1 Background

Noise transmission is a significant factor when considering indoor comfort in building designs. [3] Nowadays, increasing noise issues are limiting building functions from different aspects. Active systems have been designed to improve indoor comfort, leading, for example, to mechanical ventilation and active noise control systems. [15] Windows plays an essential role in addressing this issue as an essential building element, and relevant studies have been extensively investigated. [8,13] Increasing window thickness could be a solution; however, it inevitably results in a bulky structure. Screening related systems (like rolling shutter boxes) have been proposed to overcome the thickness issue [9], and active noise control has been demonstrated to achieve effective low-frequency attenuation. [15] On the other hand, natural ventilation and air change rate (*ACR*) are highlighted as key factors to quantify passive energy requirements [272,273] as contemporary architecture and engineering research are focusing primarily on energy-efficient approaches. With this aim, the latest development of AMMs managed to achieve tailored acoustic properties depending on the material geometrical structure more than the constituent material properties itself. [271,276] The application frequency ranges in many cases are limited by their large spatial footprint. For these reasons, it is

necessary to investigate further an ideal design and application of AMM to address both noise control and natural ventilation, adaptable to different environmental situations.

Our previous study has investigated a promising acoustic metacage window with significant results in a frequency range of 300-5KHz (see Figure 7.1.a). [262] The tunability of the AMM unit cells constituting the metacage window, related to a few geometric parameters, has been demonstrated through parametric studies. Later, a preliminary realistic adaptation was speculated as an acoustic metawindow (AMW) unit (see Figure 7.1.b). The acoustic metacage window geometry was better approximated to standard window design and tested both numerically and experimentally. The main conclusion is that significant noise reduction can be achieved while allowing a 30% of opening ratio (*OR*).

This PhD chapter aims to numerically investigate the applicability of previously used AMM on a full-scale window model (see Figure 7.1.c) and optimise the parameter settings according to different acoustic conditions (depending on the frequency range). Three specific targets highlighted from Chapter **3 Participatory approach to draw ergonomic criteria for window design** are to be considered in the design, including visual impact, acoustics, and ventilation. The visual impact is addressed by using transparent glass as the central panel (dimensions 1.2x0.6 m). The acoustics and ventilation functions are fulfilled by integrating AMM unit cells in the window frame. The window performances are then characterised by different geometric parameters of the window and the AMM unit (described in the following section). The combined variables define different acoustic impacts and *ACR* of the window system on the indoor environment. Finally, the parametric study results are compared to a standard sliding window to show the design benefits. Significant improvements from the standard window design performances could be found. New AMM-based windows are set for building engineering or architecture applications.

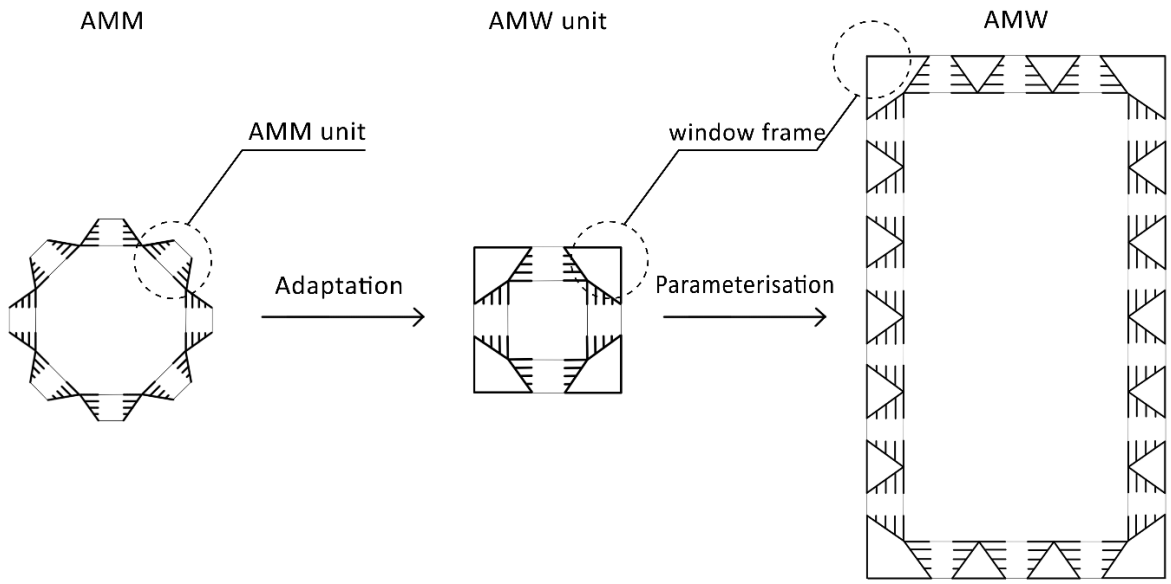

Figure 7.1 Geometrics and physics concept-flow from the acoustic metacage window, to the AMW unit and finally AMW as per its full-scale application (cross-sections).

7.2 Materials and Method

7.2.1 Geometric setting for acoustic and ACR analysis

Numerical simulations are used to evaluate the performance of the proposed full-scale AMM window. Both acoustic and *ACR* simulations are performed based on the same 3D geometric settings; however, the physics models have different governing equations and boundary conditions (specified in the following section). For each analysis, the Finite Element Method (FEM) is used to perform the parametric study. The geometric elements considered in this study are: a spherical boundary of 0.9 m radius, a 0.13m division in the middle (representing the building's wall), and the AMW attached to one side of the division (see Figure 7.2.a). The sphere's partitions are considered indoor and outdoor environments. The "inner wall" is where the AMW geometry is placed. The dimension of the central transparent panel of the AMW is 1.2 x0.6 m and is constant for all the parametric studies. The input wave (modelled as background pressure field or air velocity) passes through the AMW and radiates in through the distributed ventilation holes along the AMM units surface. As depicted in Figure 7.2.a, a few parameters are considered for this study.

The first parameter, T, represents the AMW frame thickness starting from the inner side of the division (see Figure 7.2.a). Indeed, the 3D window system can be viewed as a protrusion from a 2D plane placed on the inner wall. The previous studies highlighted that *T* influences the frequency range of acoustic applications. However, beforehand, there has never been such a parametric study to understand

which *T* dimension can activate the noise reduction on specific frequency bands. In this research *T* varies within these values: A, *T*= 0.13 m; B, *T*= 0.11 m; C, *T*= 0.09 m; D, *T*= 0.07 m; E, *T*= 0.05 m; F, *T*= 0.03 m. A variation of *T* determines a variation of the total opening areas of the AMM units in the AMW frame (see Figure 7.2.a). They vary as 0.14 m^2 (*T*=A), 0.12 m^2 (*T*=B), 0.10 m^2 (*T*=C), 0.08 m^2 (*T*=D), 0.05 m^2 (*T*=E), 0.03 m^2 (*T*=F).

The second parameter, depicted in Figure 7.2.b, is the frame height (*H*), which varies in a range of 0.04 m (*H*=4), 0.05 m (*H*=5), 0.06 m (*H*=6), 0.075 m (*H*=7.5), 0.10 m (*H*=10), 0.15 m (*H*=15). A variation of *H* results in a variation of the frontal area of each window (see Figure 7.2.b) without varying the central transparent panel dimensions. The frontal area changes within this range: 0.88m^2 (*H*=4), 0.91m^2 (*H*=5), 0.95m^2 (*H*=6), 1.01m^2 (*H*=7.5), 1.12m^2 (*H*=10), 1.35m^2 (*H*=15). A third parameter to evaluate our study is the *OR*. This unit represents the percentage ratio between the total opening areas of all the AMM units in the AMW frame and the frontal area of each window (see Figure 7.2); so, the combination of different *T* and *H* generates a variation of the *OR*. These variations are: 30% (*T*=A=0.13 m), 25% (*T*=B=0.11 m), 20% (*T*=C=0.09 m), 16% (*T*=D=0.07 m), 11% (*T*=E=0.05 m), 7% (*T*=F=0.03 m). This specific definition of the *OR* will allow comparing on a later stage the AMW's performance with common window design' ones (see Section 7.2.2 and 7.3.1).

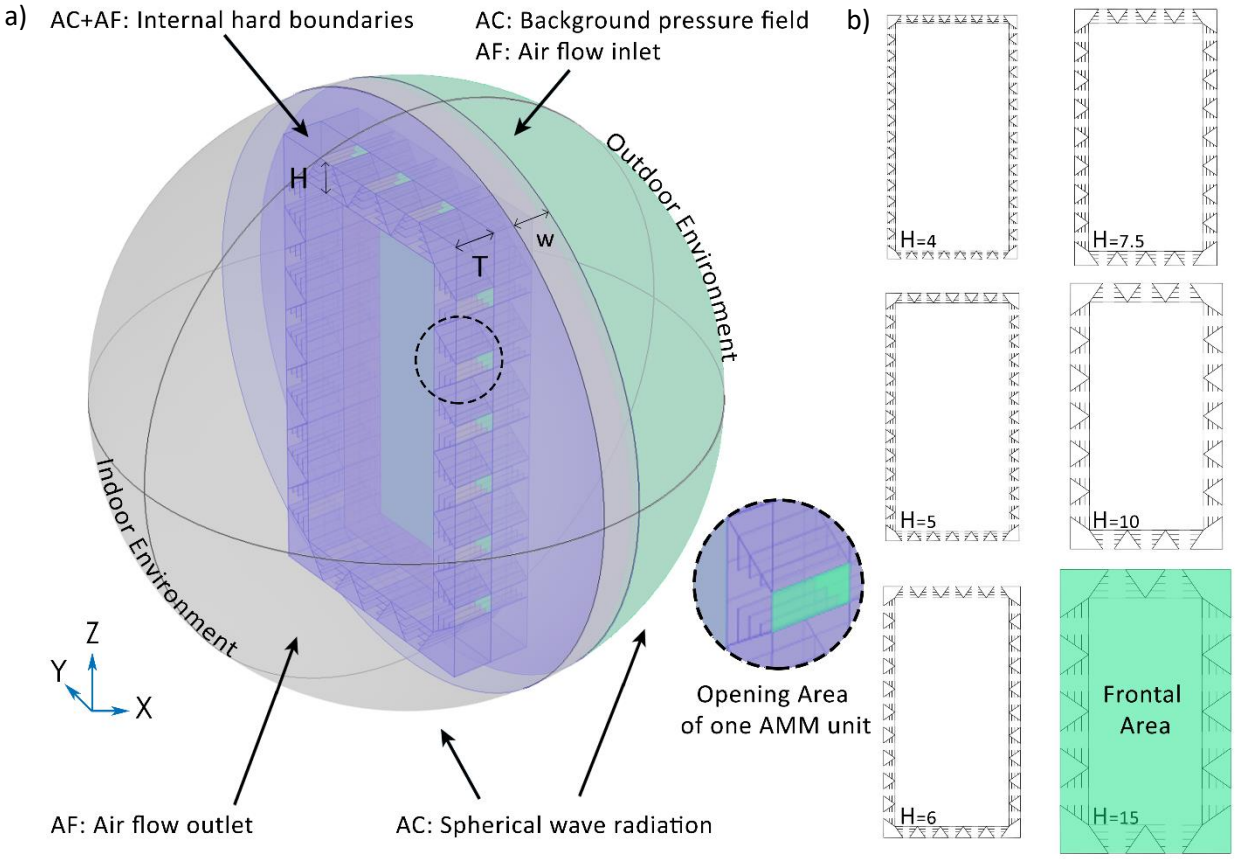

Figure 7.2 a) 3D representation of boundary conditions and parameters used in both acoustics (AC) and airflow (AF) studies. b) 2D AMW section to show the variation of the H parameter.

7.2.2 Boundary Conditions and Study Settings

The numerical model is implemented using commercial FEM software Comsol Multiphysics under Acoustics and Fluid Dynamics modules. For the first parametric investigation, semi-infinite acoustic conditions are applied to the two boundary sides of the sphere (see Figure 7.2.a). Free spherical wave radiation conditions are applied to all the spherical geometry. The separation walls and the AMW geometry are considered as interior sound hard boundaries. Sound transmission through walls of the AMW and possible viscous-thermal effect in the narrow resonator channels are neglected in this study. The 3D domain is filled with air, where air density and sound speed at room temperature are used. The outdoor boundary is characterised by a background pressure field directed towards the indoor with a pressure amplitude of 1 Pa and an airspeed of the sound of 343 m/s. TL is calculated by the reduction of sound power through the metamaterial interface (in dB). The extra sound attenuation (called ΔTL) of the AMW compared to the standard window's one is defined to show our design benefits, and it is calculated as:

$$extra\ attenuation = \Delta TL = TL_{AMW} - TL_{SW} \quad (dB) \tag{7.1}$$

where:

- TL_{AMW}= AMW's transmission loss (dB)
- TL_{SW} = Standard window's transmission loss (dB)

Regarding the mesh size for the 3D study, this model results very complex, and since the convergence of results is proven, simplification is needed, so the maximum allowed element size is 343/6/2000=0.0286 m. The study is a frequency domain analysis from 50 to 5000 Hz with a step size of 100 Hz. In the results, the *TL* is shown linearly within the simulation frequencies.

In the parametric airflow study, the same geometric boundaries are used for a laminar flow study in order to calculate the air changes per hour (*ACPH*). An air change is the number of times the air enters and exits a room from the heating, ventilating and air conditioning (HVAC) system in one hour. *ACPH* is a measurement of air volume that is added to (or removed from) a room divided by the total volume of the room; so, it measures how many times the air in the room is replaced. Higher *ACPH* values result in adequate ventilation. The formula is as follows:

$$ACPH = \frac{Q}{V} \quad (h^{-1}) \tag{7.2}$$

where:

- Q = Volumetric flow rate of air in cubic metres per hour (m^3/h) = $3600 \cdot A \cdot v$
- V = Space volume L × W × H in cubic metres (m^3)
- A = Cross-sectional area of the duct (m^2)
- v = airflow velocity (m/s)

This unit allows comparing the AMW performances to the standardised value for public buildings[315]. Moreover, with an easy time unit adaptation, air change per minute (*ACPM*) can be calculated to describe more precisely the extra opening time that AMW requires when compared to the standardised value for offices. In this case, for example, *ACPH*= 6 h^{-1} [11] while *ACPM*=0.1 min^{-1}. From this unit, another time-based indicator, air change requirement in minute (ACRM), can be defined as:

$$ACRM = \frac{1}{ACPM} \quad (min) \tag{7.3}$$

So for *ACPH*=6 h^{-1}, *ACPM*=0.1 min^{-1}, and *ACRM*=10 min. *ACRM* is then calculated for all the different AMW models, according to each *T* and *H* combination. Finally, the extra time needed for the AMW to reach the standard window (SW) *ACR* performance is calculated as:

$$extra\ time = \Delta ACRM = ACRM_{AMW} - ACRM_{SW} \quad (min) \tag{7.4}$$

where:

- $ACRM_{AMW}$ = AMW's ACRM (min)
- $ACRM_{SW}$= Standard window's ACRM (min)

For boundary conditions definition, the 3D geometry is filled with air where air density at room temperature is used. Inlet conditions are applied to the outdoor boundary surface. Normal wind velocity flow at the inlet is 1.132 m/s according to Asfour and Gadi criteria [288], depending on the height above the ground (20m) and the room height (3m). Outlet conditions with 0 Pa pressure characterise the indoor boundary. In this analysis as well, the walls of the AMW and material cells are set as interior hard boundaries. The mesh size for this 3D study is defined by a maximum element size of 0.18 m and a minimum element size of 0.03m. Indoor average air velocity is analysed in this parametric study to define *ACPH* for each configuration.

7.3 Numerical Results

7.3.1 Thickness variation and frequency range parametric study

Table 7.1.a shows the *ΔTL* mean value according to different *H* and *T*. *ΔTL* goes from a minimum of 19.37 dB to a maximum of 39.75 dB showing increasing values in relation to high *H*; so this parameter might be significant in the determination of the *ΔTL* amplitude and a more specific frequency related analysis is needed. In Table 7.1.b, individual bands (low= 0-500 Hz, middle= 500-2000 Hz, high= 2000-5000 Hz) are analysed. From a first look at this table, mostly higher frequencies result significantly affected by the AMW performance in terms of *ΔTL*; however, focusing on the frame height, the results show that when *H* increases together with the dimensions of the AMM units, they affect more significantly the low frequencies component of the soundwave.

Models with *H*=7.5, 10, 15 generates a cut off frequency in the low band, up to a significant mean *ΔTL* of 10.94, 16.10, and 12.3 dB, respectively. At the same time, bigger AMM units also determine a significant *ΔTL* at the higher bands (500-2000 and 2000-5000 Hz), making their application effective on the broad frequency range. In conclusion, within the same audible spectrum, the noise reduction performance of full-scale AMW is better than a comparable sliding window, regardless of the different thicknesses (or *OR*). Moreover, *H*=10 results to be the overall best performing model.

7.3.2 ACRH and time gap for optimal ventilation conditions

Table 7.1.c illustrates the difference in terms of AMW ACRM. These values represent the extra opening time that AMW requires when compared to the standardise value for offices (*ACRM*= 10 min) [315]. The standard value in this analysis is initially defined by DIN 1946 part 2, which is set by the German Institute for Standardisation and accepted worldwide [315], and where it is expressed in ACPH. The specific function was taken into account as an example of a public indoor environment where acoustic and ventilation comfort is crucial for the occupants. In Table 7.1.c, negative values mean that the performance of the studied model is even better than a standard window and that a shorter opening time is required to achieve the standard ACRM. Overall the shorter time required to satisfy the *ACRM* standards is between -6.52 min (= -6’31’’) and -9.18 min (= -9’11’’). There is an improvement for bigger T values (A, B, C) as the *ΔACRM* is probably due to their *OR*. The ventilation performances for these thickness values are the best among the AMW models. In future studies, the AMW *ACRM* can be compared to standardised values of other indoor functions to have a broader idea of its application in public buildings.

Table 7.1: a) ΔTL mean of the total value of the acoustic parametric study according to different AMW T or OR; b) ΔTL mean by different frequency bands: low= 50-500 Hz, middle= 500-2000 Hz, high= 2000-5000 Hz; c) ΔACRM between standardised value for offices expressed in additional opening window time (min).

(a)

	ΔTL mean total (dB)						
	4	5	6	7.50	10	15	Mean
A	19.37	21.23	24.63	30.04	39.75	34.11	28.19
B	21.73	22.53	26.93	29.63	30.47	35.30	27.77
C	18.24	22.53	27.16	28.94	32.36	34.97	27.37
D	23.81	27.15	28.90	31.47	32.84	35.88	30.01
E	19.67	23.59	30.86	34.15	34.65	34.95	29.65
F	31.43	33.26	35.31	35.87	36.28	34.17	34.39
Mean	22.37	25.05	28.96	31.68	34.39	34.90	

(b)

		ΔTL mean freq. bands (dB)						
	Freq. Bands	4	5	6	7.5	10	15	Mean
A	LOW	2.44	3.04	3.95	5.00	16.10	4.94	
	MID	18.19	17.85	18.57	19.66	31.75	38.99	21.58
	HIGH	23.34	26.56	31.79	40.24	48.48	37.51	
B	LOW	1.49	2.16	3.08	4.24	4.99	4.12	
	MID	19.77	18.83	18.33	17.97	19.24	40.60	20.37
	HIGH	26.76	28.46	36.00	40.54	41.18	38.89	
C	LOW	2.15	2.95	4.01	5.26	6.46	5.01	
	MID	18.69	18.70	19.38	20.81	28.46	43.21	20.80
	HIGH	21.23	28.36	35.67	37.74	39.49	36.85	
D	LOW	3.06	4.14	5.28	6.66	8.15	6.26	
	MID	14.17	14.13	14.77	21.52	31.26	44.18	22.39
	HIGH	32.78	38.27	40.69	41.41	38.58	37.65	
E	LOW	4.02	5.15	6.58	8.25	10.08	8.65	
	MID	7.67	7.53	8.67	17.85	25.55	36.44	21.58
	HIGH	28.79	35.32	46.81	47.48	44.12	39.46	
F	LOW	7.54	7.10	8.82	10.94	13.20	12.30	
	MID	5.28	3.89	5.06	14.21	25.91	33.09	24.58
	HIGH	49.29	53.18	55.73	51.68	46.07	39.09	
	Mean	15.93	17.53	20.18	22.86	26.61	28.18	

(c)

	ΔACRM (min)					
	4	5	6	7.5	10	15
A	-9.16	-9.18	-9.15	-9.12	-8.92	-9.00
B	-9.02	-9.05	-9.01	-8.98	-8.94	-8.86
C	-8.89	-8.85	-8.84	-8.82	-8.76	-8.68
D	-8.63	-8.61	-8.59	-8.57	-8.49	-8.36
E	-8.27	-8.22	-8.20	-8.11	-7.97	-7.81
F	-7.56	-7.46	-7.18	-6.99	-6.78	-6.52

7.4 Broadband potential optimisation of the AMW's acoustic performance

As achieved for the AMW unit (see in Chapter **5 AMM adaptation to real window design**), an acoustic optimisation is investigated for the full-scale AMW design. Since from Chapter 5, B and C Configurations resulted as the most effective perforation combinations within the AMM units panels, optimisation on the full-scale AMW design is investigated following these two approaches. Configuration B has 7% of perforation on the panels belonging to 2/4 of the same AMM units, while configuration C has 7% of the overall panels' area's perforation applied on one panel of each AMM unit. For the sake of simplicity in showing the results and since the previous section demonstrated that *H*=0.05 - 0.15 m performs optimally in noise reduction and natural ventilation, only these models will be tested. Moreover, since the *H*=0.15 m is quite a bulky window frame model which cannot be easily found on the market, this will be further excluded from the investigation. In the B and C Configurations, the resonating volume goes from 7.7 x 10^{-4} m^3 (*H*=0.05 m) to 30.8 x 10^{-4} m^3 (*H*=0.10 m), and the perforated panels within the AMW unit geometry are placed differently to investigate also in this full-scale case if the perforation position is a determinant parameter for the AMW *TL*. *TL* is here calculated following the same procedure used for the basic full-scale model (see Section **7.2.2**

Boundary Conditions and Study Settings). *ACR* did not change compared to the basic version, so ventilation evaluations are not shown here and can be considered comparable.

Figure 7.3 shows a comparison of the two schematics related to B and C Configurations *TL* characterised by *H*=0.1 m and *T*=0.13 m (A), *T*=0.11 m (B), *T*=0.09 m (C), *T*=0.07 m (D), *T*=0.05 m (E), T=0.03 m (F). These decreasing *T* values represent the closing mechanism of the AMW. So, from this schematics comparison, the effectiveness of *TL* can be appreciated simultaneously with the window opening reduction. Overall, B and C show significant TL throughout the whole frequency range (50-5000Hz). The numerical analysis determines a minimum TL potential of 10dB, which is particularly remarkable for the lower frequency range 50-500Hz. Moreover, comparing the optimised configurations (B and C) with the RMS of the original full-scale AMW TL (represented by the red line plot), the TL optimisation is overall performed broadband in both cases. Specifically, configuration C shows better performance as it is clearly below the original AMW only in the frequency ranges of 1850-1900Hz, while configuration B does not optimise TL at 1500-1600Hz, 1850-1900Hz, 3900-4100Hz. Configuration C creates a resonant condition that optimises the system better than B. This is probably because perforated panels are not coupled. Indeed, an original AMM unit (cavities-based) configuration faces a perforated one (see Figure 7.3).

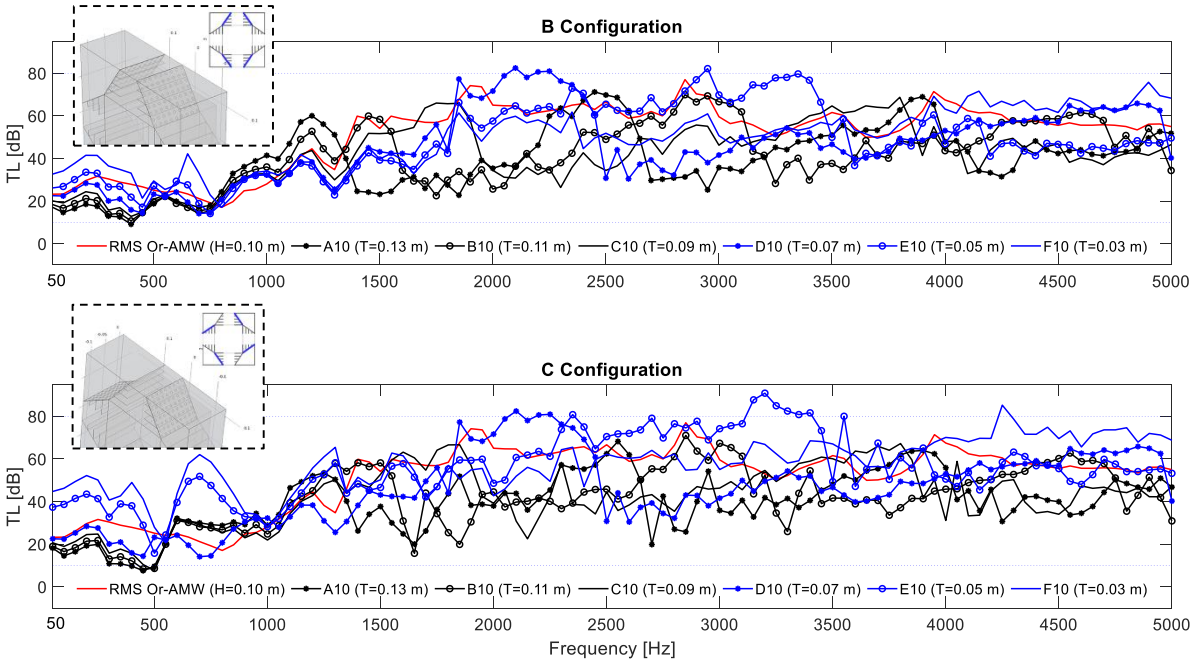

Figure 7.3 Schematics comparison of B and C Configurations TL characterised by H=0.1 m and T=0.13 m (A), T=0.11 m (B), T=0.09 m (C), T=0.07 m (D), T=0.05 m (E), T=0.03 m (F). Two blue dotted lines are plotted for TL = 10dB and TL= 80 dB as reference for the overall TL performance. The red line plot represents the RMS of the original full-scale AMW TL.

Figure 7.4 shows the TL of the optimised Configuration B and C of the full-scale AM, characterised by a frame height H=0.075m. The decreasing value of T (A=*T*=0.13m, B=*T*=0.11m, C=*T*=0.09m, D=*T*=0.07m, E=*T*=0.05m, F=T=0.03m) represent the thickness of the window with constant H, and so the performance of the AMW at different degrees of closure. Overall, significant TL is highlighted from the numerical analysis of Configurations B and C. Also, in this case, C works better than B generally throughout the frequency range 50-5000Hz and specifically if compared with the TL RMS of the original AMW(represented by the red line plot). A significant dip is highlighted between 50 and 100Hz for B, showing a magnification of the acoustic signal through this Configuration for the bigger opening degrees (T=0.13, 0.11, 0.09 m). It is possible to assume that, due to its even geometrical nature, Configuration C allows an optimised TL and overcome possible magnifications as for B (see Figure 7.4).

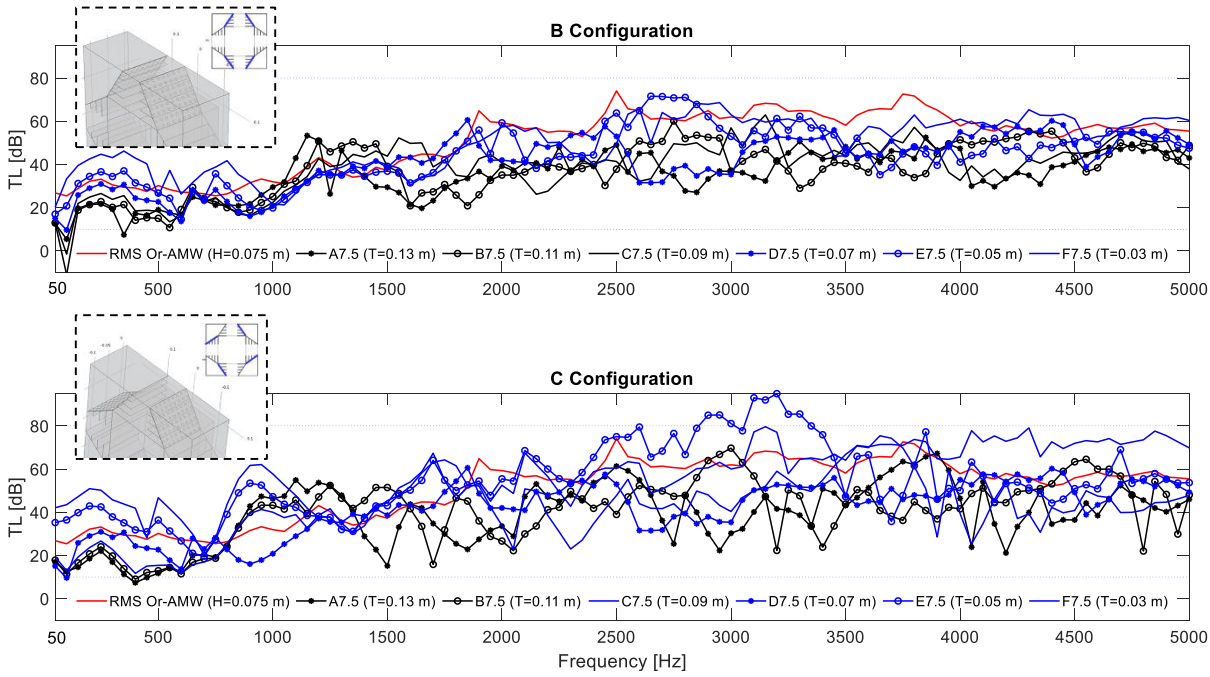

Figure 7.4 Schematics comparison of B and C Configurations TL characterised by H=0.075 m and T=0.13 m (A), T=0.11 m (B), T=0.09 m (C), T=0.07 m (D), T=0.05 m (E), T=0.03 m (F). Two blue dotted lines are plotted for TL = 10dB and TL= 80 dB as reference for the overall TL performance. The red line plot represents the RMS of the original full-scale AMW TL.

Figure 7.5 shows a comparison of the two schematics related to B and C Configurations *TL* characterised by *H*=0.06 m and decreasing *T* value represents the closing mechanism of the AMW (A=*T*=0.13m, B=*T*=0.11m, C=*T*=0.09m, D=*T*=0.07m, E=*T*=0.05m, F=T=0.03m). So, also for a frame thickness H=0.06m, the effectiveness of *TL* can be appreciated simultaneously with the window opening reduction. Overall, B and C show significant TL throughout the 50-5000Hz frequency range (minimum TL=10dB and maximum TL= 84dB). Clear advantages from Configuration C are shown from this numerical analysis, highlighting its merit again over B also in comparison with the RMS of the

original full-scale AMW TL (represented by the red line plot). TL optimisation is indeed performed broadband by model C of the AMW (50-5000Hz). Also, for a frame with H=0.06, Configuration C creates a resonant condition that clearly optimises the system better than B because perforated panels are not coupled, and even AMM unit resonance is improved if compared with a mirrored one (see Figure 7.5).

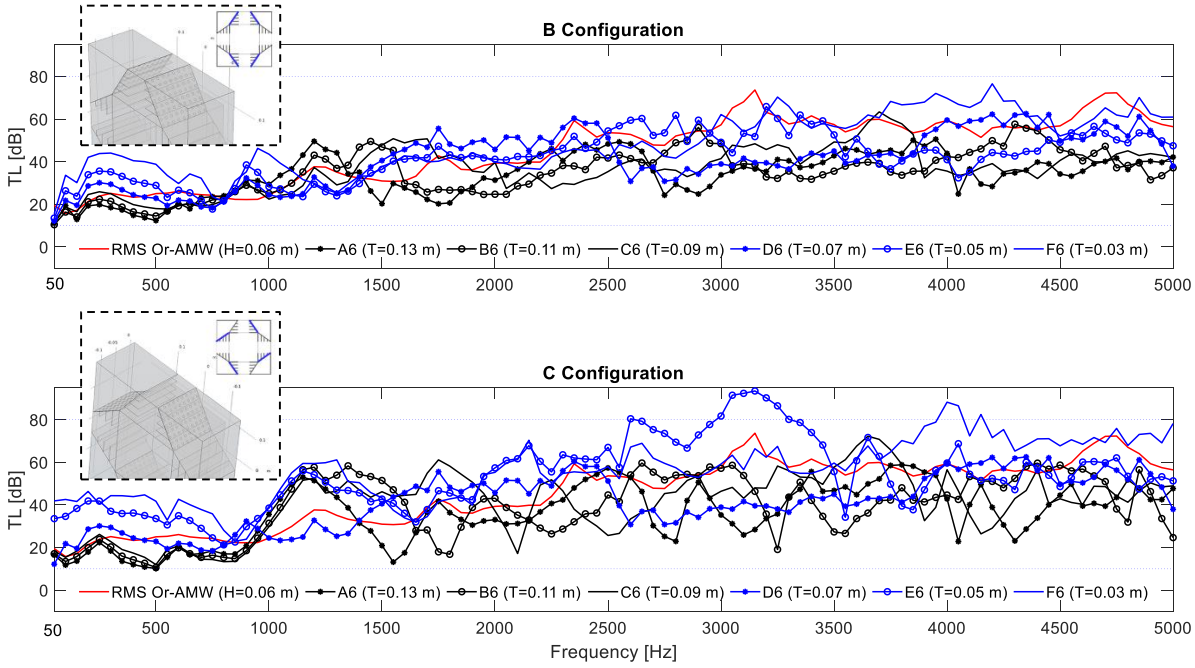

Figure 7.5 Schematics comparison of B and C Configurations TL characterised by H=0.06 m and T=0.13 m (A), T=0.11 m (B), T=0.09 m (C), T=0.07 m (D), T=0.05 m (E), T=0.03 m (F). Two blue dotted lines are plotted for TL = 10dB and TL= 80 dB as reference for the overall TL performance. The red line plot represents the RMS of the original full-scale AMW TL.

Finally, Figure 7.6 shows the TL of the optimised Configuration B and C of the full-scale AM, characterised by a frame height H=0.05m. The decreasing value of T (A=*T*=0.13m, B=*T*=0.11m, C=*T*=0.09m, D=*T*=0.07m, E=*T*=0.05m, F=T=0.03m) represent the thickness of the window with constant H again, and so the performance of the AMW at different degrees of closure. Overall, significant TL is highlighted from the numerical analysis of Configurations B and C. Also, in this case, C works slightly better than B throughout the 50-5000Hz frequency range, meaning that the smaller dimensions of the AMM unit within the frame neutralise the resonant contribution of the evenly perforated Configuration C. The comparison with the TL RMS of the original AMW(represented by the red line plot) shows overall merit towards the new optimised models(see Figure 7.6).

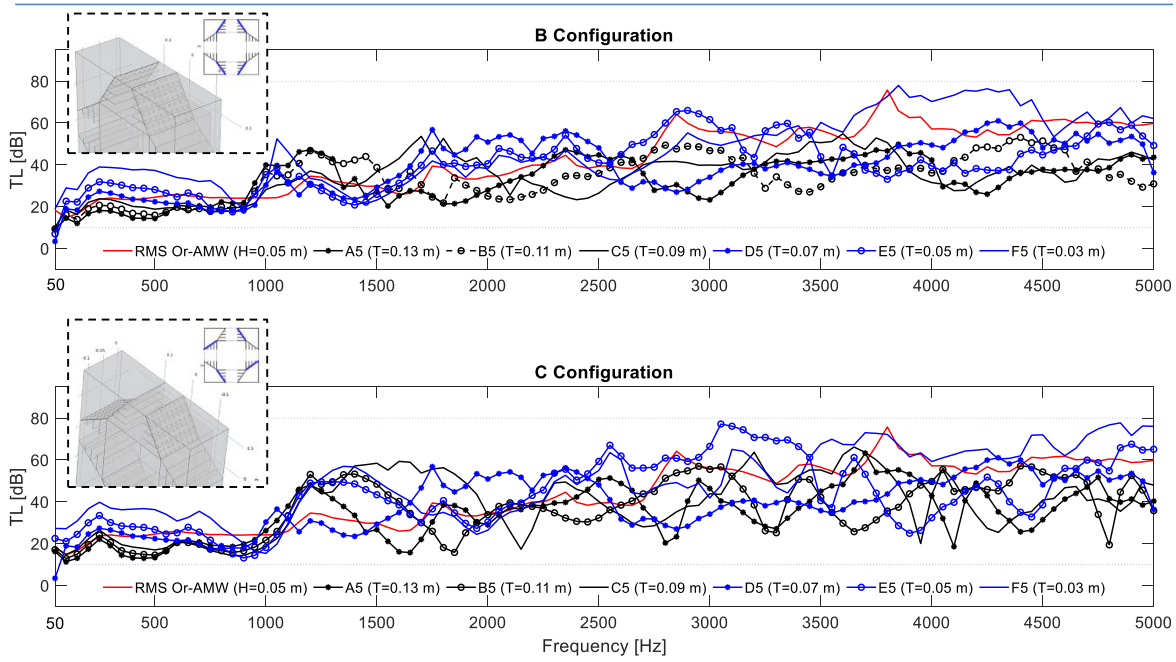

Figure 7.6 Schematics comparison of B and C Configurations TL characterised by H=0.05 m and T=0.13 m (A), T=0.11 m (B), T=0.09 m (C), T=0.07 m (D), T=0.05 m (E), T=0.03 m (F). Two blue dotted lines are plotted for TL = 10dB and TL= 80 dB as reference for the overall TL performance. The red line plot represents the RMS of the original full-scale AMW TL.

Overall, B and C Configurations work more efficiently when compared to the original configuration because, as in the case study of the AMW unit, they allow the AMM unit to have the biggest resonating volume, showing that the perforation percentage is a crucial factor for the design of such AMM window, especially at low frequencies (50-500 Hz) where they reach an average of 25 dB of *TL*. On the other side, it is important to note that the perforated panels' disposition becomes more crucial with the increase of the frame height (H). It is possible to assume that, due to its even geometrical nature, Configuration C allows an optimised TL and overcome limitations and even possible magnifications caused by B at a lower frequency range (50-100Hz). Despite its acoustic merits over the original full-scale AMW model and the B variation, Configuration C might result in more convenient for an industrialised process since this specific design could allow a fabrication in series of the AMM unit pieces, which would be all the same. This feature would represent a great simplification in the fabrication process and so an advantage over production costs and time.

7.4 Conclusions

This PhD study chapter has attempted to explore the applicability of a previously developed AMW unit system for noise reduction and natural ventilation in a full-scale window system. A total of 120 parametric analyses have been carried out in order to assess the effectiveness concerning two design

parameters: frame's thickness and height (*T* and *H*) for both a basic AMW full-scale model and broadband optimised one.

First of all, from the acoustics point of view, the basic full-scale AMW reduces the incoming noise effectively with a minimum *ΔTL* of 1.49 dB and a maximum of 55.73 dB over a standard sliding window. It was proved that, nevertheless, the customisation of the AMW design (depending on H) and the degree of opening (depending on T), the noise reduction is guaranteed.

Once the system's acoustics was proved to be efficient despite the opening degree of the AMW, natural ventilation is considered independent from the noise reduction task. This specific full-scale AMW technology allows a non-dependency with the noise exposure time, showing a significant advantage over standard window design (where users must choose over noise insulation/reduction or natural ventilation). So in this final part of the PhD study, natural ventilation is numerically proved to satisfy the ACRM standards with an overall shorter time between -6.52 min (= -6'31'') and -9.18 min (= -9'11'') (especially for bigger values of T= A, B, C). The natural ventilation efficiency is numerically verified for both acoustically basic and optimised models.

The final numerical analysis on the acoustically optimised model of AMW (in a number of different customisable designs according to T and H) finally shows that with a tailored perforated AMM unit structure [189], noise attenuation can be consistently achieved within the frequency range of 50-5000 Hz, and opening time can be increased or reduced mostly without depending on the outdoor acoustic stimuli. Furthermore, models with *T*=7.5, 10, 15 can achieve significant *TL* values with optimal *ACRM*, making this design suitable for most indoor public functions.

8. Conclusions

As highlighted in Chapter **2. Literature Review**, windows are a key feature of physical connection with the outdoor environment, yet standard windows cause discomfort when users must choose between natural ventilation and noise reduction. To fill this gap, modern technologies such as AMMs could be used as they have a wide range of applications and could perhaps resolve the previous highlighted issue if implemented into the window system; However, so far, these technologies have been developed without considering human perception and ergonomics. So this project aimed at addressing physical, perception and ergonomic issues of windows through AMMs in order to allow natural ventilation and optimised noise reduction.

8.1 Findings

In particular, three research questions were considered to fill the actual research gap through this project 1) Which are the most relevant ergonomic principles to be followed when designing a new window system? Why is it important to follow ergonomic principles in an AMM-based window?; What are the benefits of using AMMs over traditional window technologies? How is it possible to embed AMMs into ergonomic windows?; 3) Will an AMM-based window impact significantly people' perception and improve overall indoor comfort? How does this new AMM-based window relate to the ergonomic principles?

About the first research question, it was found that users perceive the ergonomic value of a window through three principles: 1. Importance of the Outdoor Connection to feel oriented, 2. Filtering the information without changing the meaning, and 3. Controlling the window system behaviours within physical boundaries. The first research question was indeed addressed through a participatory design method involving the ergonomics of the window. This Social Science and Ergonomics based methodology could be used by Engineering and Architecture researchers to investigate the optimal building feature design ergonomically according to the users' perspective. It could be possible, for example, to draw a windows design prototype depending on these three principles defining specific optimal window requirements such as incoming noise reduction without changing the meaning of the outdoor context to help the users feel oriented but also achieve indoor comfort. If implemented with the right technologies, the window design would become indeed not only the mediator between the outside inputs and the indoor comfort, but it could even modulate the first one to optimise the second.

For the second research question, it was developed a full-scale AMW which could allow noise reduction and natural ventilation while following the ergonomic principles for the window design. To

answer this research question, analytical, numerical, and experimental analyses were used first to develop an AMM unit based on the acoustic stopband related to the resonant tubular array and inspired by the acoustic black hole (ABH) effect [268]. The principles behind ABH allows having a significant noise-reducing system within a limited thickness, with several benefits over traditional materials. Secondly, the AMM unit was assembled into an AMW unit to understand the evolution of its physical properties according to the coupled spatial configuration. Finally, once the AMW unit demonstrated significant benefit from the acoustic and ventilation point of view, it was adapted to a customisable full-scale AMW, which could allow noise reduction and natural ventilation while following the ergonomic principles for the window design. The customisation resulted in being efficient for both physical problems; nevertheless, the design could be adapted to different architectonical necessities (thickness and height of the window frame could be adapted without changing the effectiveness of the AMW).

For the third and final research question, it was found that the AMW has a significant soundscape neutralisation capacity from the human perception point of view. This finding was achieved through a physics and human perception study based on laboratory measurements on the AMW unit and laboratory and online questionnaires (over 85 people) presenting seven environmental sound recordings (related to everyday life activities), presented both in their original version and modified by the AMW acoustic effect. Specifically, it was found that the AMW unit can hallow to 1) have a significant acoustic filtering capacity over the most frequently heard noise sources frequency range (by using a customised AMM system) while allowing natural ventilation; 2) mediate between the indoor and the outdoor of a building: acoustically (through the AMMs), visually (through possible filtering effects applied on the central panel), and from a ventilation point of view (by regulating the opening of the window); 3) put the users in connection with the outdoor environment: acoustically (by filtering the incoming noise without changing the meaning), visually (through the frontal transparent panel), and from a ventilation point of view (by regulating the opening of the window); 4) make the users feel oriented and perceive an improvement in the indoors affective impact, despite the non-optimal conditions (acoustically by filtering the noise sources but keeping them recognisable.

8.2 Related future research

In this project, Social science-based, ergonomic, numerical, analytical and experimental methods were used to draw a full-scale window prototype using AMMs to allow natural ventilation independently from the outdoor noise situation. This research opens a new field of investigation not limited to buildings insulation but including outdoor stimuli optimisation towards a more comprehensive indoor comfort. However, further studies could overcome some limitations and expand the specificity of this project over the following aims and objectives:

Ergonomic and focus group studies targeting specific context of climate and geographical ranges and specific indoor activities and buildings functions

The three ergonomic principles highlighted from this project are related to generic environmental conditions, indoor functions and building destination. However, a more targeted study could allow drawing customised ergonomic window design principles for each specific situation. For example, public or private buildings have a different requirement in terms of noise insulation and natural ventilation, same as different indoor functions (for example, home, work, spare time, education, and healthcare-related functions), or outdoor environmental conditions (very loud and infrastructural, very quiet and natural, very vibrant neighbourhood).

Experimental testing on full-scale AMW prototype from the acoustic and ventilation point of view

Experimental tests on the AMW unit gave sufficient information about physic and human perception based characteristics and potential; However, experimental study on the full-scale AMW might help understand other psychoacoustic effects according to bigger design and wider frequency range of noise reduction. Even if the AMW unit investigation highlighted significant merits over standard windows, full-scale tests might give a more comprehensive understanding of the AMW potential from an acoustics, natural ventilation, and human perception point of view.

CFD or experimental study on the full-scale AMW ventilation potential, targeting specific building characteristics (including floor level, geographical location, wind direction, wind velocity, room dimension);

The numerical analysis highlighted basic sufficient ventilation capacity of the AMW (either unit or full-scale); However, the outdoor ventilation boundary conditions and the indoor room

characteristics were limited (wind speed of 1.132 m/s according to Asfour and Gadi criteria [288], the perpendicular direction of airflow at the inlet, height above the ground of 20m, and the room height of 3m). Further CFD or experimental studies could allow a more comprehensive characterisation of the AMW considering a variety of floor levels (different heights where the window is placed are characterised by different wind velocity), geographical location (different wind directions might derive from this factor), and room dimension (as a bigger volume of the room needs higher volumetric flow rate of air in order to satisfy the standards of ACPH).

Bibliography

[1] Rem Koolhaas. Elements of Architecture. Milan, Italy: MARSILIO; 2014.

[2] Harvie-Clark J, Chilton A, Conlan N, Trew D. Assessing noise with provisions for ventilation and overheating in dwellings. J Build Serv Eng Res Technol 2019;40:263–73. https://doi.org/10.1177/0143624418824232.

[3] Public Health England. Review and Update of Occupancy Factors for UK homes. London: 2018.

[4] Fusaro G, Kang J. Participatory approach to draw ergonomic criteria for window design. Int J Ind Ergon 2021;82. https://doi.org/10.1016/j.ergon.2021.103098.

[5] Tang SK. A review on natural ventilation-enabling façade noise control devices for congested high-rise cities. Appl Sci 2017;7. https://doi.org/10.3390/app7020175.

[6] Du L, Lau SK, Lee SE, Danzer MK. Experimental study on noise reduction and ventilation performances of sound-proofed ventilation window. Build Environ 2020;181:107105. https://doi.org/10.1016/j.buildenv.2020.107105.

[7] Lam B, Shi D, Belyi V, Wen S, Gan WS, Li K, et al. Active control of low-frequency noise through a single top-hung window in a full-sized room. Appl Sci 2020;10. https://doi.org/10.3390/app10196817.

[8] Kang J, Brocklesby MW. Feasibility of applying micro-perforated absorbers in acoustic window systems. Appl Acoust 2005;66:669–89. https://doi.org/10.1016/J.APACOUST.2004.06.011.

[9] Asdrubali F, Buratti C. Sound intensity investigation of the acoustics performances of high insulation ventilating windows integrated with rolling shutter boxes. Appl Acoust 2005;66:1088–101. https://doi.org/10.1016/j.apacoust.2005.02.001.

[10] Waddington DC, Oldham DJ. The prediction of airflow-generated noise in mechanical ventilation systems. Indoor Built Environ 2000;9:111–7. https://doi.org/10.1177/1420326X0000900207.

[11] Harvie-Clark J, Conlan N, Wei W, Siddall M. How loud is too loud? noise from domestic mechanical ventilation systems. Int J Vent 2019;18:303–12. https://doi.org/10.1080/14733315.2019.1615217.

[12] Wang X, Luo X, Yang B, Huang Z. Ultrathin and durable open metamaterials for simultaneous ventilation and sound reduction. Appl Phys Lett 2019;115:171902. https://doi.org/10.1063/1.5121366.

[13] Kang J, Li Z. Numerical simulation of an acoustic window system using finite element method. Acta Acust United with Acust 2007;93:152–63.

[14] De Salis MHF, Oldham DJ, Sharples S. Noise control strategies for naturally ventilated buildings. Build Environ 2002;37:471–84. https://doi.org/10.1016/S0360-1323(01)00047-6.

[15] Lam B, Shi C, Shi D, Gan WS. Active control of sound through full-sized open windows. Build Environ 2018;141:16–27.

[16] Carbajo J, Ghaffari Mosanenzadeh S, Kim S, Fang NX. Sound absorption of acoustic resonators with oblique perforations. Appl Phys Lett 2020;116. https://doi.org/10.1063/1.5132886.

[17] Pan L, Martellotta F. A parametric study of the acoustic performance of resonant absorbers made of micro-perforated membranes and perforated panels. Appl Sci 2020;10. https://doi.org/10.3390/app10051581.

[18] Kusaka M, Sakagami K, Okuzono T. A Basic Study on the Absorption Properties and Their Prediction of Heterogeneous Micro-Perforated Panels : A Case Study of Micro-Perforated Panels with Heterogeneous Hole Size and Perforation Ratio. Acoustics 2021;5. https://doi.org/10.3390/acoustics3030031.

[19] Tsukamoto Y, Tomikawa Y, Sakagami K, Okuzono T, Maikawa H, Komoto Y. Experimental assessment of sound insulation performance of a double window with porous absorbent materials its cavity perimeter. Appl Acoust 2020;165:107317. https://doi.org/10.1016/j.apacoust.2020.107317.

[20] Zhou Y, Li D, Li Y, Hao T. Perfect acoustic absorption by subwavelength metaporous composite. Appl Phys Lett 2019;115. https://doi.org/10.1063/1.5107439.

[21] Li D, Jiang Z, Li L, Liu X, Wang X, He M. Investigation of acoustic properties on wideband sound-absorber composed of hollow perforated spherical structure with extended tubes and porous materials. Appl Sci 2020;10:1–11. https://doi.org/10.3390/app10248978.

[22] Horoshenkov K V., Groby J-P, Dazel O. Asymptotic limits of some models for sound propagation in porous media and the assignment of the pore characteristic lengths. J Acoust Soc Am 2016;139:2463–74. https://doi.org/10.1121/1.4947540.

[23] Yu X. Design and in-situ measurement of the acoustic performance of a metasurface ventilation window. Appl Acoust 2019;152:127–32. https://doi.org/10.1016/j.apacoust.2019.04.003.

[24] Li LJ, Zheng B, Zhong LM, Yang J, Liang B, Cheng JC. Broadband compact acoustic absorber with high-efficiency ventilation performance. Appl Phys Lett 2018;113. https://doi.org/10.1063/1.5038184.

[25] Kumar S, Lee HP. Labyrinthine acoustic metastructures enabling broadband sound absorption and ventilation. Appl Phys Lett 2020;116. https://doi.org/10.1063/5.0004520.

[26] Yang M, Sheng P. An Integration Strategy for Acoustic Metamaterials to Achieve Absorption by Design. Appl Sci 2018;8:1247. https://doi.org/10.3390/app8081247.

[27] Jiménez N, Groby J-P, Pagneux V, Romero-García V. Iridescent Perfect Absorption in Critically-Coupled Acoustic Metamaterials Using the Transfer Matrix Method. Appl Sci 2017;7:618. https://doi.org/10.3390/app7060618.

[28] Zhang J, Romero-García V, Theocharis G, Richoux O, Achilleos V, Frantzeskakis DJ. Dark solitons in acoustic transmission line metamaterials. Appl Sci 2018;8. https://doi.org/10.3390/app8071186.

[29] Gritsenko D, Paoli R. Theoretical optimization of trapped-bubble-based acoustic metamaterial performance. Appl Sci 2020;10:1–16. https://doi.org/10.3390/app10165720.

[30] Park J, Lee D, Rho J. Recent advances in non-traditional elastic wave manipulation by macroscopic artificial structures. Appl Sci 2020;10. https://doi.org/10.3390/app10020547.

[31] Li Y, Liang B, Gu ZM, Zou XY, Cheng JC. Unidirectional acoustic transmission through a prism with near-zero refractive index. Appl Phys Lett 2013;103. https://doi.org/10.1063/1.4817249.

[32] Qi S, Assouar B. Acoustic energy harvesting based on multilateral metasurfaces. Appl Phys Lett 2017;111. https://doi.org/10.1063/1.5003299.

[33] Xie Y, Shen C, Wang W, Li J, Suo D, Popa BI, et al. Acoustic Holographic Rendering with Two-dimensional Metamaterial-based Passive Phased Array. Sci Rep 2016;6:1–6. https://doi.org/10.1038/srep35437.

[34] Zhang Z, Wei Q, Cheng Y, Zhang T, Wu D, Liu X. Topological Creation of Acoustic Pseudospin Multipoles in a Flow-Free Symmetry-Broken Metamaterial Lattice. Phys Rev Lett 2017;118:1–6. https://doi.org/10.1103/PhysRevLett.118.084303.

[35] Chen S, Fan Y, Fu Q, Wu H, Jin Y, Zheng J, et al. A Review of Tunable Acoustic Metamaterials. Appl Sci 2018;8:1480. https://doi.org/10.3390/app8091480.

[36] Wu F, Xiao Y, Yu Di, Zhao H, Wang Y, Wen J. Low-frequency sound absorption of hybrid absorber based on micro-perforated panel and coiled-up channels. Appl Phys Lett 2019;114. https://doi.org/10.1063/1.5090355.

[37] Yu X, Lu Z, Cheng L, Cui F. On the sound insulation of acoustic metasurface using a sub-structuring approach. J Sound Vib 2017;401:190–203. https://doi.org/10.1016/j.jsv.2017.04.042.

[38] Köhler B, Rage N, Chigot P, Hviid CA. Thermo-active building systems and sound absorbers: Thermal comfort under real operation conditions. Build Environ 2017;128:143–52. https://doi.org/10.1016/j.buildenv.2017.11.037.

[39] Nagamachi M. Kansei engineering: A new consumer-oriented technology for product development. Int J Ind Ergon 1995;15:3–11. https://doi.org/10.1201/9780203010457.

[40] Pereira Pessôa MV, Jauregui Becker JM. Smart design engineering: a literature review of the impact of the 4th industrial revolution on product design and development. Res Eng Des 2020;31:175–95. https://doi.org/10.1007/s00163-020-00330-z.

[41] Singh R, Tandon P. User values based evaluation model to assess product universality. Int J Ind Ergon 2016;55:46–59. https://doi.org/10.1016/j.ergon.2016.07.006.

[42] Sakagami K, Okuzono T. Some considerations on the use of space sound absorbers with next-generation materials reflecting COVID situations in Japan: additional sound absorption for post-pandemic challenges in indoor acoustic environments. UCL Open Environ 2020:1–10. https://doi.org/10.14324/111.444/ucloe.000012.

[43] Joshi M, Deshpande V. A systematic review of comparative studies on ergonomic assessment techniques. Int J Ind Ergon 2019;74:102865. https://doi.org/10.1016/j.ergon.2019.102865.

[44] Seim R, Broberg O. Participatory workspace design: A new approach for ergonomists? Int J Ind Ergon 2010;40:25–33. https://doi.org/10.1016/j.ergon.2009.08.013.

[45] Kang J. An acoustic window system with optimum ventilation and daylighting performance. Noise Vib Worldw 2006:9–17.

[46] Huang H, Qiu X, Kang J. Active noise attenuation in ventilation windows. J Acoust Soc Am 2011;130:176. https://doi.org/10.1121/1.3596457.

[47] Fusaro G, D'alessandro F, Baldinelli G, Kang J. Design of urban furniture to enhance the soundscape: A case study. Build Acoust 2018;25:61–75. https://doi.org/10.1177/1351010X18757413.

[48] Torresin S, Aletta F, Babich F, Bourdeau E, Harvie-Clark J, Kang J, et al. Acoustics for supportive and healthy buildings: Emerging themes on indoor soundscape research. Sustain 2020;12:1–28. https://doi.org/10.3390/su12156054.

[49] Zwicker E, Fastl H (Hugo). Psychoacoustics : facts and models. Springer; 1999.

[50] Cicero. Oratio pro Rabirio - 54 B.C. 54AD.

[51] Poore J. Anatomy of a double-hang window. Old House J 1999.

[52] Everest FA, Pohlmann KC. Master Handbook of Acoustics. Fifth. New York Chicago San Francisco Lisbon London Madrid Mexico City Milan New Delhi San Juan Seoul Singapore Sydney Toronto: Mc Graw Hill; 2009.

[53] ISO. ISO 16383 - Acoustics — Field measurement of sound insulation in buildings and of building elements (parts 1-3). 2016.

[54] Lam B, Elliott S, Cheer J, Gan W-S. Physical limits on the performance of active noise control through open windows. Appl Acoust 2018:9–17. https://doi.org/10.1016/j.apacoust.2018.02.024.

[55] Kang J, Schulte-Fortkamp B. Soundscape and the built environment. Routledge - Taylor & Francis Group; 2017. https://doi.org/10.1201/b19145.

[56] Asdrubali F, Cotana F. Influence of filtering system on high sound insulation ventilating windows. INTER-NOISE NOISE-CON Congr Conf Preced 2000:295–302.

[57] Field CD, Fricke FR. Theory and applications of quarter-wave resonators: A prelude to their use for attenuating noise entering buildings through ventilation openings. Appl Acoust 1998;53:117–32. https://doi.org/10.1016/S0003-682X(97)00035-2.

[58] Yu X, Cui FS, Cheng L. On the acoustic analysis and optimization of ducted ventilation systems using a sub-structuring approach. J Acoust Soc Am 2016;139:279. https://doi.org/10.1121/1.4939785.

[59] Yu X, Lau SK, Cheng L, Cui F. A numerical investigation on the sound insulation of ventilation windows. Appl Acoust 2017;117:113–21. https://doi.org/10.1016/j.apacoust.2016.11.006.

[60] Al-Homoud DMS. Performance characteristics and practical applications of common building thermal insulation materials. Build Environ 2005;40:353–66. https://doi.org/10.1016/J.BUILDENV.2004.05.013.

[61] Pendry JB. Negative Refraction Makes a Perfect Lens. Phys Rev Lett 2000;66.

[62] Pendry JB, Holden AJ, Robbins DJ, Stewart WJ. Magnetism from conductors and enhanced nonlinear phenomena. IEEE Trans Microw Theory Tech 1999;47:2075–84. https://doi.org/10.1109/22.798002.

[63] Liu Z, Zhang X, Mao Y, Zhu YY, Yang Z, Chan CT, et al. Locally Resonant Sonic Materials. Sci New Ser 2000;289:1734–6.

[64] Rout S, Sonkusale S. Active Metamaterials. Cham: Springer International Publishing; 2017. https://doi.org/10.1007/978-3-319-52219-7.

[65] Weiglhofer WS, Lakhtakia A (Akhlesh), Society of Photo-optical Instrumentation Engineers. Introduction to complex mediums for optics and electromagnetics. SPIE; 2003.

[66] Zouhdi S, Sihvola AH, Vinogradov AP. Metamaterials and plasmonics : fundamentals, modelling, applications. Springer; 2009.

[67] Guenneau S, Movchan A, Pétursson G, Anantha Ramakrishna S. Acoustic metamaterials for sound focusing and confinement. New J Phys 2007;9:399–399. https://doi.org/10.1088/1367-2630/9/11/399.

[68] Shalaev VM. Optical negative-index metamaterials. vol. 1. 2007.

[69] Fang N, Lee H, Sun C, Zhang X. Sub-Diffraction-Limited Optical Imaging with a Silver Superlens. Science (80-) 2005;308:534–7.

[70] Cai W, Chettiar UK, Kildishev A V, Shalaev VM. Optical cloaking with metamaterials. Nat Photonics 2007. https://doi.org/10.1038/nphoton.2007.28.

[71] Haberman MR, Guild MD. Acoustic metamaterials. Phys Today 2016;69:42–8. https://doi.org/10.1063/PT.3.3198.

[72] Enoch S, Tayeb G, Sabouroux P, Guérin N, Vincent P. A Metamaterial for Directive Emission. Phys Rev Lett 2002;89. https://doi.org/10.1103/PhysRevLett.89.213902.

[73] Mocella V, Cabrini S, Chang ASP, Dardano P, Moretti L, Rendina I, et al. Self-Collimation of Light over Millimeter-Scale Distance in a Quasi-Zero-Average-Index Metamaterial. Phys Rev

Lett 2009;102. https://doi.org/10.1103/PhysRevLett.102.133902.

[74] Alù A, Silveirinha MG, Salandrino A, Engheta N. Epsilon-near-zero metamaterials and electromagnetic sources: Tailoring the radiation phase pattern. Phys Rev B - Condens Matter Mater Phys 2007;75:1–13. https://doi.org/10.1103/PhysRevB.75.155410.

[75] Hao J, Yan W, Qiu M. Super-reflection and cloaking based on zero index metamaterial. Appl Phys Lett 2010;96:1–4. https://doi.org/10.1063/1.3359428.

[76] Shen C, Xie Y, Li J, Cummer SA, Jing Y. Asymmetric acoustic transmission through near-zero-index and gradient-index metasurfaces. Appl Phys Lett 2016;108:223502. https://doi.org/10.1063/1.4953264.

[77] Groby JP, Huang W, Lardeau A, Aurégan Y. The use of slow waves to design simple sound absorbing materials. J Appl Phys 2015;117. https://doi.org/10.1063/1.4915115.

[78] Lu D, Liu Z. Hyperlenses and metalenses for far-field super-resolution imaging. REVIEW 2012. https://doi.org/10.1038/ncomms2176.

[79] Zhu J, Christensen J, Jung J, Martin-Moreno L, Yin X, Fok L, et al. A holey-structured metamaterial for acoustic deep-subwavelength imaging. Nat Phys Lett 2011;7:52–5. https://doi.org/10.1038/NPHYS1804.

[80] Del Grosso AE, Basso P. Adaptive building skin structures. Smart Mater Struct 2010;19. https://doi.org/10.1088/0964-1726/19/12/124011.

[81] Kronenburg R, Kronenburg D. Flexible: Architecture that Responds to Change. London: Laurence King Publishing; 2007.

[82] Romero-García V, Krynkin A, Garcia-Raffi LM, Umnova O, Sánchez-Pérez J V. Multi-resonant scatterers in sonic crystals: Locally multi-resonant acoustic metamaterial. J Sound Vib 2013;332:184–98. https://doi.org/10.1016/j.jsv.2012.08.003.

[83] Krynkin A, Umnova O, Chong AYB, Taherzadeh S, Attenborough K. Scattering by coupled resonating elements in air. J Phys D Appl Phys 2011;44. https://doi.org/10.1088/0022-3727/44/12/125501.

[84] Ma G, Sheng P. Acoustic metamaterials: From local resonances to broad horizons. Sci Adv 2016;2:e1501595–e1501595. https://doi.org/10.1126/sciadv.1501595.

[85] Lee SH, Park CM, Seo YM, Wang ZG, Kim CK. Composite Acoustic Medium with Simultaneously Negative Density and Modulus. Phys Rev Lett 2010;104.

https://doi.org/10.1103/PhysRevLett.104.054301.

[86] Bliss D, He Q, Franzoni L, Palas C. Innovative structural acoustic strategies to reduce sound transmission through lightweight flexible structures. J Acoust Soc Am 2009;125:2603–2603. https://doi.org/10.1121/1.4783909.

[87] Firth IM. On the Theory and Design of Acoustic Resonators The Journal of the Acoustical Society of America. Circ Concentric Helmholtz Reson J Acoust Soc Am 1986;80:41. https://doi.org/10.1121/1.2023505.

[88] Sandler M. HIGH COMPLEXITY RESONATOR STRUCTURES FOR FORMANT SYNTHESIS OF MUSICAL INSTRUMENTS. vol. 27. 1989.

[89] Braasch J. Understanding timbral effects of multi-resonator/generator systems of wind instruments in the context of western and non-western music. J Acoust Soc Am 2015;137:2426–2426. https://doi.org/10.1121/1.4920851.

[90] Dancila D, Rottenberg · X, Tilmans HAC, De Raedt · W, Huynen · I. INVESTIGATION OF INTERNAL NONHOMOGENOUS VOLUMES OF PERTURBATION AS TUNING AND MINIATURIZATION ELEMENTS FOR CAVITY RESONATORS. Microw Opt Technol Lett 2012;54:491/496. https://doi.org/10.1002/mop.

[91] Dancila D, Rottenberg · X, Focant · N, Tilmans HAC, De Raedt · W, Huynen · I. Compact cavity resonators using high impedance surfaces. Appl Phys A 2011;103:799–804. https://doi.org/10.1007/s00339-010-6235-6.

[92] Yang T, Saati F, Horoshenkov K V., Xiong X, Yang K, Mishra R, et al. Study on the sound absorption behavior of multi-component polyester nonwovens: experimental and numerical methods. Text Res J 2019;89:3342–61. https://doi.org/10.1177/0040517518811940.

[93] Law M, Greene LE, Johnson JC, Saykally R, Yang AP. Nanowire dye-sensitized solar cells 2005. https://doi.org/10.1038/nmat1387.

[94] Derode A, Roux P, Fink M. ACOUSTIC TIME-REVERSAL THROUGH HIGH-ORDER MULTIPLE SCATTERING. IEEE Ultrason Symp 1995;Vol.2:1091–4. https://doi.org/10.1109/ULTSYM.1995.495751.

[95] Chong YD, Ge L, Cao H, Stone AD. Coherent Perfect Absorbers: Time-reversed Lasers. 2010.

[96] Mei J, Ma G, Yang M, Yang Z, Wen W, Sheng P. Dark acoustic metamaterials as super absorbers for low-frequency sound 2012. https://doi.org/10.1038/ncomms1758.

[97] Jiménez N, Huang W, Romero-García V, Pagneux V, Groby JP. Ultra-thin metamaterial for perfect and quasi-omnidirectional sound absorption. Appl Phys Lett 2016;109. https://doi.org/10.1063/1.4962328.

[98] Cox TJ, D'Antonio P. Acoustic Absorbers and Diffusers. Third. CRC Press; 2016. https://doi.org/10.1201/9781315369211.

[99] Arenas JP, Crocker MJ. Recent Trends in Porous Sound-Absorbing Materials. Sound Vib 2010;44:12–7.

[100] Yang Z, Mei J, Yang M, Chan NH, Sheng P. Membrane-Type Acoustic Metamaterial with Negative Dynamic Mass. Phys Rev Lett 2008;101:204301:1-4. https://doi.org/10.1103/PhysRevLett.101.204301.

[101] Yang M, Ma G, Yang Z, Sheng P. Coupled Membranes with Doubly Negative Mass Density and Bulk Modulus. Phys Rev Lett 2013;110:134301:1-5. https://doi.org/10.1103/PhysRevLett.110.134301.

[102] Fleury R, Alù A. Extraordinary Sound Transmission through Density-Near-Zero Ultranarrow Channels. Phys Rev Lett 2013;111. https://doi.org/https://doi.org/10.1103/PhysRevLett.111.055501.

[103] Jing Y, Xu J, Fang NX. Numerical study of a near-zero-index acoustic metamaterial. Phys Lett A 2012;376:2834–7. https://doi.org/10.1016/j.physleta.2012.08.057.

[104] Yao S, Zhou X, Hu G. Investigation of the negative-mass behaviors occurring below a cut-off frequency. New J Phys 2010;12:103025. https://doi.org/10.1088/1367-2630/12/10/103025.

[105] Lee SH, Mahn Park C, Seo YM, Wang ZG, Kim K. Acoustic metamaterial with negative density. Phys Lett A 2009;373:4464–9. https://doi.org/10.1016/j.physleta.2009.10.013.

[106] Pierre J, Dollet B, Leroy V. Resonant Acoustic Propagation and Negative Density in Liquid Foams 2014. https://doi.org/10.1103/PhysRevLett.112.148307.

[107] Veselago V. The electrodynamics of substances with simultaneously negative values of E and m . Sov Phys Uspekhi 1968;10.

[108] Zhang S, Yin L, Fang N. Focusing Ultrasound with an Acoustic Metamaterial Network. Phys Rev Lett 2009;102. https://doi.org/10.1103/PhysRevLett.102.194301.

[109] Kaina N, Lemoult F, Fink M, Lerosey G. Negative refractive index and acoustic superlens from multiple scattering in single negative metamaterials. Nature 2015;525:77–81.

https://doi.org/10.1038/nature14678.

[110] Zigoneanu L, Popa BI, Cummer SA. Three-dimensional broadband omnidirectional acoustic ground cloak. Nat Mater 2014;13:352–5. https://doi.org/10.1038/nmat3901.

[111] Xie Y, Wang W, Chen H, Konneker A, Popa BI, Cummer SA. Wavefront modulation and subwavelength diffractive acoustics with an acoustic metasurface. Nat Commun 2014;120:1–5. https://doi.org/10.1063/1.4967738.

[112] Sun S, He Q, Xiao S, Xu Q, Li X, Zhou L. Gradient-index meta-surfaces as a bridge linking propagating waves and surface waves. Nat Mater 2012;11:426–31. https://doi.org/10.1038/nmat3292.

[113] Liang Z, Li J. Extreme Acoustic Metamaterial by Coiling Up Space. Phys Rev Lett 2012;108. https://doi.org/10.1103/PhysRevLett.108.114301.

[114] Klipsch PW. A Low Frequency Horn of Small Dimensions. J Acoust Soc Am 1941;13:137–44. https://doi.org/10.1121/1.1916155.

[115] Cheng Y, Zhou C, Yuan BG, Wu DJ, Wei Q, Liu XJ. Ultra-sparse metasurface for high reflection of low-frequency sound based on artificial Mie resonances. Nat Mater 2015;14:1013–9. https://doi.org/10.1038/nmat4393.

[116] European Parliament and Council. Directive 2002/49/EC relating to the assessment and management of environmental noise. Brussels: Publications Office of the European Union: 2002.

[117] Allard J-F, Atalla N. Propagation of sound in porous media : modelling sound absorbing materials. Wiley; 2009.

[118] Kim S, Kim Y-H, Jang J-H. On the Theory and Design of Acoustic Resonators. J Acoust Soc Am 2006;119:1975. https://doi.org/10.1121/1.2177568.

[119] Wang C, Huang L, Zhang Y. Oblique incidence sound absorption of parallel arrangement of multiple micro-perforated panel absorbers in a periodic pattern. J Sound Vib 2014;333:6828–42. https://doi.org/10.1016/j.jsv.2014.08.009.

[120] Park S-H. Acoustic properties of micro-perforated panel absorbers backed by Helmholtz resonators for the improvement of low-frequency sound absorption. J Sound Vib 2013;332:4895–911. https://doi.org/10.1016/j.jsv.2013.04.029.

[121] Cai X, Guo Q, Hu G, Yang J. Ultrathin low-frequency sound absorbing panels based on

coplanar spiral tubes or coplanar Helmholtz resonators. Appl Phys Lett 2014;105:121901. https://doi.org/10.1063/1.4895617.

[122] Wang J, Leistner P, Li X. Prediction of sound absorption of a periodic groove structure with rectangular profile. Appl Acoust 2012;73:960–8. https://doi.org/10.1016/j.apacoust.2012.04.006.

[123] Toyoda M, Kobatake S, Sakagami K. Numerical analyses of the sound absorption of three-dimensional MPP space sound absorbers. Appl Acoust 2014;79:69–74. https://doi.org/10.1016/j.apacoust.2013.12.012.

[124] Nocke C, Hilge C, Scherrer J-M. Brief review on micro-perforated sound absorbers. J Acoust Soc Am 2012;131:3420–3420. https://doi.org/10.1121/1.4708824.

[125] Horoshenkov K V., Hurrell A, Groby J-P. A three-parameter analytical model for the acoustical properties of porous media. J Acoust Soc Am 2019;145:2512–7. https://doi.org/10.1121/1.5098778.

[126] Groby J-P, Huang W, Lardeau A, Aurégan Y. The use of slow waves to design simple sound absorbing materials. J Appl Phys 2015;117:124903. https://doi.org/10.1063/1.4915115.

[127] Gibson LJ, Ashby MF. Cellular Solids: Structure and Properties. 2nd ed. Cambridge University Press; 1997.

[128] Noor AK, Anderson MS, GreeneJ WH, Xi WW. Continuum Models for Beam-and Platelike Lattice Structures. AIAA J 1978;16. https://doi.org/10.2514/3.61036.

[129] Jin M, Hu Y, Wang B. Compressive and bending behaviours of wood-based two-dimensional lattice truss core sandwich structures. Compos Struct 2015;124:337–44. https://doi.org/10.1016/j.compstruct.2015.01.033.

[130] Lexcellent C (Christian). Shape-Memory Alloys Handbook. Wiley; 2013.

[131] Hutchinson RG. Mechanics of lattice materials. University of Cambridge, 2004.

[132] Bower AF. Applied Mechanics of Solids. CRC Press; 2009.

[133] Evans KE. Auxetic polymers: a new range of materials. vol. 15. 1991. https://doi.org/10.1016/0160-9327(91)90123-S.

[134] Lees C, Vincent J, Hillerton J. Poissons ratio in skin. Biomed Mater Eng 1991;1:19–23.

[135] Valant M, Axelsson A-K, Aguesse F, Alford NM. Molecular Auxetic Behavior of Epitaxial Co-

Ferrite Spinel Thin Film. Adv Funct Mater 2010;20:644–7. https://doi.org/10.1002/adfm.200901762.

[136] Kumar GP, Ismail M, Nguyen YN, Liang LH, Cui F. Fatigue modeling in percutaneous caval valved stents. Procedia Eng 2017;214:98–106. https://doi.org/10.1016/j.proeng.2017.08.188.

[137] Körner C, Liebold-Ribeiro Y. A systematic approach to identify cellular auxetic materials. Smart Mater Struct 2014. https://doi.org/10.1088/0964-1726/24/2/025013.

[138] Grima JN, Evans KE. Auxetic behavior from rotating triangles. J Mater Sci 2006;41:3193–3196. https://doi.org/10.1007/s10853-006-6339-8.

[139] Mousanezhad D, Haghpanah B, Ghosh R, Magid Hamouda A, Nayeb-Hashemi H, Vaziri A. Elastic properties of chiral, anti-chiral, and hierarchical honeycombs: A simple energy-based approach. Theor Appl Mech Lett 2016;6:81–96. https://doi.org/10.1016/j.taml.2016.02.004.

[140] Zhao Z-L, Li B, Feng X-Q. Handedness-dependent hyperelasticity of biological soft fibers with multilayered helical structures. Int J Non Linear Mech 2016;81:19–29. https://doi.org/10.1016/j.ijnonlinmec.2015.12.002.

[141] Oliverio M, Digilio MC, Versacci P, Dallapiccola B, Marino B. Shells and heart: Are human laterality and chirality of snails controlled by the same maternal genes? Am J Med Genet Part A 2010;152A:2419–25. https://doi.org/10.1002/ajmg.a.33655.

[142] Qing H, Mishnaevsky L. 3D hierarchical computational model of wood as a cellular material with fibril reinforced, heterogeneous multiple layers. Mech Mater 2009:1034–49. https://doi.org/10.1016/j.mechmat.2009.04.011.

[143] Ortiz C, Boyce MC. Bioinspired Structural Materials. Sci New Ser 2008;319:1053–4. https://doi.org/10.1126/science.ll55477.

[144] Fratzl P, Weinkamer R. Nature's hierarchical materials. Prog Mater Sci 2007;52:1263–334. https://doi.org/10.1016/j.pmatsci.2007.06.001.

[145] Espinosa HD, Juster AL, Latourte FJ, Loh OY, Gregoire D, Zavattieri PD. Tablet-level origin of toughening in abalone shells and translation to synthetic composite materials. Nat Commun 2011;2. https://doi.org/10.1038/ncomms1172.

[146] Aizenberg J, Weaver JC, Thanawala MS, Sundar VC, Morse DE, Fratzl P. Skeleton of Euplectella sp.: Structural Hierarchy from the Nanoscale to the Macroscale. 22 A Chrestin, U Merkt, Appl Phys Lett 1985;297:2387. https://doi.org/10.1126/science.1113523.

[147] Wang J-S, Wang G, Feng X-Q, Kitamura T, Kang Y-L, Yu S-W, et al. Hierarchical chirality transfer in the growth of Towel Gourd tendrils. Sci Rep 2013;3. https://doi.org/10.1038/srep03102.

[148] Zhao Z-L, Zhao H-P, Wang J-S, Zhang Z, Feng X-Q. Mechanical properties of carbon nanotube ropes with hierarchical helical structures. J Mech Phys Solids 2014:64–83. https://doi.org/10.1016/j.jmps.2014.06.005.

[149] Alderson KL, Evans KE. Auxetic materials: the positive side of being negative. Eng Sci Educ J 2000;9:148–54. https://doi.org/10.1049/esej:20000402.

[150] Scarpa F, Smith FC, Chambers B, Burriesci G. Mechanical and electromagnetic behaviour of auxetic honeycomb structures. Aeronaut J 2003;107:175–83. https://doi.org/10.1017/s000192400001191x.

[151] Scarpa F, Ciffo LG, Yates JR. Dynamic properties of high structural integrity auxetic open cell foam Related content Vibration transmissibility and damping behaviour for auxetic and conventional foams under linear and nonlinear regimes. Smart Mater Struct 2004;13:49–56. https://doi.org/10.1088/0964-1726/13/1/006.

[152] Haghpanah B, Oftadeh R, Papadopoulos J, Vaziri A. Self-similar hierarchical honeycombs. Proc R Soc A 2013. https://doi.org/10.1098/rspa.2013.0022.

[153] Bettini P, Airoldi A, Sala G, Landro L Di, Ruzzene M, Spadoni A. Composite chiral structures for morphing airfoils: Numerical analyses and development of a manufacturing process. Compos Part B 2009. https://doi.org/10.1016/j.compositesb.2009.10.005.

[154] Mizzi L, Attard D, Gatt R, Pozniak AA, Wojciechowski KW, Grima JN. Influence of translational disorder on the mechanical properties of hexachiral honeycomb systems. Compos Part B 2015;80:84–91. https://doi.org/10.1016/j.compositesb.2015.04.057.

[155] Li Y, Assouar BM. Acoustic metasurface-based perfect absorber with deep subwavelength thickness. Appl Phys Lett 2016;108. https://doi.org/10.1063/1.4941338.

[156] Lynd DT, Harne RL. Strategies to predict radiated sound fields from foldable, Miura-ori-based transducers for acoustic beamfolding. J Acoust Soc Am 2017;141:480. https://doi.org/10.1121/1.4974204.

[157] Zou C, Lynd DT, Harne RL. Acoustic Wave Guiding by Reconfigurable Tessellated Arrays. Phys Rev Appl 2018;9. https://doi.org/10.1103/PhysRevApplied.9.014009.

[158] Babaee S, Overvelde JTB, Chen ER, Tournat V, Bertoldi K. Reconfigurable origami-inspired acoustic waveguides. Sci Adv 2016;2:e1601019–e1601019. https://doi.org/10.1126/sciadv.1601019.

[159] Thota M, Li S, Wang KW. Lattice reconfiguration and phononic band-gap adaptation via origami folding. Phys Rev B 2017;95:64307. https://doi.org/10.1103/PhysRevB.95.064307.

[160] Thota M, Wang KW. Reconfigurable origami sonic barriers with tunable bandgaps for traffic noise mitigation. J Appl Phys 2017;122:144902. https://doi.org/10.1063/1.4991026.

[161] Turner N, Goodwine B, Sen M. A review of origami applications in mechanical engineering. J Mech Eng Sci 2016;230:2345–2362. https://doi.org/10.1177/0954406215597713.

[162] Hull TC. The Combinatorics of Flat Folds: a Survey. Springfield, MA: 2013.

[163] Lang RJ. TreeMaker - Robert J. Lang Origami 2010. https://langorigami.com/article/treemaker/ (accessed November 14, 2018).

[164] Demaine ED, O'Rourke J. Geometric folding algorithms : linkages, origami, polyhedra. Cambridge University Press; 2007.

[165] Bern M, Demaine E, Eppstein D. A disk-packing algorithm for an origami magic trick. In: International conference on fun with algorithms. 1998.

[166] Folding/one-cutting a Betsy Ross star from a Square 2017. https://www.ushistory.org/BETSY/more/flagfoldcut2.htm (accessed March 14, 2021).

[167] Tachi T. Rigid foldable thick origami tachi. Comput Sci 2010. https://doi.org/10.1201/b10971-24.

[168] Review T, Palma C-A, Cecchini M, Samorì P. Predicting self-assembly: from empirism to determinism. Chem Soc Rev 2012;41:3701–4088. https://doi.org/10.1039/c2cs15302e.

[169] Judy JW, Muller RS. Magnetically actuated, addressable microstructures. J Microelectromechanical Syst 1997;6:249–55. https://doi.org/10.1109/84.623114.

[170] Whitney JP, Sreetharan PS, Ma Y. Monolithic fabrication of millimeter-scale machines Related content Pop-up book MEMS 2012. https://doi.org/10.1088/0960-1317/22/5/055027.

[171] Whitney JP, Sreetharan PS, Ma KY, Wood RJ. Pop-up book MEMS. J Micromechanics Microengineering 2011;21. https://doi.org/10.1088/0960-1317/21/11/115021.

[172] Hawkes E, An B, Benbernou NM, Tanaka H, Kim S, Demaine ED, et al. Programmable matter

by folding. Proc Natl Acad Sci 2010;107:12441–5. https://doi.org/10.1073/pnas.0914069107.

[173] Ramadoss R, Lee S, Lee YC, Bright VM, Gupta KC. Fabrication, assembly, and testing of rf mems capacitive switches using flexible printed circuit technology. IEEE Trans Adv Packag 2003;26:248–54. https://doi.org/10.1109/TADVP.2003.817968.

[174] Liu Y, Boyles JK, Genzer J, Dickey MD. Supporting Information for: Self-Folding of Polymer Sheets Using Local Light Absorption. Soft Matter 2012.

[175] Liu Y, Mailen R, Zhu Y, Dickey MD, Genzer J. Simple geometric model to describe self-folding of polymer sheets. Phys Rev E 2014;89:42601. https://doi.org/10.1103/PhysRevE.89.042601.

[176] Kuribayashi K, Tsuchiya K, You Z, Tomus D, Umemoto M, Ito T, et al. Self-deployable origami stent grafts as a biomedical application of Ni-rich TiNi shape memory alloy foil 2006. https://doi.org/10.1016/j.msea.2005.12.016.

[177] Ahmed S, Ounaies Z, Frecker M. Investigating the performance and properties of dielectric elastomer actuators as a potential means to actuate origami structures. Smart Mater Struct 2014. https://doi.org/10.1088/0964-1726/23/9/094003.

[178] Yang FQ. Relation between surface stress and surface energy for an elastic sphere: Effects of deformation and Maxwell stress. Sci China Physics, Mech Astron 2017;60:8–11. https://doi.org/10.1007/s11433-017-9081-2.

[179] Pelrine R, Kornbluh R, Kofod G. High-Strain Actuator Materials Based on Dielectric Elastomers. Adv Mater 2000;12:1223–5. https://doi.org/10.1002/1521-4095(200008)12:16<1223::AID-ADMA1223>3.0.CO;2-2.

[180] Pelrine R, Kornbluh R, Pei Q, Joseph J. High-speed electrically actuated elastomers with strain greater than 100%. Science (80-) 2000;287:5454.

[181] Van Knippenberg R, Habraken A, Teuffel P. Deployable structures using non-singular rigid foldable patterns. Procedia Eng 2016;155:388–97. https://doi.org/10.1016/j.proeng.2016.08.042.

[182] Kobayashi H, Kresling B, Vincent JF V. The Geometry of Unfolding Tree Leaves. vol. 265. 1998.

[183] Hunt GW, Ario I. Twist buckling and the foldable cylinder: An exercise in origami. Int J Non Linear Mech 2005;40:833–43. https://doi.org/10.1016/j.ijnonlinmec.2004.08.011.

[184] Fuchi K, Diaz AR, Rothwell EJ, Ouedraogo RO, Tang J. An origami tunable metamaterial. J Appl Phys 2012;111:11303. https://doi.org/10.1063/1.4704375.

[185] Griffith S, Calisch S, Gilman T, Gaebler F. Origami-inspired Prototyping. R&D - Strateg Innov 2012:24–6.

[186] Balkcom DJ, Mason MT. Robotic origami folding. Int J Robot Res Vol 2008;27:613–627. https://doi.org/10.1177/0278364908090235.

[187] Clough RW. The Finite Element Method in Plane Stress Analysis. Proc. Second ASCE Conf. Electron. Comput., Pittsburgh: 1960, p. 345–78.

[188] Bathe K-J. Finite Element Procedures. 2nd ed. London: Englewood Cliffs, N.J.; 2014.

[189] Fusaro G, Yu X, Lu Z, Cui F, Kang J. A Metawindow with optimised acoustic and ventilation performance. Appl Sci 2021;11:1–16. https://doi.org/10.3390/ app11073168.

[190] Kumar S, Xiang TB, Lee HP. Ventilated acoustic metamaterial window panels for simultaneous noise shielding and air circulation. Appl Acoust 2020;159. https://doi.org/10.1016/j.apacoust.2019.107088.

[191] Trott DW, Gobbert MK. Finite Element Convergence Studies Using COMSOL 4 . 0a and LiveLink for MATLAB. Integr Vlsi J 2010:1–16.

[192] Sabatini R, Snively JB, Bailly C, Hickey MP, Garrison JL. Numerical Modeling of the Propagation of Infrasonic Acoustic Waves Through the Turbulent Field Generated by the Breaking of Mountain Gravity Waves. Geophys Res Lett 2019;46:5526–34. https://doi.org/10.1029/2019GL082456.

[193] Morton KW, Mayers DF. Numerical Solution of Partial Differential Equations, An Introduction. Cambridge University Press; 2005.

[194] Jin B-J, Kim H-S, Kang H-J, Kim J-S. Sound diffraction by a partially inclined noise barrier. Appl Acoust 2001;62:1107–21.

[195] Cutanda-Henríquez V, Juhl PM. An axisymmetric boundary element formulation of sound wave propagation in fluids including viscous and thermal losses. J Acoust Soc Am 2013;134:3409–18. https://doi.org/10.1121/1.4823840.

[196] Farley S, Evison R, Rackham N, Nicolson R, Dawson J. The Behaviour Analysis Coding System – An applied, real-time approach for measuring and improving interactive skills. Cambridge Handb. Gr. Interact. Anal., Cambridge University Press.; 2016, p. 1–14.

[197] Rossing TD, Schroeder MR, Hartmann WM, Fletcher NH, Dunn F, Campbell DM, editors. Springer Handbook of Acoustics. New York: Springer; 2007.

https://doi.org/https://doi.org/10.1007/978-0-387-30425-0_23.

[198] ISO 10534-1: 1996. Acoustics – Determination of sound absorption coefficient and impedance in impedance tubes – Part 1: Method using standing wave ratio. International Organisation for Standardisation; 1996.

[199] ISO 10534-2: 1998. Acoustics – Determination of sound absorption coefficient and impedance in impedance tubes – Part 2: Transfer function method. International Organisation for Standardisation; 1998.

[200] ISO 354:2003. Acoustics – Measurement of sound absorption in a reverberation room, 2003. International Organisation for Standardisation; 2003.

[201] Nobile MA. The measurement of absorption coefficient and acoustic impedance using spherical waves and a transfer function method. J Acoust Soc Am 1987;82:S11–S11. https://doi.org/10.1121/1.2024624.

[202] Beranek LL, Sleeper HP. The Design of Anechoic Sound Chambers. J Acoust Soc Am 1946;18:246–246. https://doi.org/10.1121/1.1902429.

[203] Dobychina EM, Snastin M V., Efimov EN, Shevgunov TY. Unmanned Aerial Vehicle Antenna Measurement Using Anechoic Chamber. TEM J 2020;9:1480–7. https://doi.org/10.18421/TEM94-21.

[204] Pywell M, Midgley-Davies M. Aircraft-sized anechoic chambers for electronic warfare, radar and other electromagnetic engineering evaluation. Aeronaut J 2017;121:1393–443. https://doi.org/10.1017/aer.2017.89.

[205] Wang T, Zhou M. A method for product form design of integrating interactive genetic algorithm with the interval hesitation time and user satisfaction. Int J Ind Ergon 2020;76:102901. https://doi.org/10.1016/j.ergon.2019.102901.

[206] Dianat I, Vahedi A, Dehnavi S. Association between objective and subjective assessments of environmental ergonomic factors in manufacturing plants. Int J Ind Ergon 2016;54:26–31. https://doi.org/10.1016/j.ergon.2015.12.004.

[207] Tang P, Sun X, Cao S. Investigating user activities and the corresponding requirements for information and functions in autonomous vehicles of the future. Int J Ind Ergon 2020;80:103044. https://doi.org/10.1016/j.ergon.2020.103044.

[208] Bayoumi M. Energy saving method for improving thermal comfort and air quality in warm

humid climates using isothermal high velocity ventilation. Renew Energy 2017;114:502–12. https://doi.org/10.1016/j.renene.2017.07.056.

[209] Pitt JC, Shew A. Handbook of human factors and Ergonomics. John Wiley & Sons; 2012. https://doi.org/10.4324/9780203735657.

[210] Handbook of perception and human performance. New York: Wiley; 1986.

[211] Frings C, Wentura D. Self-priorization processes in action and perception. J Exp Psychol Hum Percept Perform 2014;40:1737–40. https://doi.org/10.1037/a0037376.

[212] Brunetti R, Indraccolo A, Mastroberardino S, Spence C, Santangelo V. The impact of cross-modal correspondences on working memory performance. J Exp Psychol Hum Percept Perform 2017;43:819–31. https://doi.org/10.1037/xhp0000348.

[213] Warren PA, Gostoli U, Farmer GD, El-Deredy W, Hahn U. A re-examination of "Bias" in human randomness perception. J Exp Psychol Hum Percept Perform 2018;44:663–80. https://doi.org/10.1037/xhp0000462.

[214] Yang W, Moon HJ. Combined effects of acoustic, thermal, and illumination conditions on the comfort of discrete senses and overall indoor environment. Build Environ 2019;148:623–33. https://doi.org/10.1016/j.buildenv.2018.11.040.

[215] Lupyan G. Objective Effects of Knowledge on Visual Perception. J Exp Psychol Hum Percept Perform 2017;43:794–806. https://doi.org/10.1037/xhp0000343.supp.

[216] Klepeis NE, Nelson WC, Ott WR, Robinson JP, Tsang AM, Switzer P, et al. The National Human Activity Pattern Survey (NHAPS): A resource for assessing exposure to environmental pollutants. J Expo Anal Environ Epidemiol 2001;11:231–52. https://doi.org/10.1038/sj.jea.7500165.

[217] Frontczak M, Andersen RV, Wargocki P. Questionnaire survey on factors influencing comfort with indoor environmental quality in Danish housing. Build Environ 2012;50:56–64. https://doi.org/10.1016/j.buildenv.2011.10.012.

[218] Samet JM, Spengler JD. Indoor Environments, and Health: Moving into the 21st Century. Am J Public Health 2003;93:1489–93. https://doi.org/10.2105/AJPH.93.9.1489.

[219] Leaman A. Dissatisfaction and office productivity. Facilities 1995;13:13–9. https://doi.org/10.1108/02632779510078120.

[220] Seppänen OA, Fisk W. Some quantitative relations between indoor environmental quality and

work performance or health. HVAC&R Res 2006;12:957–73. https://doi.org/10.1080/10789669.2006.10391446.

[221] U.S. Environmental Protection Agency. Indoor Air Pollution: an Introduction for Health Professionals. Co-Sponsored by: The American Lung Association (ALA), the Environmental Protection Agency (EPA), the Consumer Product Safety Commission (CPSC), and the American Medical Association (AMA): 1994.

[222] Council WGB. Green offices that keep staff healthy and happy are improving productivity & boosting businesses' bottom line, finds report 2010. https://www.worldgbc.org/news-media/green-offices-keep-staff-healthy-and-happy-are-improving-productivity-boosting-businesses (accessed March 31, 2021).

[223] Wang J, Zhang T, Wang S, Battaglia F. Numerical investigation of single-sided natural ventilation driven by buoyancy and wind through variable window configurations. Energy Build 2018;168:147–64. https://doi.org/10.1016/j.enbuild.2018.03.015.

[224] Djongyang N, Tchinda R, Njomo D. Thermal comfort: A review paper. Renew Sustain Energy Rev 2010;14:2626–40. https://doi.org/10.1016/j.rser.2010.07.040.

[225] Torresin S, Albatici R, Aletta F, Babich F, Oberman T, Kang J. Acoustic design criteria in naturally ventilated residential buildings: New research perspectives by applying the indoor soundscape approach. Appl Sci 2019;9. https://doi.org/10.3390/app9245401.

[226] Sakellaris IA, Saraga DE, Mandin C, Roda C, Fossati S, De Kluizenaar Y, et al. Perceived indoor environment and occupants' comfort in European "Modern" office buildings: The OFFICAIR Study. Int J Environ Res Public Health 2016;13. https://doi.org/10.3390/ijerph13050444.

[227] Pierson C, Wienold J, Bodart M. Review of Factors Influencing Discomfort Glare Perception from Daylight. LEUKOS - J Illum Eng Soc North Am 2018;14:111–48. https://doi.org/10.1080/15502724.2018.1428617.

[228] Nagamachi M. Requisites and practices of participatory ergonomics. Int J Ind Ergon 1995;15:371–7. https://doi.org/10.1016/0169-8141(94)00082-E.

[229] Naweed A, Ward D, Gourlay C, Dawson D. Can participatory ergonomics process tactics improve simulator fidelity and give rise to transdisciplinarity in stakeholders? A before–after case study. Int J Ind Ergon 2018;65:139–52. https://doi.org/10.1016/j.ergon.2017.07.011.

[230] Bridger RS. Introduction to Ergonomics. vol. 53. Taylor & Francis; 2003. https://doi.org/10.1017/CBO9781107415324.004.

[231] Kitzinger J, Barbour RS. Introduction: The challenge and promise of focus groups. In: Barbour RS, Kitzinger J, editors. Dev. Focus Gr. Res. Polit. Theory Pract., London: SAGE; 1999, p. 1–20.

[232] Henry Ollagnon. Propositions pour une gestion patrimoniale des eaux souterraines. L'expe´rience de la nappe phre´atique d'Alsace. 1979:33–73.

[233] Barbour R. Doing Focus Groups. London: SAGE Publications Ltd; 2007. https://doi.org/10.4135/9781849208956.

[234] Wilkinson S. Focus group methodology: a review. Int J Soc Res Methodol 1998;1:181–203. https://doi.org/10.1080/13645579.1998.10846874.

[235] Morgan D. Focus Groups as Qualitative Research. 2455 Teller Road, Thousand Oaks California 91320 United States of America : SAGE Publications, Inc.; 1997. https://doi.org/10.4135/9781412984287.

[236] Blumer H. Symbolic interactionism : perspective and method. University of California Press; 1986.

[237] Seale C. The quality of qualitative research. Sage Publications; 1999.

[238] Callaghan G. Accessing Habitus: Relating Structure and Agency through Focus Group Research. Sociol Res Online 2005;10:1–12. https://doi.org/10.5153/sro.1129.

[239] Bourdieu P. In other words : essays towards a reflexive sociology. Stanford University Press; 1990.

[240] Environment T. The Tavistock Institute - Our History 2007. https://www.tavinstitute.org/who-we-are/our-history/ (accessed January 19, 2018).

[241] Charmaz K. Constructing Grounded Theory: A Practical Guide through Qualitative Analysis. SAGE; 2006.

[242] Melia KM. Producing "plausible stories": interviewing student nurses. In: Dingwall G, Miller R, editors. Context Method Qual. Res., London: SAGE; 1997, p. 26–36.

[243] Kelle U. Theory Building in Qualitative Research and Computer Programs for the Management of Textual Data. Sociol Res Online 1997;2.

[244] Kuzel AJ. Sampling in qualitative inquiry. Doing Qual. Res., SAGE Publications, Inc.; 1992, p. 31–44.

[245] Mays N, Pope C. Rigour and qualitative research. BMJ 1995;311:109–12.

[246] Puchta C, Potter J. Asking elaborate questions: Focus groups and the management of spontaneity. J Socioling 2002;3:314–35. https://doi.org/10.1111/1467-9481.00081.

[247] Owen S. The practical, methodological and ethical dilemmas of conducting focus groups with vulnerable clients. J Adv Nurs 2001;36:652–8.

[248] Deininger M, Daly SR, Lee JC, Seifert CM, Sienko KH. Prototyping for context: exploring stakeholder feedback based on prototype type, stakeholder group and question type. Res Eng Des 2019;30:453–71. https://doi.org/10.1007/s00163-019-00317-5.

[249] Corbin JM, Strauss AL, Strauss AL. Basics of qualitative research : techniques and procedures for developing grounded theory. Sage Publications; 2008.

[250] Kim KM, Lee K pyo. Collaborative product design processes of industrial design and engineering design in consumer product companies. Des Stud 2016;46:226–60. https://doi.org/10.1016/j.destud.2016.06.003.

[251] Adelson B. Developing strategic alliances: A framework for collaborative negotiation in design. Res Eng Des - Theory, Appl Concurr Eng 1999;11:133–44. https://doi.org/10.1007/s001630050010.

[252] Mcdonagh-philp Mied D, Bruseberg A. Using Focus Groups to Support New Product Development. Inst Eng Des J 2000;5:1–6.

[253] Veenstra VS, Halman JIM, Voordijk JT. A methodology for developing product platforms in the specific setting of the housebuilding industry. Res Eng Des 2006;17:157–73. https://doi.org/10.1007/s00163-006-0022-6.

[254] Macnaghten, P. and Myers G. Focus groups. London: SAGE; 2004.

[255] Dokmeci Yorukoglu PN, Kang J. Development and testing of indoor soundscape questionnaire for evaluating contextual experience in public spaces. Build Acoust 2017;24:307–24. https://doi.org/10.1177/1351010X17743642.

[256] Glaser BG, Strauss AL. The Discovery of Grounded Theory: Strategies for Qualitative Research. vol. 1. Aldine Transcaction; 1967. https://doi.org/10.2307/2575405.

[257] Realyvásquez-Vargas A, Maldonado-Macías AA, García-Alcaraz JL, Cortés-Robles G, Blanco-Fernández J. A macroergonomic compatibility index for manufacturing systems. Int J Ind Ergon 2018;68:149–64. https://doi.org/10.1016/j.ergon.2018.07.007.

[258] Zhou D, Chen J, Lv C, Cao Q. A method for integrating ergonomics analysis into maintainability

design in a virtual environment. Int J Ind Ergon 2016;54:154–63. https://doi.org/10.1016/j.ergon.2016.06.003.

[259] Shankar P, Morkos B, Yadav D, Summers JD. Towards the formalization of non-functional requirements in conceptual design. Res Eng Des 2020;31:449–69. https://doi.org/10.1007/s00163-020-00345-6.

[260] Santolaya JL, Lacasa E, Biedermann A, Muñoz N. A practical methodology to project the design of more sustainable products in the production stage. Res Eng Des 2019;30:539–58. https://doi.org/10.1007/s00163-019-00320-w.

[261] Fusaro G, Yu X, Cui F, Kang J. Development of a window system with acoustic metamaterial for air and noise control. Proc. 10th Int. Conf. Comput. Methods, Singapore: 2019.

[262] Fusaro G, Yu X, Cui F, Kang J. Development of a metamaterial for acoustic and architectonical improvement of window design. Proc 23rd Int Conf Acoust 2019;2019-Septe:1977–83. https://doi.org/10.18154/RWTH-CONV-239567.

[263] Fusaro G, Yu X, Kang J, Cui F. Development of metacage for noise control and natural ventilation in a window system. Appl Acoust 2020;170:107510. https://doi.org/10.1016/j.apacoust.2020.107510.

[264] Yu X, Fang H, Cui F, Cheng L, Lu Z. Origami-inspired foldable sound barrier designs. J Sound Vib 2019;442:514–26. https://doi.org/10.1016/j.jsv.2018.11.025.

[265] Shen C, Xie Y, Li J, Cummer SA, Jing Y. Acoustic Metacages for Omnidirectional Sound Shielding. J Acoust Soc Am 2017;141.

[266] Belyi V, Gan WS. Integrated psychoacoustic active noise control and masking. Appl Acoust 2019;145:339–48. https://doi.org/10.1016/j.apacoust.2018.10.027.

[267] Crooker MJ. Handbook of Noise and Vibration Control. vol. 58. John Wiley & Sons; 2007. https://doi.org/10.2307/1119589.

[268] Guasch O, Arnela M, Sánchez-Martín P. Transfer matrices to characterize linear and quadratic acoustic black holes in duct terminations. J Sound Vib 2017;395:65–79. https://doi.org/10.1016/j.jsv.2017.02.007.

[269] Cotana F, Pisello AL, Moretti E, Buratti C. Multipurpose characterization of glazing systems with silica aerogel: In-field experimental analysis of thermal-energy, lighting and acoustic performance. Build Environ 2014;81:92–102. https://doi.org/10.1016/j.buildenv.2014.06.014.

[270] Kim SH, Lee SH. Air transparent soundproof window. AIP Adv 2014;4. https://doi.org/10.1063/1.4902155.

[271] Shen C, Xie Y, Li J, Cummer SA, Jing Y. Acoustic metacages for sound shielding with steady air flow. J Appl Phys 2018;123:124501. https://doi.org/10.1063/1.5009441.

[272] Lim HS, Kim G. The renovation of window mechanism for natural ventilation in a high-rise residential building. Int J Vent 2018;17:17–30. https://doi.org/10.1080/14733315.2017.1351733.

[273] Sorgato MJ, Melo AP, Lamberts R. The effect of window opening ventilation control on residential building energy consumption. Energy Build 2016;133:1–13. https://doi.org/10.1016/j.enbuild.2016.09.059.

[274] UK Space Management, Group. UK Higher Education Space Management Project Review of space norms. 2006.

[275] Tong YG, Tang SK, Kang J, Fung A, Yeung MKL. Full scale field study of sound transmission across plenum windows. Appl Acoust 2015;89:244–53. https://doi.org/10.1016/j.apacoust.2014.10.003.

[276] Li Y, Jiang X, Li R-Q, Liang B, Zou X-Y, Yin L-L, et al. Experimental Realization of Full Control of Reflected Waves with Subwavelength Acoustic Metasurfaces. Phys Rev Appl 2014;2:1–11. https://doi.org/10.1103/PhysRevApplied.2.064002.

[277] Cummer SA, Popa B-I, Schurig D, Smith DR, Pendry J, Rahm M, et al. Scattering Theory Derivation of a 3D Acoustic Cloaking Shell. Phys Rev Lett 2008;100:1–4. https://doi.org/10.1103/PhysRevLett.100.024301.

[278] Ghaffarivardavagh R, Nikolajczyk J, Glynn Holt R, Anderson S, Zhang X. Horn-like space-coiling metamaterials toward simultaneous phase and amplitude modulation. Nat Commun 2018;9:1–8. https://doi.org/10.1038/s41467-018-03839-z.

[279] Selamet A, Ji ZL. ACOUSTIC ATTENUATION PERFORMANCE OF CIRCULAR EXPANSION CHAMBERS WITH EXTENDED INLET/OUTLET. J Sound Vib 1999;223:197–212. https://doi.org/10.1006/jsvi.1998.2138.

[280] Sellen N, Cuesta M, Galland M-A. Noise reduction in a flow duct: Implementation of a hybrid passive/active solution. J Sound Vib 2006;297:492–511. https://doi.org/10.1016/j.jsv.2006.03.049.

[281] Von Grabe J, Svoboda P, Bäumler A. Window ventilation efficiency in the case of buoyancy ventilation. Energy Build 2014;72:203–11. https://doi.org/10.1016/j.enbuild.2013.10.006.

[282] Bayoumi M. Impacts of window opening grade on improving the energy efficiency of a façade in hot climates. Build Environ 2017;119:31–43.

[283] Lee KJB, Jung MK, Lee SH. Highly tunable acoustic metamaterials based on a resonant tubular array. Phys Rev B 2012;86:184302. https://doi.org/10.1103/PhysRevB.86.184302.

[284] Woong Jung J, Eun Kim J, Woo Lee J. Acoustic metamaterial panel for both fluid passage and broadband soundproofing in the audible frequency range. Appl Phys Lett 2018;112:41903. https://doi.org/10.1063/1.5004605.

[285] Yu N, Genevet P, Aieta F, Kats MA, Blanchard R, Aoust G, et al. Flat optics: Controlling wavefronts with optical antenna metasurfaces. IEEE J Sel Top Quantum Electron 2013;19:4700423. https://doi.org/10.1109/JSTQE.2013.2241399.

[286] Qian E, Fu Y, Fu Y, Chen H. Total omnidirectional reflection by sub-wavelength gradient metallic gratings. EPL 2016:34003. https://doi.org/10.1209/0295-5075/114/34003.

[287] Barjau A. On the one-dimensional acoustic propagation in conical ducts with stationary mean flow. J Acoust Soc Am 2007;122:3242. https://doi.org/10.1121/1.2799478.

[288] Asfour OS, Gadi MB. A comparison between CFD and Network models for predicting wind-driven ventilation in buildings. Build Environ 2007;42:4079–85. https://doi.org/10.1016/j.buildenv.2006.11.021.

[289] Zhu WJ, Shen WZ, Sørensen N. High-order numerical simulations of flow-induced noise. Int J Numer METHODS FLUIDS 2010;66:17–37. https://doi.org/10.1002/fld.2241.

[290] Delprat N. Rossiter's formula: A simple spectral model for a complex amplitude modulation process? Phys Fluids 2006;18. https://doi.org/10.1063/1.2219767.

[291] Stinson MR, Champoux Y. Propagation of sound and the assignment of shape factors in model porous materials having simple pore geometries. J Acoust Soc Am 1992;91:685–95. https://doi.org/10.1121/1.402530.

[292] Allam S, Abom M. A New Type of Muffler Based on Microperforated Tubes. J Vib Acoust 2011;133. https://doi.org/10.1115/1.4002956.

[293] Włodarczyk EA, Szkiełkowska A, Skarżyński H, Miaśkiewicz B, Skarżyński PH. Reference values for psychoacoustic tests on Polish school children 7–10 years old. PLoS One 2019;14:1–21.

https://doi.org/10.1371/journal.pone.0221689.

[294] Peel MC, Finlayson BL, McMahon TA. Updated world map of the Köppen-Geiger climate classification. Hydrol Earth Syst Sci 2007;11:1633–44. https://doi.org/10.1002/ppp.421.

[295] International Organization for Standardization. ISO 7726 Ergonomics of the thermal environment — Instruments for measuring physical quantities. International Organisation for Standardisation; 1998.

[296] Torresin S, Albatici R, Aletta F, Babich F, Kang J. Assessment methods and factors determining positive indoor soundscapes in residential buildings: A systematic review. Sustain 2019;11. https://doi.org/10.3390/su11195290.

[297] Aletta F, Oberman T, Axelsson Ö, Xie H. Soundscape assessment : towards a validated translation of perceptual attributes in different languages. Inter-Noise 2020.

[298] Héroux ME, Babisch W, Belojevic G, Brink M, Janssen S, Lercher P, et al. WHO environmental noise guidelines for the European Region. Euronoise 2018 2018:2589–93.

[299] Lionello M, Aletta F, Kang J. A systematic review of prediction models for the experience of urban soundscapes. Appl Acoust 2020;170. https://doi.org/10.1016/j.apacoust.2020.107479.

[300] Mitchell A, Oberman T, Aletta F, Erfanian M, Kachlicka M, Lionello M, et al. The soundscape indices (SSID) protocol: A method for urban soundscape surveys- Questionnaires with acoustical and contextual information. Appl Sci 2020;10. https://doi.org/10.3390/app10072397.

[301] ISO 12913-1:2014. Acoustics - soundscape - part 1: definition and conceptual framework. 2014.

[302] Stockfelt T. Sound as an existential necessity. J Sound Vib 1991;151.

[303] Kang J, Choroumouziadou K, Sankatamis K. Soundscape of European cities and landscapes. Research report COST TUD Action TD0804. Oxford: 2013.

[304] Pedrielli F, Carletti E, Casazza C. Just noticeable differences of loudness and sharpness for earth moving machines. Proc - Eur Conf Noise Control 2008:1231–6. https://doi.org/10.1121/1.2933219.

[305] Di Blasio S, Shtrepi L, Puglisi GE, Astolfi A. A cross-sectional survey on the impact of irrelevant speech noise on annoyance, mental health and well-being, performance and occupants' behavior in shared and open-plan offices. Int J Environ Res Public Health 2019;16.

https://doi.org/10.3390/ijerph16020280.

[306] Haapakangas A, Hongisto V, Liebl A. The relation between the intelligibility of irrelevant speech and cognitive performance—A revised model based on laboratory studies. Indoor Air 2020;30:1130–46. https://doi.org/10.1111/ina.12726.

[307] ISO. Acoustics - Method for calculating Loudness - Part 1: Zwicker Method, ISO 532-1. Switzerland, Geneva: 2017.

[308] Xiao J, Aletta F. A soundscape approach to exploring design strategies for acoustic comfort in modern public libraries: A case study of the Library of Birmingham. Noise Mapp 2016;3:264–73. https://doi.org/10.1515/noise-2016-0018.

[309] Kosters J, Kunz M, van den Bosch KA, Andringa TC, Zuidema SU, Luijendijk HJ, et al. Validation of a modified ambiance scale in nursing homes. Aging Ment Heal 2020;0:1–7. https://doi.org/10.1080/13607863.2020.1747049.

[310] Hoerzer S, Trudeau MB, Edwards WB, Nigg BM. Intra-rater reliability of footwear-related comfort assessments. Footwear Sci 2016;8:155–63. https://doi.org/10.1080/19424280.2016.1195451.

[311] McGraw KO, Wong SP. Forming Inferences about Some Intraclass Correlation Coefficients. Psychol Methods 1996;1:30–46. https://doi.org/10.1037/1082-989X.1.1.30.

[312] Bruton A, Conway JH, Holgate ST. Reliability: What is it, and how is it measured? Physiotherapy 2000;86:94–9. https://doi.org/10.1016/S0031-9406(05)61211-4.

[313] Chinn S. Statistics in respiratory medicine. 2. Repeatability and method comparison. Thorax 1991;46:454–6. https://doi.org/10.1136/thx.46.6.454.

[314] Cortina JM. What Is Coefficient Alpha? An Examination of Theory and Applications. J Appl Psychol 1993;78:98–104. https://doi.org/10.1037/0021-9010.78.1.98.

[315] DIN Deutsches Institut für Normung. DIN EN 16798-17 Energy performance of buildings - Ventilation for buildings - Part 17: Guidelines for inspection of ventilation and air conditioning systems, German version EN 16798-17:2017. 2017.

Appendix A - Online Questionnaire related to experiment described in Chapter 6

Information sheet:

Evaluation of metamaterials controlled Soundscape: listening test through headphones.

Sheffield Research Ethics Committee Approval ID Number: 033686

You are being invited to participate in a research project conducted by staff members of the **Acoustics Group at Sheffield University**. Before you decide to take part, it is important for you to understand why the research is being done and what participation will involve. **This has been approved as "low risk" research, as it only consists of a listening experience of everyday sounds and a questionnaire about them**.

Participation is voluntary. Please take time to read the following information carefully and discuss it with others if you wish. Ask us if there is anything that is not clear or if you would like more information. Take time to decide whether or not you want to take part. **Thank you for reading this**.

1. What is the project's purpose?

This project explores the subjective perception of outdoor and indoor public spaces. In particular, we ask what you think about the overall quality of various acoustic environments, what sound sources you can recognise from the recording of urban space and how you assess their loudness levels.

2. Why have I been chosen?

You are invited to participate in this study because you are an adult (above 18 years old) with proficiency in Italian or English languages. We plan to recruit a minimum of 20 people for this experiment to capture the variability of the general population in detail.

3. Do I have to take part?

Participation in this experiment is voluntary, and it is up to you to decide whether or not to take part. If you do decide to take part, you will be asked to sign a consent form. You can withdraw at any time without providing a reason. If you choose to withdraw, your responses will not be considered in the analyses, and any data you might have already provided up to that point will be

permanently deleted. After completing the experiment and submitting all the forms, we will not be able to retract your responses.

4. What will happen to me if I take part?

After reading the experiment description and giving consent to participate in the study, you will be asked to complete a short headphones screening (approximately 3 minutes). Given the successful completion of this step, you will then move to the main experiment.

You will listen to 14 different acoustic scenarios over consecutive sessions. Each recording will be 30 seconds long. After each acoustic scene, you will be asked to complete a questionnaire consisting of **5 short questions. You will be asked to rate the perceived quality of sounds along a pre-specified scale, rate what category of sounds dominates in the recording, enter verbal information about your perception of the sound sources, and judge the perceived loudness of the acoustic environment.** Although the time for answering those questions is not limited, please try and answer them as soon as possible so that the impression of the acoustic environment you just listened to is still fresh in your mind.

At the end of the assessment part, we will ask you a few basic demographic questions (e.g., age, gender, perceived well-being). This is to verify differences in acoustic preference according to gender or age. In any case, the questionnaire will be completely anonymous so that it won't be possible to identify you from your responses.

There will be short breaks in between the blocks to allow you to rest. On the whole, it is expected that each experiment **lasts no longer than 30 minutes in one sitting.**

5. What are the possible disadvantages and risks of taking part?

There are no risks associated with this study. Rest assured that if you carefully follow instructions in the calibration and screening test, sound levels will be set much below the threshold of what can be considered as potentially harmful noise exposure. Yet, if, for any reason (even not related to the sounds) you feel uncomfortable during the experiment, please feel free to terminate the experiment.

6. What are the possible benefits of taking part?

There are no immediate benefits for those people participating in the project. Their involvement in this study will help further our understanding of environmental sounds and sound-related information regarding the use of acoustic metamaterials. At a more general level, we hope that your participation in this study will also help you become more aware and acknowledge your sound surroundings' importance. Your participation will certainly help us to shape acoustically enjoyable public environments.

7. What if something goes wrong?

If you are concerned with any part of this research, please contact our local line managers or our UK line manager.

UK, IT line manager 1: Gioia Fusaro, gfusaro1@sheffield.ac.uk, +39 3495404068

UK line manager 2: Wen-Shao Chang, w.chang@sheffield.ac.uk, +44 (0) 114 2220370

UK, line manager 3: Jian Kang, j.kang@ucl.ac.uk, +44(0)2031087338

However, suppose you feel that your complaint has not been handled to satisfaction. In that case, you can contact the manager of Sheffield School of Architecture Research Ethics Committee: Dr Chengzi Peng, c.peng@sheffield.ac.uk, +44(0)114 222 0318.

8. Will my taking part in this project be kept confidential?

All the information that we collect about you during the research will be kept strictly confidential. You will not be able to be identified in any subsequent reports or publications. The project line managers will assign a code to your name at the beginning of the study to eventually track back your participation and keep your participation anonymous for future data elaborations. All the personal information we gather will be kept confidentially between the line managers of this project.

9. What will happen to the results of the research project?

Results from this study will be presented at international conferences and published in international journals. Results will always be presented in an aggregated and anonymised way, so confidentiality is always assured, and you will never be able to be identified as a participant.

10. Data Protection Privacy Notice

The controller for this project will be the University of Sheffield (UoS). The UoS Data Protection Officer provides oversight of UoS activities involving personal data processing and can be contacted at the head of data protection and legal services (Luke Thompson) email address: luke.thompson@sheffield.ac.uk.

This 'local' privacy notice sets out the information that applies to this particular study. Further details on how UoS uses participant information can be found in our 'general' privacy notice: https://www.sheffield.ac.uk/govern/data-protection/privacy/general .

The information required to be provided to participants under data protection legislation (GDPR and DPA 2018) is provided across both the 'local' and 'general' privacy notices.

The categories of personal data used will be as follows:

- Age (to detect differences in acoustic perception/preference according to age);
- Gender (to detect differences in acoustic perception/preference according to gender).

The lawful basis that would be used to process your personal data will be a task's performance in the public interest.

Your personal data will be processed so long as it is required for the research project.

If you are concerned about how your personal data is being processed, or if you would like to contact us about your rights, please contact UoS in the first instance at luke.thompson@sheffield.ac.uk .

11. Who is organising and funding the research?

The University of Sheffield is sponsoring this research.

Contact for further information: If you would like more information, please contact one of the Researchers:

- Ms Gioia Fusaro gfusaro1@sheffield.ac.uk
- Dr Wen-Shao Chang, w.chang@sheffield.ac.uk
- Prof Jian Kang j.kang@ucl.ac.uk

Thank you for reading this information sheet and for considering taking part in this research study.

>>NEXT PAGE>>

Consent Form:

Please complete this form after reading the Information Sheet and/or an explanation about the research.

Thank you for considering taking part in this research. The person organising the research must explain the project to you before you agree to take part. If you have any questions arising from the Information Sheet or explanation that was already given to you, please ask the researcher before deciding whether to join in.

1. I confirm that I have read and understood the Information Sheet for the above study. I have had an opportunity to consider the information and what will be expected of me. I have also had the chance to ask questions that have been answered to my satisfaction and participate in this listening experiment.
2. I understand that I will be able to withdraw my data up to the end of the experimental session.
3. I consent to participate in the study. I understand that my personal information (gender, age) will be used for the purposes explained to me. I understand that according to data protection legislation, 'public task' will be the lawful basis for processing.
4. I understand that all personal information (in this case, gender and age) will remain confidential and that all efforts will be made to ensure I cannot be identified. I understand that my data gathered in this study will be stored anonymously and securely. It will not be possible to identify me in any publications.
5. I understand that my information may be subject to review by responsible individuals from the University for monitoring and audit purposes.

6. I understand that my participation is voluntary and that I am free to withdraw at any time without giving a reason. I understand that if I decide to withdraw, any personal data I have provided up to that point will be deleted.
7. I understand that I will not benefit financially from this study or from any possible outcome it may result in in the future.

☐

I consent

>>NEXT PAGE>>

Get Ready!

Before you start, we would like to make sure that you are **sitting comfortably** in a quite room wearing a pair of **headphones** for the experiment. If possible, please turn off sound notifications on your messengers.

>>NEXT PAGE>>

Headphones Calibration

It is important for us to ensure the **realistic exposure**, so all recordings of everyday urban sounds you will hear are within the same volume range as the following calibration sounds. Their level is set not to exceed anything you encounter in your daily life.

However, if you find it hard to adjust the sound level or the loud sample is too disturbing to you, please feel free to quit the experiment.

On the next page, you will be instructed about how to set the headphones calibration and how to access the audiogram test.

>>NEXT PAGE>>

Headphones Calibration and Personal Audiogram Instructions

Headphones Calibration and Personal Audiogram Instructions

We now invite you to access the Headphones Calibration and Personal Audiogram test kindly. This preliminary test will take about 5 minutes. At the end of this preliminary test, we kindly ask you to save your personal audiogram and headphones volume with the personal ID we have assigned you p2. Thank you!

By clicking the link below, you will be sent to an online page for the Audiogram test. There is no right or wrong answer, so just answer according to how you perceive the testing sounds.

Once set, please **DO NOT** change the volume settings during the experiment.

>>NEXT PAGE>>

ParticipantSARE sent to the online calibration test at https://hearingtest.online/

Once the test is completed their audiogram is saved by their ID number and the headphones are calibrated. In the case their audiogram doesn't show any severe hearing losses, they can continue the online questionnaire.

>>NEXT PAGE>>

Soundscape test

Let's begin! If you have finished the personal audiogram test, you can keep going with the acoustic environments questionnaire by clicking on the next icon. During the experiment, you will hear a set of recordings (of 30 seconds each) of public places. Please listen to the recordings and answer the following questions.

>>NEXT PAGE>>

Screen 1

When you are ready, please press play and listen to the recording of the public space. After you have listened to the recording, please answer the following questions about the acoustic environment you heard.

1. While listening, please write down in the following tab any sound sources you can identify in this sound environment (please separate each sound source with a comma).

>>NEXT PAGE>>

Screen 2

2. How did you hear the following four sounds?

Scale: Not at all, A little, Moderately, A lot, Dominates completely

Traffic Noise (cars, buses, trains, aeroplanes, etc.)

Other noise (e.g. sirens, construction, industry, loading of goods)

Sounds from human beings (e.g. conversation, laughter, children at play, footsteps)

Natural sounds (e.g. singing birds, flowing water, wind in vegetation)

>>NEXT PAGE>>

Screen 3-4

3. For each of the 8 scales below, to what extent do you agree or disagree that the outdoor public space you heard is...

Scale: Strongly agree, Somewhat agree, Neither, Somewhat disagree, Strongly disagree

Pleasant

Chaotic

Vibrant

Uneventful

Calm

Annoying

Eventful

Monotonous

>>NEXT PAGE>>

Screen 5

5. Overall, how would you describe the outdoor public space you have just heard?

Scale: Very good, Good, Neither bad nor good, Bad, Very bad

6. How loud would you say this environment was?

Scale: Not at all, Slightly, Moderately, Very, Extremely

>>NEXT PAGE>>

Please indicate for each of the five statements below which is the closest to how you have been feeling over the last two weeks.

Scale: All of the time, Most of the time, More than half of the time, Less than half of the time, Some of the time, None of the time

1. I have felt cheerful and in good spirits

2. I have felt calm and relaxed

3. I have felt active and vigorous

4. I woke up feeling fresh and rested

5. My daily life has been filled with things that interest me

Thank you for completing the questionnaire!
Please continue to fill a short demographic form which will help us contextualise your answer.

>>NEXT PAGE>>

Demographic Questionnaire

Thank you for completing the Acoustic Questionnaire!

Before exiting the experiment, please fill a Short Demographic Questionnaire. All the information will be treated with respect to your privacy and will be stored anonymously according to the ID code that was assigned to you.

1. How old are you?

2. What is your gender?

Male, Female, Trans, Non-Binary, I prefer not to answer

3. Please specify your ethnicity

Asian or Pacific Islander, Black or African American, Hispanic or Latino, Native American or Alaskan Native, White or Caucasian, Multiracial or Biracial

4.Have you ever been diagnosed with any hearing problems or neurological disorders affecting hearing?

Yes, No

5. What is the highest level of education you have completed?

Primary school, Secondary school up to 16 years, Higher or secondary or further education (A-levels, BTEC, etc.), College or university, Post-graduate degree, Prefer not to say

6. What is your occupational status?

Student, Unemployed, Full-time employment, Part-time employment, Self-employed, Home-maker, Retired

7. What is your occupational/study activity?

8. Is your occupational/study activity mostly related to outdoor or indoor spaces?

Indoor, Outdoors

9. Do you practise sport?

Yes, No

9.b If yes, do you practice it indoors or outdoors?

Indoor, Outdoors

10. Has the actual Pandemic situation influenced your previous answers compared to those you would have given before COVID?

Yes, No

10.b If yes, in which way?

11. According to the following scale, how do you judge your actual condition in terms of working/study environmental quality compared to the pre-COVID one?

Much worst, Slightly worst, Unvaried, Slightly better, Much better

12. In which geographical area are you taking this questionnaire?

13. What is the temperature in the room you are in? (Please specify if you are using Celsius or Fahrenheit degrees)

13.b How would you rate the room where you are?

Too cold, Slightly cold, Comfortable, Slightly warm, Too warm

14. How humid is the room where you are?

Too dry, Slightly dry, Comfortable, Slightly humid, Too humid

15. How is the lighting condition in the room where you are?

Too dark, Slightly dark, Comfortable, Slightly bright, Too bright

16. How noisy is the acoustic environment of the room where you are?

Very noisy, Slightly noisy, Slightly quite, Very quite

17. Would you be interested in a system that allows natural ventilation and, at the same time, reduce the incoming noise?

Not interested at all, Not very much interested, Slightly interested, Very much interested

>>NEXT PAGE>>

Debriefing

Thank you for completing the Environmental Sound and Demographic Questionnaire! You have now finished the experiment successfully and contributed to the advancement of our research on Building Acoustics!!!

How would you rate this questionnaire experience?

Negative, Quite negative, Neutral, Quite Positive, Positive

Your opinion is precious to us! Please, leave a comment about the experiment modality. If you think there is anything to improve, please write it below.